DOE RESPONSES TO REQUEST FOR ADDITIONAL INFORMATION

(TAC NO. L22283)

DOE RESPONSES TO REQUEST FOR ADDITIONAL INFORMATION (TAC NO. L22283)

CHAPTER 1: INTRODUCTION AND GENERAL DESCRIPTION OF INSTALLATION

1-1 Request:

Identify structures, systems, and components (SSC) of the Three Mile Island Unit 2 (TMI-2) Independent Spent Fuel Storage Installation (ISFSI), including the dry casks that are important to safety.

Response:

The identification of structures, systems and components that are important to safety is provided in SAR Chapter 3, Section 3.4 "Classification of Structures, Components, and Systems". Section 3.4 provides a discussion of the criteria, a discussion of the classification of each structure, component, or system of the TMI-2 ISFSI. Section 3.4 also provides a Table 3.4-1 "NUHOMS® Major Components and Safety Classification", which summarizes the classification in accordance with the criteria discussed in Section 3.4.

Proposed SAR Rewrite:

No rewrite of Chapter 1 is required. However it should be noted that, in response to Item 3-8 of the Request for Additional Information (RAI), Table 3.4-1 will be revised to clarify the classifications in the table for consistency, relative to entire components versus subcomponents. (See Response to RAI Item 3-8).

1-2 Request:

Include a brief summary (not to exceed one page) of information on principal site characteristics, waste products generation, activities conducted at the ICPP that my affect TMI-2 ISFSI operations, and the quality assurance (QA) program, all of which are presented in more detail elsewhere in the SAR.

Response:

See proposed SAR rewrite

Proposed SAR Rewrite:

Section 1.1 will be revised to include the following (new) subsections:

1.1.3 TMI-2 ISFSI Site Characteristics (NEW)

Chapter 2 of this document provides the site characteristics relating to the Idaho National Engineering and Environmental Laboratory (INEEL), the Idaho Chemical Processing Plant (ICPP), and the INEEL TMI-2 ISFSI. It includes the meteorology, hydrology, seismology, geology, and volcanism of the area. It describes the geographical location, the population distribution within and around the INEEL, land and water use, and associated site activities. It also provides an evaluation of the site with respect to plant safety. Following is a summary of TMI-2 ISFSI site conditions:

- Probable Maximum Flood (PMF) Plain Elevation (Feet): 4917.0 above sea level (ASL)
- Ambient Temperature (Extremes):
  Highest: 103°F.
  Lowest: Minus 50°F.
- Average Monthly Temperature Extremes:
  Maximum: 87°F (in July).
  Minimum: 4°F (in January)
- Annual Precipitation:
  Average: 8.71 inches
  Highest: 14.40 inches
  Lowest: 4.50 inches
  Average Yearly Snowfall: 26 inches
- Seismic Zone 2B per the Uniform Building Code
- Design Basis Tornado:
  Maximum wind speed: 200 mph
  Rotational speed: 160 mph
  Translational Speed: 40 mph
  Pressure Drop: 1.5 psi
- Snow Load: 30 pounds per square foot (psf)
- Frost Depth: 5 feet
- Existing Ground Level Elevation (Feet): 4915 (ASL).

1.1.4 (Previously 1.1.3) Activities and Facilities to be Licensed

No change from existing text

1.1.5 Waste Product Generation (NEW)

Chapter 6 of this document addresses site-generated waste confinement and management. In summary, maintenance of the HEPA grade filters in the dry shielded canister (DSC) vent system is the only activity that will generate waste during the operating design life of the system. This waste will be in the form of dry radioactive waste. On the average, the filters could be replaced five times during the 50-year life of the system. It is estimated this would consist of about one cubic foot per DSC over the design life of the TMI-2 ISFSI (a total of less than 30 ft^3). Decommissioning activities at the time of TMI-2 ISFSI closure is estimated to generate less than 10 ft^3 per module (a total of less than 300 ft^3). The horizontal storage module (HSM) and concrete basemat would be disposed of as clean free release material after radiological surveys and any necessary decontamination.

1.1.6 Activities Conducted at ICPP that may affect TMI-2 ISFSI Operations (NEW)

The TMI-2 ISFSI will be located within the site boundaries of the ICPP with several other DOE owned facilities and DOE managed programs. The INEEL has its own large security police force, a fire department, medical staff, emergency response teams, and full-time ICPP shift plant supervision. Thus, the INEEL infrastructure will be considered to serve equivalent functions as independent local agencies (similar to local city or county) do for typical commercial licensed sites.

Normal ICPP operations will not affect operation of the TMI-2 ISFSI. Emergency situations, unrelated to the TMI-2 ISFSI operations, which would require personnel to evacuate the plant area, or take cover, could cause temporary interruptions to normal TMI-2 ISFSI operations (loading, unloading and surveillance). The interruptions would not compromise safety.

1.1.7 Quality Assurance Program (NEW)

The QA Program selected for this project satisfies the requirements of 10 CFR Part 72, Subpart G. The QA Program will ensure that essential technical and quality requirements for structures, systems, and components (SSCs) classified as important to safety are achieved and documented throughout all design, fabrication, construction, testing, operations, modifications and decommissioning activities. Chapter 11 of this document provides a detailed description of the QA program.

The basic quality assurance program is the DOE's Office of Civilian Radioactive Waste Management's Quality Assurance Requirements and Description, DOE/RW-0333P, Revision 5 (QARD). All SSCs are analyzed to determine whether their functions or physical characteristics are essential to the safety function. Those items are classified as "important to safety", and are subject to the applicable requirements of the QARD. The program will be implemented through use of approved, controlled implementing procedures.

CHAPTER 2: SITE CHARACTERISTICS

2-1 <u>Request:</u>
Provide the following with respect to withdrawal and use of water on the Idaho National Engineering and Environmental Laboratory (INEEL).

(a) A map that show wells where water withdrawal is occurring on the INEEL site with particular reference to the ICPP and the TMI-2 ISFSI location. As a minimum include all wells located within a minimum of an 8-km (5 mi) radius of the TMI-2 ISFSI. Note that Figure 2.5-2 provides some information, but it is not sufficient.

<u>Response</u>
Attachment 1 provides the requested information. It shows the location of the INEEL production wells and their location with respect to the TMI-2 ISFSI.

<u>Proposed SAR Rewrite:</u>
Attachment 1 will be added to Section 2.5 of the SAR in the next update.

<u>Request:</u>
(b) ***Depth of water well and formation from which water is extracted.***
(c) ***The quantity of water withdrawn annually at each well within the 8-km (5 mi) radius.***
(d) ***A discussion of the use of the water from each well with particular reference to any consumption by humans or animals.***

<u>Response:</u>
See the proposed SAR rewrite below

<u>Proposed SAR Rewrite:</u>
Table 2.5-(x) lists the INEEL production wells, the depth of the well, the depth to water at the well, and the annual volume of water withdrawn from each well. All wells withdraw water from the main body of the Snake River Plain Aquifer. The water withdrawn from each well is used for potable water on the Site, for ground maintenance, and necessary facility operations.

TABLE 2.5-(x): INEEL Production Wells and Annual Volume Pumped

Well Name	Depth of well (ft bls)[a]	Depth to Water (ft bls)	Annual Volume (gal)
ANP-01	360	208	2.561E+06
ANP-02	340	211	1.433E+06
ANP-08	309	218	3.908E+05
Badging Facility well	644	489	5.760E+04
CFA-1	639	468	1.473E+07
CFA-2	681	471	1.448E+05
CPP-01	586	460	1.834E+08[b]
CPP-02	605	460	1.834E+08[b]
CPP-04	700	462	1.834E+08[b]
CPP-05	695	447	1.834E+08[b]
EBR-1	1075	596	4.491E+04
EBR II-1	745	632	2.767E+06[c]
EBR II-2	753	630	2.767E+06[c]
FET-1	330	199	1.427E+06
FET-2	455	200	5.067E+05
Fire Station well	516	420	1.057E+04
NRF-1	535	363	2.594E+06
NRF-2	529	362	9.368E+06
NRF-3	546	363	9.802E+04
NRF-4	597	363	1.649E+07
Rifle Range well	620	508	9.115E+04
RWMC Production	685	568	4.824E+05
SPERT-1	653	456	3.871E+05
SPERT-2	1217	463	3.450E+05
TRA-01	600	453	3.595E+07
TRA-03	602	456	2.074E+06
TRA-04	965	463	9.006E+07

a. Feet below land surface (ft bls)
b. Annual volume data is the total for wells CPP-1, CPP-2, CPP-4, and CPP-5.
c. Annual volume data is the total for both wells EBR II-1 and EBR II-2.
Note: All wells are withdrawing water from the main body of the Snake River Plain Aquifer and are used as drinking water wells with the exception of wells ANP-08, Fire station well, and NRF-4 which are production wells for facility operations.

2-2 Request:

Provide the following for the instruments gathering the meteorological data (section 2.3.3): (a) site description, including location, elevation of the instrument package, physiographic placement of the site (i.e., situated in a valley, on a flood plain, or on a hill), and type and extent of vegetation at or near the site; (b) types of sensors employed; (c) examples of recording of the sensor output; (d) instrument surveillance records; and (e) data acquisition and reduction methods.

Response

Attachment 2 (*U.S. Department of Commerce, National Oceanic and Atmospheric Administration letter, Kirk L. Clawson to Mr. Joe Carlson, dated November 24, 1997*), provides the requested information

Proposed SAR Rewrite

None

2-3 Request:

Provide in section 2.3.3 of the SAR, a representative sample of the data acquired in the actual on-site meteorological monitoring conducted at the TMI-2 ISFSI.

Response

This information is included in **Attachment 2** (See RAI 2-2 above).

Proposed SAR Rewrite

This information will be included in the next SAR rewrite.

2-4 Request:

Provide the following with respect to analysis approaches, assumptions, and additional supporting information with respect to flood analysis in section 2.4.

(a) Topographic maps showing 1 ft contours at the ICPP.

Response

A topographic map with 1 ft contours is not available. A topographic map showing 2 ft contours is provided as **Attachment 3**.

Proposed SAR Rewrite

Figure 2.6-39 will be replaced with the **Attachment 3** map.

Request:

(b) Explicit steps taken to derive the probable maximum precipitation over the ICPP and the resultant probable maximum flood (PMF).

Response

A probable maximum precipitation (PMP) and PMF on the Big Lost River is discussed in Section 2.4.3. A PMP is unlikely to be centered over the ICPP due to semi-arid climate and location on the Snake River plain.

Proposed SAR Rewrite
The 3rd paragraph of section 2.4.2.3 will be deleted

Request:
(c) Discussion on the assumptions and uncertainties associated with the water level that would result from a PMF at the ICPP.

Response
See response to RAI 2-4(b)

Proposed SAR Rewrite
Same as RAI 2-4(b)

2-5 Request:
Provide the following with respect to groundwater hydrology in section 2.5:

(a) ***Classification of Snake River Aquifer as a sole source aquifer.***

Response
See proposed SAR rewrite.

Proposed SAR Rewrite
The Snake River Plain Aquifer, one of the largest and most productive groundwater resources in the United States, underlies the INEEL. The aquifer is listed as a Class I aquifer and was designated by the EPA as a sole source aquifer in 1991. Groundwater from this aquifer supplies essentially all drinking water consumed within the Eastern Snake River Plain

Request:
(b) A survey of current groundwater users, water usage, pumping rate, and draw downs in the area surrounding the INEEL.

Response
See proposed SAR rewrite.

Proposed SAR Rewrite
Irrigated agriculture provides a significant portion of the economic base for the people of southern Idaho, and the Snake River Plain Aquifer plays a major role in meeting irrigation requirements. The aquifer provides ground water for irrigation of over one third of the three million irrigated acres of the Snake River Plain. It is estimated that over 127,000 people depend on the aquifer for domestic and municipal water needs. Total domestic water consumption is approximately

46,000 ac-ft/yr and ground water discharge from well pumpage equals approximately 1.92 million ac-ft. [Ref. (new)]

Will add the following (new) reference to Section 2.8 SAR: EPA 910/9-90-020, *"EPA Support Document for the EPA Designation of the Eastern Snake River Plain Aquifer as a Sole Source Aquifer"*, August 1990

2-6 <u>**Request:**</u>
Provide the following to improve the quality of some figures in section 2.6.1, and to give sufficient information.

(a) Revise Figure 2.6-12 to make it a larger scale geologic map that is more comprehensible and covers a similar area as the current version of Figure 2.6-12. The figure should include:
(1) surface geology and brief description,
(2) location of major facilities (besides TMI-2, ISFSI),
(3) bedrock outcrops and brief description,
(4) areas of sediment coverage and brief description of the sediments,
(5) locations of cross sections shown in Figures 2.6-14 through 2.6-16, and
(6) a stratigraphic column

<u>**Response**</u>
An enlarged map and explanation have been developed **[Attachment 4]**. It is presented in 11x17 format as a fold-out map. It shows the locations of the ICPP site and other major facilities at INEEL. It also shows the locations of cross sections shown in Figures 2.6-14, -15, and -16. The explanation (legend) describes the geologic units on the map.

<u>**Proposed SAR Rewrite:**</u>
The SAR section will be revised to replace the old Figure 2.6-12 with new Figure **[Attachment 4]**.

<u>**Request:**</u>
(b) A brief description of each layer shown in Figures 2.6.13 through 2.6-16 and the geological engineering significance such as types of rock or sediments, permeability, strength under cyclic loading, seismic wave velocities, and consolidation characteristics. Explain the symbols used to represent the stratigraphic layers (such as BC, DE, E, F, EF, and DEB).

<u>**Response:**</u>
See proposed SAR rewrite below:

<u>**Proposed SAR Rewrite:**</u>

Insert the following text as the last paragraph of section 2.6.1.2.2.2, TMI-2 ISFSI Site, Stratigraphy.

Based on analysis of geophysical logs of wells, examination of drill core from coreholes, chemical analyses of core samples, and radiometric age determinations, twenty-three basalt lava-flow groups have been identified in the first 700 feet beneath ICPP. These flow groups have been "named" with the letter designations shown in Figures 2.6-14 through 2.6-16. Because the detailed stratigraphic work was initiated at the Radioactive Waste Management Complex, about 9 km south of the TMI-2 ISFSI site at ICPP, the "named" groups there have been extended to correlative units beneath the ICPP area. Additional groups have been identified beneath the ICPP area and thus letter designations such as DE-1, DE-2, etc. have been developed. In general, flow group B is the youngest at ICPP and flow group I is the oldest. The age of flow group B is between 100,000 and 200,000 years and the age of flow group I is about 640,000 years.

Correlations based on regional mapping and analysis of well and drill hole data from throughout INEEL provide knowledge of the source areas for some of the flow groups. Many others, however, have unknown source areas and unknown areal distributions because their source vents have been buried by later flows or sediments and the current distribution of drill-holes has not provided sufficient subsurface information to identify all vent locations.

Flow group I erupted from AEC Butte, which lies less than 2 km north of TRA, and covers a large portion of southern INEEL. It has a distinctive chemistry and petrography that allows for easy identification in geophysical logs (gamma logs) and drill core. Flow group F is easily recognized by its paleomagnetic properties because it was emplaced during a short period of reversed magnetic polarity about 565,000 years ago. It probably flowed into the ICPP area from a vent to the southwest, somewhere in the Arco Volcanic Rift Zone.

Basalt lava flow groups make up about 85% of the upper 700 feet of stratigraphy beneath ICPP. The remaining 15% consist of sediment interbeds, which are not named in the cross sections. The surficial sediment ranges in thickness from a few feet to about 80 feet, with the thickest areas lying west of ICPP and south of TRA. Surficial sediment is mostly composed of sandy and silty gravels deposited by the Big Lost River during late Pleistocene time. Sediment interbeds from deeper in the section are composed of both eolian silts and sands, and alluvial sediments.

For more detailed descriptions of the units see Attachment 6 [new figure developed to show detailed stratigraphic column for the TMI-2 ISFSI site in response to comment 2-6 (c)]. A site-specific shear wave velocity profile is provided in that figure, and mechanical properties of the surficial sediment and the uppermost basalt lava flow are given in Table 2.6-16.

<u>Request:</u>

(c) ***Description of the stratigraphic units shown in Figures 2.6-3 and 2.6-11 should provide information to include, but not be limited to:***
   (1) ***age, and***
   (2) ***lithologic and geological engineering characteristics such as types of rock or sediments, permeability, strength under cycle loading, seismic wave velocities, and consolidation characteristics, particularly for new stratigraphic units.***

<u>Response:</u>

A replacement for Figure 2.6-3 has been prepared [**Attachment 5**]. It shows the complete stratigraphic column from Precambrian to Holocene. In addition, a more detailed stratigraphic column of the upper 3 km beneath the TMI-2 ISFSI site has been prepared [**Attachment 6**]. It contains a shear wave velocity profile and radiometric ages for those units for which ages have been determined.

<u>Proposed SAR Rewrite:</u>

Make a note on existing Figure 2.6-3 that refers the reader to **Attachments 5 and 6**. Alternatively, **Attachments 5 and 6** could be inserted into the document to replace Figure 2.6-3.

<u>Request:</u>

(3) ***A structural map showing bedrock surface contours and identifying specific structural features of significance, such as folds, faults, synclines, anticlines, basins, and domes.***

<u>Response:</u>

A map of the TMI-2 ISFSI site and immediate surroundings has been prepared [**Attachment 7**]. It shows locations of 1997 drill holes and contours of depth to bedrock.

<u>Proposed SAR Rewrite:</u>

The following discussion will be inserted into Chapter 2 the SAR during the next rewrite:

Lithologic relationships in numerous drill holes and wells in the ICPP area show no evidence for folding or faulting in the subsurface. Although some basalt lava flows are present in parts of the area and absent in others, it has been demonstrated that they have not been structurally disrupted (Add new Reference "Smith & Hersley, 1997). Their discontinuous distribution is due to pinching out of lavas that flowed into the Big Lost River valley from vents to the southeast and southwest.

The slope of the bedrock surface from a "plateau" of about 25 ft depth in the southeastern part of the TMI-2 ISFSI Site to about 60 ft depth in the northwest part of the TMI-2 ISFSI Site is typical of the rough topography on the upper surfaces of Snake River Plain lava flows. The typical shape of the upper surface of a lava flow is irregular and rugged. High "plateaus" correspond to inflated areas, where the lava beneath the solidified crust remained in place and solidified, freezing in the full thickness of the lava flow. Low areas correspond to basins and pits, where lava has escaped from beneath the solidified crust and allowed the crust to collapse to elevations as much as 30 to 40 feet below the inflated areas. The margins of the pits and craters are commonly marked by concentric fissures developed in the crust as it collapsed because of removal of support from below. None of the TMI-2 ISFSI site drill holes encountered such a fissure.

2-7 <u>Request:</u>
Revise Figure 2.6-9 to provide a comprehensible and good quality site topographic map covering the similar area as the current version of Figure 2.6-9. Include the following:

(a) Systematic elevation contours with finer intervals, which would give a clear picture of various important topographic elements such as the axial ridge of the Eastern Snake River Plain (ESRP), the buttes, sinks, depressions and mounds, and the steepness of slopes.

<u>Response</u>:
A detailed topographic map has been prepared. It is presented in two formats: and 8.5"x11" size **[Attachment 8]** and a 1:100,000-scale map **[Attachment 9]**. It has 5 ft and 40-ft contour intervals (depending on the local relief), it shows the major INEEL facilities, and it shows the locations of drill holes. Also, many of the major topographic and geographic features are labeled, such as the axial ridge of the ESRP, the Big Lost River, the sinks areas, and the major buttes.

<u>Proposed SAR Rewrite:</u>
Figure 2.6-9 will be replaced with Attachment 8.

<u>Request:</u>
(b) Paths of various rivers and their names, including the Snake River (if not located in the map area, should indicate so in the text), including their direction of flow.

<u>Response</u>:
The Big Lost River's path is shown on the topo map **[Attachments 8 and 9]**. Note: The Big Lost River is prevented by the axial ridge of the ESRP from flowing into the Snake River. The Snake River flows to the southwest along the southern margin of the ESRP about 30 km to the southeast of the INEEL.

<u>Proposed SAR Rewrite:</u>
None required. The above note is included in both Attachment 8 and 9.

<u>Request:</u>

(c) ***Characteristics of recent sedimentary deposits (especially those that have engineering significance, i.e., liquefaction potential) such as river deposits, wind deposits, and the deposits of lakes and ponds in closed depressions, especially near the TMI-2 ISFSI site.***

Response:
This is covered in the response to comments 2-6 (b) and 2-14.

Proposed SAR Rewrite:
SAR revision per proposed response to comments 2-6(b) and 2-14

Request:
(d) ***Description of landforms in the vicinity of the TMI-2 ISFSI, such as braided channels and irregular flow lobes of basalt lavas.***

Response:
The ICPP lies just southeast of the channel of the Big Lost River in the south-central part of the INEEL (Figure 2.6-9) **[Attachments 8 and 9]**. In this area, the Big Lost River has a broad low-relief floodplain about 6 km wide that is bounded on the southeast and northwest by outcrops of basalt lava flows (Figure 2.6-12) **[Attachment 4]**. The current channel of the river and the ICPP lie near the middle of the floodplain. The ICPP is constructed on Late Pleistocene alluvial gravels above the Holocene floodplain, which lies to the northwest of the river channel between ICPP and TRA. The Holocene floodplain is characterized by numerous abandoned channels and perhaps braided channels of the Big Lost River. The presently active channel, which is dry most of the time, is incised into the Holocene floodplain deposits by about 1.5-2 meters, and is floored by sands and fine gravels of light tan color. The Pleistocene floodplain deposit on which the ICPP is located shows no evidence in air photographs of recent channels or braids of the river. A subdued meander-scroll topography is present over large areas of the Pleistocene surface, especially to the south and southwest of ICPP. The surface is covered by sagebrush and the meander-scrolls are recognizable mainly from tonal anomalies on air photographs. Based on degree of soil development, the deposits that make up this surface were laid down during periods of high runoff during retreat of the most recent (Pinedale) glaciers, probably in the range of 15,000 to 20,000 years ago (SAR Reference 2.55).

The landforms outside the floodplain are dominated by lava flow surface morphology that has been subdued somewhat by deposition of loess and fine eolian sand in low areas and in the lee of ridges and hills. The lava flow surfaces are characterized by rugged but low-relief topography. Due to deflation of parts of the surface during waning stages of volcanic activity, there are numerous closed basins separated by undeflated ridges. The largest of the basins (up to several 10s of meters across) commonly contain thin playa deposits which cover the basin floors. The ridges are riddled with anastomosing fissures that are roughly parallel to the margins of the collapse basins. Many of the outcrops show columnar jointing that produces a hexagonal or polygonal pattern of fractures on the outcrop surface.

Proposed SAR Rewrite:
Insert the two paragraphs above as the first two paragraphs of the Areal Geology section of section 2.6.1.2.2.2 TMI-2 ISFSI Site.

2-8 Request
Address the following items related to the interbedded basalts and sediments:

(a) Compare the current thickness of the sediments (9 to 18 m at the TMI-2 ISFSI site) with typical thickness of the interbedded sediments and discuss the possibility of future volcanic activity or probability of volcanic activity during the projected operating period of the proposed TMI-2 ISFSI.

Response:
Volcanic activity and volcanic hazards are discussed in SAR Section 2.6.6 (Volcanism). Following is a discussion of sediment thickness distribution.

The thickness of surficial sediment at the TMI-2 ISFSI (25->50 feet) is greater than that of most interbeds in the vadose zone beneath the site. The interbeds in the vadose zone (down to about 400 feet) average about 8.6 ft (2.6 m) in thickness and range from 3 ft (1m) to 15 ft (4.7m). Greater interbed thicknesses occur at greater depth in the sequence **[Attachment 6]**. At depths of about 500 m (1600 ft) and greater, several interbeds of thickness 30 to 100 ft (10 to 30 m) occur, and the average interbed thickness from 500 m to the base of the basalt-sediment sequence is about 28 ft (8.4m). On an INEEL-wide basis, sediment interbed thickness distributions with depth are similar to that beneath the TMI-2 ISFSI site. For all INEEL wells and drill holes the thickness of interbeds tends to be smaller at depths less than 1000 feet (mean =17 ft; median = 9 ft) than at depths greater than 1000 feet (mean = 38 ft; median = 25 ft). In addition, the thickness of interbeds tends to be greater in the northern part of INEEL (median ~ 16 ft) than in the southern and southeastern parts (median ~ 7 ft).

Although the surficial sediment at the TMI-2 ISFSI site is composed of alluvial gravels, the composition of sediments in most interbeds directly beneath the TMI-2 ISFSI site ranges from silty sand to clayey silt, probably of mostly alluvial and eolian origin. Some of the deeper, thicker interbeds contain significant alluvial materials, including sands and gravels and, at the northern end of the ICPP near the course of the Big Lost river, some of the interbeds within the vadose zone contain sands and gravels.

Proposed SAR Rewrite:
Insert the two paragraphs above as the last two paragraphs of the Stratigraphy ~~section of~~ section 2.6.1.2.2.2 TMI-2 ISFSI Site. They should follow the insertion suggested for 2-6 (b).

Request:

(b) Provide a site-specific Late Tertiary to Quaternary stratigraphic column at the TMI-2 ISFSI site, clearly indicating the interbedded characteristics, thickness of layers and their physical and engineering characteristics, mineral composition, origin, and degree (some kind of quantitative measure) of consolidation.

Response:

A detailed stratigraphic column is presented for the TMI-2 ISFSI site **[Attachment 6]**. Physical and engineering characteristics of surficial sediments are given in Table 2.6-16. Knowledge of the engineering characteristics of interbeds is very sketchy, due to their lack of importance to the foundation design of facilities. They typically occur at depths much greater than the bottoms of foundations, they are unsaturated to depths of several hundred feet, and their thicknesses are so small that there is great difficulty in obtaining in-situ properties and in obtaining samples for laboratory analysis.

At the New Production Reactor (NPR) site, which lies about 2.5 miles to the east of the TMI-2 ISFSI site, geotechnical analyses of several interbeds in the depth range of 70 to 300 feet have been done (Golder Associates, 1991, Geotechnical Soils Testing Laboratory Results for the New Production Reactor; EGG-NPR-10688) **[Attachment 10]**. In addition, cross hole seismic surveys have been done there to measure compression wave and shear wave velocities of basalts and interbeds to a depth of about 300 feet (Weston Geophysical Corporation, 1991, Geophysical Investigation, New Production Reactor Complex, Idaho National Engineering Laboratory; EGG-NPR-10689). The NPR site is farther from the Big Lost River than the TMI-2 ISFSI site, and thus likely to have a greater proportion of eolian silty sedimentary interbeds than at the TMI-2 ISFSI site. Nevertheless, this is the only geotechnical information that exists for interbeds in the ICPP area and it is presented for completeness.

The geotechnical data is summarized in **Attachment 10**, and shows that, in contrast to ICPP surficial sediments, the materials at the NPR Site are mostly sand and clay/silt instead of gravels. The cross-hole seismic surveys show interbed shear wave velocity at about 200 feet depth is about 300 m/sec, and compression-wave velocity is about 460 m/sec.

Proposed SAR Rewrite:

The 3 paragraphs above will be inserted after all other insertions into the Stratigraphy section of section 2.6.1.2.2.2 TMI-2 ISFSI Site.

2-9 Request:

Provide the following with respect to section 2.6.2:

(a) *Revise Figure 2.6-17 to clearly mark the pertinent geographical features that are referred to in the text in describing fault geometry, for example state border lines, names such as Great Rift, Intermountain Seismic Belt, Centennial Tectonic Belt, Hebgen Lake, etc. Include all of the important faults and their names.*

(b) *Provide a clear fault map identifying all capable faults listed in section 2.6.2.3.2 and section 2.6.3.5. Include in Figures 2.6-10, 2.6-17, 2.6-19, 2.6.24, and 2.6-25 the names of the faults and their segments, and names of geographical locations (places) referred to in the text in describing the fault geometry. Specifically identify the Pass Creek and Arco segments of the Lost River fault, the Blue Dome and Nicholia segments of the Beaverhead fault, and places such as Caribou Range, Snake River Range, and Rexburg.*

(c) *Revise Figure 2.6-10 to develop a map similar to the fault map for the volcanic rift zones (VRZ) with the TMI-2 ISFSI site location indicated. Specifically, show the VZR for the Great Rift, the Arco, and the Lava Ridge-Hells Half Acre. Alternatively, Figure 2.6-41 should be used or referred to in section 2.6.2.3.3.*

Response:
A new map has been developed showing all important faults, fault segments, volcanic rift zones, seismically active zones, and major historic earthquakes to replace Figures 2.6-10, 2.6-17, 2.6-19, 2.6-25, and 2.6-25 **[Attachment 11]**. In addition, two maps showing all earthquake epicenters from 1850 to 1995 have been prepared. One is plotted on regional shaded relief topography with faults **[Attachment 12]**, and the other is plotted on a state outline map with faults **[Attachment 13]**. A fourth map showing the seismic source zones has been developed **[Attachment 14]**. Also, a fifth map, showing the INEEL seismic network stations and earthquakes within 100 miles of the INEEL has been developed **[Attachment 15]**.

Proposed SAR Rewrite:
The maps will be included in the next SAR rewrite.

Request:
(d) *Revise Figure 2.6-32 in an appropriate scale to show all of the seismic sources, including both area and fault sources and the location of the TMI-2 ISFSI site. Consider eliminating earthquake epicenter locations in this figure to make it clearer.*

Response:
See **Attachment 14**.

Proposed SAR Rewrite:
Attachment 14 will be added in the next SAR rewrite

<u>Request:</u>
(e) Clarify whether or not the "radial distance" in table 2.6-4 is from the earthquake epicenter to the proposed TMI-2 ISFSI site.

<u>Response</u>:
Radial distance in this table is not from the TMI-2 ISFSI site, but instead from the geographic center of the INEEL, at Latitude 43° 42'N and Longitude 112° 48'W.

<u>Proposed SAR Rewrite:</u>
Will indicate the location of the radial distance origin as described above.

<u>Request:</u>
(f) Indicate the units for ground acceleration, velocity, and displacement in table 2.6-5.

<u>Response</u>:
Ground acceleration (g, % of acceleration due to gravity), velocity (cm/sec), and displacement (cm).

<u>Proposed SAR Rewrite:</u>
The units will be included in the next SAR rewrite.

<u>Request:</u>
(g) Provide a well drawn figure showing the epicenters of all the earthquake listed in table 2.6-7 and associated structures with the names clearly indicated.

<u>Response</u>
See new figures presented in **Attachments 11, 12, and 13,** and the proposed rewrite of section 2.6.2.2.2 (**Attachment 22** showing underline/strikeout changes) which is consistent with the new figures.

<u>Proposed SAR Rewrite:</u>
Attachments 11, 12 and 13 will be included in the next SAR update.

<u>Request:</u>
(h) Revise Figures 2.6-28 through 2.6-31 to make earthquake intensity contour maps readable and to locate the proposed TMI-2 ISFSI site.

<u>Response</u>
Six new isoseismal maps are supplied, all plotted on a state outline map of the western U.S. with major cities and the ICPP site located. They are the 1905 Shoshone earthquake **[Attachment 16]**, the 1983 Borah Peak earthquake **[Attachment 17]**, the 1975 Pocatello Valley earthquake **[Attachment 18]**, the 1959 Hebgen Lake earthquake **[Attachment 19]**, the 1975 Yellowstone National

Park earthquake **[Attachment 20]**, and the 1994 Draney Peak earthquake **[Attachment 21]**.

Proposed SAR Rewrite
These maps will be included in the next SAR update.

2-10 Request:
Discuss in section 2.6.2.2, the effects of historical earthquakes on the proposed site. Provide more information with regard to the actual or interpreted effects of moderate-to-large earthquakes (those listed in tables 2.6-4 and 2.6-7) on the proposed TMI-2 ISFSI site. Estimate ground acceleration (and/or Modified Mercalli Intensity) at the TMI-2 ISFSI site associated with these earthquakes based on empirical or stochastic ground motion attenuation relations or simply according to earthquake intensity maps obtained through historical records.

Response:
The information has been added to the proposed SAR rewrite below.

Proposed SAR Rewrite:
See **Attachment 22** for proposed SAR rewrite of sections 2.6.2.2.2 and 2.6.2.2.3 (showing underline/strikeouts).

2-11 Request:
Eliminate inconsistent discussions of fault activities given in sections 2.6.2.3.2 and 2.6.2.3.5 address the following items:

(a) The maximum earthquake magnitude for the southern Lemhi fault. and the closest distance from the southern termination of Lemhi fault to the TMI-2 ISFSI.
(b) The maximum earthquake magnitude along the Lost River fault.
(c) The closest distance from the Beaverhead fault to the TMI-2 ISFSI site.
(d) The faulting mechanism of the northwest boundary of the ESRP.

Response
See proposed SAR rewrite below

Proposed SAR Rewrite:
See **Attachment 22** for proposed SAR rewrite of sections 2.6.2.3.2, 2.6.2.3.5, and Table 2.6-7 (showing underline/strikeouts).

2-12 Request:
Eliminate inconsistent information about the ESRP Volcanic Zones given in sections 2.6.2.3.3 and 2.6.2.3.5 and other background provinces (such as the ESRP, Northern Basin, Range, Idaho Batholith, and Yellowstone Plateau).

Response:
See proposed SAR rewrite below

Proposed SAR Rewrite:
See **Attachment 22** for proposed rewrite of Sections 2.6.2.3.3 and 2.6.2.3.5 (with underline/strikeout).

2-13 Request:
Present major findings and provide design bases and associated justifications for the deterministic and probabilistic seismic hazard analyses discussed in the SAR.

(a) ***Present specific results in section 2.6.2.3.7.1.1. such as peak ground accelerations, for the ICPP site based on the 1990 deterministic study.***
(b) ***Give more detailed information on the current deterministic seismic hazard evaluation at the ISFSI site, including selections and associated justifications for the maximum credible earthquake, minimum source-to-site distance, and ground motion attenuation relations. Provide a brief discussion on how this most up-to-date deterministic seismic hazard evaluation differs from previous similar evaluations.***
(c) ***Justify that the 0.36-g design value is satisfactory for the facility under consideration taking into account the latest deterministic and probabilistic seismic hazard values and applicable NRC regulatory requirements and regulatory guides.***

Response:
The information is presented in the proposed SAR rewrite.

Proposed SAR Rewrite:
Replace section 2.6.2.3.7, Table 2.6-11, and Table 2.6-12 of the SAR with a complete new write-up as shown in **Attachment 22**. The changes are too numerous to show using the underline/strikeout method.

2-14 Request:
Provide an interpretation of the soil properties (sediments) and bedrock at the ICPP presented in table 2.6-16. Provide an explanation of how the results from various measurements relate to safety concerns and how they are used in the design to assure safety. Provide an analysis of the stability of the foundations, based on the design ground motion from the design earthquake using appropriate response spectrs and calculate a safety factor.

Response: (Part 1) – Explanation for parameters listed in Table 2.6-16

Discussion of soil property parameters at ICPP and the TMI-2 ISFSI site:

Dry density is the weight of solids per cubic foot of soil. It is determined by weighing the soil after drying in an oven to remove moisture. Also called unit weight, reported in lbs/square ft. It is used in development of many of the other parameters of soil, including dynamic damping, and helps to evaluate the potential for liquefaction. Values for ICPP soils are typical of those for sandy gravels worldwide.

Relative density is a measure of the soil density at a particular site with respect to the possible range of densities for that particular soil type. It is a measure of how densely or compactly the particles are packed together. Relative density is calculated by a ratio of dry densities (density in densest state times density of sample minus density in loosest state divided by density of sample times difference between density in densest state and the density in loosest state) and usually reported in percent (meaning percent of density in densest state). The relative densities reported for soils at ICPP are mostly in the range of 40 to 100%, corresponding to dense to very dense sands, and thus have a low potential for further compaction and for liquefaction.

Moisture content is the weight of water per unit weight of solids. It is useful for establishing requirements for compaction, if compaction is required. It influences the potential for liquefaction. Since the moisture contents of gravels and sands from the TMI-2 ISFSI site is so low, generally less than 20%, reflecting the unsaturated condition of the soils, there is very little potential for either liquefaction or for consolidation (see description of consolidation below).

Porosity is the fraction or percentage of bulk volume that is not occupied by solids, or, in other words the fraction or percentage of bulk volume occupied by voids or pores. It is a general indicator of the potential of the soil for further compaction, an obviously closely related to density and relative density. Porosities reported for ICPP soils are 30 to 40% and are slightly lower than porosities for most graded gravels and sands composed of rounded grains (36-46%). Again, this suggests a relatively low potential for further reduction in pore volume by compaction or settling.

Strength characteristics are parameters that describe the resistance to shear. They are "C", which is cohesion or interparticle attraction, and ϕ, which is the angle of internal friction or the resistance to interparticle slip. The sandy gravels at ICPP have "C" values of 0, indicating that they are cohesionless. The angle of internal friction for ICPP sandy gravels ranges from 35° to 45° and corresponds to values for dense sands. This indicates a relatively high resistance to interparticle slip. Natural cohesionless materials (sand and gravels) range from <30° for very loose sands to >45° for very dense sands.

Vp is the velocity at which seismic compression waves travel through the material, often referred to as P-wave velocity. Used for seismic hazards assessments. The values reported for ICPP and for the TMI-2 ISFSI site (400 to 1000 m/sec) are typical of values for gravels and sands worldwide.

Vs is the velocity at which seismic shear waves travel through the material, often referred to as S-wave velocity or shear velocity. It is an important input parameter for the stochastic ground motion model used for seismic hazards assessment at ICPP and the TMI-2 ISFSI site. Also, it is very important in estimation of the amplification of ground motion by the upper layer of soil at the site. It is also useful for evaluation of liquefaction potential (see section on Liquefaction Potential, below). Reported Vs for ICPP and the TMI-2 ISFSI site range from about 230 to 600 m/sec and are typical of values for stiff soils and cohesionless sands and gravels worldwide.

Damping is a measure of the vibrational energy absorbing characteristic of the soil. It is used in seismic design of foundations and structures. Although some tests have been done on sieved and reconstituted samples from ICPP, little confidence is given to the results. Since it is not possible to obtain undisturbed samples at ICPP for lab tests, Dames and Moore (1976) recommend using the average of measured damping values for sand (from Seed and Idriss, 1970).

Shear Modulus (G') is the ratio of shear stress to shear strain. It is used to estimate the foundation frequency and displacement amplitudes during seismic ground shaking. For earthquake ground motion estimations it is usually measured in the lab using undisturbed samples from the soils at the site. It can be measured in the lab using either cyclic loading or resonant column apparatii. Because undisturbed samples of the coarse sandy gravels at ICPP and the TMI-2 ISFSI site cannot be obtained, the values reported have been measured in the lab using sieved and reconstituted samples from ICPP soils or estimated using empirical equations. It can also be estimated by multiplying the soil density by the shear wave velocity squared.

Poisson's Ratio is the ratio of transverse to axial strain. It describes the amount of lateral bulging that accompanies axial compression in rock or soil samples. It is an input parameter for calculation of soil spring constant (i.e., modulus of subgrade reaction), of the dynamic shear modulus, and also allows estimation of Vs from measured Vp. Most natural soils and rocks have values between 0 and 0.5. Values measured at ICPP range from 0.27 to 0.45. Most sands worldwide have values from 0.3 to 0.35, so the alluvial soils at ICPP are fairly typical.

Static modulus of elasticity (E) is the ratio of stress increment to the strain that it produces. It is essentially the slope of the stress-strain curve for elastic or nearly elastic materials, and is often not constant throughout the range of possible stresses. It also varies with load, as seen in Table 2.6-16.

Bulk Modulus (K) describes the rate of density change with change in confining pressure. It is used in the determination of the amount of settlement that will occur beneath a structure. It is closely related to the static modulus of elasticity, and Table 2.6-16 reports similar values for these two parameters.

Consolidation characteristics consist of Cv, the coefficient of consolidation, and Cc, the compression index. They provide a measure of the time dependent volume change due to an applied load in saturated soils. In saturated conditions the applied load is commonly supported initially by pore pressure, and over time the pore fluid is forced from the voids and the load is gradually transferred to the soil framework (grains). Consolidation is defined as the time-dependent volume reduction accompanying this transfer of the load. For unsaturated, cohesionless, granular soils (as those at the TMI-2 ISFSI site) the transfer of load to the soil framework is immediate and there is very little time dependent behavior. This is illustrated by the very low Cv and Cc values reported for ICPP soils. The term consolidation may not be applicable to unsaturated granular soils, and some geotechnical engineers prefer to use the term settlement.

<u>Proposed SAR Rewrite:</u>
The soil properties will be added to next revision of the SAR

<u>Response 2-14 (Part 2) *Provide an analysis of foundation stability and calculate a safety factor.*</u>

Safety factors for seismic events are provided in section 8.2.3, Earthquake Accident Analysis. A general discussion of foundation stability is provided in the following paragraphs.

All of the geotechnical data for soils at the ICPP and TMI-2 ISFSI site show that the site will be stable with respect to landsliding, slumping, and liquefaction during earthquake ground shaking. Although most of the data provided in Table 2.6-16 represents samples from outside the TMI-2 ISFSI site, it is generally applicable to the TMI-2 ISFSI site because the soils encountered in the subsurface throughout the ICPP site are virtually identical. There are minor variations in relative percentages of gravel, sand, and silt, and most places exhibit crude stratification of sand-rich and sand-poor layers, but the stratigraphy is remarkably uniform throughout the ICPP area. Specific indicators of soil stability include very gentle surface gradient, unsaturated conditions, low water contents of the soils, high blow counts in standard penetration tests, high shear wave velocity, large grain size. Following is a discussion of each of these factors.

There is no potential for landsliding or slumping because the topography of the site is essentially flat **[Attachment 3]**. Maximum surface gradients are in the range of 10 feet per mile.

The surface soils are over 400 feet above the water table and have water contents of 20% or less. It is possible that saturated conditions could exist locally and temporarily due to flooding or to the proximity to percolation ponds. However, no saturation of surficial sediments has been observed at or near the TMI-2 ISFSI site during the history of operations at ICPP. The percolation ponds are located at the far south end of ICPP and do not have influence on the surficial sediment conditions at the TMI-2 ISFSI site. Temporary saturation of sediments has been observed in the vicinity of the Big Lost River at the far north end of the ICPP during times when the river flows through the area, but the TMI-2 ISFSI site is so far from the river's course that it has never been affected. Even if an exceptionally large flood caused temporary saturation of the soils at the TMI-2 ISFSI site, other factors (discussed below) would still prevent the occurrence of liquefaction or subsidence during potential seismic events.

During drilling of several boreholes in and around the TMI-2 ISFSI site in the fall of 1997, standard penetration tests (SPT) were performed at intervals during the drilling. The ranges observed for the TMI-2 ISFSI site are plotted in **Attachment 23** showing SPT (N)-Blows per foot vs. cyclic stress ratio (from Seed et al., 1983). The range of values in which liquefaction is possible is 4 - 35, and increases with increasing cyclic stress ratio. Although we do not know the cyclic stress ratio of ICPP and TMI-2 ISFSI soils, the figure shows that all but one or two tests have over 35 blows per foot, ranging up to 178 for depths of about 5 feet and to 224 for depths of about 20 feet. In fact, for depths of about 20 feet the lowest blows per foot is about 70, twice the number below which liquefaction is possible.

Shear wave velocity is another parameter which can help evaluate the potential for liquefaction. Shear wave velocities were determined in 7 boreholes in and around the TMI-2 ISFSI site in the fall of 1997. The ranges of values measured are plotted in **Attachment 23** showing cyclic stress ratio verses shear wave velocity (from Kayen, 1992 and Seed et al., 1983). Only one borehole (#5) has velocities low enough at a depth of about 5 feet to encroach on the liquefaction field, but the large grain size at that spot (57% gravel) precludes development of excess pore pressure and liquefaction will not occur.

The potential for liquefaction is also influenced by the grain size of the soil. Particle size distributions for samples from the boreholes ~~at~~ the TMI-2 ISFSI site **[Attachment 23]** show that the material consists of 48 to 68% gravel, the rest being made up of sand and silt. Soils in which liquefaction has been observed to occur are typically uniform, saturated sands. Gravels such as those at the TMI-2 ISFSI site have not been known to liquefy because the pore size is so large (due to the gravel-sized particles) that excess pore pressure cannot be maintained.

Geotechnical data supporting the discussion above are contained in **Attachment 23**. This Attachment includes a table of shear wave velocities, a table of Standard Penetration Test blow counts, graphic plots of seismic velocity profiles of boreholes, plots of blow counts and shear wave velocities vs. cyclic stress ratio, particle size distribution plots, and a graphic log for each of 13 boreholes drilled at and near the TMI-2 ISFSI site in the fall of 1997.

Proposed SAR Rewrite:

The information will be included in the next SAR rewrite.

2-15 Request:

Provide the locations, ages, and volumes of basaltic volcanoes in the Arco VRZ and Axial volcanic zone to evaluate possible spatial and temporal inhomogeneities in basaltic volcano formation. These data are summarized in table 2.6-15 and referenced as "table 3" in Figure 2.6-41.

Response:

Maps showing the locations of volcanic vents, locations and ages of samples for which ages have been determined, and volumes of lava fields for which volumes have been calculated are included **[Attachment 24]**. The volcanic vent map is an 8.5x11 inch map with volcanic vents plotted on topography. The map which shows the locations and ages of radiometrically dated samples is the Kuntz et al., 1994, Geologic map of the INEL and adjoining areas; US Geological Survey Map I-2330, 1:100,000 scale. The volumes of lava fields are written in red ink on a copy of the geologic map of INEEL presented in Attachment 4. Volumes of lava fields range from 0.01 km^3 to 6 km^3. The Hells Half Acre lava field and the Wapi lava field are among the largest on the Snake River Plain, with volumes of about 6 km^3. Estimates of volume have been made only for Holocene (Qba) lava fields (SAR Reference 2.45).

Note: As noted in the December 10, 1997 meeting with the NRC, LMITCO indicated we had only one copy of Map I-2330. This copy would be included in NRC's Document Control Center Package. Additional copies of the map can be obtained through:

U.S. Geological Survey Map Distribution
Box 25286, Federal Center, Denver, DO 80225

Proposed SAR Rewrite:

The map will be added to the SAR in the next rewrite.

2-16 <u>Request</u>:
Provide individual measurement of lava-flow length and area, which are summarized in section 2.6.6.2.3.3.

<u>Response:</u>
A table showing individual measurements of lava flow length and area for all those lava flows that occur within the boundaries of the Geologic Map of the INEL and Adjoining Areas (USGS Map I-2330) is included **[Attachment 25]**.

<u>Proposed SAR Rewrite:</u>
None

CHAPTER 3: PRINCIPAL DESIGN CRITERIA

3-1 Request:

Provide a summary of estimates of the amount of ^{235}U, total U; $^{239}Pu + ^{241}Pu$, and total Pu in each canister and an evaluation of the uncertainties in the estimates that are provided in various referenced documents such as Lassahn (1993). Provide a summary of the calculations made using the ORIGEN-II code to estimate the activation products, actinides, and fission products inventories resulting from irradiation at TMI-2 that have been referenced in an SAR for the NUPAC 125-B Fuel Shipping Cask (Nuclear Packaging, 1991) but no direct reference or the original document has been made in the TMI-2 SAR.

Response (Part 1):

Attachment 26, "Summary of TMI-2 Canister Weights, Uncertainties, and Methodology Used to Determine Uncertainties" contains a summary of the Lassahn database on canister contents "Uranium and Plutonium Contents of TMI-2 Defueling Canisters" Lassahn (1993). The attachment contains the canister inventory results, uncertainties associated with the inventory data, and the methodology used to obtain the uncertainties.

Response (Part 2):

Attachment 27, "TMI-2 Isotopic Inventory Calculations" is a report documenting the most recent ORIGEN-II analysis for the TMI-2 reactor core. These results are based on the power history documented in LASL report "TMI-2 Decay Power: LASL Fission Product and Actinide Decay Power Calculations for the President's Commission on the Accident at Three Mile Island," LA-8041-MS, March 1980.

Attachment 28 is a letter report that shows comparisons between measured and calculated fission product inventory data for TMI-2. This evaluation was performed because ORIGEN-II does not accurately model fission product production early in reactor core life.

Proposed SAR Rewrite:

None

3-2 Request:

Provide consistent information regarding the average decay heat power per canister given in tables 1.2-1 and 3.1-1 that exhibit values of 15 and 29 W. respectively. (The latter figure is in agreement with the text of the report). Provide results of the analyses of vented samples of the gases generated during storage at Test Area North (TAN).

Response (Part 1):

Table 1.2-1 lists the calculated average decay heat power for all canisters whereas Table 3.1-1 contains the bounding value to be used for calculation purposes. This value was obtained by multiplying the average canister decay heat by the ratio of 1.879 to obtain the average canister decay heat for the peak core power.

A footnote will be added to Table 3.1-1 that distinguishes this value from that reported in Table 1.2-1.

Proposed SAR Rewrite:
Table 3.1-1 will be revised to add the following footnote:

29 watts/canister was obtained by multiplying the average canister decay heat of 15 watts/canister by the hot channel peaking factor of 1.879.

Response: (Part 2)
No analyses have been performed to date of vented gas samples. **Attachment 29**, "Test Plan Summary for Measuring Gases and Particulate Vented from the TMI-2 Canisters", is a draft plan for analyzing canister releases during the following periods:
1) Prior to canister dewatering/movement of the core material from TAN to ICPP,
2) During the dewatering and drying process, and
3) During dry storage at ICPP. Specific radionuclides to be addressed are measurable particulates (^{137}Cs, ^{90}Sr, etc.), ^{129}I, ^{85}Kr and ^{3}H.

In addition, measurements of radiolytic hydrogen will be performed. Results of each phase of the test program will be submitted to NRC when completed. The phase 1 measurements will be completed by 9/30/98. Phase 2 measurements will be obtained periodically during the TMI-2 canister dewatering/drying campaign. The Phase 3 measurements will be performed after the canisters are placed into dry storage at the TMI-2 ISFSI.

Proposed SAR Rewrite:
None – information only – not required as input to the SAR.

3-3 Request:
Provide information regarding any potential degradation of the Boral that may have occurred in the TAN pool. Present an evaluation of the current condition of the mixture of low-density concrete, glass bubbles, and water (Babcock and Wilcox, 1986) emplaced in the space between the shroud and the canister shell and the potential effect on the integrity of the stainless steel shroud that may be affected by crevice corrosion or other degradation processes.

Response:
There is no information on the condition of the boral in the TAN pool and the extent of possible corrosion; however, evaluations that have been performed indicate that crevice corrosion of the stainless steel covering the boral should be insignificant and no damage to the boral is expected. Water samples removed

from several TMI-2 canisters have been evaluated to assess elemental content and the effect on the stainless steel liner. As indicated in **Attachment 30,** "Summary of Information on the Response of TMI-2 Canisters to Chemical Corrosion", the concentrations of corrosive ions (e.g., chloride) is quite low in the canister water samples analyzed. Chloride concentrations measured are 10^{-4} to 10^{-5} M and are considerable less than the 2 x 10^{-3} M that would be expected to be of concern per discussions with Southwest Research Institute during the December meeting in San Antonio. No chloride corrosion would be expected on the surface of the canister exposed to the fuel debris and pool water.

In addition, analyses were performed to assess corrosion of the stainless steel covered boral exposed to the light concrete (LICON). In this analysis to assess the potential for crevice corrosion, analyses of the LICON were performed to determine the chloride concentration in the LICON and to assess the quantity that might be leachable. These analyses indicated (as shown in attachment 30) that the measured chloride content of the LICON is ≤ 26 micrograms per gram of LICON and would not be expected to result in any significant corrosion.

Proposed SAR Rewrite:
None

3-4 **Request**:
Provide information regarding the possibility of pyrophoric conditions that may be introduced due to complete dryness of very fine particles of fuel if zirconium from the fuel cladding has not been completely oxidized to zirconia.

Response:
No pyrophoricity of the TMI-2 fuel debris is expected base on studies performed to assess pyrophoricity of the fuel debris. See **Attachment 31,** "Summary of Studies Performed to Address the Pyrophoricity of TMI-2 Fuel Debris"

Proposed SAR Rewrite:
None

3-5 **Request:**
Provide an explanation in table 3.1-3 as to why a specific power of 27.14 MW/MTU (i.e., core average) was assumed as opposed to a peak core specific power that is a factor 1.879 times greater (50.99 MW/MTU) than what was assumed in Chapter 7 for calculating radionclide inventories.

Response:
The number in the table is a "typo". The correct number is 50.99 MW/MTU.

Proposed SAR Rewrite:
Will add a note to Table 3.1-3 of the SAR which states, "This specific power is consistent with the average TMI-2 core burnup. The above listed source terms

were calculated using this specific power multiplied by a hot channel peaking factor of 1.879 as discussed in Chapter 7 (page 7.2-1) of this SAR.

3-6 Request:

Provide correct references to fuel particle sizes in the filter canisters as discussed on page 3.3-7, section B, line 10.

Response:

The correct reference is "TMI-2 Defueling Canisters Final Design Technical Report" (SAR reference 3.4) Section C, Table 1.

Proposed SAR Rewrite:

The correct reference will be made in the next SAR revision.

3-7 Request:

Provide further justification for the assumption that the fuel is at a density of 10 g/cm^3 as discussed on page 3.3-9, paragraph 4, lines 11-14.

Response:

The density of the fuel pellets in the TMI-2 core is provided in "TMI-2 Accident Core Heat-Up Analysis, NSAC-25, Nuclear Associates International and Energy Incorporated, June 1981." **Attachment 32** contains specific (pertinent) information from this report

Proposed SAR Rewrite:

NSAC 25 will be added as a reference in the next SAR rewrite.

3-8 *Request:*

Provide clarification on the classification of the entire dry shielded canister (DSC) on page 3.4-1.

Response:

The classification of each individual part is provided in the Safety Analysis Report Drawings included in Appendix A. The Parts list on the drawings has a column titled "Quality Category". Parts are listed as NITS ("not important to safety") or Category A ("important to safety"). Also it should be noted that, in response to discussion of this RAI Item 3-8 in San Antonio, December 10, 1998, Table 3.4-1 will be revised to clarify the classifications in the table for consistency, relative to classification of entire components versus subcomponents. The Dry Shielded Canister (DSC) has subcomponents which are important to safety as well as subcomponents which are not important to safety; therefore, the classification is provided in the table by subcomponent breakdown. For consistency, the classification of the Horizontal Storage Module (HSM) in Table 3.4-1 will be modified to show safety classification by subcomponent only.

Proposed SAR Rewrite:

Table 3.4-1 will be revised as noted in above response in the next SAR revision.

3-9 Request:
Provide a discussion on the potential for soil liquefaction during a seismic event and the net effect on the systems to perform their intended safety functions.

Response:
See response to RAI 2-14, part 2.

Proposed SAR Rewrite:
The information in response to RAI 2-14, part 2 will be included in the next SAR rewrite.

3-10 Request:
Provide greater detail in section 3.1.2 of the specific issues of sealing and venting the DSC.

Response:
The DSC is sealed to ensure that any flow of gases in or out of the DSC, during storage, is through a HEPA filter. This is accomplished by welding the closure plates in place and leak testing the welds. The inner cover is welded and inspected to the same criteria as the outer cover plate. The plates are welded to the shell and seal welded together at the purge and vent ports to provide redundant closures. Both the purge and vent ports are covered with vent housings that are sealed to the outer cover plate with dual metallic seals. During leak testing and transfer/transport activities the filters are closed by installing cover plates which are sealed to the vent housings with dual metallic seals. Acceptance leak testing is done with the DSC inside the cask by pulling a vacuum in the DSC, back filling with helium, sealing the cask, then pulling a vacuum in the annulus between the cask and the DSC with the discharge routed through a helium leak detector. When the DSC is placed in the HSM the test/transport covers are removed to allow the DSC to vent to atmosphere, thereby, removing radiolytically generated hydrogen from any residual moisture contained inside the DSC.

The filters are screwed into the filter housing using an elastomeric gasket under the flange of the filters. Filters are sintered carbon encased in stainless steel bodies originally developed for long term hydrogen gas venting of radiological waste containers. There are four, two-inch diameter filters located in the vent cover housing and one, two inch diameter filter located in the purge port vent cover housing. The vent port accesses the DSC in the headspace immediately above the top of the TMI canisters. This allows for direct removal of any gases emitted by the canisters. The purge port connects to a mechanical tube that goes to the bottom of the DSC to allow for gas circulation in the system. This also allows for complete purging of the DSC.if, as discussed in section 4.3, any abnormally high gas build-ups are noted. Both the purge port filter and vent port filter housings ports that allow for sampling of gases within the DSC.

Additionally, the test/transport covers can be installed over the filters to allow equalization of gases within the DSC so representative gas samples can be obtained. The filter housings also have leak test ports for remotely testing the filter housing to DSC seals. The vent and purge ports can be accessed through the rear of the HSM during DSC storage. The HSM filter access holes exit the HSM rear wall through a vented steel door.

Proposed SAR Rewrite:
The additional information will be added during the next SAR rewrite.

3-11 Request:
Provide acceptance criteria in section 3.1.2.1 for equipment design and testing.

Response:
All equipment will be functionally tested, including load tests as appropriate, to demonstrate that each item meets its operational requirements. The cask and DSC are designed, tested and documented as Safety Related equipment to ensure that they will meet all design conditions. The non-safety related support equipment is designed and built to meet commercial codes and standards and functionally tested. This equipment is not required to meet accident-related criteria as its failure can't result in an unanalyzed safety condition. For example the lifting yoke will be load tested to ANSI 14.6 and dimensionally checked by fit up to the MP-187 trunnions, the trailer will be load tested, the hydraulic ram and the skid positioning systems will be functionally tested to the design limits of the systems. Following the individual functional and load tests, a dry runs(s) will be performed for the complete transportation and transfer parts of the system using dummy DSC loads simulating the TMI-2 fuel debris canisters. This test(s) will ensure that all parts of the system meet their functional requirements and correctly interface with the other components.

Proposed SAR Rewrite:
This information will be added during the next SAR rewrite.

3-14 Request:
Provide details on the procedure used to develop the max/min pressure coefficients in table 3.2-2 on page 3.2-11.

Response:
Max/min pressure coefficients in Table 3.2-2 of Revision 0 are incorrect. Table 3.2-2 is revised as shown below. Also note an error on page 3.2-2, at mid-page as stated "...in Figure 2 and Table 8.4 of ANSI A58.1-1982.", revise Table 8.4 to read Table 8. The next revision to the SAR will incorporate these changes.

Table 3.2-2
Design Pressures for Tornado Wind Loading

Wall ① Orientation	Velocity Pressure (psf)	Gust Response Factor	Max/Min Pressure Coefficient	Max/Min ② Design Pressure (psf)
North	94	1.32	+0.80	99
East	94	1.32	-0.70	-87
South	94	1.32	-0.50	-62
West	94	1.32	-0.70	-87
Roof	94	1.32	-0.70	-87

Notes:

1. Wind direction assumed to be from North. Wind loads for other directions may be found by rotating table values to desired wind direction. For example, if the wind was from the east, the design pressure would be 99 psf on the east wall, -62 psf on the west wall, and -87 psf on the roof, north, and south walls.
2. Negative values indicate suction pressure.

Proposed SAR Rewrite:
The above changes will be made at the next SAR rewrite.

3-15 Request:
Provide in section 3.2.3.2 (page 3.2-4) sufficient details to determine the nature of these frequencies and how they will affect design. Some details are given in Chapter 8, but these are not sufficient. Provide specific details on what these modes are and how they were calculated. Describe the modeling in sufficient detail. For example, the roof of the HSM is attached to the walls but there is no real restraint between the vertical wall and the roof other than the vertical displacement.

Response:
A description of the model of the HSM and the DSC support structure developed to evaluate the frequencies provided in Section 3.2.3.2, the model boundary conditions and coupling of the roof structure to the base unit is provided in **Attachment 33.**

Proposed SAR Rewrite:
None

CHAPTER 4: INSTALLATION DESIGN

4-1 Request:

Provide the following information, necessary for the evaluation of the acceptability of the DSC closure welds and DSC coating:

(a) Welding specifications applied to the final closure seal welds on the DSC.
(b) Discussion on how degradation of the zinc-based coating is prevented during welding operations performed on the DSC. Discussion on the effect of temperatures during closure welding on the zinc coating and the resulting effects of molten zinc, if released, on the integrity of the TMI-2 canisters.
(c) Description of the design and operating characteristics of the specific DSC zinc coating to be used (i.e., composition, method of application, etc.) and its interaction with the lubricants used on the rails in the HSM, corrosion susceptibility to local gases mixed with moisture and locally formed acids, and stainless steel in contact with the zinc coating.

Response:

Resolution of this item is still in progress. See DOE letter OPE-SNF-98-050, dated February 12, 1998.

4-2 Request:

Justify the absence of a reference code or standard for the DSC Internal Structure from the table in section 4.2.3.

Response:

The design and safe operation of the TMI-2 DSC does not rely upon the integrity of the internal basket structure. As described in section 4.2.5.2, the basket is considered to be a non-structural, non-load bearing system of plates that is included in the DSC for operational convenience in the loading/unloading of the TMI-2 canisters. The TMI-2 canisters do not rely upon the structural support of the basket in the event of a drop accident or other unspecified occurrence.

Proposed SAR Rewrite:

None

4-3 Request:

Provide the following information to evaluate the DSC vent system and high-energy efficiency air (HEPA) filters:

(a) Design and test data (manufacturers, or test) to verify that the HEPA filters have an efficiency of greater than 99.97 percent for particulates down to 0.3 microns for the environments that bound the INEEL,

(b) Off-normal and accident conditions considered to ensure the filters operation continues to be safe.

Response:
The testing and requirements for the filters are described in Section 4.3. The filters will be tested for penetration of particulate and airflow capacity consistent with ANSI/ASME N510-1989 and the manufacturer's procedures. The tests are also used to demonstrate the filter capabilities after freeze/thaw cycles, impact testing and vibration testing. The filters have been test cycled between -195.4°C and +140°C without any reduction in filter performance. The manufacturer's test data will be added to the SAR as an appendix.

The filters have been evaluated over the full range of conditions expected for both normal and off-normal events at the TMI-2 ISFSI. Since the filters are passive and protected from the environment, there are no postulated accident conditions that would cause the filters to fail. However, in an attempt to bound all possibilities, the two failure conditions, of either completely plugged vents or filters that fail open are evaluated in Chapter 8. The failed open events are combined with a massive failure of the TMI-2 canisters to provide a large release fraction source term. The plugged vent case, unlikely due to the redundancy of the vents, is covered by the analysis of the potential gas build-up, that would be detected by the scheduled gas sampling program. In the unlikely case that the sampling program failed to detect the plugged event the potential gas build up for the plugged vents for a one-year period is evaluated.

Proposed SAR Rewrite:
The manufacture's testing report will be added as an appendix during the next revision of the SAR. The statement in 4.3 will be added as a reference to the appendix.

4-4 Request:
Justify the appropriateness of referencing the Sacramento Municipal Utility District (SMUD) SAR in section 4.7.3.2

Response:
The references to the SMUD SAR's for the 10CFR71 and 10CFR72 operations are appropriate as these provide a controlled source of the operational limits for the MP187 cask proposed for use on the INEEL project. As both documents are presently undergoing licensing review it would not be appropriate to provide duplicate information in this SAR license application.

Proposed SAR Rewrite:
None

CHAPTER 5: OPERATION SYSTEMS

5-1 Request:

Describe the test, analysis, research data showing that the proposed method of dewatering will provide an environment inside the canister that meets the acceptance criteria.

Response:

Testing on actual loaded TMI-2 fuel, filter, and knockout type canisters, selected to represent anticipated worst case conditions, will be performed to demonstrate the viability of the drying system and methodology to infer that the acceptance criteria of 8.8E-5 g/cc will be met for the fuel debris. The TMI-2 canisters will be dried and tested for dryness prior to loading in the DSC. The figure provided below was created using the ideal gas law. If bulk liquid water is present in the TMI-2 canisters, vacuum would be lost when the drying system vacuum pump is shut down. The family of curves indicates that for a given equilibrium vacuum value up to 80 Torr, the density of the moderator will be less than the 8.8E-5 g/cc acceptance criteria.

Proposed SAR Rewrite:

The following sentence will be added to 10.3.1(2) on page 10.3-1: "The acceptance criteria for the dryness of the TMI-2 canisters prior to loading into the DSC is a moderator density of less than or equal to 8.8E-5g/cc."

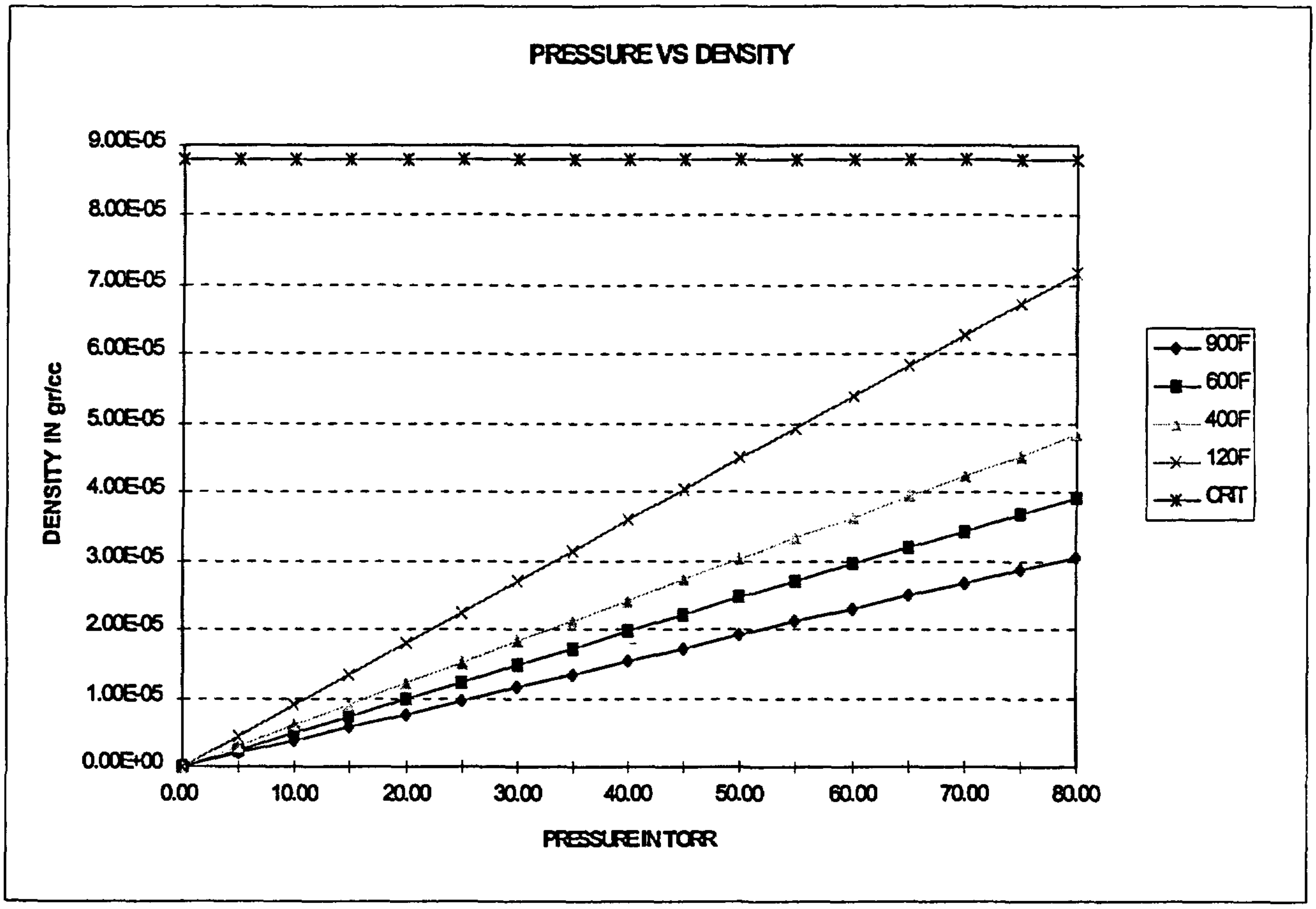
PRESSURE VS DENSITY
9.00E-05
8.00E-05
7.00E-05
6.00E-05
5.00E-05
4.00E-05
3.00E-05
2.00E-05
1.00E-05
0.00E+00
DENSITY IN gr/cc
0.00
10.00
20.00
30.00
40.00
50.00
60.00
70.00
80.00
PRESSURE IN TORR
900F
600F
400F
120F
CRIT

CHAPTER 6: SITE-GENERATED WASTE CONFINEMENT AND MANAGEMENT

6-1 Request:

Describe the effluent and environmental monitoring program at the ISFSI site. Include in this description the types of samples taken, sampling locations, collection frequency, method of collection, and type of radionuclide analysis with lower limits of detection.

Response:

The requested information is described in Section 7.6.1 of the SAR. Also, the information is presented in the INEEL Site Wide Environmental Monitoring Program Report [DOE/ID 12082(96)], which was previously furnished to the NRC. [Reference J. Hagers to C. Haughney, "*Response to Request for Additional Information to Prepare an Environmental Impact Statement (Docket 72-20) (OPE-SFP-97-335),* dated November 19, 1997]

Proposed SAR Rewrite:

None

CHAPTER 7: RADIATION PROTECTION

7-1. Request:

Provide justification for the statement on page 7.2-2, paragraph 4, line 3 that " temperatures in excess of 1600°C would be required to release the volatile fission products from the fuel matrix." This statement is counterintuitive since the boiling points from I_2 and Cs are 184°C and 669°C, respectively. With this information in mind, provide justification for not modeling the source term for the release of radioiodine similarly to ^{3}H and ^{85}Kr. It is noted that if ^{129}I release is modeled similarly to the noble gases as suggested on page 4 of Staley (1996). ^{129}I may become the most significant dose contributor of those nuclides listed in table 7.2-3.

Response: (Part 1)

Significant release of volatile fission products at temperatures below the dissolution temperature of the fuel is limited as the volatiles are retained in the reactor fuel until dissolution of the fuel begins. Supporting information is provided in **Attachment** 34, "Fission Product Release from Nuclear Fuel Rods as a Function of Temperature."

Proposed SAR Rewrite:

None

Response: (Part 2)

The ^{129}I dose listed in Table 7.2-3 was modeled as a particulate radionuclide release rather than a noble gas release because most radioiodine that was at exposed surfaces of the fuel material was dissolved into the coolant early in the accident with the balance being located in the fuel matrix. This fraction is not expected to be significantly released during the drying operation. Consequently, the potential for release is expected to be more similar to particulates than noble gases."

Proposed SAR Rewrite:

None

7-2 Request:

Provide more justification for neglecting the peak does rates due to neutrons in column one on the last two lines of this table [see table 7.3-1 (page 7.3-6]. Since the neutron peak dose rates are approximately equal to the gamma peak dose rates for other entries in this quadrant of the table, it would expect the neglected peak neutron dose rates to be about equal to their respective peak gamma does rates.

Response:

The basis for neglecting the neutron dose rates on the DSC shield plug and at the DSC vent port is the two-dimensional discrete ordinates transport computer code

(DORT) (SAR Ref. 7.11) model of the DSC in the MP187 cask described in Section 7.3.2.2(C) of this SAR. At the DORT node corresponding to the surface of the DSC top cover, the calculated neutron dose rate is 3.5 mrem/hr and the calculated gamma dose rate is 234.6 mrem/hr (the magnitude of the gamma dose rate reported by DORT is greater than that shown in table 7.3-1 because the DORT model includes back-scatter from the MP187 top cover plate). Based on these results, the neutron dose rate on the surface of the DSC top shield plug is expected to be less than 1.5% of the total dose rate and has, therefore, been neglected.

The apparent discrepancy between this result and the cask top and bottom dose rates shown in table 7.3-1 is due to the lack of neutron shielding in the ends of the MP187 cask. The MP187 top cover plate consists of 6.5 inches of stainless steel which attenuates gammas significantly more effectively than neutrons. The neutron dose rate, therefore, represents a greater fraction of the total MP187 top (and bottom) surface dose rate than it does for the DSC shield plug dose rate. Note that because the HSM is shielded by concrete instead of steel, the neutron dose rate represents less than 1% of the total for the HSM front and rear surfaces, which is more consistent with the fraction stated for the DSC shield plug.

Proposed SAR Rewrite:

Note 1 of table 7.3-1 in the SAR will be revised to state, "Analysis performed only for gamma-ray doses. Neutron doses represent less than 1.5% of the total doses at these locations based on the DORT model described in section 7.3.2.2(C) and have been neglected."

7-3 Request:

Provide justification on page 7.2-2, paragraph 4, line 7 for the assumption that only one percent of particulates and solids released from the fuel to air in the canister reach the HEPA filter.

Response:

The 1% particulate release to air from fuel will be measured during the fission product release to be performed prior to beginning operation of the drying system. A quantitative measure of the release of particulate will be completed. The results of the test will be provided to NRC when completed. Supporting information is available in **Attachment 35** "Summary of Fission Product Release Test Results."

Proposed SAR Rewrite:

None

CHAPTER 8: ANALYSIS OF DESIGN EVENTS

8-1 Request:
Provide the following additional information with respect to analysis approach, models, and results contained in Section 8.1.

(a) Example of input and corresponding output computer file listings for both the thermal analysis (i.e., HEATING 7 code) and structural analysis (i.e., ANSYS code).

Response:
Thermal analysis:
The critical HEATING 7 input and output files used in the thermal analysis are included as a hardcopy **[Attachment 36]** (available on a diskette upon request).

The critical input and output files for the NUHOMS®-12T HSM thermal analysis are 103°F ambient off-normal case which results in maximum HSM temperatures and also maximum side wall gradient and -50°F ambient accident case which results in maximum HSM roof gradient as shown in Table 8.1-8 of the SAR.

HEATING Input / Output Files

CASES	HEATING7 Input File Name	HEATING7 Output File Name and Date/Time
103°F ambient, Off-Normal NUHOMS-12T HSM	TMI-4D1.INP	TMI-4D1.OUZ
-50°F ambient, Accident NUHOMS-12T HSM	TMI-4D5.INP	TMI-4D5.OUZ
103°F ambient, Accident NUHOMS-12T DSC	TMI103A.INP	TMI103A.OUT 09/12/96,17:43:26

Structural Analysis:
A hard copy of critical input/output files is included as **Attachment 37** (available on a diskette upon request).

Proposed SAR Rewrite:
None

Request:
(b) Complete set of mechanical and thermal properties for materials used in the thermal and structural analyses, beyond those listed in tabled 8.1-3, 8.1-6, and 8.1-7. Include Young's modulus, Poisson's ratio, coefficient of thermal

expansion, thermal conductivity, and strength properties for all materials used in the HSM and DSC analyses.

Response:
Stainless steel thermal conductivity values are conservatively used for the neutron absorbing material (Boral). The thermal properties of all the other materials used in the thermal analysis (thermal conductivity and emissivity) are given in the SAR Tables 8.1-6 and 8.1-7.

Provision of input files in response to RAI Item Number 8.1 (a) provides the requested data.

Proposed SAR Rewrite:
None

Request:
(c) Details on how view factors are established for the radiation heat transfer analysis across the air gap between the DSC and HSM, as well as across air gaps within the DSC between the TMI-2 canisters and the DSC shell.

Response:
HSM concrete walls and ceiling, and between the DSC outer surface and the HSM floor. The effective emissivity for the various surfaces is calculated as shown below using parallel surfaces with a view factor of unity:

The effective emissivity between parallel surfaces is given by:

$$\varepsilon_{eff} = \frac{1}{(\frac{1}{\varepsilon_1}) + (\frac{1}{\varepsilon_2}) - 1}$$

1. The effective emissivity of the gap between the DSC shield plug and TMI-2 canister outer surface in the axial direction is given by:

$$\varepsilon_1 = \varepsilon_2 = 0.587$$

$$\therefore \; \varepsilon_{eff} = \frac{1}{\frac{1}{0.587} + \frac{1}{0.587} - 1} = 0.4154$$

$$\therefore \; \sigma * \varepsilon = 0.4154 * 1.984E\text{-}13 = 8.2412E\text{-}14 \; \frac{Btu}{\text{min-}inch^2 \; {}^\circ R^4}$$

where σ is the Stephen Boltzman constant.

2. Similarly the effective emissivity between the DSC shell and concrete surfaces is given by:

$$\varepsilon_{DSCShell} = 0.587 \quad \varepsilon_{Concrete} = 0.90$$

$$\therefore \quad \varepsilon_{eff} = \frac{1}{\dfrac{1}{0.9} + \dfrac{1}{0.587} - 1} = 0.551$$

$$\therefore \quad \sigma * \varepsilon = 0.551 * 1.984E\text{-}13 = 1.093E\text{-}13 \quad \frac{Btu}{\text{min-}inch^2 \; {}^\circ R^4}$$

where σ is the Stephen Boltzman constant.

3. The effective emissivity between the parallel concrete surfaces for all conditions is given by:

$$\varepsilon_1 = 0.90 \quad \varepsilon_2 = 0.90$$

$$\therefore \quad \varepsilon_{eff} = \frac{1}{\dfrac{1}{0.90} + \dfrac{1}{0.90} - 1} = 0.818$$

$$\therefore \quad \sigma * \varepsilon = 0.818 * 1.984E\text{-}13 = 1.623E\text{-}13 \quad \frac{Btu}{\text{min-}inch^2 \; {}^\circ R^4}$$

where σ is the Stephen Boltzman constant.

4. The effective emissivity between the steel outside surface (HSM Door) and ambient for all conditions is given by:

$$\varepsilon_1 = 0.587 \quad \varepsilon_{ambient} = 1.0$$

$$\therefore \quad \varepsilon_{eff} = \frac{1}{\dfrac{1}{0.587} + \dfrac{1}{1.0} - 1} = 0.587$$

$$\therefore \quad \sigma * \varepsilon = 0.587 * 1.984E\text{-}13 = 1.1645E\text{-}13 \quad \frac{Btu}{\text{min-}inch^2 \; {}^\circ R^4}$$

where σ is the Stephen Boltzman constant.

5. The effective emissivity between the concrete outside surfaces and ambient for all conditions is given by:

$$\varepsilon_I = 0.80 \quad \varepsilon_{ambient} = 1.0$$

$$\therefore \ \varepsilon_{eff} = \frac{1}{\frac{1}{0.80} + \frac{1}{1.0} - 1} = 0.80$$

$$\therefore \ \sigma * \varepsilon = 0.80 * 1.984E\text{-}13 = 1.587E\text{-}13 \ \frac{Btu}{\text{min-}inch^2 \ {}^\circ R^4}$$

where σ is the Stephen Boltzman constant. Note that a concrete emissivity of 0.80 is used instead of 0.90 which is conservative for the maximum concrete temperature calculation.

Proposed SAR Rewrite:
None

Request:
(d) ***Examples of how the stress intensities for the DSC and its support structure, as shown in tables 8.1-11 through 8.1-13, are determined from the ANSYS results and how the membrane stresses are separated from the total stresses.***

Response:
The program ANSYS outputs stress intensities directly. Stresses can also be separated into membrane, bending, membrane plus bending, peak and total stress categories. For convenience, these portions of the ANSYS manuals are reproduced here.

The column heading for Table 8.1-13 should read "Calculated Stress" and delete the word "intensity" as the DSC support structure steel design is done to AISC code requirements, not ASME.

Proposed SAR Rewrite:
These changes will be made in the next SAR revision

Request:
(e) Examples of how the HSM reinforced concrete bending and shear forces, as shown in table 8.1-15, are determined from the ANSYS results.

Response:
See **Attachment 38** for response

Proposed SAR-Rewrite
None

Request:

(f) *Clarification of HSM HEATING 7 results of 45°F ambient air analysis, as tabulated in Figure 8.1-2, to show cross-sectional plane* where results are taken, as well as depict locations where surface temperatures are being read (i.e., HSM inner and outer wall surfaces, HSM inner and outer roof surfaces, DSC shell surface, etc.). Also provide further clarification of how heat loading is applied in the simplified NUHOMS®-12T DSC used in the HSM thermal analysis (Figure 8.1-1).

Response:

Figure 8.1-1 is marked to show the cross-sectional plane where the results of Figure 8.1-2 are taken. Figure 8.1-2 has been clarified to include the locations where the surface temperature results are taken.

The heat load is applied as a volumetric heat density of 9.646E-5Btu/min-in^3 over the fueled portion of the TMI-2 canister. The calculation of volumetric heat density is shown below:

Volumetric Heat Density is calculated as follows:

$$\ddot{Q} = \frac{0.86kW * \frac{3412\ (Btu/hr)}{kW} * \frac{hr}{60\ \text{min}}}{\pi (33.595)^2\ inch^2 * 143\ inch}$$

where 33.595" and 143" are the DSC cavity internal radius and the TMI-2 canister cavity length respectively. This heat density is applied to the fueled portion of the TMI-2 canister in the thermal models.

Proposed SAR Rewrite:

None

8-2 **Request:**

Discuss why stress intensities are not computed for the bottom shield plug as they are for the top shield plug as shown in tables 8.1-11 and 8.1-12, since both are defined as important to safety (see table 3.4-1).

Response:

The plugs are defined as Important To Safety (ITS) for their shielding properties. The top shield plug must also support its own weight during installation when it must be installed over the fuel debris canisters, during transportation, and for a postulated bottom end drop accident event.

The bottom shield plug is supported by the inner and outer bottom cover plates during all normal operating and postulated accident events and, therefore, no strength properties are required to meet its ITS function.

<u>Proposed SAR Rewrite:</u>
None

8-3 <u>Request</u>:
Provide details concerning the radial gap between the TMI-2 canisters and the holes in the DSC spacer discs in which the canisters are inserted. Justify that the thermal and structural results for the DSC and basket assembly encompass the possible case of non-uniform thermal loading (i.e., DSC basket assembly containing TMI-2 fuel canisters having a maximum thermal output on one side versus much lower thermal output on the other side).

<u>Response:</u>
The TMI-2 canisters have an outside diameter of 14.00 inches and are inserted into 14.50-inch diameter holes in the spacer disc creating a diametric gap of 0.25 inch. This gap is guaranteed by the gage test.

The basket is non-safety related and as such asymmetric thermal stresses are not a concern. The DSC shell is carbon steel and as such non-uniform temperature distribution will be kept to a minimum. Canister removal/insertion is not a problem as heating/expansion of discs will keep openings aligned.

The maximum temperature gradient in the DSC shell caused by the case of non-uniform thermal loading (i.e. DSC basket assembly containing TMI-2 fuel canisters having a maximum thermal output on one side versus a much lower thermal output on the other side) is estimated as follows:

The maximum DSC shell temperature is calculated assuming all the TMI-2 canisters in a DSC are with the highest decay heat load. The minimum DSC shell temperature is calculated assuming all the TMI-2 canisters in the DSC are with the lowest (zero) decay heat load. A conservative bounding of the effect of non-uniform thermal loading is to assume these maximum and minimum temperatures occur in a given DSC at the same time. Using the results from Table 8.1-9 of the SAR, the maximum temperature gradient across the DSC shell due to non-uniform thermal loading will be 52.8° F (97.8 - 45) for normal conditions, 54.8° F (4.8 - (- 50)) for off-normal conditions and 80.8° F (183.8 - 103) for accident conditions.

A simple ratio of the stress from the calculations of the generic DSC (with a thermal gradient of 75° F and a maximum associated stress of 12.6 ksi) shows a maximum stress under normal conditions for the TMI-2 DSC:

$$f_{max/TMI-2} = 12.6\ (52.8/75)$$

$$= 8.9\ \text{ksi}$$

Proposed SAR Rewrite:
None

8-4 Request:
Provide clarification for the statement. "Error! Reference source not found" section 8.1.1.3 (page 8.1-8).

Response:
This is a message that the automatic referencing system of WORD could not find the appropriate reference for this section an was not caught during proofreading. This should read "The applied load is shown in **Figure 8.1-10.**"

Proposed SAR Rewrite:
This will be changed in the next revision of the SAR.

8-5 Request:
Discuss and present results showing how stresses within welds are calculated around the top and bottom cover plates.

Response:
Resolution of this item is still in progress. See DOE letter OPE-SNF-98-050, dated February 12, 1998.

Proposed SAR Rewrite:
TBD

8-6 Request:
Provide clarification in section 8.2 as to which postulated accidents and events (occurring with a low frequency) are of Type III and which are of Type IV. On page 8.1-1 of the SAR, design events are classified into four categories: Type I-normal (occur regularly). Type II-off normal (occur once during a calendar year), and Type III and IV-postulated accidents and events (occur with a low frequency). However, in section 8.2. which covers accident analysis, no distinction is made between Types III and IV events.

Response:
The use of the event type classifications is misleading, as it is not carried consistently into the SAR. To remove the confusion caused by these terms we propose eliminating them from 8.1 and replacing them with the more readily understood, and consistent, terminology "normal operating, off-normal operating and accident" classifications. This terminology is also more consistent with the base documents used to prepare the SAR and the latest NUREG 1536.

Proposed SAR Rewrite:
The second paragraph of Section 8.2 (page 8.1-1) will be reworded to read as follows:

"In accordance with NRC Regulatory Guide 3.48 [8.1], the design events identified by ANSI/ANS57.9-1984 [8.2] form the basis for the accident analyses performed for the NUHOMS®-12T system. **Three categories of design events are defined. Normal operating and Off-normal events are addressed in Section 8.1. Accident conditions as postulated in ANSI/ANS 57.9-1984 due to natural phenomena and manmade events are addressed in Section 8.2.** These events provide a means of establishing that the NUHOMS-12T system design satisfies the applicable operational and safety acceptance criteria as delineated herein.

CHAPTER 10: OPERATING CONTROLS AND LIMITS

10-1 <u>Request</u>:

Provide a better description of the current conditions of the TMI-2 canisters and the controls and limits for dewatering and drying of the canisters as a replacement of the inert requirements included in 10 CFR 72.236(a).

<u>Response:</u>

The condition of the TMI-2 canisters is addressed in Item 3-3 part 2. The 10 CFR 72.23 requirement for an inert atmosphere in a storage system is based on the need to prevent degradation of the fuel cladding as a confinement/containment boundary. An inert atmosphere is a requirement for licensing a standard storage container; however, the TMI-2 fuel debris is severely degraded with no intact cladding. Consequently, there is no basis for the inert atmosphere.

Achieving canister dryness is accomplished in a two-stepped process – dewatering and drying. Dewatering the canisters removes the bulk of the free water by pushing the water out of the canisters with pressurized air. The acceptance criteria is an unrestricted airflow through the canister as indicated by flow monitoring equipment on the dewatering skid. The remaining water will be removed during drying.

The dewatered canisters are then placed into the heated vacuum drying system where the remaining water is removed from the canisters. The acceptance criteria of a moderator density less than or equal to 8.8E-5 g/cc was established to ensure all free water has been removed from the canister internals. The method of verification is to hold a vacuum of 80 Torr or less for a specified period of time as noted in RAI 5-1.

Testing on new (nonradioactive) and actual radioactive TMI-2 fuel, filter, and knockout type canisters is being performed to demonstrate the viability of the drying system and methodology to infer that the acceptance criteria of 8.8E-5 g/cc will be met for the fuel debris. The TMI-2 canisters will be dried prior to loading in the DSC.

<u>Proposed SAR Rewrite:</u>

None

10-2 <u>Request</u>:

Provide information regarding the present condition of Boral and the B_4C ***pellets as neutron absorbers to ensure that control of criticality will be maintained under credible conditions, as per 10 CFR 72.236(c).***

<u>Response:</u>

This question is addressed as part of RAI Item 3-3.

Proposed SAR Rewrite:
None

10-3 **Request:**
State in the SAR the catalysts composition and characteristics as an oxygen and hydrogen recombiner this is to assure that no detrimental effects can be expected from its presence.

Response:
The composition of hydrogen recombiner materials and their expected behavior are addressed in **Attachment 40**, "J. O. Henrie, B. D. Bullough, and D. J. Flesher, *Catalyst Tests for Hydrogen Control in Canisters of Wet Radioactive Wastes*, GEND-062, August 1987".

In summary, there are two types of recombiners utilized in the TMI-2 canisters. One type is Engelhard Deoxo Type 18467, a palladium-on-alumina catalyst, previously designated as Engelhard Deoxo-D, Nuclear-Grade Al6430. The other is a wet-proof, silicone-coated platinum-on-aluminum catalyst manufactured by AECL. The two types exist in a mixture of 80% Engelhard Deoxo Type 18467 and 20% AECL .

Proposed SAR Rewrite:
A summary description of the recombiners will be included in the next SAR revision.

10-4 **Request:**
Provide a rationale for the choice of a 5-year interval for surveillance of leak testing of DSC vent housing seals and monitoring of HSM dose rates.

Response:

Leak Testing - The 5-year interval for leak testing of the vent housing seals is based on the characteristics of the seal and the environment they will see. The seal is a metallic seal made of materials that are more noble than the contacting materials. The seals have an infinite shelf life according to the manufacturer. The seals are completely passive, sealing against a negligible pressure differential in a static situation, with little temperature fluctuation. The seals are also adjacent to open vents. Therefore there is no known postulated event or environment that will change the sealing situation and a long interval between leak tests is warranted. Also as the housings are tightened in a metal to metal configuration the consequences of a seal leaking are small. Therefore the gain from frequent tests, compared to the exposure that workers would receive in performing the tests, is small. A five-year interval was chosen to provide a reasonable check on seals throughout the TMI-2 ISFSI lifetime and is consistent with ALARA principles. The seals are initially tested to demonstrate a minimum leak rate of 1×10^{-7} cc/sec with helium as the seals are part of the transportation secondary containment boundary. This is three orders of magnitude greater than the leak tightness requirements for storage considerations.

Dose Rate: - The 5-year interval for the monitoring of the HSM dose rates will be deleted and will be changed to be in accordance with the Radiation Protection Program.

Proposed SAR Rewrite:
Will delete the 5-year interval for monitoring dose rates and require dose rate monitoring in accordance with the ICPP Radiation Protection Program.

LISTING OF RAI ATTACHMENTS

1. Map showing production wells at the INEEL [Ref. RAI 2-1]
2. *U.S. Department of Commerce, National Oceanic and Atmospheric Administration letter, Kirk L. Clawson to Mr. Joe Carlson, dated November 24, 1997* [Ref. RAI 2-2 and 2-3]
3. Topographic Map Showing 2-ft Contours at the ICPP [Ref. RAI 2-4]
4. Large-scale Geological Map of the INEEL [Ref. RAI 2-6(a) and 2-7(d)]
5. Figure 2.6-3: Precambrian to Quaternary stratigraphic section [Ref. RAI 2-6(c)]
6. Figure 2.6-(x): Late Tertiary and Quaternary stratigraphic section at TMI-2 ISFSI site [Ref. RAI 2-6(c) and 2-8]
7. Map of the TMI-2 ISFSI site showing locations of 1997 boreholes and contours of bedrock [Ref. RAI 2-6(c)]
8. 8.5x11 inch topographic map of INEEL [Ref. RAI 2-7]
9. 1:100,000-scale topographic map of the INEEL [Ref. RAI 2-7]
10. Summary table of geotechnical results for the New Production Reactor site [Ref. RAI 2-8(b)]
11. Large-scale fault map of the region [Ref. RAI 2-9]
12. Earthquake epicenters (1850-1995) plotted on shaded relief fault map [Ref. RAI 2-9]
13. Earthquake epicenters (1850-1995) plotted on state outline map [Ref. RAI 2-9]
14. Map showing seismic source zones used in probabilistic seismic hazards assessment [Ref. RAI 2-9]
15. Map showing locations of the INEEL seismic network stations and earthquakes within 100 miles of INEEL from 1972-1995 [Ref. RAI 2-9(h)]
16. Isoseismal map for the 1905 Shoshone earthquake [Ref. RAI 2-9(h)]
17. Isoseismal map for the 1983 Borah Peak earthquake [Ref. RAI 2-9(h)]
18. Isoseismal map for the1975 Pocatello Valley earthquake [Ref. RAI 2-9(h)]
19. Isoseismal map for the 1959 Hebgen Lake earthquake [Ref. RAI 2-9(h)]
20. Isoseismal map for the 1975 Yellowstone Park earthquake [Ref. RAI 2-9(h)]
21. Isoseismal map for the 1994 Draney Peak earthquake [Ref. RAI 2-9(h)]
22. Proposed SAR Rewrite of Sections 2.6.2.2.2, 2.6.2.2.3, 2.6.2.3.2, 2.6.2.3.3, 2.6.2.3.5, 2.6.2.3.7, Table 2.6-11, and Table 2.6-12 [Ref. RAI 2-10, 2-11, 2-12 and 2-13]
23. Geotechnical data package for the TMI-2 ISFSI site [Ref. RAI 2-14 (Part 2)] Consisting of:
    - Map of the TMI-2 ISFSI site showing locations of 1997 boreholes
    - Table of blow counts determined in Standard Penetration Tests
    - Table of seismic velocities determined by downhole seismic logging
    - Summary diagram of seismic velocity profiles of boreholes at the TMI-2 ISFSI site
    - Graph showing TMI-2 ISFSI site blow-counts plotted on a cyclic stress ratio vs. blow count diagram
    - Graph showing TMI-2 ISFSI site shear wave velocities plotted on a cyclic stress ratio vs. shear wave velocity diagram
    - Seismic velocity profiles of individual boreholes at the TMI-2 ISFSI site
    - Lithologic logs and completion diagrams for boreholes at the TMI-2 ISFSI site
    - Particle size distribution test reports for surficial sediment samples collected from the 1997 boreholes at and near the TMI-2 ISFSI site

24. Maps showing the locations of volcanic vents, locations of radiometric age determinations, and volumes of lava fields [Ref. RAI 2-15]
25. Table of individual measurements of lava flow length and area [Ref. RAI 2-16]
26. Summary of TMI-2 Canister Weights, Uncertainties, and Methodology Used to Determine Uncertainties [Ref. RAI 3-1 (Part 1)]
27. TMI-2 Isotopic Inventory Calculations [Ref. RAI 3-1 (Part 2)]
28. Letter report showing comparisons between measured and calculated fission product inventory data for TMI-2 [Ref. RAI 3-1 (Part 2)]
29. Test Plan Summary for Measuring Gases and Particulate Vented from the TMI-2 Canisters [Ref. RAI 3-2 (Part 2)]
30. Summary of Information on the Response of TMI-2 Canisters to Chemical Corrosion [Ref. RAI 3-3]
31. Summary of Studies Performed to Address the Pyrophoricity of TMI-2 Fuel Debris [Ref. RAI 3-4]
32. TMI-2 Accident Core Heat-Up Analysis, NSAC-25, Nuclear Associates International and Energy Incorporated, June 1981 [Ref. RAI 3-7]
33. Model of HSM and DSC Support Structure [Ref. RAI 3-15]
34. Fission Product Release from Nuclear Fuel Rods as a Function of Temperature [Ref. RAI 7-1 (Part 1)]
35. Summary of Fission Product Release Test Results [Ref. RAI 7-3]
36. HEATING 7 input and output files used in the thermal analysis [Ref. RAI 8-1(a)]
37. Structural Analysis input files [Ref. RAI 8-1(a)]
38. Examples of how the HSM reinforced concrete bending and shear forces, as shown in table 8.1-15, are determined from the ANSYS results [Ref. RAI 8-1(e)]
39. J. O. Henrie, B. D. Bullough, and D. J. Flesher, *Catalyst Tests for Hydrogen Control in Canisters of Wet Radioactive Wastes*, GEND-062, August 1987 [Ref. RAI 10-3]

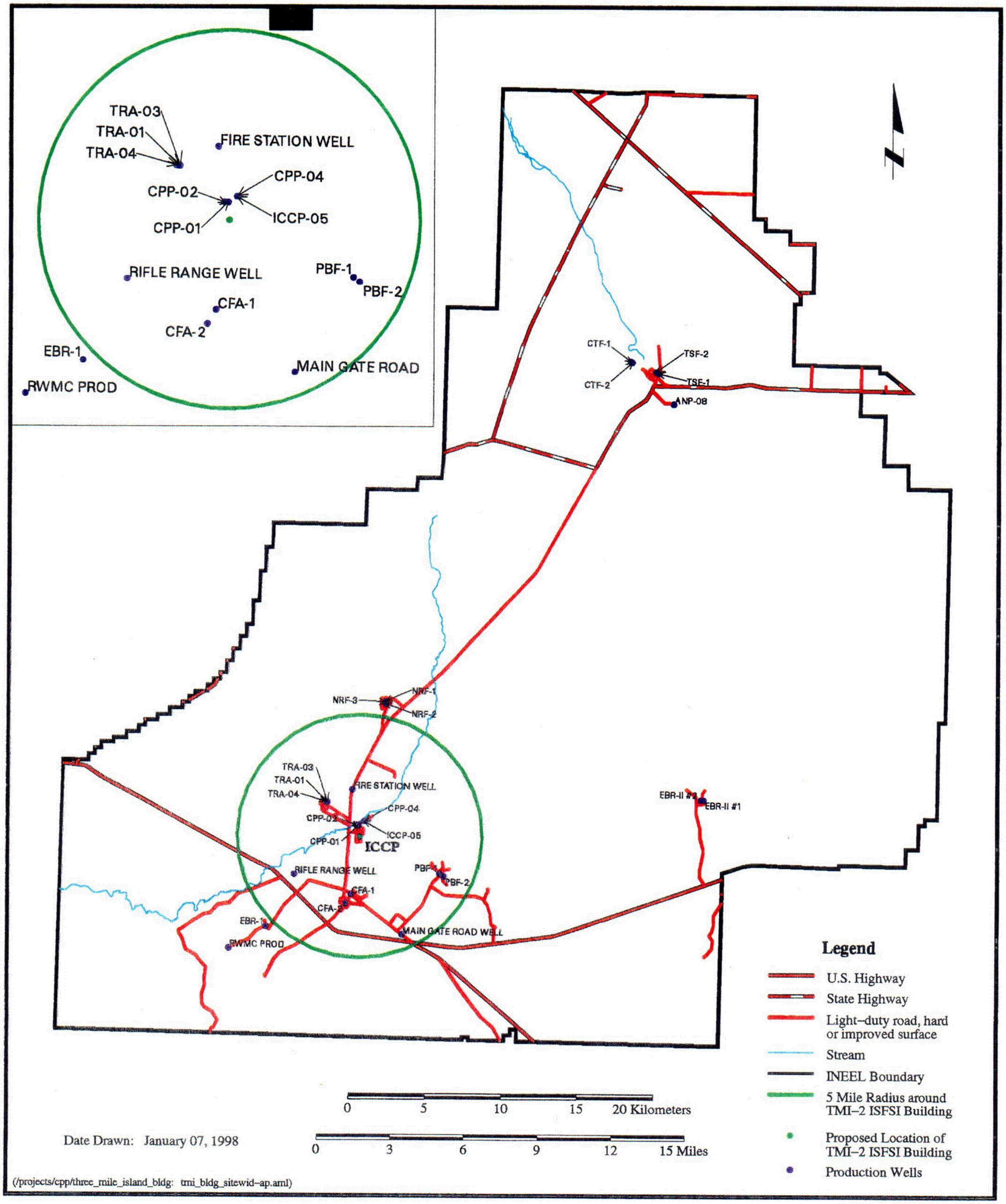

Figure 2.5-(x): Map Showing Production Wells at the INEEL

C-01

U.S. DEPARTMENT OF COMMERCE
National Oceanic and Atmospheric Administration
ENVIRONMENTAL RESEARCH LABORATORIES
ARL Field Research Division
1750 Foote Drive
Idaho Falls, ID 83402-4901

November 24, 1997

Mr. Joe Carlson
Lockheed Martin Idaho Technologies Company
INEEL Spent Nuclear Fuel Program
P.O. Box 1625
Idaho Falls, ID 83415-3114

Dear Joe:

I have prepared the attached information in response to your fax dated 18 November 1977. I have addressed the Request for Additional Information comments 2-2 and 2-3 as they pertain to Section 2.3.3 of the INEEL TMI-2 Safety Analysis Report. This should satisfy the RAI. If you have additional questions, please call me at 6-2742.

Sincerely,

Kirk L. Clawson

Kirk L. Clawson
Research Meteorologist

Attachments

ATTACHMENT 2

Response to Request for Additional Information 2-2 & 2-3
Application for a License for an Independent Spent Fuel Storage Installation
to Store the TMI-2 Fuel Debris 2.3.2 and 2.3.3

The Grid 3 facility is located about 1.6 miles north of ICPP on a broad, flat plain (see accompanying map). The vegetation is primarily sagebrush and rabbit brush and covers approximately 70% of the ground. The tallest vegetation is approximately 1 m. No trees are in the area. The fetch is level for several miles in all directions.

The site is equipped with a 64 m tower for measuring 3 levels of temperature and 2 levels of wind. All sensors are polled each second and then the data are averaged for a 5 minute period. Statistics such as wind direction standard deviation, and air temperature maxima and minima are calculated by the attached datalogger. The data are collected every five minutes using a radio link between the station and the NOAA offices. The data are then merged into the NOAA mesonet database with data from more than 30 other meteorological stations. A sample output for Grid 3 from the mesonet database is attached. The datalogger that is used to control and monitor the meteorological instruments is the Campbell Scientific Model CR-10X. The datalogger program is attached. The specifications for the meteorological sensors are given in the attached table.

A routine calibration of all instruments and datalogger is conducted semi-annually. The most recent semi-annual report is attached. Any malfunctioning equipment is replaced at that time. In addition, the data are subjected to a routine QC screening every weekday by a trained meteorologist. The QC procedures are both automated and manual. All suspect data is flagged and any equipment malfunction is noted. The malfunctioning sensor is immediately replaced.

Height	Meteorological Variable	Sensor	Manufacturer	Model
1 m	Precipitation	Heated Rain Guage	Friez Engineering Co.	5405H
2 m	Aspirated Air Temperature	Type E Thermocouple	Met One Instruments	Model 076B Radiation Shield
2 m	Relative Humidity		Vaisala	Humitter 50U
2 m	Solar Radiation	Pyranometer	Licor	LI200X
10 m	Aspirated Air Temperature Difference	Type E Thermocouple	Met One Instruments	Model 076B Radiation Shield
10 m	Wind Speed	Anemometer	Met One Instruments	Model 5397/NOAA
10 m	Wind Direction	Wind Vane	Met One Instruments	Model 5387/NOAA
64 m	Aspirated Air Temperature Difference	Type E Thermocouple	Met One Instruments	Model 076B Radiation Shield
64 m	Wind Speed	Anemometer	Met One Instruments	Model 5397/NOAA
64 m	Wind Direction	Wind Vane	Met One Instruments	Model 5387/NOAA

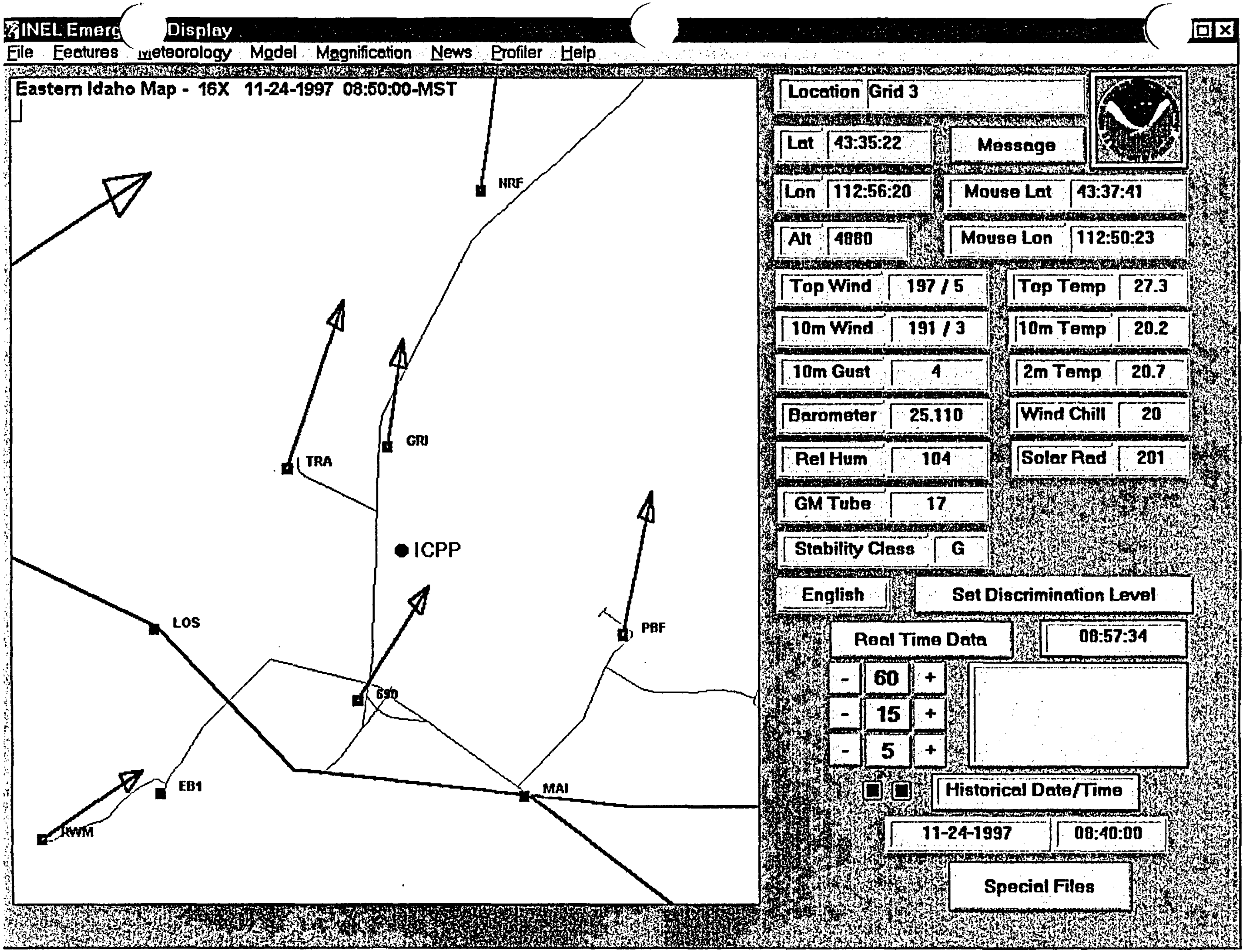
INEL Emerg Display
File
Features
Meteorology
Model
Magnification
News
Profiler
Help
Eastern Idaho Map - 16X 11-24-1997 08:50:00-MST
NRF
TRA
GRI
ICPP
LOS
PBF
EB1
RWM
MAI
Location
Grid 3
Lat
43:35:22
Message
Lon
112:56:20
Mouse Lat
43:37:41
Alt
4880
Mouse Lon
112:50:23
Top Wind
197 / 5
Top Temp
27.3
10m Wind
191 / 3
10m Temp
20.2
10m Gust
4
2m Temp
20.7
Barometer
25.110
Wind Chill
20
Rel Hum
104
Solar Rad
201
GM Tube
17
Stability Class
G
English
Set Discrimination Level
Real Time Data
08:57:34
60
15
5
Historical Date/Time
11-24-1997
08:40:00
Special Files

Example Grid 3 Data Output

```
Date (YYMMDD),Time (hhmm),GRI BVlt (Volts),GRI CRTmp (Degrees F.),GRI DPts,GRI HVol,GRI NRad (microR/hr),GRI
15S (MPH),GRI 15D (Degrees),GRI 15SD (Degrees),GRI 15G (MPH),GRI 2Tmp (Degrees F.),GRI 15Tmp (Degrees F.),GRI
[illegible]T (Degrees F.),GRI 2MinT (Degrees F.),GRI 2RH (Percent),GRI SRad (Watts/m2),GRI Rain (Inches),GRI TopS
[illegible]H),GRI TopD (Degrees),GRI TopSD (Degrees),GRI TopG (MPH),GRI TopT (Degrees F.),GRI BP (Inches Hg)
971124,555,12.94,18.09,300,0,16.51,3.5,208,4.5,4.1,11.75,15.46,11.86,11.62,98.6,0.7,0,4.2,348,3.4,4.6,27.02,25.09
971124,600,12.94,18.05,300,0,15.97,3.2,219,4,3.9,11.66,15.08,11.79,11.52,98.6,0.7,0,5.2,352,8.3,5.8,26.72,25.089
971124,605,12.92,18.05,300,0,16.4,3.4,212,8.6,3.7,11.39,14.16,11.57,11.25,98.3,0.8,0,5.2,356,7.7,6,26.5,25.092
971124,610,12.93,18.01,300,0,16.68,3.2,208,3.9,3.7,11.28,13.62,11.35,11.19,98.4,0.7,0,4.8,354,3.5,5.8,25.73,25.094
971124,615,12.92,17.97,300,0,17.76,3.6,213,5.1,4.2,11.32,13.21,11.39,11.23,98.5,0.9,0,4.3,358,4.5,5,25.63,25.095
971124,620,12.94,17.93,300,0,16.12,3.8,215,5.1,4.5,11.28,13.86,11.41,11.16,98.4,0.7,0,3.9,357,8.1,4.9,25.39,25.096
971124,625,12.94,17.93,300,0,17.01,3.8,215,3,4.2,11.12,12.81,11.26,11.01,98.2,0.8,0,3.4,9,7.4,4.2,25.05,25.098
971124,630,12.94,17.9,300,0,16.61,3.7,215,5.5,4.1,10.94,12.47,11.08,10.81,98.1,0.7,0,3.4,1,11.3,4.5,25.35,25.098
971124,635,12.94,17.82,300,0,17.28,3.4,224,4,3.9,10.83,12.24,10.98,10.67,98.1,0.9,0,4.2,352,12.6,4.8,26.03,25.097
971124,640,12.94,17.74,300,0,17.17,3.2,211,6.3,3.5,10.62,12.04,10.72,10.47,97.9,0.8,0,3.9,9,11.3,4.9,25.68,25.098
971124,645,12.94,17.7,300,0,16.44,3.3,205,2.1,3.5,10.4,12.04,10.53,10.26,97.8,0.7,0,3.5,16,5.9,3.8,25.68,25.1
971124,650,12.93,17.62,300,0,16.71,3.3,197,5.8,3.5,10.36,12.07,10.47,10.26,98,0.8,0,3.5,38,9.7,3.9,25.4,25.099
971124,655,12.93,17.55,300,0,17.14,3.3,206,4.2,3.6,10.53,12.15,10.8,10.31,98.3,0.9,0,2.9,37,6,3.5,24.53,25.102
971124,700,12.93,17.47,300,0,16.76,3.5,205,3.5,3.7,10.87,12.18,10.99,10.74,98.4,1,0,3.6,36,4.6,3.9,24.81,25.102
971124,705,12.93,17.38,300,0,16.14,3.1,205,3.4,3.4,10.9,12.15,10.98,10.81,98.2,0.9,0,4,31,4,5,24.7,25.103
971124,710,12.93,17.31,300,0,16.97,3.1,210,4.2,3.5,10.72,11.97,10.85,10.53,98,0.9,0,3.6,33,7.5,4.7,24.32,25.105
971124,715,12.93,17.28,300,0,17.48,3.2,208,6.3,3.8,10.35,11.71,10.56,10.15,97.6,1,0,3.7,39,7.7,5,24.05,25.105
971124,720,12.93,17.15,300,0,16.33,3.2,211,6.5,3.4,10.08,11.71,10.22,9.9,97.6,1.2,0,3.6,43,9.9,4.9,24,25.105
971124,725,12.93,17.11,300,0,16.15,3.4,202,3.9,3.7,9.73,11.95,10,9.5,97.3,2,0,2.8,59,8.1,3.6,23.81,25.106
971124,730,12.92,17.01,300,0,16.66,3.8,199,5.3,4.2,9.68,12.38,9.86,9.59,97.7,4.6,0,2.9,50,9.5,3.6,23.72,25.107
971124,735,12.92,16.92,300,0,14.6,4.2,198,3.9,5,10.06,12.49,10.49,9.77,98.2,7.8,0,2.2,63,17.5,3.1,24.06,25.105
971124,740,12.92,16.84,300,0,16,4.5,196,2.9,5,10.94,12.56,11.37,10.44,99,11.4,0,1,101,19.1,1.9,24.26,25.104
971124,745,12.92,16.81,300,0,17.14,4,193,4.4,4.5,11.75,12.51,12.13,11.35,99.3,14.2,0,1.8,105,16.5,2.5,24.3,25.103
971124,750,12.92,16.77,300,0,17.18,3.3,202,8.2,3.9,12.31,12.54,12.45,12.07,99.3,17,0,1.9,80,24.3,2.3,24.46,25.103
[illegible]24,755,12.92,16.77,300,0,15.87,3.4,217,6,4.4,12.43,12.43,12.52,12.36,99.1,27.5,0,1.4,62,63.1,3.1,24.79,25.103
[illegible]24,800,12.92,16.81,300,0,16.02,2.9,208,7,3.4,12.54,12.47,12.65,12.42,99.1,35.2,0,1.2,39,19.7,3.2,25.32,25.103
971124,805,12.92,16.84,300,0,17.61,3.6,211,7.4,4.6,12.72,12.69,12.81,12.6,99.2,44.9,0,1.6,54,91.1,3.2,25.35,25.103
971124,810,12.92,16.93,300,0,16.3,3.7,216,9.4,4.3,12.92,12.97,13.14,12.76,99.5,58.6,0,0.8,334,86.8,2,26.11,25.102
971124,815,12.92,17.01,300,0,16.9,3.2,211,7.1,3.9,13.32,13.21,13.6,13.08,99.7,73.1,0,0.6,345,17.1,1.6,26.72,25.104
971124,820,12.92,17.17,300,0,16.2,3.4,218,8.6,4.1,14.02,13.87,14.43,13.57,100.3,85.9,0,0.6,275,70.7,0.6,26.4,25.109
971124,825,12.92,17.35,300,0,15.89,3.3,222,6.7,4,14.79,14.61,15.13,14.38,100.7,100.3,0,0.6,283,35,0.6,26.62,25.111
971124,830,12.92,17.63,300,0,16.04,3.2,220,8,3.9,15.48,15.21,15.91,15.08,101,120,0,1.5,245,29.5,2.7,26.19,25.113
971124,835,12.92,17.97,300,0,16.22,3.1,220,6.5,3.7,16.34,16.11,16.88,15.87,101.6,116.1,0,0.9,257,12.1,1.8,26.73,25.111
971124,840,12.92,18.36,300,0,16.84,3.2,206,11,4.1,17.53,17.37,18.21,16.84,102.3,133.7,0,1.7,227,12.3,2.7,27.56,25.111
971124,845,12.93,18.86,300,0,16.29,3.1,206,10.3,4.2,18.97,18.78,20.06,18.16,103.3,191.9,0,3.4,214,4.6,4.1,27.64,25.11
971124,850,12.93,19.4,300,0,16.76,3.5,191,6.9,4.3,20.65,20.25,21.29,19.97,103.9,201.2,0,4.5,198,7.2,5,27.29,25.11
971124,855,12.93,20.05,300,0,16.45,2.9,186,7.6,4,22.04,21.44,22.76,21.2,104.5,222,0,4.5,182,3.9,6.2,27.14,25.109
971124,900,12.92,20.81,300,0,14.27,3.3,186,8,4.7,23.22,22.46,23.65,22.65,104.7,226.5,0,5,181,2.3,6.7,27.02,25.108
971124,905,12.92,21.64,300,0,15.36,3.4,178,7.3,4.5,24.17,23.42,24.71,23.49,105.1,205.1,0,6,179,3.2,7.2,26.34,25.109
971124,910,12.93,22.5,300,0,16.59,2.7,172,10.2,4.1,24.98,24.3,25.25,24.64,105.2,174.2,0,6.6,183,4.6,8,25.92,25.111
971124,915,12.93,23.44,300,0,16.51,2.5,170,11.7,3.7,25.02,24.29,25.17,24.83,104.7,171.4,0,7.2,193,4.1,7.6,25.45,25.112
971124,920,12.93,24.34,300,0,15.97,2.6,170,14.1,4.2,25.09,24.31,25.54,24.79,105,251.4,0,7.1,196,7.6,7.7,25.52,25.109
971124,925,12.92,25.23,300,0,16,3,190,11.2,3.9,25.71,25.02,26.25,25.35,105.4,268.8,0,6.8,209,3.3,7.6,25.77,25.11
971124,930,12.93,26.13,300,0,14.76,3.2,197,8.4,3.9,26.59,26.04,26.98,26.17,105.9,302.7,0,6.3,205,7.1,7.3,25.68,25.112
971124,935,12.94,27.02,300,0,14.69,3.2,183,8.7,4.3,27.3,26.64,27.59,26.86,106.1,325.3,0,5.4,202,8.6,6.9,25.98,25.112
971124,940,12.93,27.91,300,0,15.22,3.2,188,7.4,3.9,27.58,26.71,27.78,27.35,106,300.3,0,4.7,203,13.2,6.2,26.02,25.114
971124,945,12.93,28.79,300,0,16.16,2.9,189,12.5,4.2,27.61,26.79,27.87,27.46,105.9,266.2,0,4.9,206,10.5,5.9,26.07,25.118
971124,950,12.93,29.68,300,0,15.58,2.2,190,15.7,3.7,27.73,27.06,27.9,27.56,106,346.4,0,4.6,208,7.1,7,26.67,25.12
971124,955,12.93,30.57,300,0,15.48,2.1,190,13.6,3.1,28.12,27.65,28.39,27.82,106.3,298.7,0,3.6,223,12.5,4.7,27.05,25.121
971124,1000,12.93,31.45,300,0,17.16,2.5,180,15,3.8,28.65,28.05,29.01,28.02,106.6,371.5,0,3.6,198,14.5,4.6,27.44,25.12
[illegible]124,1005,12.93,32.37,300,0,16.75,3,182,20.3,5,29.18,28.57,29.45,28.79,106.7,371.5,0,3.3,206,20,4.9,27.94,25.121
[illegible]24,1010,12.93,33.34,300,0,16.04,3.2,188,20.7,5.6,29.56,29.05,29.97,29.32,106.8,371.6,0,4,207,11.6,5.7,28.3,25.122
[illegible]124,1015,12.94,34.3,300,0,14.41,3.5,176,10.2,4.7,30,29.39,30.1,29.92,106.9,367,0,3.2,191,13.9,4.2,28.95,25.123
971124,1020,12.94,35.41,300,0,15.06,2.5,164,15.9,4.8,30.26,29.54,30.53,30.05,106.9,380.1,0,3.2,160,15,4.3,29.46,25.122
```

Datalogger Program

Program: DATALOGU

Programmer: Randy Johnson   Date: Apr. 16, 1996

Update L: 08/07/91 - Shortened output labels
File Name: DATALOGL.DLD
DATALOGL.DOC

Update M: 08/21/91 - Add Calibration flag (Flag 1) and skip around averaging when inputs are out of order or being calibrated.
Signature: 25404
File Name: DATALOGM.DLD
DATALOGM.DOC

Update N: 06/22/93 - Deleted M version additions that set flag 1. The program will recompile and work better with the new edlog also.
File Name: DATALOGN.DLD
DATALOGN.DOC

Update O: 12/06/93 - Changed the nuc. radiation mult. to .002 from .05 to work with the new circuit that uses a one shot multivibrator circuit. Will try for a while to see if it works.
File Name: DATALOGO.DLD
DATALOGO.DOC

Update P: 09/15/94 - The thermocouple inputs were changed to be full differential.

Update Q: 01/11/95 - Changed to allow use of calibrated solar radiation sensors (resistor included at end of cable) with an output of 5mV/1000 W. Requires a new multiplier of 200.

The station number input on the I/O pins is no longer required. The station version dates were removed. This eliminated input locations 1, 2 and 3. These were also removed from the output records.

Update R: 08/15/95 - Changed thermocouple type from type T to type E.

Update S: 02/05/96 - Soil temperatures are no logner used. All reference and instructions associated with soil temp. removed.

Instructions are added to allow a solar radiation standard to compare and calibrate the Licor solar radiation sensor. The difference between the licor and the Eppley is stored in input memory location 2.

Update T: 03/15/96 - New 40 hole choppers are added to the wind speed units so the multiplier used for wind speed was changed.

The old 207 probes were changed to use Visala 0-1v probes.

Update U: 04/16/96 - The precipitation total routine was modified to make sure both the daily and 5 minute totals have been incremented. This fixed a problem caused when a tip came in between the 5 min and daily output total instructions.

Stations:

Stn#	Stn	Type	RF95 Switchs Open
2	ST1	4	2
3	ST2	4	1,2
4	EB1	4	3
5	Rptr	Repeater	1,3
11	BAS	3	1,2,4
12	BIG	3	3,4
13	BLA	3	1,3,4
14	BLU	3	2,3,4
15	CRA	3	1,2,3,4
16	DEA	3	5
17	HAM	3	1,5
18	HOW	3	2,5
19	IDA	3	1,2,5
20	KET	3	3,5
21	MIN	3	1,3,5
22	MON	3	2,3,5
23	NRF	3	1,2,3,5
24	PBF	3	4,5
25	ROV	3	1,4,5
26	SAN	3	2,4,5
27	TER	3	1,2,4,5
28	TRA	3	3,4,5
36	ABE	2	3,6
37	ARC	2	1,3,6
38	DUB	2	2,3,6
39	RIC	2	1,2,3,6
40	ROB	2	4,6
41	RWM	2	1,4,6
42	SUG	2	2,4,6
43	TAB	2	1,2,4,6
	FOR (FORT HALL)		3,4,6
	RES (RES-		1,3,4,6

53	CFA	1	1,3,5,6
54	EBR	1	2,3,5,6
55	GRI	1	1,2,3,5,6
56	LOF	1	4,5,6
57	690	1	1,4,5,6
63	TEST	1	1,2,3,4,5,6

Analog Input Channel Usage:

1.	Nuclear Radiation	**3**
2.	15M Wind Direction	**3**
3.	2 M 107 Temp, 15M T/C	**3**
4.	15M T/C	**3**
5.	2 M Relative Humidity	**2**
6.	Solar Radiation	**2**
7.	Top Wind Dir, Top T/C	**1**
8.	Top T/C	**1**
9.	Barometric Pressure	**1**
10.		
11.	Eppley Radiometer Low	**3**
12.	Eppley Radiometer Hi	**3**

Pulse Input Channel Usage:

1.	15M Wind Speed	**3**
2.	Top Wind Speed	**1**

Excitation Channel Usage:
1. Wind Direction/s
2. Relative Humidity

Control Port Usage, Key *6A0

1.	Address 0	input
2.	Address 1	input
3.	Address 2	input
4.	Address 3	input
5.	Address 4	input
6.	Address 5	input
7.	Precipitation	input
8.	HiVol Control	output

Input Memory Usage, Key *6A

1. Eppley PSP Radiometer W/M
2. Delta Solar (Eppley PSP - Licor) (W/M)
4. Battery Voltage
5. CR10 Temperature
6. HiVol Status
7. Background Radiation
8. 15M Wind Speed
9. 15M Wind Direction
10. 2M Temperature
11. 15M Temperature
12. 2M Relative Humidity
13. Solar Radiation
14. Precipitation
15. Top Wind Speed
16. Top Wind Direction
17. Top Temperature

18. Barometric Pressure
19. Precipitation test word
20.
21.
22. 1 (used to calculate # of measurements)

Output Array 1 Definitions (5 Minute), Key *71A

0.	Station date and time	*4*
1.	Battery Voltage (Volts)	*4*
2.	CR10 Temperature (Deg. C.)	*4*
3.	Repititions in interval	*4*
4.	HiVol Status, average	*4*
5.	Nuclear Radiation (mR/hr)	*3*
6.	15 Meter Wind Speed (MPS)	*3*
7.	15 Meter Wind Direction (Degrees)	*3*
8.	15 Meter Wind Standard Deviation	*3*
9.	15 Meter Wind Gust	*3*
10.	2 Meter Temperature	*3*
11.	15 Meter Temperature	*3*
12.	2 Meter Max Temperature	*3*
13.	2 Meter Min Temperature	*3*
14.	2 Meter Relative Humidity	*2*
15.	Solar Radiation (Watts per square meter)	*2*
16.	Precipitation (inches)	*2*
17.	Top Wind Speed (meters per second)	*1*
18.	Top Wind Direction (degrees)	*1*
19.	Top Standard Deviation	*1*
20.	Top Wind Gust	*1*
21.	Top Temperature (degrees C)	*1*
22.	Barometric Pressure (inches of Mercury)	*1*
23.	Eppley PSP Radiometer (Watts per square meter)	*3*

Output Array Definintions (Daily), Key *72A

0. Date and Time
1. Battery Voltage
2. CR10 Temperature
3. Repititions (86,000 per day)
4. Average Nuclear Radiation
5. Maximum 15M Wind Gust
6. Average 2M Temperature
7. Maximum 2M Temperature
8. Minimum 2M Temperature
9. Average Solar Radiation
10. Total Precipitation for Day
11. Maximum, Top of Tower, Wind Gust
12. Average Barometric Pressure
13. Maximum Barometric Pressure
14. Minimum Barometric Pressure
15. Eppley PSP Radiometer

{5MinData,
BV1t,CRTmp,

```
DPts,HVol,NRad,15S,15D,
15SD,15G,2Tmp,15Tmp,2MaxT,
2MinT,2RH,SRad,Rain,TopS,
TopD,TopSD,TopG,TopT,BP,EpRad}


{DalyData,
BVlt,CRTmp,
DPts,NRad,15G,2Tmp,2MaxT,
2MinT,SRad,Rain,TopG,BP,
MaxBP,MinBP,EpRad}


*      1        Table 1 Programs
  01: 1         Sec. Execution Interval

01:   P20       Set Port(s)
  01: 7888      C8..C5=output/input/input/input
  02: 8888      C4..C1=input/input/input/input

02:   P10       Battery Voltage
  01: 4         Loc [:Batt_Volt]

03:   P17       Module Temperature
  01: 5         Loc [:CR10_Temp]

04:   P30       Z=F
  01: 1         F
  02: 0         Exponent of 10
  03: 22        Z Loc [:One      ]

05:   P25       Read Ports
  01: 128       Mask (0..255)
  02: 6         Loc [:HiVol_On ]

06:   P1        Volt (SE)
  01: 1         Rep
  02: 14        250 mV fast Range
  03: 2         IN Chan
  04: 7         Loc [:NucRad_mR]
  05: 10        Mult
  06: .168      Offset

07:   P3        Pulse
  01: 1         Rep
  02: 1         Pulse Input Chan
  03: 20        High frequency; Output Hz.
  04: 8         Loc [:15M_S_MPS]
  05: .03977    Mult
  06: .26822    Offset
```

```
08:  P4        Excite,Delay,Volt(SE)
  01: 1        Rep
  02: 15       2500 mV fast Range
  03: 1        IN Chan
  04: 1        Excite all reps w/EXchan 1
  05: 1        Delay (units .01sec)
  06: 2500     mV Excitation
  07: 9        Loc [:15M_D_Deg]
  08: .142     Mult
  09: 0        Offset

09:  P11       Temp 107 Probe
  01: 1        Rep
  02: 3        IN Chan
  03: 2        Excite all reps w/EXchan 2
  04: 10       Loc [:2MTemp_C ]
  05: 1        Mult
  06: 0        Offset

10:  P14       Thermocouple Temp (DIFF)
  01: 1        Rep
  02: 21       2.5 mV 60 Hz rejection Range
  03: 2        IN Chan
  04: 2        Type E (Chromel-Constantan)
  05: 10       Ref Temp Loc
  06: 11       Loc [:15MTemp_C]
  07: 1        Mult
  08: 0.0000   Offset

11:  P1        Volt (SE)
  01: 1        Rep
  02: 25       2500 mV 60 Hz rejection Range
  03: 5        IN Chan
  04: 12       Loc [:2M_RelHum]
  05: .10000   Mult
  06: 0.0000   Offset

12:  P1        Volt (SE)
  01: 1        Rep
  02: 13       25 mV fast Range
  03: 6        IN Chan
  04: 13       Loc [:Solar_Rad]
  05: 200      Mult
  06: 0        Offset

13:  P3        Pulse
  01: 1        Rep
  02: 2        Pulse Input Chan
  03: 20       High frequency; Output Hz.
  04: 15       Loc [:Top_S_MPS]
  05: .03977   Mult
  06: .26822   Offset
```

```
14:  P4        Excite,Delay,Volt(SE)
  01: 1        Rep
  02: 15       2500 mV fast Range
  03: 7        IN Chan
  04: 1        Excite all reps w/EXchan 1
  05: 1        Delay (units .01sec)
  06: 2500     mV Excitation
  07: 16       Loc [:Top_D_Deg]
  08: .142     Mult
  09: 0        Offset

15:  P14       Thermocouple Temp (DIFF)
  01: 1        Rep
  02: 21       2.5 mV 60 Hz rejection Range
  03: 4        IN Chan
  04: 2        Type E (Chromel-Constantan)
  05: 10       Ref Temp Loc
  06: 17       Loc [:TopTemp_C]
  07: 1        Mult
  08: 0.0000   Offset

16:  P1        Volt (SE)
  01: 1        Rep
  02: 15       2500 mV fast Range
  03: 9        IN Chan
  04: 18       Loc [:BPres_"Hg]
  05: .17718   Mult
  06: 2362.4   Offset

17:  P37       Z=X*F
  01: 18       X Loc BPres_"Hg
  02: .01      F
  03: 18       Z Loc [:BPres_"Hg]

Multiplier for Eppley
S# 10809F4 = 160 Factory Cal 10/95
S# 15648F3 = 98.814 Factory Cal 1970

18:  P2        Volt (DIFF)
  01: 1        Rep
  02: 23       25 mV 60 Hz rejection Range
  03: 6        IN Chan
  04: 1        Loc [:EppRad    ]
  05: 160      Mult
  06: 0        Offset

19:  P35       Z=X-Y
  01: 1        X Loc EppRad
  02: 13       Y Loc Solar_Rad
  03: 2        Z Loc [:SolarDiff]

Start 5 minute output
```

```
20:  P84        Output Record
  01: 0         Seconds into interval
  02: 300       Seconds interval
  03: 0         No. of records

21:  P70        Sample
  01: 2         Reps
  02: 4         Loc

22:  P72        Totalize
  01: 1         Rep
  02: 22        Loc One

23:  P71        Average
  01: 2         Reps
  02: 6         Loc HiVol_On

24:  P69        Wind Vector
  01: 1         Rep
  02: 0         Samples per sub-interval
  03: 0         Polar Sensor/(S, D1, SD1)
  04: 8         Wind Speed/East Loc 15M_S_MPS
  05: 9         Wind Direction/North Loc 15M_D_Deg

25:  P73        Maximize
  01: 1         Rep
  02: 0         Value only
  03: 8         Loc 15M_S_MPS

26:  P71        Average
  01: 2         Reps
  02: 10        Loc 2MTemp_C

27:  P73        Maximize
  01: 1         Rep
  02: 0         Value only
  03: 10        Loc 2MTemp_C

28:  P74        Minimize
  01: 1         Rep
  02: 0         Value only
  03: 10        Loc 2MTemp_C

29:  P71        Average
  01: 2         Reps
  02: 12        Loc 2M_RelHum

30:  P72        Totalize
  01: 1         Rep
  02: 14        Loc Prec*.01"

31:  P32        Z=Z+1
  01: 19        Z Loc [:PrecpTest]
```

```
32:  P89        If X<=>F
  01: 19        X Loc PrecpTest
  02: 3         >=
  03: 2         F
  04: 30        Then Do

33:  P30        Z=F
  01: 0         F
  02: 0         Exponent of 10
  03: 14        Z Loc [:Prec*.01"]

34:  P30        Z=F
  01: 0         F
  02: 0         Exponent of 10
  03: 19        Z Loc [:PrecpTest]

35:  P95        End

36:  P69        Wind Vector
  01: 1         Rep
  02: 0         Samples per sub-interval
  03: 0         Polar Sensor/(S, D1, SD1)
  04: 15        Wind Speed/East Loc Top_S_MPS
  05: 16        Wind Direction/North Loc Top_D_Deg

37:  P73        Maximize
  01: 1         Rep
  02: 0         Value only
  03: 15        Loc Top_S_MPS

38:  P71        Average
  01: 1         Rep
  02: 17        Loc TopTemp_C

39:  P78        Resolution
  01: 1         High Resolution

40:  P71        Average
  01: 1         Rep
  02: 18        Loc BPres_"Hg

41:  P78        Resolution
  01: 0         Low Resolution

42:  P71        Average
  01: 1         Rep
  02: 1         Loc EppRad

End of 5 minute output
Begin Daily Output
```

```
43:  P84        Output Record
  01: 0         Seconds into interval
  02: 86400     Seconds interval
  03: 10        No. of records

44:  P70        Sample
  01: 2         Reps
  02: 4         Loc

45:  P78        Resolution
  01: 1         High Resolution

46:  P72        Totalize
  01: 1         Rep
  02: 22        Loc One

47:  P78        Resolution
  01: 0         Low Resolution

48:  P71        Average
  01: 1         Rep
  02: 7         Loc NucRad_mR

49:  P73        Maximize
  01: 1         Rep
  02: 0         Value only
  03: 8         Loc 15M_S_MPS

50:  P71        Average
  01: 1         Rep
  02: 10        Loc 2MTemp_C

51:  P73        Maximize
  01: 1         Rep
  02: 0         Value only
  03: 10        Loc 2MTemp_C

52:  P74        Minimize
  01: 1         Rep
  02: 0         Value only
  03: 10        Loc 2MTemp_C

53:  P71        Average
  01: 1         Rep
  02: 13        Loc Solar_Rad

54:  P72        Totalize
  01: 1         Rep
  02: 14        Loc Prec*.01"

55:  P32        Z=Z+1
  01: 19        Z Loc [:PrecpTest]
```

```
56:  P89         If X<=>F
  01: 19         X Loc PrecpTest
  02: 3          >=
  03: 2          F
  04: 30         Then Do

57:  P30         Z=F
  01: 0          F
  02: 0          Exponent of 10
  03: 14         Z Loc [:Prec*.01"]

58:  P30         Z=F
  01: 0          F
  02: 0          Exponent of 10
  03: 19         Z Loc [:PrecpTest]

59:  P95         End

60:  P73         Maximize
  01: 1          Rep
  02: 0          Value only
  03: 15         Loc Top_S_MPS

61:  P78         Resolution
  01: 1          High Resolution

62:  P71         Average
  01: 1          Rep
  02: 18         Loc BPres_"Hg

63:  P73         Maximize
  01: 1          Rep
  02: 0          Value only
  03: 18         Loc BPres_"Hg

64:  P74         Minimize
  01: 1          Rep
  02: 0          Value only
  03: 18         Loc BPres_"Hg

65:  P78         Resolution
  01: 0          Low Resolution

66:  P71         Average
  01: 1          Rep
  02: 1          Loc EppRad

67:  P           End Table 1


*       2        Table 2 Programs
  01: 0          Sec. Execution Interval
```

```
01:  P         End Table 2

*     3        Table 3 Subroutines

01:  P85       Beginning of Subroutine
  01: 97       Subroutine Number

02:  P30       Z=F
  01: 1        F
  02: 0        Exponent of 10
  03: 14       Z Loc [:Prec*.01"]

03:  P4        Excite,Delay,Volt(SE)
  01: 1        Rep
  02: 25       2500 mV 60 Hz rejection Range
  03: 1        IN Chan
  04: 1        Excite all reps w/EXchan 1
  05: 15       Delay (units .01sec)
  06: 2500     mV Excitation
  07: 9        Loc [:15M_D_Deg]
  08: .142     Mult
  09: 0.0000   Offset

04:  P95       End

05:  P         End Table 3

*     A        Mode 10 Memory Allocation
  01: 35       Input Locations
  02: 100      Intermediate Locations
  03: 0        Final Storage Area 2

*     C        Mode 12 Security
  01: 0000     LOCK 1
  02: 0000     LOCK 2
  03: 0000     LOCK 3
```

 Input Location Assignments (with comments):

Key:
T=Table Number
E=Entry Number
L=Location Number

```
T:  E:  L:
1: 18:  1:  Loc [:EppRad    ]
1: 19:  2:  Z Loc [:SolarDiff]
1:  2:  4:  Loc [:Batt_Volt]
1:  3:  5:  Loc [:CR10_Temp]
1:  5:  6:  Loc [:HiVol_On ]
1:  6:  7:  Loc [:NucRad_mR]
1:  7:  8:  Loc [:15M_S_MPS]
1:  8:  9:  Loc [:15M_D_Deg]
3:  3:  9:  Loc [:15M_D_Deg]
1:  9: 10:  Loc [:2MTemp_C ]
1: 10: 11:  Loc [:15MTemp_C]
1: 11: 12:  Loc [:2M_RelHum]
1: 12: 13:  Loc [:Solar_Rad]
1: 33: 14:  Z Loc [:Prec*.01"]
1: 57: 14:  Z Loc [:Prec*.01"]
3:  2: 14:  Z Loc [:Prec*.01"]
1: 13: 15:  Loc [:Top_S_MPS]
1: 14: 16:  Loc [:Top_D_Deg]
1: 15: 17:  Loc [:TopTemp_C]
1: 16: 18:  Loc [:BPres_"Hg]
1: 17: 18:  Z Loc [:BPres_"Hg]
1: 31: 19:  Z Loc [:PrecpTest]
1: 34: 19:  Z Loc [:PrecpTest]
1: 55: 19:  Z Loc [:PrecpTest]
1: 58: 19:  Z Loc [:PrecpTest]
1:  4: 22:  Z Loc [:One      ]
```

Page 14   Input Location Labels:

1:EppRad	6:__________	11:15MTemp_C	16:__________
2:SolarDiff	7:NucRad_mR	12:2M_RelHum	17:TopTemp_C
3:__________	8:__________	13:Solar_Rad	18:__________
4:__________	9:__________	14:Prec*.01"	19:PrecpTest
5:__________	10:__________	15:__________	20:__________

#1160

Replaced ... [illegible]

APPENDIX 14-2 SEMIANNUAL CALIBRATION AND MAINTENANCE FORM

Station GRI Date Start 10-22-97 Date End 10-22-97

Time Start 11:40 Time End 1300

Wind Direction Calibration - Top / 2 meters (Circle Top or 2)

Old serial# H3064 New serial# ________

1. Check orientation on known point(s). Correct if off. Orientation bearing 18.2

   Old value 16.2 Corrected to 18.3

2. Test that the torque is within the 0.11 oz. in spec.
   Remove wind vane and check torque with calibration counterweight.
   If torque lifts counterweight past vertical, replace unit. Make this check with unit in horizontal position.

   Checked OK ✓ Replaced unit ________

3. Check linearity. Using linearity plate, set the wind vane at 180 degrees. Then step through 225°, 270°, 315°, 360°, 0°, 45°, 90°, 135°. Actual values should be within ± 5°.

   180 180.5 225 226.1 270 271.2 315 317.0 360 ______

   0 1.00 45 45.7 90 90.5 135 135.8

   Checked OK ✓ Replaced unit ________

4. Replace wind vane and reorient to known point(s).

Wind Direction Calibration 10/15 meters (Circle 10 or 15)

Old serial# H3085 New serial# ________

1. Check orientation on known point(s). Correct if off. Orientation bearing 18.2
   Old value 17.6 Corrected to ________

Station GRI Date 10-22-97

Wind Direction Calibration 10/15 meters (Circle 10 or 15) (continued)

2. Test that the torque is within the 0.11 oz. in spec.
Remove wind vane and check torque with calibration counterweight.
If torque lifts counterweight past vertical, replace unit. Make this check with unit in horizontal position.

Checked OK ________ Replaced unit ________

3. Check linearity. Using linearity plate, set the wind vane at 180 degrees. Then step through 225°, 270°, 315°, 360°, 0°, 45°, 90°, 135°. Actual values should be within ± 5°.

180 179.9 225 224.2 270 269.8 315 313.9 360 ______

0 1.6 45 45.0 90 90.2 135 135.2

Checked OK ✓ Replaced unit ________

4, Replace wind vane and reorient to known point(s).

Wind Speed Calibration - Top / 2 meters (Circle Top or 2)

Old serial# H1114 New serial# ________

1. This test will check that the torque is within the .003 oz. in spec.
2. Remove cups and check torque with calibration counterweight. If torque lifts weight past vertical, replace unit. Make this check with unit in horizontal position.

Checked OK ✓ Replaced unit ______Bearings______

Wind Speed Calibration - 10/15 meters (Circle 10 or 15)

Old serial# H1118 New serial# ________

1. Test that the torque is within the 0.003 oz. in spec.
2. Remove cups and check torque with calibration counterweight. If torque lifts weight past vertical, replace unit. Make this check with unit in horizontal position.

~~Checked~~ OK BAD Replaced unit ______Bearings ✓

Station GRI Date 10·22·97

Temperature Calibration - Top of Tall Towers

Clip calibration thermometer to aspirator intake and compare thermometer reading to keypad reading. Average reading for 5 min. Replace if difference is greater than ± 1° C.

Thermometer 6.2 minus Keypad 6.0 equals 0.2

Temperature Calibration - 10/15 meters (Circle 10 or 15)

Clip calibration thermometer to aspirator intake and compare thermometer reading to keypad reading. Average reading for 5 min. Replace if difference is greater than ± 1° C.

Thermometer 7.4 minus Keypad 7.2 equals 0.2

Temperature Calibration - 2 meters

Clip calibration thermometer to aspirator intake and compare thermometer reading to keypad reading. Average reading for 5 min. Replace if error is greater than ± 1° C. Replace if delta T for lower level is ± 0.1° C different than delta T at upper levels.

Thermometer 7.9 minus Keypad 7.8 equals 0.1

Precipitation Gage (Annually, usually in Spring. Items 1 and 7 both Spring and Fall)

Serial# 4

1. Remove and clean tipping bucket.
2. Wet down funnel. Reinstall funnel.
3. Measure 230.0 ml of water into drip bottle.
4. Drip at a rate no faster than 1 tip/30sec into funnel. Allow 10 tip to occur.
5. Stop flow of water and measure remaining liquid.
6. Measured amount should be between 34.7 and 54.7 ml. for a 12" diameter gage. Check bucket and fix if incorrect amount.

Number of tips ______ Amount of water left ___-___

This test checks the tipping bucket calibration of 185.3 ml per 0.1 inches of precipitation for a 12" diameter gage.

Fill a plastic bag with ice/water slush. Place the bag in the funnel over the thermostat and verify that the heater turns on.

Station GRI Date 10·22·97

Precipitation Gage (Continued)

7. Thermostat check - to be performed in Fall. The opposite side of the funnel should heat when the thermostat operates correctly. Replace the thermostat if the heater does not heat. Repeat the ice/water test.

Check OK ______ Replaced unit ______

Relative Humidity Calibration

Using sling or battery powered psychrometer and psychometric calculator.

Old serial# ______ New serial# ______

System RH 54.9 Actual RH 50 (as based on dry bulb and wet bulb)

Dry Bulb 46 Wet Bulb 38

Replace if greater than ± 5% difference. Check calibration.

If unit is replaced, recheck calibration

System RH ______ Actual RH ______ (as based on dry bulb and wet bulb)

Dry Bulb ______ Wet Bulb ______

Barometer Calibration

Old serial# 270089 New serial# ______ C

System value 25.077 Actual value 25.050

Replace if off by ± 0.043 inches of mercury. Check calibration.

Checked OK ______ Replaced unit ______

System value ______ Actual value ______

Pyranometer

Clean upper surfaces with a clean, soft cloth and clean water, if needed. Check level and re-level if needed. Re-leveled NO/OK

Station GRI Date 10·22·97

High volume Sampler:

Remote on ok ✓ Remote off ok ✓

Serial Numbers:	Wind Direction Top/2 (Circle Top or 2)	H3064
	Wind Direction 10/15 (Circle 10 or 15)	H3085
	Wind Speed Top/2 (CircleTop or 2)	H1114
	Wind Speed 10/15 (Circle 10 or 15)	H1118
	Precipitation Gage	4
	Relative Humidity	
	Barometer	270089 CD320706
	Pyranometer	PY13763
	CR-10	09108 CD283138
	Radio	924 CD283147
	RF95	1254

Comments:

WS 10 m replaced bearings

Signatures:

ET performing maintenance Thomas W. Stro... Date 10-22-97

Engineer reviewing report Randy Johnson Date 11-20-97

QAO reviewing report Warren ... Date 11-25-97

Attachment 3

THIS PAGE IS AN OVERSIZED DRAWING OR FIGURE,

THAT CAN BE VIEWED AT THE RECORD TITLED:
"TOPOGRAPHIC MAP SHOWING 2-FT CONTOURS AT THE ICPP"

WITHIN THIS PACKAGE

D-01

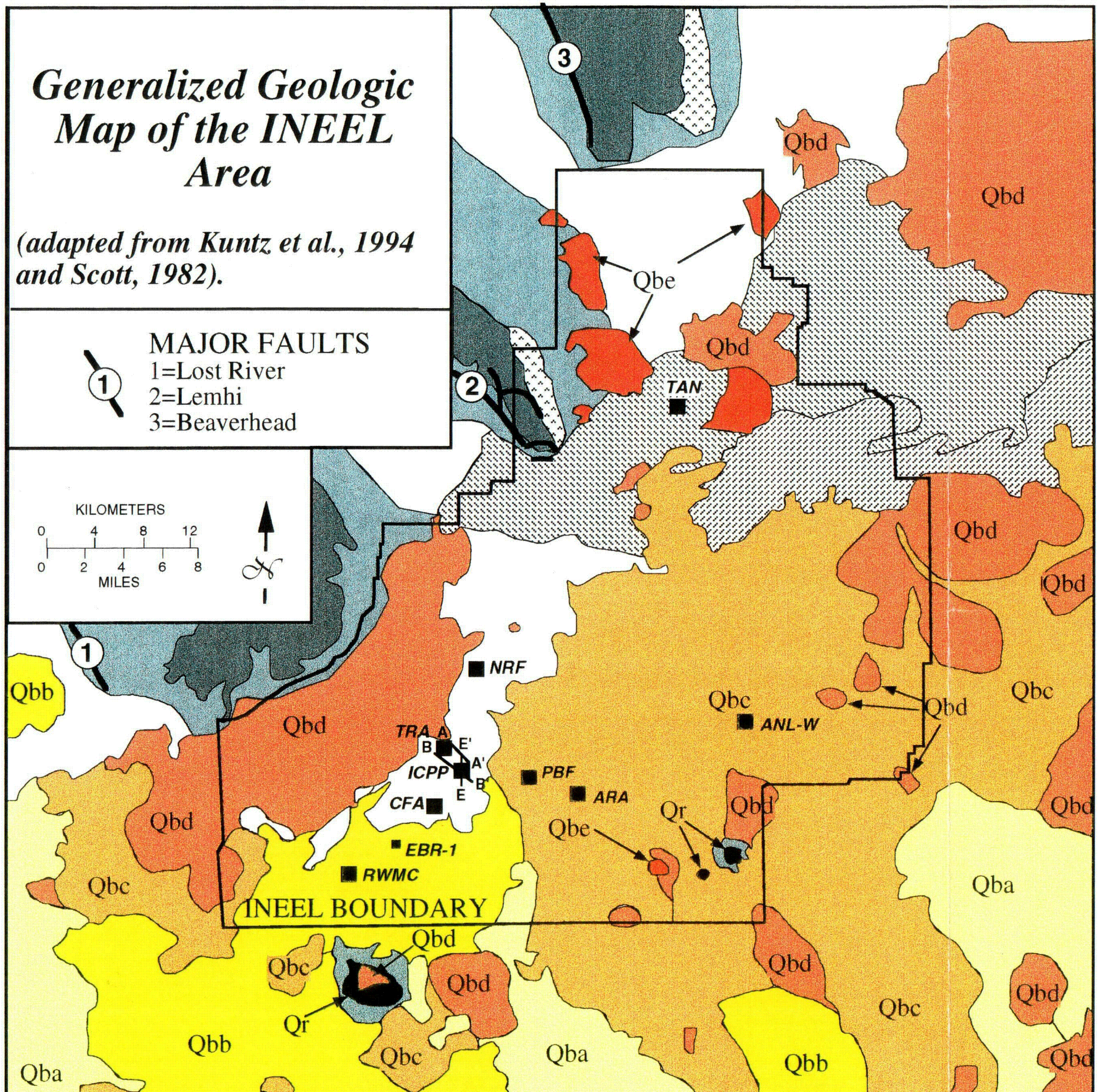

Mainstream Alluvium. Includes deposits of modern flood plains (Holocene) and older deposits in terraces above modern floodplains (upper to middle Pleistocene). Composed mostly of gravel and sand with minor silt and clay. Older deposits host well developed soils and partial to complete loess cover. Up to 20 m thick in southern INEEL, and much thicker in mainstreams to the north.

Alluvial Fans Deposits. Debris flow and stream deposits of clast supported pebble and boulder gravels with matrix of silty sand to clayey silt. Holocene to upper Pliocene. Middle to lower Pleistocene units commonly locally faulted along the west flanks of the Lost River, Lemhi, and Beaverhead Ranges. Includes colluvial debris fans on steep slopes of East, Middle, and Big Southern Buttes.

Eolian Deposits. Very fine to coarse sand in mostly stabilized dunes, 1 to 5 m thick. Some areas of active deflation and migrating sand. Holocene to upper Pleistocene.

Lacustrine Deposits. Mostly lake floor deposits of Pleistocene Lake Terreton. Silty clay to sandy silt. 1 to >100 m thick. Locally includes sandy lake margin deposits and Holocene playa deposits.

BEDROCK UNITS

Basaltic Lava Flows. Black to gray pahoehoe and a'a lava flows, with bedded, oxidized, scoria, cinders, and ash near vents. Locally weathered and oxidized. Olivine basalts composed of crystals of olivine, pyroxene, plagioclase, titanomagnetite, and ilmenite in a matrix of brown glass.

Qba Holocene to uppermost Pleistocene (<15 kyr). No cover of eolian or alluvial deposits.

Qbb Upper to Middle Pleistocene (15-200 kyr). Locally covered by up to 1 m of eolian sand and loess.

Qbc Middle Pleistocene (200-400 kyr). Covered by as much as several m of eolian sand and loess.

Qbd Middle to Lower Pleistocene (400-730 kyr). Mostly covered by several m of eolian sand and loess.

Qbe Lower Pleistocene (>730 kyr) Mostly covered by several m of eolian sand and loess. Reversed magnetic polarity.

Quaternary Rhyolite (Qr)

Qr

Rhyolite Domes. Pleistocene (0.3-1.2 Myr) tan to pink, flow laminated rhyolite, with minor vent breccia and banded obsidian composed of microcrystaline intergrowths of quartz, and alkali fledspar with rare phenocrysts of quartz clinopyroxene, and magnetite.

Tertiary Volcanics

Volcanic Rocks. Basaltic lava flows, rhyolitic ash flow tuffs, and rhyolitic lava flows. Mostly Miocene and Pliocene (~4-12 Myr).

Pre-Tertiary Rocks

Pre-Tertiary Rocks. Late Precambrian to Triassic. Mostly Mississippian shelf carbonates of the Overthrust Belt. Also includes Permian to Triassic fine clastic deposits and phosphatic silts; Cambrian to Ordovician quartzites, sandstone, conglomerates, and siltstones; Devonian dolostones and argillites; and Precambrian sandstones and quartzites.

A E' B A' B' E

Positions at cross sections shown in figures 2.6-14, 2.6-15, and 2.6-16.

9802200317-02

C-02

ATTACHMENT 5

Geologic Age	Formation and Brief Description	Thickness (m)
Quaternary	Surficial deposits of playas (silty sand to clayey silt), floodplains (sandy gravel to silty sand), alluvial fans (sandy gravels to silty sands), and thin eolian blankets (loess and fine sand).	Playas: <30m Floodplains: ~20m on INEEL Eolian: 1-10m
	Rhyolitic lavas, breccias, and obsidians of Big Southern, East, and Cedar Buttes, and an unnamed butte along the axis of the ESRP. 0.3-1.2 Myr.	2500 at Big Southern Butte
Quaternary and Tertiary	**Snake River Group.** Interbedded clastic sediments and basaltic lava flows of the Snake River Plain. Sediments are unlithified to poorly lithified alluvial (gravels, sands, minor silt), lacustrine (silty clays to sandy silts), and eolian (silts and sands) deposits. Basaltic lavas are black to dark gray pahoehoe and minor a'a flows with near-vent scoria, cinder, and ash deposits. Age range - 2 kyr to ~4.5 Myr. Rocks and sediment older than about 1.2 Myr are present only in the subsurface. Comprises almost all of the rocks within the ESRP.	700-1500
Tertiary	Various basaltic lava flows of late-Tertiary age, rhyolitic ash flow tuffs of the **Heise volcanic field** (4.3-7 Myr), older rhyolitic ash flow tuffs (7-12 Myr), and Eocene **Challis volcanics**. All outcrop outside the ESRP in the mountains northwest of the INEEL. Heise and older tuffs occur in deep drill holes within the ESRP.	Total thickness unknown
Triassic	**Dinwoody Fm.** Siltstone and micaceous shale.	>55
Permian	**Phosphoria Fm.** Limestone, chert, phosphatic siltstone, phosphorite, and dolostone.	60
Permian to Mississippian	**Snaky Canyon Fm.** Interbedded limestone, dolostone, and minor sandstone.	1200
Pennsylvanian -Mississippian	**Bluebird Mt. Fm.** Sandstone w/interbedded limestone and minor dolostone. Straddles period boundary.	100
Mississippian	From younger to older, consists of **Bluebird Mtn., Arco Hills, Railroad Canyon, Surrett Canyon, South Creek, Scott Peak, and Middle Canyon Fms.** Mostly fossiliferous limestones w/interbedded sandstones, siltstones, and shales.	1000-1500
Mississippian -Devonian	**McGowan Creek and Three Forks Fms.** Gray argillites, siltstones, and limestones.	64-163
Devonian	**Jefferson Fm.** Sandy to silty gray dolostone and limestone.	60-300
Ordovician	**Fish Haven Dolostone.** Gray, massive dolostone.	18-300
	Kinnikinic Quartzite. Vitreous orthoquartzite.	100-230
	Summerhouse Fm. Quartzite w/calcareous sandstone and siltstone.	0-60
Cambrian	**Tyler Peak Fm.** Sandstone, shale, and quartzite.	265
Precambrian	**Swager Fm, Lemhi Group, and Wilbert Fm.** Arkosic, conglomeratic sandstones and quartzites.	320-400

Notes: ESRP = eastern Snake River Plain. Double lines = unconformities. Precambrian to Triassic units outcrop only in the mountains north and south of the ESRP.

ATTACHMENT 6

Detailed Stratigraphic Column and Shear Wave Velocity Profile for the TMI-2 ISFSI Site.

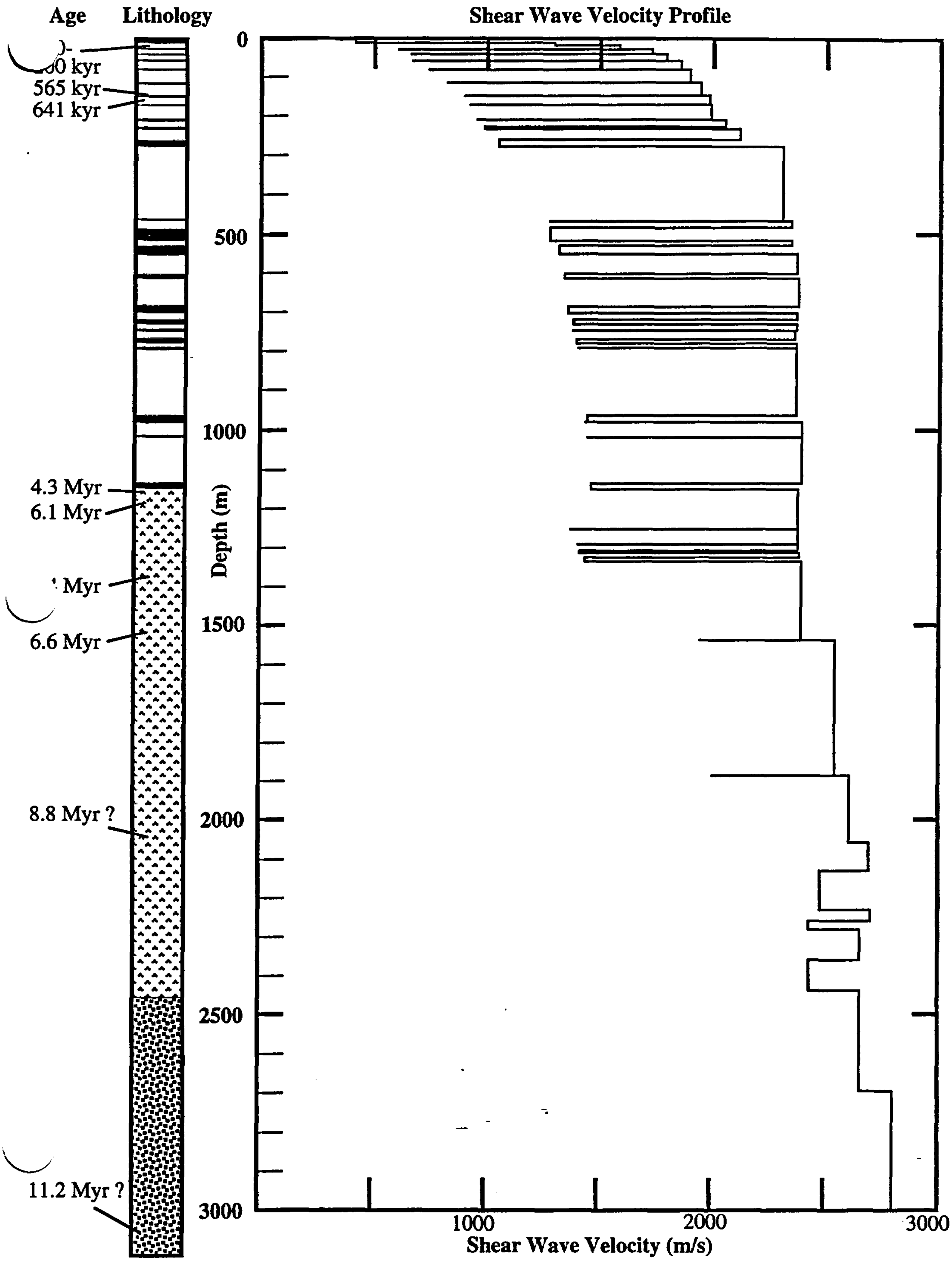

EXPLANATION

Composite lithology from site-specific drilling at the TMI-2 ISFSI site (0-25m), and drill holes USGS-47 (25-200m), USGS-48 (200-230m), ATR Disposal Well (230-365m), WO-2 (230-1524m), and INEL-1 (1524-3130m). Shear wave velocities are measured near the surface (Agbabian Associates, 1995, 1997; Dames and Moore, 1976, 1977; EG&G, 1984; Northern Testing and Engineering, 1987, and Golder Associates, 1992) and calculated from measured compression wave velocities (sonic logs) in INEL-1 and other deep drill holes (2.53).

Basalt lava flows of the Snake River Group. Mostly vesicular pahoehoe with variable fracturing and alteration. Hard, competent rock composed of phenocrysts of olivine, pyroxene, plagioclase, titanomagnetite, and ilmenite in a matrix of brown glass. Subhorizontal platy fracturing near upper and lower contacts, with columnar jointing in interiors of flows. Rubble zones common at upper and lower contacts. Weak hydrothermal alteration and mineral fillings of voids occur near the base of the unit. Age ranges from about 200,000 years near the surface to about 4 million years at the base of the Snake River Group at 1144 m depth.

Sediments of the Snake River Group. Unlithified to poorly lithified clastic, terrigenous sediments. Composed mostly of sandy to clayey silts of eolian origin, and sandy to silty gravels of alluvial origin. Age ranges from latest Pleistocene at the surface to about 4 million years at the base of the unit.

Rhyolitic ash flow tuffs. Mostly welded tuffs of the Heise volcanic field (age 4.3 to ~7 Myr), but also includes rhyolitic welded tuffs that may be older than the Heise volcanics. Thin zones of unwelded tuff (corresponding to low velocity zones) and vitrophyre occur throughout the sequence. Nearly all fractures are sealed by hydrothermal minerals including calcite, quartz, hematite, pyrite, chlorite, and clay minerals.

Rhyodacite. Dense hydrothermally altered and recrystallized aphanitic rhyodacite porphyry. Contains broken and resorbed phenocrysts of plagioclase, sanidine, and quartz. Origin uncertain; could be either a thick welded ash flow tuff or a subvolcanic intrusive rock.

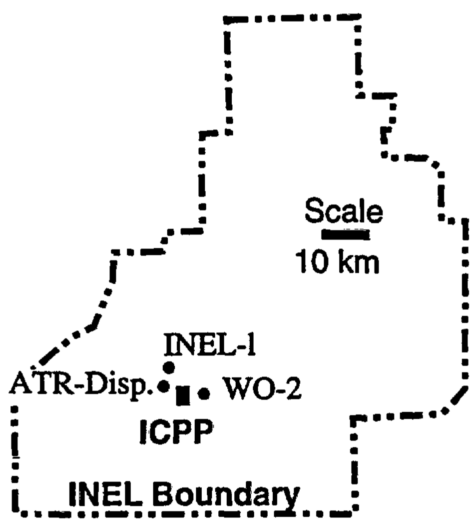

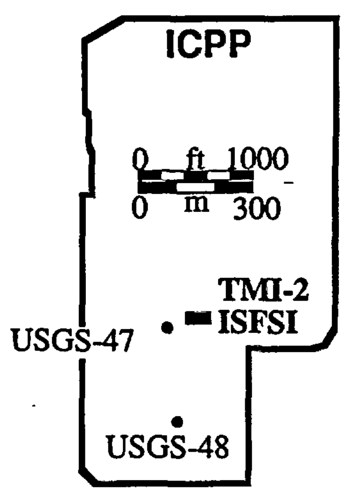

Index maps showing locations of drill holes used in composite stratigraphic sections for the TMI-2 ISFSI site.

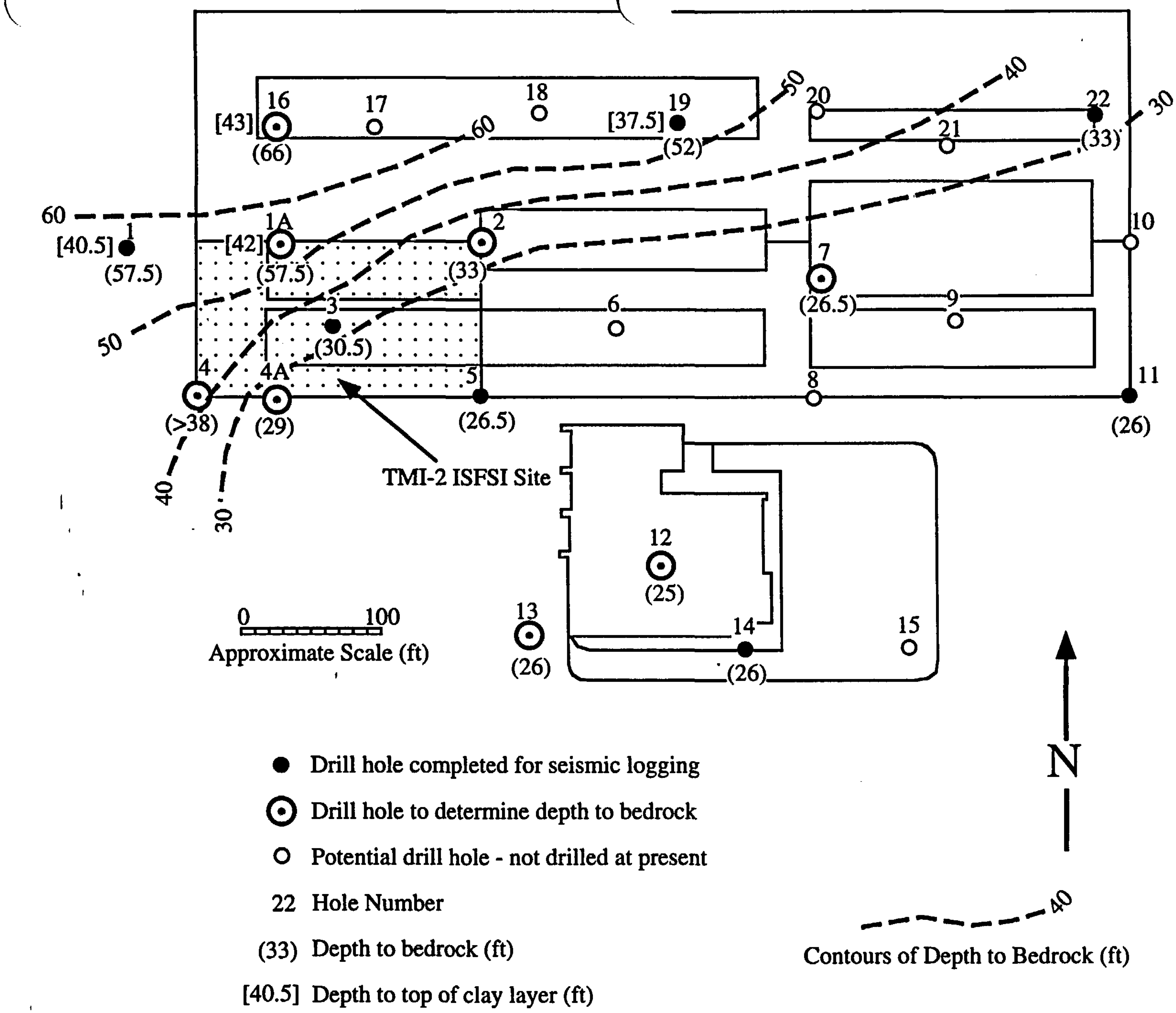

Map of the TMI-2 ISFSI site and immediate surroundings, showing locations of 1997 drill holes and contours of depth to bedrock

ATTACHMENT 7

IT I ruell 8

Idaho National Engineering and Environmental Laboratory

Topography and Wells

Legend

- U.S. Highways
- State Highways
- Light-duty road, hard or improved surface
- Stream
- INEEL Boundary
- Box outlines for facility well maps
- NWI-Mapped Wetlands/ Playas/Spreading Areas
- Cities
- Wells
- Facility area wells

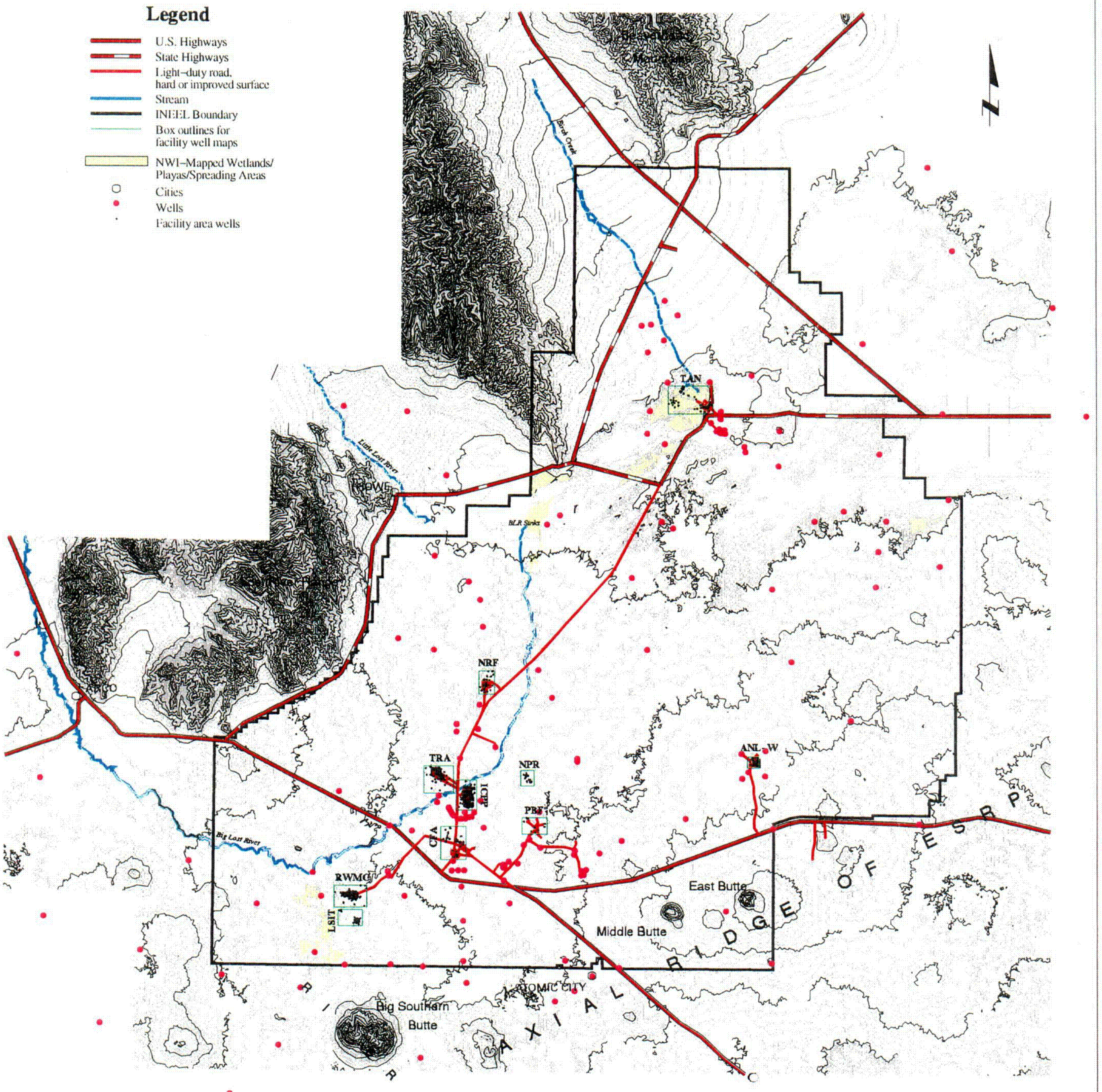

Note: The Big Lost River is prevented by the axial ridge of the ESRP from flowing into the Snake River. The Snake River flows in a southwesterly direction along the ESRP about 30 km to the southeast of the INEEL.

0 10 20 30 Kilometers

0 5 10 15 20 Miles

Contour Interval: 5ft. & 40ft.
Index Contours: 200ft.
Projection: STATE PLANE
Units: FEET
Zone: 3701

INEEL SPATIAL ANALYSIS LABORATORY

Date Drawn : January 20, 1998

(/projects/ineel/contour_maps: 100k_general_wells_anno-ap.aml)

C-03

Attachment 9

THIS PAGE IS AN OVERSIZED DRAWING OR FIGURE,

THAT CAN BE VIEWED AT THE RECORD TITLED: "IDAHO NATIONAL ENGINEERING AND ENVIRONMENTAL LABORATORY TOPOGRAPHY AND WELLS"

WITHIN THIS PACKAGE

D-02

TABLE 1
PAGE 1 OF 2
GEOTECHNICAL TESTING SUMMARY SHEET

BORING	SAMPLE	DEPTH (ft)	USC	PERCENTAGE OF GRAVEL	PERCENTAGE OF SAND	PERCENTAGE OF CLAY/SILT	PLASTICITY LL	PLASTICITY PL	PLASTICITY PI	NATURAL MOIST %	DRY DENSITY (pcf)	SPECIF GRAV	SHEAR STRENGTH phi	SHEAR STRENGTH C (psi)
DC-1		107.3-108.1	SM	2	51	47				35.7				
DC-1		108.1-111.6	CL	1	24	75	26	13	13	25.8				
DC-1		236.6-237.3	SM	0	61	39	NP	NP	NP	32.3		2.68		
DC-1		244.0-244.8	SP-SM	4	85	11				25.9				
DC-1		249.4-250.2	ML	0	44	56	26	23	3	26.6		2.63		
DC-1		257.3-258.5	CL	0	5	95	42	19	23	26.1				
DC-2		70.0-70.6	SM	7	68	25								
DC-2		104.6-105.7	SM	0	72	28				31.1	75.2			
DC-2		236.0-236.7	CL	0	30	70	41	13	28					
DC-2		255.9-256.5	CL	3	6	91	40	16	24					
DC-2		296.5-296.9	SM	4	56	40								
DC-4		112.9-113.9	ML	2	46	52				29.6	86.8			
DC-4		236.6-238.0	SP-SM	13	80	7				36.8	76.4			
DC-4		241.7-243.0	CL	0	9	91	38	18	20	27.9	93.7			
DC-4		248.0-249.0	SM	15	61	24				22.3				
DC-4		254.7-255.3	CL	0	5	95	42	17	25	23.5	97.8			

Note: Blanks indicate that no test was requested.

Golder Associates

Attachment 10 - NPR Site Data

TABLE 2
PAGE 2 OF 2
GEOTECHNICAL TESTING SUMMARY SHEET

BORING	SAMPLE	DEPTH (ft)	USC	PERCENTAGE OF GRAVEL	SAND	CLAY/SILT	PLASTICITY LL	PL	PI	NATURAL MOIST %	DRY DENSITY (pcf)	SPECIF GRAV	SHEAR STRENGTH phi	C (psi)
A-26		147.4-148.1	SM	0	60	40				36.4	75.9			
A-26		156.0-156.5	CL	2	26	72				28.8	91.5			
IC-5		105.0-105.5	CL	0	15	85	26	16	10	19.9				
IC-5		110.6-111.0	CL	1	15	84	30	17	13	24.2				
IC-10		111.8-112.3	CL-ML	1	9	90	27	20	7	26.5				
IC-10		112.3-113.0	CL	2	10	88	29	16	13	26.4				
IC-10		117.9-118.5	CL	2	29	69	34	22	12	27.9				
SI-13		108.7-109.3	CL	1	11	88	32	16	16	20.6	100.6		28	10
SI-13		109.3-110.0	CL	3	24	73	27	16	11	17.7	96.2		28	10
SI-13		110.0-111.0	CL	1	26	73	23	15	8	16.1				
SI-14		104.8-105.8	SM	1	60	39	NP	NP	NP	17.9	110.3	2.79	44	0
SI-14		233.5-235.5	SM	25	33	42	NP	NP	NP	13.4	108.4			
SI-16	(SILT)	107.0-108.9	CL	1	26	73								
SI-16	(SAND)	107.0-108.9	SM	10	66	24								
SI-16		107.0-107.6	ML				NP	NP	NP	29.6	95.3		37	0
SI-16		107.6-108.4	CL-ML				22	15	7	17.0	108.7		37	0
SI-16		110.3-112.3	CL	0	25	75	26	18	8	20.5	105.4		28	10
IC-7		72.9-73.9	SM	32	39	29								
12	12-IC-1	1.0	CL	0	37	63								
12	12-IC-2.4	2.4	CL	0	33	67								
17	17-S-2	2	CL	1	38	61								
17	17-S-4	4	SM	7	51	42								
17	17-S-6	6	CL	0	27	63								
17	17-S-7.3	7.3	SC	2	49	49								

Note: Blanks indicate that no test was requested.

Golder Associates

Attachment 10 - NPR Site Data

Attachment 11

THIS PAGE IS AN OVERSIZED DRAWING OR FIGURE,

THAT CAN BE VIEWED AT THE RECORD TITLED:

"FAULTS, VOLCANIC RIFT ZONES AND HISTORIC EARTHQUAKES IN THE INEEL REGION SHADED RELIEF MAP"

WITHIN THIS PACKAGE

D-03

Attachment 12

THIS PAGE IS AN OVERSIZED DRAWING OR FIGURE,

THAT CAN BE VIEWED AT THE RECORD TITLED:
"EARTHQUAKE EPICENTERS IN THE INEEL REGION 1850 - 1995 SHADED RELIEF MAP"

WITHIN THIS PACKAGE

D-04

Attach 1B

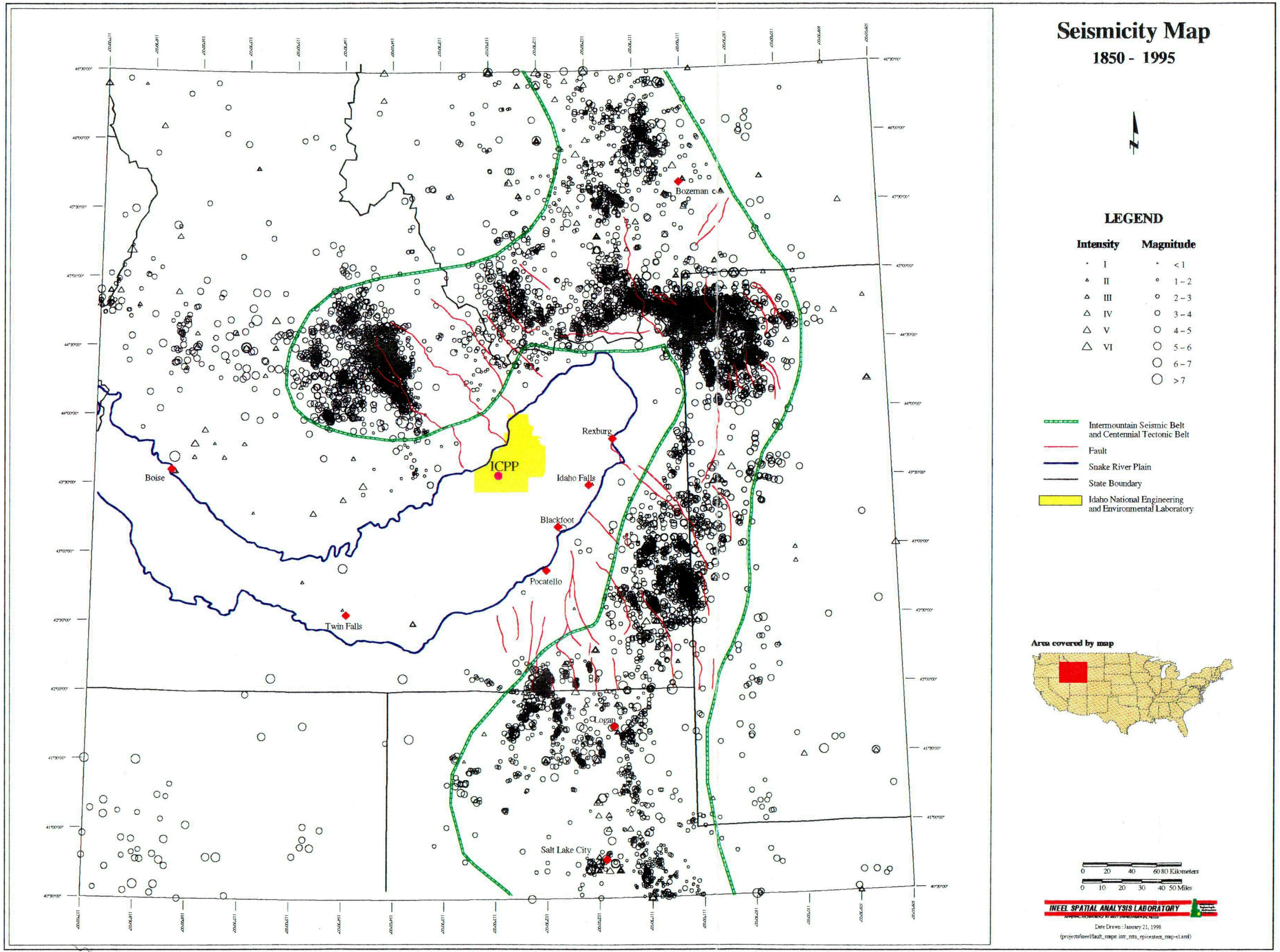

ANSTEC APERTURE CARD

Also Available on Aperture Card

9802200317-06

C-03

Attachment 15

THIS PAGE IS AN OVERSIZED DRAWING OR FIGURE,

THAT CAN BE VIEWED AT THE RECORD TITLED:
"MAP OF INEEL SEISMIC NETWORK STATIONS AND EPICENTERS OF EARTHQUAKES LOCATED IN A 100 MILE RADIUS OF THE CENTER OF THE INEEL, 1972 - 1995
SHADED RELIEF MAP"

WITHIN THIS PACKAGE

D-05

Attachment 14

THIS PAGE IS AN OVERSIZED DRAWING OR FIGURE,

THAT CAN BE VIEWED AT THE RECORD TITLED: "SEISMIC SOURCE ZONES SHADED RELIEF MAP"

WITHIN THIS PACKAGE

D-06

ATTACHMENT 16

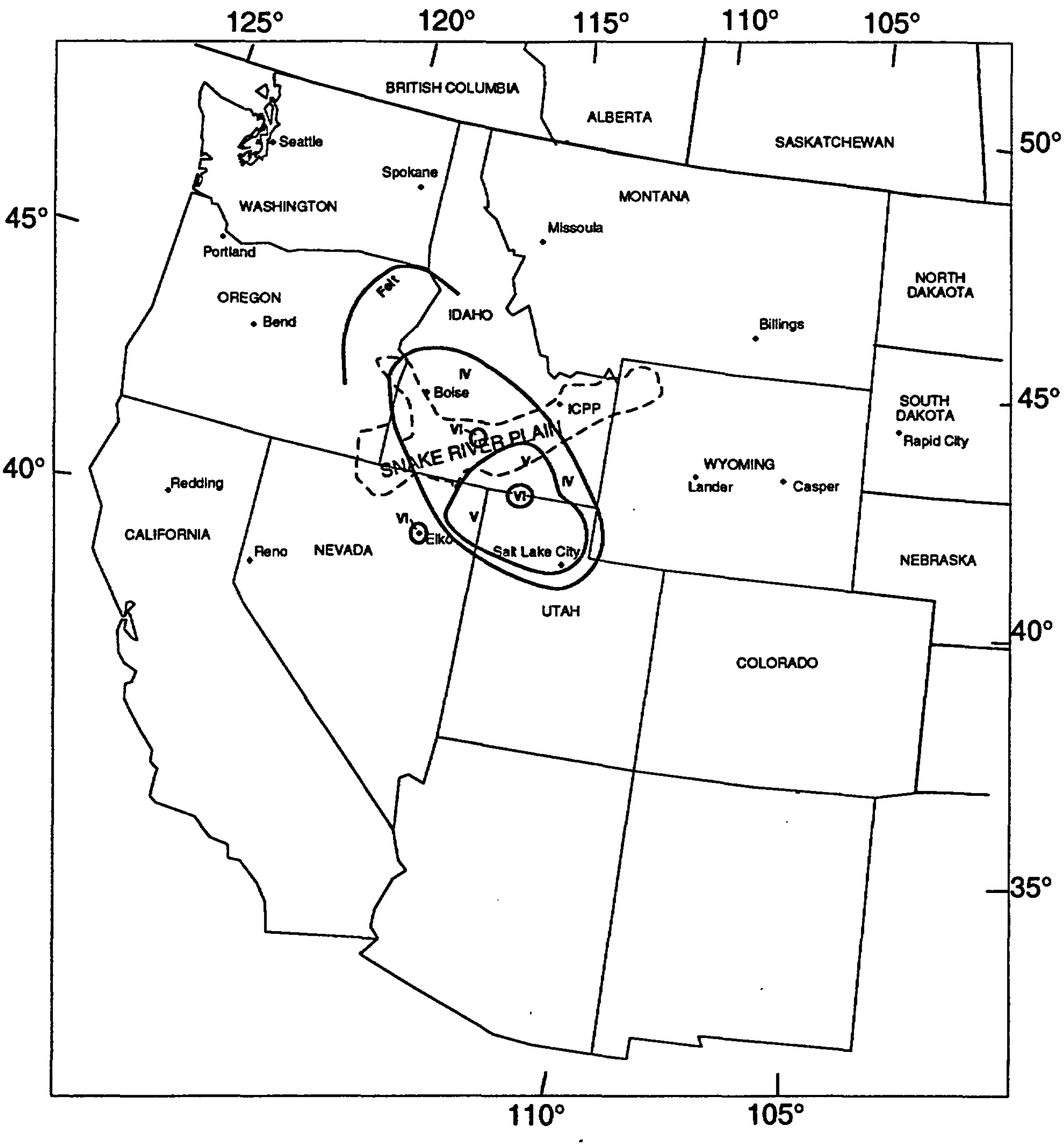

1905 Shoshone Earthquake

ATTACHMENT 17

1983 Borah Peak Earthquake

ATTACHMENT 18

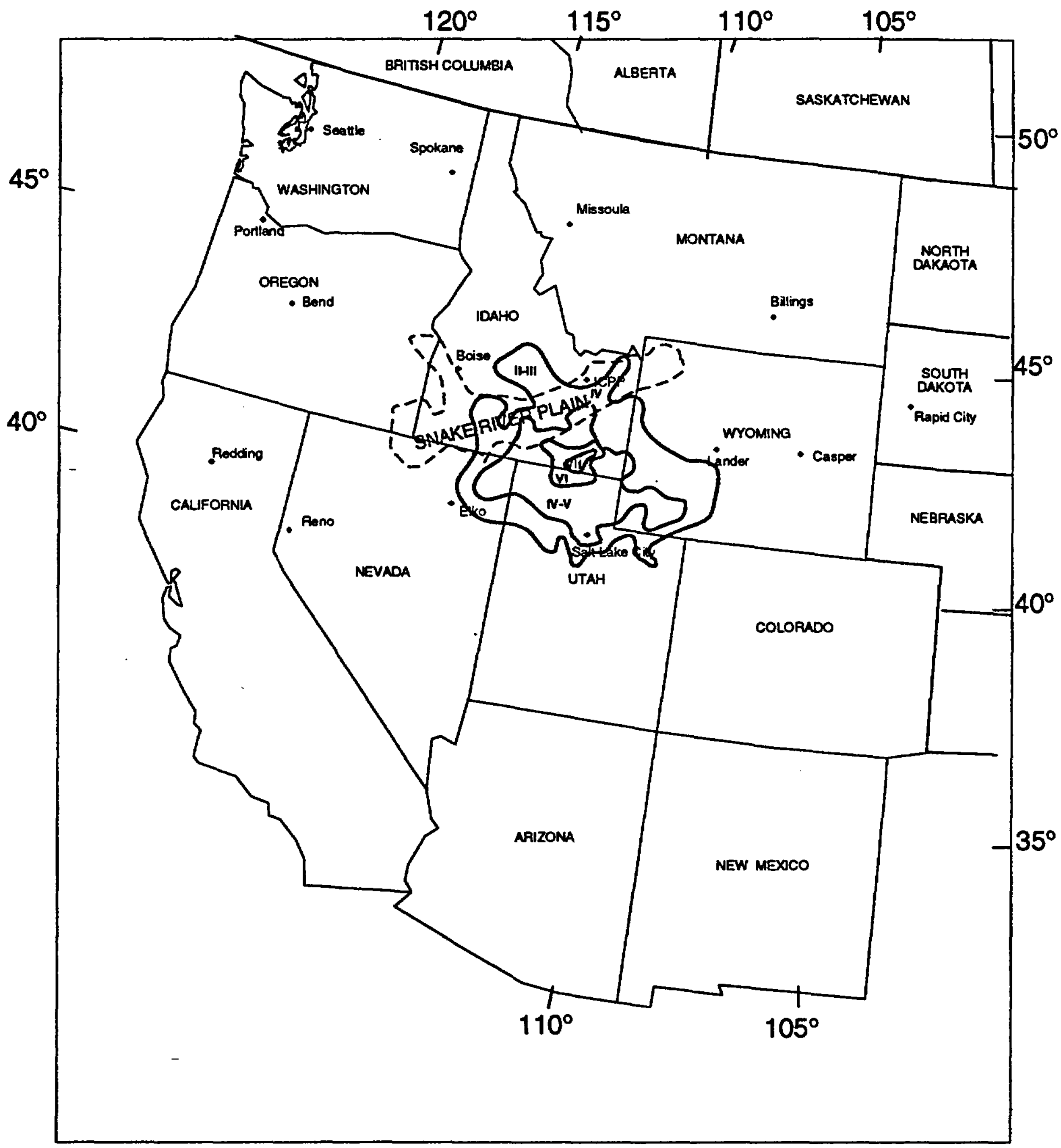

1975 Pocatello Valley Earthquake

ATTACHMENT 19

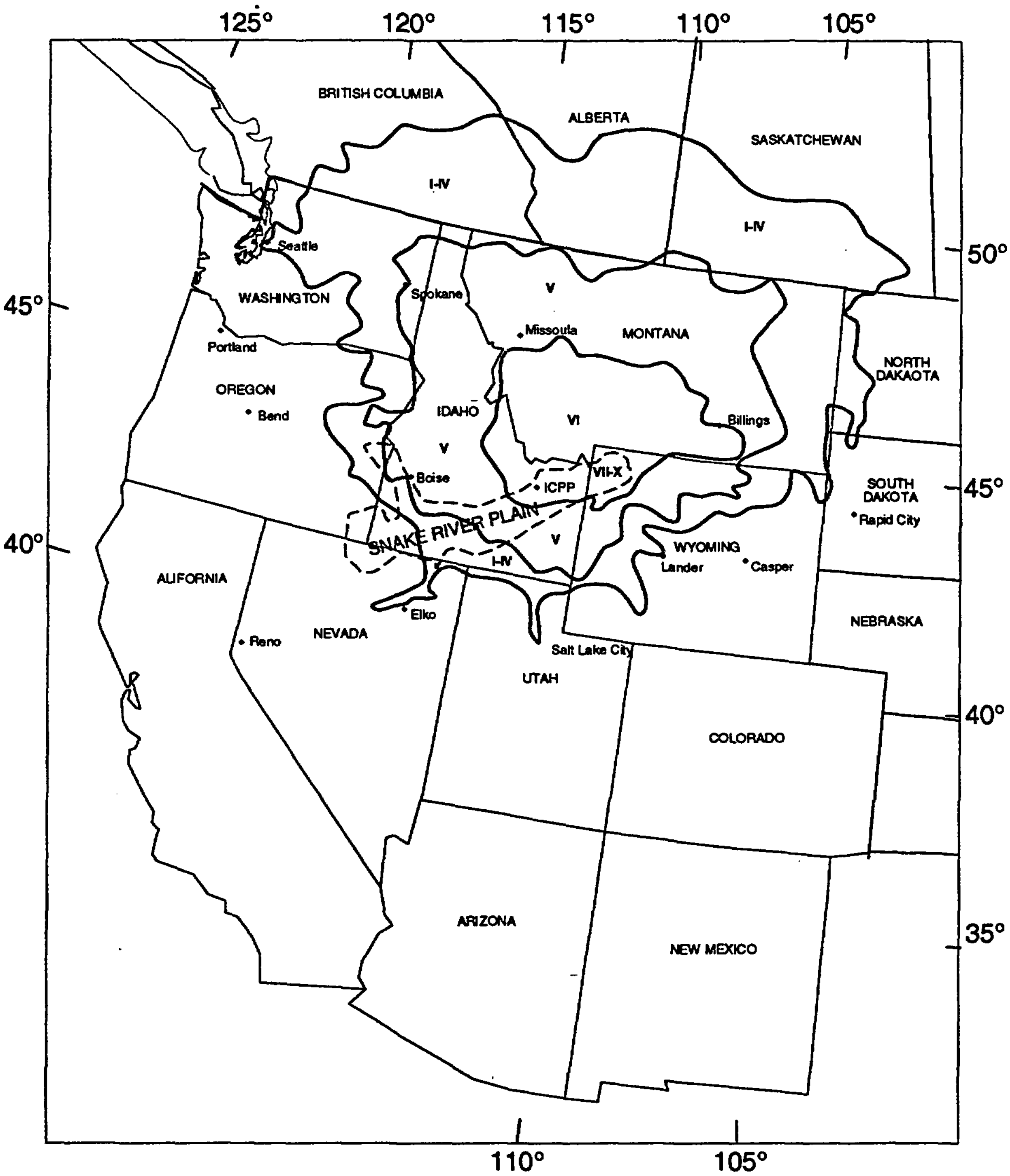

1959 Hebgen Lake Earthquake

ATTACHMENT 20

1975 Yellowstone Park Earthquake

ATTACHMENT 21

1975 Dràney Peak Earthquake

ATTACHMENT 22

2.6.2.2.2 Earthquake Data (Showing Additions and Deletions)

Earthquakes of magnitudes > 2.0 for the time period 1884-1995 (shown in Figure 2.6-17) ~~are~~ were compiled ~~by Woodward-Clyde Consultants [2.52],~~ from the following sources:

Agency	Dates
INEEL	1986-1995
United States Geological Survey (USGS)	1986-1995
Montana Bureau of Mines and Geology (MBMG)	1986-1995
United States Bureau of Reclamation (USBR)	1986-1995
University of Utah Seismograph Stations (UUSS)	1986-1995
Engdahl and Rinehart, (1988; 1991)	1884-1985

The earthquake compilation was initially developed by Woodward-Clyde Consultants [2.52] for the time period 1884-1989. It was updated by Woodward-Clyde Federal Services [2.53] to include earthquakes occurring in 1991 and 1992, and again by Woodward-Clyde Federal Services (1997) to include earthquakes occurring during 1993-1995.

For the central ISB, the earthquake record extends back to November 10, 1884, the date of the first documented earthquake (Richter magnitude (M_L) 6.3), which occurred near Paris, Idaho. Prior to the 1960's, seismographic coverage of the ESRP and surrounding Basin and Range was relatively poor, with only earthquakes larger than magnitude 5.0 recorded by seismographs worldwide. The detection of earthquakes prior to this time was based on felt and damage reports made by local residents. Such epicentral locations may be in error by 100 km or more [2.52]. Over 90 % of the earthquakes shown in Figure 2.6-17 have occurred during 1970-1995. The epicenters have been determined from localized seismic networks within the intermountain region. Epicentral errors for this time period could range from 1 to more than 20 km depending the number and spatial distribution of the seismic stations recording the event.

In the early 1960's, seismographs were installed in the intermountain area by the UUSS and, in 1971, on the ESRP by INEL. The USGS installed and operated a seismic network at Yellowstone National Park, Wyoming from 1970-1981 and, the UUSS, from 1983 to present. Seismic stations were installed near Teton Dam, Idaho (currently operated by Ricks College) beginning in 1980, in southwestern Montana (MBMG) starting in 1981, and in western Wyoming near Jackson Lake (USBR) during 1986. With additional seismic stations, smaller magnitude earthquakes could be detected.

Based on the number of seismic stations operating over specific time intervals, periods of completeness can be established for various magnitudes. The periods of completeness are the time periods over which independent earthquakes (excluding aftershocks) can be considered to be completely detected [2.52]. Table 2.6-3 shows the periods of completeness for various magnitudes of the earthquake data shown in Figure 2.6-17 ~~(~~[based on 2.71; 2.72; 2.73; 2.52]. ~~A listing of earthquake data from 1884 to 1992 is contained in Woodward-Clyde Federal Services [2.53]. A listing for 1992 to present is in preparation.~~ The completeness periods indicate that, for historic times, the data base for larger magnitude earthquakes is more complete than for smaller magnitude events.

2.6.2.2.3 Moderate to Large Earthquakes (Showing Additions and Deletions)

Moderate to large earthquakes of magnitude ≥ 5.5 have occurred within 200-mile radius of the ISFSI site and are shown in Figure 2.6-18. For these events, Table 2.6-4 lists the largest magnitude computed, moment magnitude if computed, and Modified Mercalli intensities ~~which are based on damage at the epicenter~~documented in the vicinity of the ISFSI site. Since earthquakes (M ≥ 2.5) occur at distances greater than 50 km from the ISFSI site, only events of M ≥ 5.5 are listed in Table 2.6-4. ~~Figure 2.6-18 shows their locations relative to basin-and-range normal faults and the ESRP.~~Of the events listed in Table 2.6-4, six have documented effects related to the ISFSI site.

1959 Hebgen Lake Earthquake. The largest earthquake in the region, surface-wave magnitude (M_s) 7.5, occurred within the ISB on August 17, 1959 at Hebgen Lake, Montana (Figure 2.6-18) [2.74]. It was located 190 km northeast of the ISFSI site. The ISFSI site was located in Modified Mercalli intensity zone VI (Figure 2.6-30). Although the earthquake was felt at the INEEL, it caused no damage to INEL facilities [2.75].

1983 Borah Peak Earthquake. The M_s 7.3, Borah Peak, Idaho earthquake occurred on October 28, 1983 in the CTB at a distance of 89km from ICPP. The earthquake resulted from normal faulting along the Lost River fault [2.76]. The epicenter for this event was located in the Thousand Springs valley near the western flank of Borah Peak [2.77]. Substantial damage occurred to masonry structures in the local communities of Mackay and Challis, Idaho near the epicentral area [2.78].

The ISFSI site was located in Modified Mercalli ~~Intensity~~ intensity zone VI during the earthquake (see Figure 2.6-28; [2.78]). Inspections of existing facilities near the ISFSI site following the earthquake revealed no apparent structural or component damage that would compromise structural integrity at ICPP or at the nearby Advanced Test Reactor (ATR). The ATR automatically scrammed without incident when the Plant Protective System's trip was triggered by earthquake ground motions which exceeded the 0.01 g threshold level of the trip [2.75].

Currently, the INEEL operates 24 strong motion accelerographs (SMA's). They are located at various levels (i.e., basement, first floor, roof tops) within critical facilities and at free-field sites (not within buildings). There are five instruments located at the ICPP, two of which are at the FAST facility, only a few 10's of feet from the ISFSI site. Instruments within facilities record the response of the building to the earthquake ground shaking and, at free-field sites, the level of earthquake ground motions at the earth's surface. At the time of the Borah Peak earthquake, the INEEL had 15 SMA's in operation. Peak horizontal accelerations recorded at INEEL ranged from 0.022-0.078 g for basement and free-field sites [2.79].

Table 2.6-5 shows the corrected peak accelerations, velocities, and displacements measured by the SMAs at ICPP facilities which were 89 km from the Borah Peak epicenter [2.80]. See Jackson et al., [2.80] for copies of the corrected acceleration, velocity, and displacement time-histories and response and Fourier spectra for the vertical and two horizontal components for these SMAs.

2.6.2.3.2 Identification and Description of Earthquake Sources: Faults (Showing **Additions and Deletions)**

Faults of several ages and origins occur in the INEL region. Some of them are old and inactive, presenting no earthquake threat, whereas others are capable of generating earthquakes that could affect INEL facilities. Detailed correlation of faults with earthquakes is presented in Section 2.6.2.3.4 - Correlation of Earthquake Activity with Geologic Structures or Tectonic Provinces.

Mesozoic thrust faults occur in the mountain ranges bordering the ESRP (Figure 2.6-4; [2.40; 2.39]). They formed during a period of east-directed thrusting related to the Sevier orogeny. They are gently westward-dipping structures that separate major Paleozoic thrust sheets. These faults are mostly inactive at the present time because the compressional forces that created them at about 60 Ma are no longer in existence. However, it is possible that steeply dipping parts (ramps) of some of the thrust faults have been reactivated by basin-and-range normal faults in Late Tertiary to Recent times [2.90].

Eocene to Oligocene normal faults trend northward across the Lost River, Lemhi, and Beaverhead ranges north of the ESRP [2.91]. Although these faults have several kilometers of accumulated displacement, their orientation with respect to the present stress field is such that they have little tendency for movement. Therefore they are not active today and pose no threat for earthquake hazards.

Basin-and-Range normal faults (Figure 2.6-19) of Miocene to Recent age bound the present northwest trending mountain ranges north and south of the ESRP [2.92]. These faults have accumulated 1 to 3 km of displacement in the past 4-7 Ma and are still active today as evidenced by fault scarps cutting latest Quaternary and Holocene alluvial fan deposits and by the occurrence of the 1983 Borah Peak earthquake. Table 2.6-6 summarizes the important characteristics of most Basin-and-Range normal faults around the ESRP.

The closest of these faults to INEL facilities, the Lost River, Lemhi, and Beaverhead faults (Figure 2.6-19), each bound the southwest side of a mountain range, producing typical Basin-and-Range half graben. These are large normal faults that extend from the northern margin of the ESRP northwards to the Salmon River. Based on seismic and paleoseismic investigations, they are capable of generating earthquakes of magnitude 7 or larger [2.93; 2.94]. Because of their size, activity, and proximity to many INEL facilities, they control much of the INEL seismic hazard.

Lemhi fault. Detailed paleoseismic and structural investigations have been performed on the southern Lemhi fault [2.94 and 2.95]. Results are:

1. Segmentation of the southern Lemhi fault is redefined based on timing of paleoseismic events and on detailed mapping of the structure of the fault in bedrock and surficial deposits (Figure 2.6-20).

2. The most recent earthquake events on the various segments ranges from ~~17~~15,000 to ~~25~~24,000 years ago (Figure 2.6-21).
3. There is evidence for temporal clustering of earthquake events (ie clusters of several events over a few thousand years separated by long intervals (10's of thousands of years) of quiescence.
4. Maximum magnitudes of earthquakes in the southern part of the fault is ~~about~~ M_w7.15 [2.52, 2.53].
5. Bedrock structural features of the southern part of the fault suggest that Quaternary displacement dies out at the south end of the Lemhi Range and that significant seismogenic fault movements do not extend onto the ESRP (Figure 2.6-22). Seismic reflection lines along the extended trace of the fault onto the ESRP also show that recognizable offset of rock layers does not extend for more than 1 km from the end of the range [2.96]
6. The horizontal distance from the inferred southern termination of the fault to the TMI-1 ISFSI is approximately 26.5 km.
7. The best estimate of ~~s~~Slip rate ~~estimates~~ for the southern segment of the fault range from 0.15 mm/year~~ to 1.0 mm/yr~~. In the 1996 probabilistic seismic hazard investigation the slip rate is allowed to range up to 1 mm/year to account for uncertainties in temporal clustering characteristics [2.53].

Lost River fault. The Lost River fault is slightly farther from the ISFSI site than the Lemhi fault, but poses similar seismic hazard because potential maximum magnitudes are slightly larger. Detailed paleoseismic and structural investigations of the segments closest the INEL, the Arco and Pass Creek segments [2.95; 2.97; 2.98], produced the following results:

1. Activity on both segments is younger than previously believed. The ages of the two most recent events on the Arco segment are between 21±4 and 20±4 Ka (±2σ), and the ages of the three most recent events on the Pass Creek segment are between 18±3 and 17±4 Ka. Because of the overlap in age estimates (within 2σ), the two most recent events on both segments may have been contemporaneous.
2. Ages of individual earthquake events indicate temporal clustering (i.e., clusters of several events over a few thousand years separated by long intervals [tens of thousands of years] of quiescence). Recurrence intervals vary from around 1000 years or less to 40,000 years or more on both segments.
3. Paleomagnitude estimates based on vertical displacements yield a range of moment magnitudes (M_W) from 6.6 to 7.3 for the Arco segment and 6.7 to 7.5 for the Pass Creek segment. The range of values results from assumptions as to whether measured displacements represent average or maximum values of displacement. Maximum magnitude estimates based on segment length for the Arco segment are M_W 6.6-6.8 and for the Pass Creek segment M_W 6.7.
4. The Arco segment may extend south of the terminus of the Lost River range for several kilometers onto the ESRP and into the northwestern end of the Arco volcanic rift zone.
5. The horizontal distance from the southern exposed trace of the fault to the INEL TMI-2 ISFSI is 29 km.

6. The best estimate of s~~S~~lip rate ~~estimates~~ for the southern segment of the fault is 0.12 mm/year. In the 1996 probabilistic seismic hazard assessment slip rate was allowed to range from 0.05 mm/year to 1.0 mm/year to account for uncertainties in temporal clustering characteristics.

Beaverhead fault. Although considerably farther from the INEL TMI-2 ISFSI (~52 km) than the Lemhi and Lost River faults, earthquakes on this fault will contribute to the probabilistic hazard assessment. No trenching investigations have been done for the fault, but surface mapping and studies of scarp characteristics [2.99; 2.100] furnish general information about its paleoseismology. The southernmost two segments of the Beaverhead fault (the Blue Dome and Nicholia segments), those closest to the INEL, seem to have quite different faulting histories. The Blue Dome segment (the southernmost segment) has no scarps in alluvium, even though the range front is steep and straight, suggesting geologically recent faulting. Both the range front morphology and the lack of scarps in alluvium suggest that the most recent surface faulting predated about 100,000 years BP. In addition, the exposure of bedrock on both sides of the fault scarp at the southern end of the range suggests that total vertical displacement is much smaller here than in segments farther north. Slip rate estimates for the Blue Dome segment range from 0.02 mm/year to 0.3 mm/year. In contrast, the Nicholia segment (the next segment to the north of the Blue Dome segment) is characterized by scarps that cut all alluvium except Holocene alluvium. In fact, scarps in Pinedale-age alluvium suggests that the most recent earthquake event was about 15,000 years ago and slip rate estimates range up to 1.0 mm/year.

Grand Valley-Star Valley fault. Although this fault is located at great distance from the INEL area it may also contribute to the probabilistic hazard. Field investigations by Anders and others [2.81], Piety and others [2.101], and McCalpin and others [2.102] have shown that the northern part of this fault system was very active from about 4 to 2 million years ago, but since then has been inactive. The southern end of the fault, in the Alpine and Star Valley area, however, has experienced late Pleistocene and Holocene earthquake activity.

An additional point of interest for this fault is the interpretation by some authors that it extends onto the ESRP as far as the town of Rexburg [2.103]. If this interpretation is true, and if the associated displacement is late Pleistocene or Holocene, then the fault could have considerable significance from a tectonic perspective, and the reason(s) for its extension onto the Plain must be understood because of the implications for faults closer to INEL.

The northwest boundary of the ESRP has been investigated as a possible source of earthquakes that could contribute to the seismic hazards of INEL facilities [2.104]. The abrupt termination of northwest-trending mountain ranges at the margins of the ESRP (Figure 2.6-2), the abrupt discontinuity seen in some refraction seismic sections across the boundary [2.105; 2.84], and the aseismic nature of the ESRP compared to the surrounding seismically active mountainous regions [2.81] all suggest that some sort of discontinuity exists at the ESRP margins. Several mechanisms can be envisioned for boundary faults along the margins of the the ESRP. These mechanisms include: 1. normal faulting caused by extension perpendicular to the axis of the ESRP [2.106], 2. strike-slip faulting caused by differential extension between the ESRP and the surrounding basin and range province, 3. scissors faulting caused by rotation of Basin and Range mountain blocks against non-rotating crust in the ESRP, and 4. caldera collapse faulting caused by large-volume silicic eruptions during the development of the Heise volcanic field [2.107, 2.108; 2.109; 2.33).

No support for the normal faulting mechanism (mechanism 1) has been discovered during the 3 decades of investigations since 1964. In fact, the realization that the formation of the ESRP is related to migration of the crust over the Yellowstone hotspot [2.29; 2.32], the lack of any geologic evidence for large normal faults along the margins of the ESRP [2.110; 2.111], and the determination that the entire region is subjected to northeast-directed extension [2.43] has removed any support for normal faults at the boundary of the ESRP. In fact the ESRP is a broad subsiding volcanic basin and bears very little resemblance to continental rifts, such as the Rio Grande Rift or the East African Rift, which are large graben structures bounded by normal faults. Support for the strike-slip faulting mechanism (mechanism 2) also does not exist. In fact, recent strain-rate (extension-rate) estimates for the ESRP [2.70] are consistent with those estimated for areas outside the ESRP [2.69] (see section 2.6.2.2.1 for additional discussion). Although the scissors faulting mechanism (mechanism 3) seems conceptually viable, the amount of displacement that might accumulate over the past million years or so will likely be less than 500 meters, and will be very difficult to recognized in geologic materials. To date, no evidence for such faults exist. Geologic and geophysical evidence exists for the presence of caldera boundary faults (mechanism 4) beneath the ESRP. See the section below entitled "Late Tertiary caldera boundary faults" for a discussion.

While it is true that a NE-trending fault or faults may exist at depth [2.105], the only suggestion of active faulting consists of the presence of a small NE-trending topographic scarp on an alluvial fan on the SE side of the Arco Hills [2.55]. That scarp was trenched in 1989 by the Idaho Geological Survey under contract to EG&G Idaho. The resulting trench logging showed that no faulting occurs there [2.112] and that the scarp was formed by some surficial processes, perhaps eolian modification of a fire scar.

Non-tectonic lineaments on and near INEL can be observed from the air, on aerial photographs, and on satellite images. One of the most pronounced of these lineaments, the Principal Lineament, has been studied extensively and shown to be caused by eolian modifications to a large fire scar [2.113]. This process produces many lineaments and perhaps even small topographic scarps on the ESRP. Other lineaments are caused by unmodified fire scars, linear stream drainages, alignments of vegetative or soil contrast with unknown causes, fluvial (stream, river) deposits, paleoflood deposits, and eolian deposits (dunes) [2.114; 2.112]. A discussion of lineaments near the ISFSI site is presented in Section 2.6.3.2 - Evidence of site fault offset.

Late Tertiary caldera boundary faults are postulated to exist in the silicic volcanic rocks beneath the Snake River Group. There are several bases for this postulation:

1. Calderas like those that exist on the Yellowstone Plateau today must have been associated with the late-Tertiary silicic volcanic fields occurring along the margins of the ESRP.
2. In some areas (southern ends of the Lemhi and Beaverhead Ranges near INEL, and northern ends of the Caribou and Snake River Ranges near Rexburg) structures interpreted to be caldera boundary structures have been recognized [2.107].
3. The great thicknesses of silicic volcanic rocks observed in INEL deep exploration holes, INEL-1 and WO-2 (Figure 2.6-11), suggest that they were emplaced into an intra-caldera setting.

The exact sizes, shapes, and locations of the buried calderas is uncertain, but interpretations have been made (Figures 2.6-6 and 2.6-19) on the basis of geophysical anomalies, positions of volcanic fields, flow-direction indicators in ash flow sheets, and paleomagnetic data [2.107; 2.115]. Several general observations are possible, however. Caldera size is such that some of them are likely to span the entire width of the ESRP. Caldera shape, and thus the configuration of associated caldera boundary faults, are generally circular to oval. Given the tendency for calderas to overlap each other (Figures 2.6-6 and 2.6-19], it is likely that most of the ESRP boundary is characterized by caldera boundary faults buried beneath the edges of the Snake River Group. Caldera boundary faults can explain, in a manner consistent with data and concepts, Pankratz and Ackermann's [2.105] interpreted buried fault along the northwest margin of the ESRP.

Several lines of evidence, summarized in section 2.6.6.2.1, show that the calderas are no longer active because the causative heat source has moved to a new position beneath Yellowstone. The possibility of reactivation of the faults due to contemporary tectonism should be considered, but does not seem to be a cause for concern for two reasons. 1. Since the faults have a circular to oval configuration, they are not likely have long sections oriented properly for movement in contemporary stress fields. 2. No late-Pleistocene or Holocene faulting that could be related to reactivation of these faults is observed on the ESRP [2.114].

2.6.2.3.3 Identification and Description of Earthquake Sources: Volcanic Rift Zones and Axial Volcanic Zone (Showing Additions and Deletions)

Volcanic vents on the ESRP are concentrated in NW-trending and NE-trending linear belts (Figure 2.6-10). The NW-trending belts have associated ground deformation features and are referred to as volcanic rift zones (VRZ's). The ground deformation features are fissures, faults, grabens, and monoclines that form due to dilational stresses above the tops of basalt dikes as magma moves from depth to the surface. Three well defined volcanic rift zones occur in the INEL region of the ESRP, the Great Rift VRZ (which extends southeastward from Craters of the Moon National Monument), the Arco VRZ (which extends SE from Arco across the southwestern corner of the INEL), and the Lava Ridge-Hells Half Acre VRZ (which extends from the south end of the Lemhi Range to the Hells Half Acre lava field) (Figure 2.6-10). In addition, a fourth volcanic rift zone, the Howe-East Butte VRZ, has been postulated, but it is an ill-defined zone consisting only of a few vents that are several hundred thousand years old [2.45].

By analogy with active volcanic rift zones in other parts of the world (for example, Iceland and Hawaii), it can be inferred that volcanic rift zones are sources of earthquakes during periods of volcanic activity (see section 2.6.6 - Volcanism). The magnitudes of volcanic rift zone earthquakes are small (M<5.5), but because of their proximity to INEL facilities their contributions to both deterministic and probabilistic seismic hazards have been assessed [2.52; 2.53].

Some volcanic vents on the ESRP are concentrated in a northeast-trending zone along the axis of the ESRP (Figure 2.6-10). This is called the Axial Volcanic Zone (AVZ) to distinguish it from volcanic rift zones. It is important to make this distinction because the AVZ does not contain northeast-trending ground deformation features that would qualify it to be a volcanic rift zone. The few ground deformation features that do occur in the AVZ are NW-trending fissures. This indicates that the volcanic vents in the AVZ are fed by NW trending dikes and that, even though it is not a volcanic rift zone, seismicity can be associated with volcanism there. Thus it also ~~plays an important role~~ has been evaluated in deterministic and probabilistic seismic hazards assessment [2.52; 2.53].

2.6.2.3.5 Showing Additions and Deletions

2.6.2.3.5.1 Lemhi Fault - ~~South Creek~~Howe Segment

The ~~South Creek~~Howe segment, located at the southern end of the Lemhi fault, is closest part of the Lemhi fault to INEL (Figure 2.6-32). The ISFSI site is located about ~~20~~ 26.5 km from the closest point of rupture along the Howe ~~fault~~ segment [2.~~51~~53]. The most recent event (MRE) occurred between 15,000 and 24,000 years ago [2.94]. The lengths of the Howe and Fallert Springs (the segment just to the north of the Howe segment; Figure 2.6-21) segments are approximately 15-20 km and 25-30 km, respectively [2.160; 2.161; 2.99]. Recent paleoseismic investigations (four trenches excavated across the segments) by Woodward-Clyde Consultants [2.52; 2.94] indicate that the MRE could have ruptured portions of both the Howe and Fallert Springs segments resulting in a total length of 35 km. For the MRE, maximum and average displacements are 2.5 m and 1.5 m, respectively [2.94]. The maximum magnitude estimated for the southern Lemhi fault is 7.15 based on empirical data from Wells and Coppersmith [2.143] using: 1) surface rupture length; 2) subsurface rupture length, 3) rupture area (length x downdip extent; 31 x 21 km; Figure 2.6-33); 4) maximum displacement; and 5) average displacement [2.52; 2.53]. The slip rate of 0.1 mm/yr for both the Howe and Fallert Springs segments is lower than the estimated 0.3 mm/yr for the Thousand Springs segment of the Lost River fault indicating that the Howe segment is less active [2.76].

2.6.2.3.5.2 Lost River Fault - Arco Segment

The Arco segment is located at the southern-most end of the Lost River fault and is the closest part of the fault to INEL (Figure 2.6-32). The north and south ends of the Arco segment have been mapped at different locations by various investigators. The northern terminus was orginally mapped at King Mountain [2.55; 2.164], but has more recently been established at Ramshorn Canyon [2.76; 2.162; 2.91; 2.97]. Woodward Clyde Federal Services [2.53] use the Ramshorn Canyon terminus in their detailed analysis of fault behavior. The location of the southern terminus is less certain. Fault structures are mapped along the main range front to a point about 1 km south of Arco, where they disappear under alluvium in the Arco Basin (21 km total length, 9 km west of the INEL boundary). Additional scarps are mapped about 2 km south of the range-front scarps in an area west of Butte City [2.92]. Most evidence [2.163; 2.53] supports a location just west-southwest of Butte City (25 km total length, 7 km west of the INEL boundary). Wu and Bruhn [2.97] suggest that the terminus may lie 7 km southeast of Butte City at a set of monoclinal flexures in the northwestern end of the Arco volcanic rift zone (30 km total length, 1 km west of the INEL boundary).

The most recent and penultimate events on the Arco segment occurred between 21±4 Ka and 20±4 Ka, possibly with contemporaneous rupture on the Pass Creek segment to the north. ~~The best estimate of~~ M~~m~~aximum magnitude estimates for the Arco segment ~~is M_W7.0, with uncertainty of about ±¼ of a magnitude unit~~range from 6.6 to 7.3 [2.98]. The uncertainty in magnitude is due to uncertainty in rupture length, uncertainty in assumptions that the measured displacements represent average or maximum values, and the apparent discrepency between length-based and displacement-based magnitudes (See section 2.6.2.3.2 and reference 2.98 for further details). The net vertical displacement at the Arco Peak site (on the Arco segment) averages 1.2 to 1.5 meters per event. The ~~average vertical~~best estimate of slip rate between 58 and 20 Ka is 0.12 mm/year [2.76; 2.98].

2.6.2.3.5.3 Beaverhead Fault - Blue Dome Segment

The Blue Dome segment is located at the southern-most end of the Beaverhead fault (Figure 2.6-32). The ISFSI site is located ~~45-50~~52 km from the closest point of rupture along the Blue Dome segment. ~~Based on scarp morphology~~Stickney and Bartholomew [2.66] estimate~~,~~ the MRE ~~occurred~~ at more than 30,000 years ago ~~[2.66]~~. More ~~r~~Recent ~~unpublished~~ mapping in the area suggests that it has not been active for several hundred thousand years because no scarps are present on Quaternary alluvial fans [2.99; 2.100]. The length of the segment is estimated to be about 25 km [2.99]. ~~Since no detailed paleoseismic investigations have been conducted along this segment and faults northwest of INEL are undergoing similar deformational processes,~~ Woodward-Clyde Consultants [2.52] estimates a maximum magnitude of 7.0 for an earthquake on along the Blue Dome fault based on analogy to the Lemhi and Lost River faults further to the west. ~~No data are available to quantitatively estimate a slip rate, but~~ Sseveral investigators suggest that this segment has ~~an activity~~a slip rate rate ~~similar to the southern segments of the Lemhi and Lost River faults~~of 0.02 to 0.3 mm/year [2.76; 2.81].

2.6.2.3.5.4 ESRP Boundary Faults

The ISFSI site is located about 14 km from the postulated ESRP boundary fault (Figure 2.6-32). Deep seismic refraction profiling across the northwest boundary of the ESRP near the INEL suggests the presence of a buried northeast-trending fault parallel to the ESRP boundary [2.105]. Scott [2.55] suggested that a northeast-trending topographic scarp observed on an alluvial fan along the southeast side of the Arco Hills may be a result of past movement on the boundary fault. Breckenridge and Othberg [2.112] excavated a trench across the scarp. Their trench logs indicated that no fault offset was present within the alluvial fan deposits. They concluded that the scarp may have developed redistribution of eolian sediments along an old fire scar.

Other investigations have been conducted on northeast-trending faults at the southern terminations of the Lemhi Range and Beaverhead Mountains near the margins of the ESRP [2.110; 2.111; 2.95]. Results of their studies indicate that these faults were active more than 2 million years ago (Ma). Based on the following lines of evidence these faults are not considered significant seismogenic sources: 1) their northeast trend is not consistent with the direction of the active northwest-trending normal faults which are produced by regional extensional stress field; 2) they do not displace sediments and volcanic rocks younger than 2 Ma; and 3) their lengths are small, generally less than 10 km, and they have small total displacements. Furthermore, even if they were active, their small fault lengths and displacements show that the largest magnitudes possible are magnitude 5.0. This magnitude does not exceed the magnitudes of earthquakes that could occur in the Arco volcanic rift zone or in the ESRP background source zone at equal or closer distances [2.52; 2.53].

2.6.2.3.5.5 ESRP Volcanic Zones

Volcanic vents are not randomly distributed on the ESRP, but occur in discrete zones. Most vents occur in northwest-trending volcanic rift zones and a concentration of vents also occurs along the axis of the ESRP (the Axial Volcanic Zone - see section 2.6.2.3.5.5.4, below). Volcanic rift zones on the ESRP contain a variety of structures, other than volcanic vents, that suggest an association with shallow northwest-trending dikes in the subsurface (see for example Figure 2.6-40 in section 2.6.6.2.3.1). These structures include fissures, fissure swarms, fault scarps, and monoclines, all of which have been observed in active volcanic rift zones of Iceland and Hawaii and demonstrated to be associated with shallow dike intrusion [2.135; 2.136]. The great age range of exposed volcanic rift zones on the ESRP (from over 1 million years to 2000 years; 2.33; 2.45] suggest that basaltic volcanism throughout the history of the ESRP has been fed by volcanic rift zone processes. The northwest trend of volcanic rift zones and the dikes that produce them is controlled by the regional northeast-directed extensional stress field [2.43]. The same stress field produces northwest-trending normal faults, northwest-trending fault-block mountain ranges, in the Basin-and-Range province to the north and south of the ESRP.

The long-term (~4My to present) intrusion of northwest-trending basalt dikes into the ESRP has accommodated northeast-directed extension that was elsewhere accommodated by normal faulting [2.127]. The supplanting of normal faulting and its associated earthquakes in the ESRP by dike intrusion is the mechanism that best explains the relatively aseismic nature of the ESRP with respect to the surrounding Basin-and-Range province and Yellowstone Plateau [2.126; 2.138].

2.6.2.3.5.5.1 Arco Volcanic Rift Zone

The Arco volcanic rift zone extends from the southern end of the Lost River Range across the southwestern corner of the INEL (Figure 2.6-32). The ISFSI site is about 14 km away from the closest point on the boundary of the rift zone. The rift zone is about ~~6-~~8 km wide and 20 km long [2.165; 2.166, 2.54]. Small normal faults within the rift zone are 5-6 km in length, have maximum cumulative vertical offsets of about 12 m (multiple offsets) and are postulated to extend to a depth of 2 km below the surface [2.132; 2.165; 2.166; 2.52; 2.53]. A set of fissures in the Box Canyon graben area are colinear with the small normal faults (5 km length; Table 2.6-10) bounding the graben which results in a total length of 8 km. Based on the compilation of earthquake data for active rift zones (Table 2.6-9) a maximum magnitude of 5.5 is assumed possible for future dike-injection events within the rift zone. This is consistent with a magnitude of 5.2 based on the assumption that an earthquake associated with dike injection ruptures a fault area of 16 km^2 (length x depth; 8 x 2 km; Figure 2.6-33) [2.52; 2.53]. The most recent volcanic activity within the central part of the volcanic rift zone appears to have been about 95,000 years ago [2.167; 2.166; 2.165; 2.168]. The 10,000 to 13,000 year old Cerro Grande and North and South Robbers lava flows occur at the southern end of the VRZ, at ~~the~~ its intersection of the Arco volcanic rift zone with the Axial Volcanic Zone [2.54].

2.6.2.3.5.5.2 Lava Ridge-Hell's Half Acre Volcanic Rift Zone

The Lava Ridge-Hell's Half Acre (LR-HHA) volcanic rift zone extends from the southern end of the Lemhi range across the INEL to the southeastern corner (Figure 2.6-32). The ISFSI site is about 28 km away from the closest point on the boundary of the rift zone. The rift zone is 3-6 km wide and 50 km long. At the southern end of the rift zone, two sets of fissures, which may or may not be associated with small normal faults (~~1.4 km~~LaPoint monocline in Table 2.6-10), are about 4 km in length [2.114]. Since portions of the fissures are covered by younger lava flows, the fissure sets could extend 11 km farther south. A maximum magnitude of 5.5 was assumed possible for earthquakes associated with future dike-injection events within the LR-HHA rift zone based on the compilation of earthquake data shown in Table 2.6-9. This is consistent with a magnitude of 5.5 which was estimated using fault area (15 x 3 km = 30 km^2) and assuming rupture along the entire fissure lengths [2.52; 2.53]. The most recent volcanic activity within the LR-HHA rift zone occurred with the eruption of the Hell's Half Acre Volcanic Field, at its intersection with the Axial Volcanic Zone about 5,200 years ago [2.167; 2.166].

2.6.2.3.5.5.3 Howe-East Butte Volcanic Rift Zone

The postulated Howe-East Butte (H-EB) volcanic rift zone extends across the central portion of the INEL from the range-front south of Howe to East Butte (Figure 2.6-32). It is poorly expressed surficially and is mostly covered by fluvial and lacustrine sediment [2.169] (See section 2.6.6.2.3.1 - Volcanic Rift Zones). The ISFSI site is located within the postulated H-EB volcanic rift zone. Woodward-Clyde Consultants [2.52; 2.53] consider the maximum magnitude for the H-EB to be 5.5 similar to the Arco and LR-HHA volcanic rift zones. Volcanic vents in the H-EB volcanic rift zone are dated at 580,000 to 641,000 years old [2.54], and a conservative minimum age for the H-EB volcanic rift zone is 230,000 years, based on the age of lava flows from the Axial Volcanic Zone that cover volcanic rift zone structures and vents [2.54].

2.6.2.3.5.5.4 Axial Volcanic Zone

The Axial Volcanic Zone (AVZ) is located along the ESRP axis and crosses portions of the INEL's southern and eastern boundary. The ISFSI site is about 13 km from the closest point of the AVZ boundary. Dike-induced ~~features~~ structures are located near the intersections of the Arco and LR-HHA volcanic rift zones with the AVZ. Thus, a maximum magnitude of 5.5 is assumed possible based on the interpretation that dike injection mechanisms in the AVZ are similar to those in other ESRP volcanic rift zones.. The most recent volcanic activity took place about 5,000 years ago at the Hells Half Acre lava field [2.167,2.54].

2.6.2.3.5.6 ESRP Background Province

Although instrumental seismicity indicates that the ESRP is relatively aseismic, an earthquake similar in size to the 1905 Shoshone event is considered possible within the ESRP. For estimating ground motions at INEL, an earthquake of maximum magnitude 5.5 is postulated to occur anywhere within a 25 km radius of each facility. This is referred to as a "background earthquake" and is commonly used for design of commercial nuclear reactors to assess effects from earthquakes that may occur on unknown faults (those without surface exposures).

2.6.2.3.5.7 Northern Basin and Range Background Province

The northern Basin and Range background source region surrounds the ESRP. Excluding known normal faults which are capable of generating magnitude ≅7.0 events, a background earthquake with a maximum magnitude of 6.75 is possible within this source region on unknown or "blind" faults [2.52; 2.53]. Doser [2.170] suggests that earthquakes of magnitude 6.0-6.75 could occur in the ISB without producing surface rupture, and thus would leave no geologic record of their occurrence. An example of this phenomena is the 1975 M_L 6.0 Pocatello Valley earthquake near the Idaho-Utah border (See Section 2.6.2.3.4.2.~~1~~2 - Intermountain Seismic Belt). This event occurred on a "blind" (not evident in surface geology) cross-fault which trended transverse to the trend of nearby Basin and Range normal faults [2.171].

2.6.2.3.5.8 Idaho Batholith Background Province

The Idaho Batholith is seismically quiet region and its boundaries are defined by the extent of granitic rocks associated with the batholith. No extensive or well-defined Quaternary faults are mapped within the Idaho Batholith [2.52; 2.53]. Although seismographic coverage is poor (a detection threshold of $M \geq 3$), it appears to have a low seismic potential [2.65]. Woodward-Clyde Consultants [2.52; 2.53] estimated the maximum magnitude to be M_w 5.5.

2.6.2.3.5.9 Yellowstone Plateau Background Province

The Yellowstone Plateau is the topographically high region of the Yellowstone volcanic field and surrounding areas. The elevation of the plateau averages ~2500 m and, in addition to the Yellowstone Caldera, it includes the Beartooth uplift to the east, the Hebgen Lake fault zone to the west, and the Teton Range to the south [2.85]. It is an area of extremely high heat flow, profuse seismicity, abundant geothermal activity, low seismic velocity, low gravity, and rapid vertical crustal movements, all of which suggest high temperatures and perhaps magma bodies at relatively shallow depths in the crust [2.85]. Since detailed recording began in 1973, the maximum magnitude of seismicity within the Yellowstone caldera has been about 4.5 and the focal depths have been less than 10km. Outside the caldera and along the caldera rim, Yellowstone Plateau seismicity attains a greater focal depth (~20km) and greater magnitude. It includes the 1959 Hebgen Lake (M_S 7.5) event, largest earthquake in the ISB and the 1975 Yellowstone Park M_L 6.1) earthquake. Thus, the maximum magnitude of Yellowstone Plateau seismicity is assumed to be M_s 7.5 for the INEL probabilistic seismic hazards assessment [2.52; 2.53].

2.6.2.3.7 Maximum Earthquake (Complete Rewrite)

2.6.2.3.7.1 INEEL Seismic Hazard Studies

Both deterministic and probabilistic seismic hazard assessments to evaluate potential earthquake ground motions have been conducted at the INEEL since the early1970's for establishing seismic design criteria. Since that time, ground motion seismology and federal regulations (NRC and DOE) have continued to evolve, and geoscience investigations have continued at INEEL. To keep pace with these changes, site-specific deterministic and probabilistic ground motion studies were completed for all INEEL facility areas during the 1990's [2.51; 2.53]. These results formed the basis for Woodward-Clyde Federal Services [2.179] to evaluate site-specific probabilistic and deterministic ground motions at the ISFSI site. Recent changes in NRC requirements for independent fuel storage facilities allow for the use of probabilistic seismic design parameters. The ISFSI design earthquake parameters are based on the recent probabilistic results [2.179] and are discussed Section 2.6.2.3.7.2.

The following sections discuss the results of both probabilistic and deterministic studies that are applicable to the ICPP, the host site for the TMI 2 ISFSI. Both discussions are provided because DOE-ID is nearing completion on an update of the INEEL Architectural Engineering (AE) Standards [2.174] to include probabilistic seismic design parameters for the ICPP. In the initial license application submittal, the ISFSI is designed to the deterministic seismic criteria which were in contained within the INEEL AE Standards [2.174] at that time.

The INEEL AE Standards incorporates the results of seismic hazard studies in the form of seismic design parameters, peak ground accelerations and response spectra. These seismic parameters are the criteria formally approved for use in design of INEEL facilities. The criteria provide technical direction and guidance in the development of designs for construction type work performed for DOE-ID at the INEEL. The peak horizontal accelerations for rock in the AE Standards [2.174] are based on deterministic studies conducted in the 1970's [2.175; 2.176; 2.177; 2.178] and are supported by the results of the 1990 site-wide deterministic study conducted by Woodward-Clyde Consultants [2.51].

2.6.2.3.7.1.1 Deterministic Seismic Hazard Studies Applicable to the ISFSI Site

The deterministic studies conducted in the 1970's were based on empirical attenuation relationships of maximum acceleration on rock as functions of magnitude and distance (Table 2.6-11). Limited paleoseismic studies at the southern ends of the Lost River and Lemhi faults and speculation that future earthquakes would be of similar size to earthquakes that had previously occurred in the basin and range (i.e., 1915 M 7.8 Pleasant Valley, Nevada earthquake), led some investigators to select a maximum credible earthquake of M_L 7.75 at a distance of 24 km from the ICPP. Using the empirical attenuation relationship developed by Seed et al. (1969) (which includes very few rock recordings), the evaluation resulted in a peak horizontal acceleration of 0.33 g for rock at the New Waste Calcining Facility (NWCF) at the ICPP (~320 m north of the ISFSI site) [2.175; 2.177]. The investigators also estimated a horizontal acceleration of 0.46 g for 50 ft of soil (sand and gravel) based on an amplification factor of 1.4 derived from the lumped-mass method which incorporated representative dynamic soil properties.

In 1977, Agbabian Associates [2.178] reviewed the previous deterministic evaluations conducted for INEEL facilities (this included NWCF) with respect to NRC requirements for a nuclear reactor. They recommended an alternative deterministic approach using an empirical attenuation relationship that incorporated worldwide earthquake recordings that had been developed by Woodward-Clyde Consultants [2.176]. They suggested a maximum credible earthquake of M_L 6.75 (taking into account fault surface lengths and the lack of historical earthquakes of M_L 7.75 in the Idaho region) at a distance of 24 km from the Lost River fault. This resulted in a peak horizontal acceleration of 0.30 g for rock (Table 2.6-11).

At about this same time, studies to develop seismic design criteria for other INEEL facilities near the ICPP were being conducted. Based on the results of these studies and those for ICPP, the DOE-ID issued the first draft of the INEEL AE Standards which contained peak accelerations to be used for design of INEEL facilities (DOE, 1978; Harris, 1989). This document directed that future designs at the ICPP for bedrock were to use a peak horizontal acceleration of 0.24 g and a vertical acceleration 2/3 that of the horizontal acceleration.

The 1990 deterministic study was conducted by Woodward-Clyde Consultants [2.51] at the request of DOE-ID to update the seismic design criteria contained within the INEEL AE Standards. This deterministic study estimated peak ground accelerations for ICPP based on the largest earthquake (M_w 6.9) that could occur along the Lemhi fault at a distance of 21 km. This evaluation incorporated all available results from geoscience investigations pertaining to the earthquake source and subsurface stratigraphy beneath the ESRP (crustal structure) and ICPP (near-surface stratigraphy).

Woodward-Clyde Consultants [2.51] developed a site-specific geologic profile beneath two facility areas at the ICPP to assess the nature of seismic-wave propagation. The geologic profiles were used with the stochastic numerical modeling technique known as the Band-Limited-White-Noise (BLWN) ground motion model combined with random vibration theory to determine site-specific accelerations. Sensitivity analyses indicated that the size of the earthquake (stress drop) and near-surface geology (kappa) had the most significant affects on the levels of earthquake ground motions.

Peak horizontal accelerations and response spectra were estimated for the 16th, 50th, and 84th percentiles. The peak horizontal acceleration at the 84th percentile for rock at a site (called FPR) within 200 m of the ISFSI is 0.20 g and for a soil site (called SIS) within 600 m of the ISFSI site, 0.30 g. This suggests an amplification factor of about 1.5 between these two sites at the ICPP (Table 2.6-11).

In this same study, the vertical to horizontal ratio was evaluated using regional recordings of earthquakes at the INEEL facility areas. The average was 0.72 for rock sites which is consistent with the standard value of 2/3. The results of the 1990 deterministic study were incorporated into the INEEL AE Standards. These results suggested that the peak accelerations determined from the 1970's studies are conservative.

The 1996 site-specific deterministic evaluation conducted for the ISFSI site [2.179] was based in part on the stochastic numerical modeling methodology of the 1990 deterministic evaluation [2.51] and incorporated results of recent fault-trenching studies conducted along the Lemhi and Lost River faults [2.94; 2.98]. The Lemhi fault is the closest basin-and-range normal fault to the ISFSI site and controls the deterministic seismic hazard. The paleoseismic characteristics and geometry of this fault indicate that it has the potential for a M_w 7.1 earthquake at a distance of 22 km from the ISFSI site.

The same attenuation relationships (empirical and stochastic numerical models) from the 1996 probabilistic study were used in the deterministic analysis and were weighted the same as in the 1996 probabilistic evaluation (discussed in section 2.6.2.3.7.1.2). The deterministic evaluation resulted in a peak horizontal acceleration of 0.28 g for rock at the 84th percentile (Table 2.6-11). A soil acceleration of 0.56 g was estimated by using an amplification factor of 2 (based on the site-specific probabilistic results in section 2.6.2.3.7.1.3).

2.6.2.3.7.1.2 Probabilistic Seismic Hazard Studies Applicable to the ISFSI Site

In 1977, a probabilistic seismic hazard study was conducted by Agbabian Associates [2.178]for the NWCF site at the ICPP to calculate the probability of experiencing the design earthquake during the service life of the facility (Table 2.6-12). The procedure used the mathematical model of Der-Kiureghian and Ang (1977). The investigators used three source areas having magnitude range from 6.75-7.5 with corresponding intensities of IX-X and recurrence intervals based on a limited historical earthquake catalog. They developed intensity attenuation relationship using five regional earthquakes (1935 MMI VII Helena Montana; 1959 MMI X Hebgen Lake, Montana;1962 MMI VII Richmond, Utah; 1967 MMI VII Tushar-Sevier Central Utah; and 1975 MMI VII Pocatello Valley, Idaho). Their results suggested that for a peak horizontal acceleration of 0.40 g on rock, there is 0.01% chance of exceedance in 100 years.

In the 1984 probabilistic seismic hazard study, Terra Corporation calculated probabilities of peak horizontal accelerations for the Argonne National Laboratory West site on INEEL. They developed seismic hazard maps for all of the INEEL including the ICPP. Their methodology used the Tera (1978) model developed from the work of Mortgat et al (1977) and Mortgat and Shah (1979). They specified nine source regions, three of which included the major range-bounding faults (Lost River, Lemhi, and Beaverhead). The magnitudes for the source regions ranged from 6.5 to 7.75. The recurrence intervals for the sources regions were derived from a 17-year earthquake record of the local region. The attenuation relationship was based on Campbell (1982) and Tera (1984) incorporating values of crustal attenuation determined from regional earthquake recordings (Singh and Herrmann, 1983) and the results of the ESRP refraction survey [2.84]. For the ICPP, the resulting seismic hazard maps show 0.18 g at a return period of 1,000 years and 0.30 g at a return period of 10,000 years (Table 2.6-12).

The 1996 probabilistic seismic hazards evaluation by Woodward-Clyde Federal Services [2.53] was conducted for all INEEL facility areas including the ICPP. This study has undergone extensive peer review and provides the basis for developing seismic design parameters to be used at INEEL.

The probabilistic methodology used in the study is based on Cornell (1968) and Youngs and Coppersmith (1990). It provides for explicit inclusion of the range of scientifically defensible seismologic and tectonic interpretations including seismic source characterization and ground motion attenuation models (consistent with approaches contained in NRC Regulatory Guide 1.165, "Identification and Characterization of Seismic Sources and Determination of Safe Shutdown Earthquake Ground Motions," Sections C 1 through 3). Uncertainties in conceptual models and parameters were incorporated into the hazard through use of logic trees. Sensitivity analyses were performed to examine the important contributors to the total hazard and to the uncertainties in the hazard. This evaluation incorporated results of all geologic, seismologic, and geophysical investigations conducted for INEEL since the 1960's.

Earthquake magnitudes and recurrence rates were assessed for all earthquake sources which contribute to potential ground motions at the ICPP site. The four closest sources (Figure 2.6-32) that contribute to the hazard at ICPP include:

1) Basin and Range normal faults which are characterized by magnitudes ranging from M_w 6.5 to 7.75 based on fault dimensions (surface length, displacements, and area) and recurrence methods are based on slip rates or recurrence intervals.

2) Northern Basin and Range background seismicity which is characterized by magnitudes ranging from M_w 6.25 to 6.75 and recurrence models are based on the historical earthquake record (1884-1992).

3) ESRP background seismicity which is characterized by magnitudes ranging from M_w 5.0 to 6.0 based on the possible occurrence of the 1905 Shoshone earthquake within the Snake River Plain. Because the ESRP is aseismic, the recurrence is estimated by assuming that 1/3 of the time earthquakes of this magnitude range occur in the ESRP and 2/3 of the time earthquakes of this magnitude range occur outside the ESRP.

4) Volcanic rift zones of the ESRP which are characterized by magnitude ranging from M_w 4.5 to 5.5 based on analogy with other active volcanic rift zones and measurements of fault dimensions for small normal faults produced by dike injection within the volcanic rift zones. The recurrence intervals are based on the recurrence of volcanism (Table 2.6-15).

A site-specific attenuation relationship was developed for the ICPP site using the stochastic numerical ground motion modeling approach [2.51; 2.53] and results of shear-wave velocity measured in boreholes at the ISFSI site and ICPP (see Attachment 6). In addition, four empirical ground motion attenuation relationships, which represent the uncertainty in empirical modeling of earthquake ground motions, were used in the study. The site-specific stochastic attenuation relationship was weighted at 0.6 because it is representative of the ESRP geological conditions which are vastly different for typical California sites. The empirical attenuation relationships (Idriss, 1991; Sadigh et al., 1993; Joyner and Boore, 1982; Campbell and Bozorgnia, 1994) were weighted individually based on their relative applicability (Geomatrix, 1995), but total to a combined weight of 0.4.

Results of the INEEL seismic hazard evaluation significant to the ISFSI include [2.53]:

- The ISFSI is located within the ESRP, which is characterized by a very low rate of seismicity and small magnitude earthquakes. Thus, the background earthquakes within the ESRP contribute very little to the hazard at the ISFSI.

- There is very little contribution from the volcanic rift zones because the volcanic episodes have long recurrence intervals (>15,000 yrs) and any associated seismicity is characterized by small magnitude (< 5.5) earthquakes.

- In general, the stochastic relationship results in lower motions at short periods than the empirical relationships because of the interbedded volcanic stratigraphy which has a lower velocity gradient in the upper 1 km than homogeneous rock and the alternating high and low velocities which tend to dampen out high frequency ground motions.

- At shorter return periods (<2000 yrs) the hazard is dominated by the northern Basin and Range background seismicity due in part to the extremely low level of seismicity in the ESRP and the long recurrence intervals of the Basin and Range faults.

- The Basin and Range faults contribute more to the hazard at 10,000 yrs because this return period approaches the average recurrence interval of the faults.

The results of the 1996 probabilistic seismic hazard evaluation are for rock in the form of mean peak horizontal accelerations and uniform equal hazard spectra for return periods of 500, 1,000, 2,000, and 10,000 years. For the ICPP, the peak horizontal acceleration is 0.13 g at a return period of 2,000 years (Table 2.6-12).

2.6.2.3.7.1.3 Site-Specific Probabilistic Evaluation for ISFSI Seismic Design Parameters

The results of the 1996 INEEL probabilistic study are being used to develop site-specific probabilistic design earthquake ground motion parameters, accelerations and response spectra, for the ISFSI. The response spectra for rock surface conditions are based on the mean uniform hazard spectra (UHS) computed for the site-specific probabilistic analysis at ICPP [2.53]. The UHS were deaggregated to determine the contributions from dominant earthquakes at low and intermediate frequencies. The UHS were supplemented by these results to derive the smoothed rock surface response spectra at damping values of 2, 5, 7, and 10% for 1,000, 2,000, and 10,000 years return periods. Figure 2.6-35 show the 5% damping curves for the specified return periods [2.179].

The peak horizontal acceleration for rock at a 2,000 year return period is 0.13 g (Table 2.6-11). In addition to the horizontal accelerations, Woodward-Clyde Federal Services [2.179] also calculated vertical accelerations for rock (0.06 g for 1,000 yrs; 0.08 g for 2,000 yrs; 0.13 g for 10,000 yrs) and response spectra (see reference [2.179] for spectra).

Since the ISFSI basemat will be founded in surficial sediments, the design earthquake accelerations and response spectra will include the soil response. A soil velocity profile to a depth of 23 m was developed using shallow seismic and downhole shear-wave measurements (234 m/s to 604 m/s) obtained from boreholes at the ISFSI site (see Attachment 21) supplemented by data obtained from other boreholes at the ICPP [2.56].

The soil response was incorporated by calculating power spectra that are spectrally matched to the horizontal rock spectra and propagating these spectra through the one-dimensional soil column using a frequency-domain equivalent-linear formulation similar to the program SHAKE [2.180]. This is accomplished by deconvolving the rock power spectra from the soil-rock interface down to a depth of 1 km and then propagating them back up through the rock and soil profiles. Thirty runs were made randomizing the layer thicknesses and velocities to incorporate uncertainties in sediment thickness and shear-wave velocities over the area of the ISFSI site. The total mean thickness of the soil 15.2 m was varied by $\pm$ 6.1 m.

The preliminary mean peak horizontal acceleration for soil surface conditions is 0.30 g[a] at 2,000 years. The horizontal accelerations for the other return periods are shown in Table 2.6-12. The peak vertical acceleration is 0.21 g[a] at 2,000 years (and the others: 0.16 g at 1,000 yrs; 0.33 g at 10,000 yrs). The soil response spectra for return periods of 1,000, 2,000, and 10,000 years at a damping of 5 % for the horizontal and vertical components are shown in Figures 2.6-36 and 2.6-37, respectively. The curves for damping values of 2, 7, and 10% are contained within Woodward-Clyde Federal Services [2.179].

Time histories were also calculated for the ISFSI site. They were developed by combining a Fourier amplitude spectrum with a phase spectrum from an observed strong ground motion record using the procedure of Silva and Lee (1987). The strong ground motion records are from the 1989 M_w Loma Prieta, California and 1980 Irpinia M_w 6.9 earthquakes recorded on rock sites.

2.6.2.3.7.2 ISFSI Seismic Design Parameters

The design basis horizontal acceleration for the ISFSI, including effects for soil amplification is 0.30 g[a] for a 2,000 year return period. The smoothed response spectra used for design is shown in Attachment 23. These design values were chosen because they are consistent with NRC regulations for an independent fuel storage facility and the revisions to the INEEL AE Standards. The design basis parameters are site-specific probabilistic results which incorporate all that in known about the geology and seismology of the ESRP region and ISFSI site at this time [2.53; 2.179; Attachment 21].

Under the initial license application submittal to the NRC the ISFSI seismic design is based on the deterministic 0.36 g peak horizontal acceleration used in conjunction with the NRC Regulatory Guide 1.60 spectra (consistent with the criteria in the INEEL AE Standards [2.174] at that time). A comparison between the probabilistic response spectra at 0.30 g with the NRC Regulatory Guide 1.60 spectra at 0.36 g shows that the design for the ISFSI site at the deterministic value of 0.36 g exceeds the probabilistic 0.30 g value at all frequencies and results in a more conservative design **(Included as part of this Attachment)**. Thus, the current ISFSI design will resist stresses induced by seismically transmitted peak horizontal accelerations up to 0.36 g.

Footnote
a - This value is preliminary and may possibly change based on incorporation of recently acquired data from boreholes drilled at the ISFSI site.

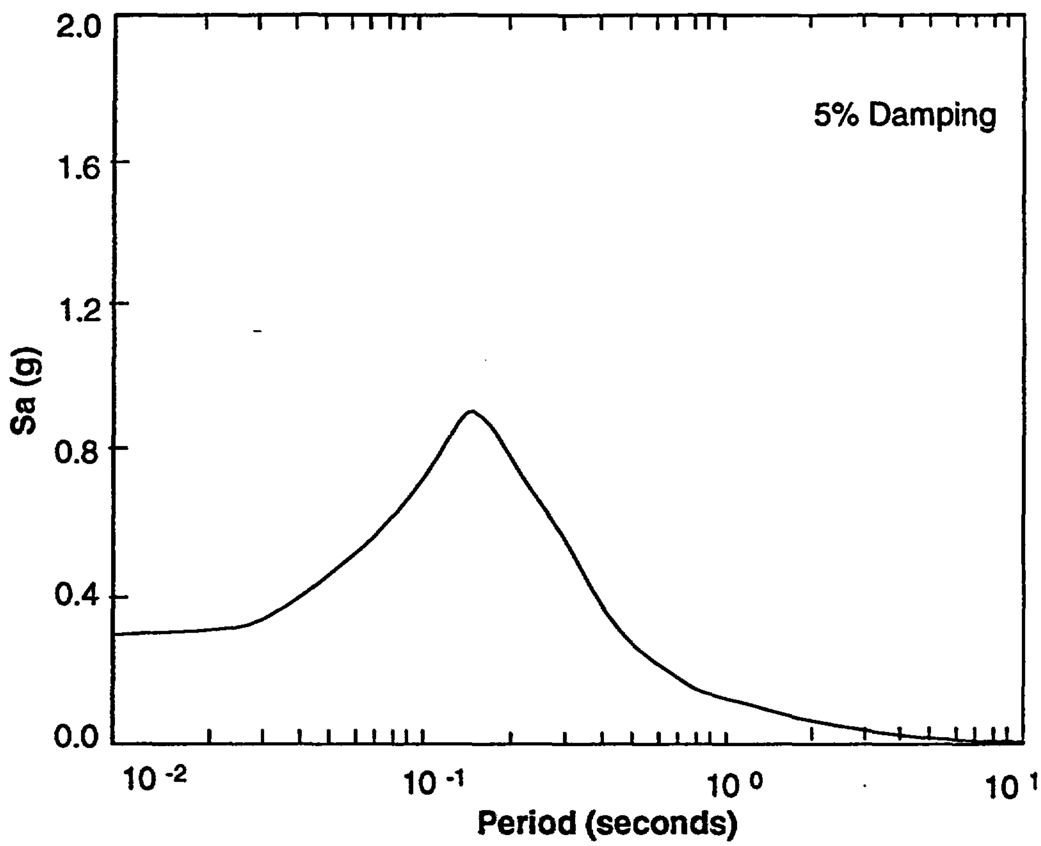

LEGEND

——— 2,000 years, smoothed, PHA=0.30g*

*The response spectra is preliminary and may possibly change based on incorporation of recently acquired data from boreholes drilled at the ISFSI site.

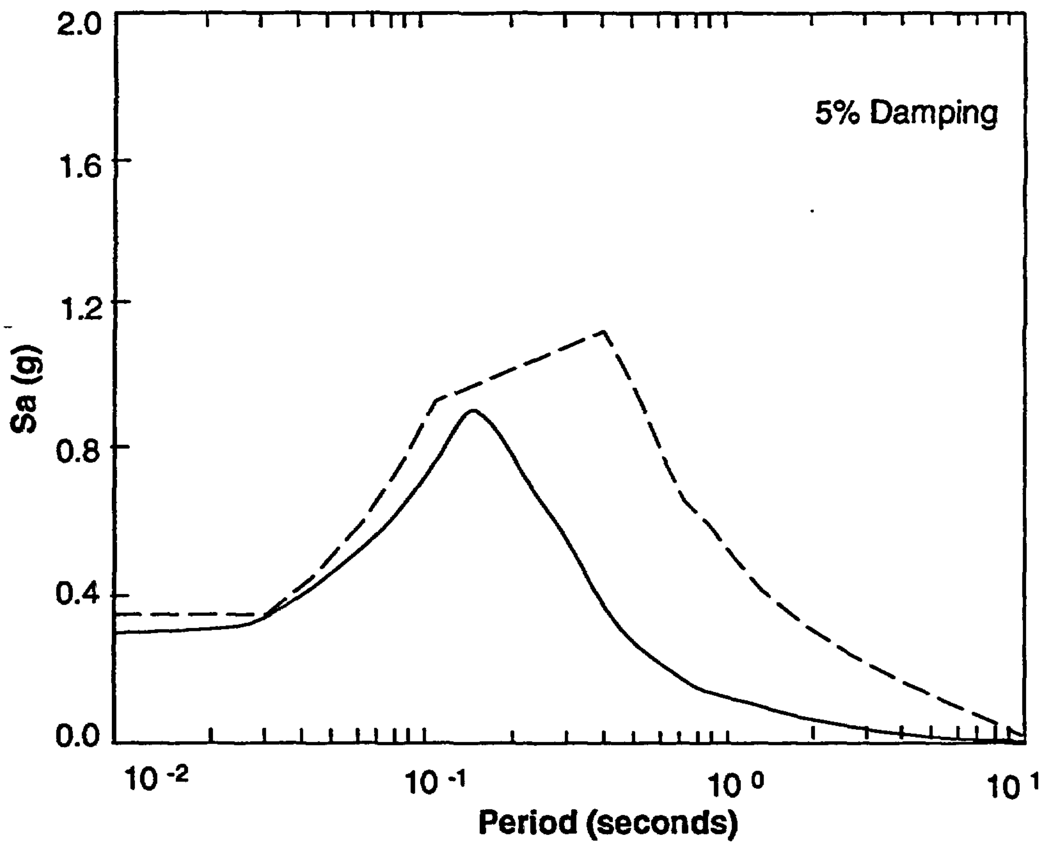

LEGEND

– – – – – NUREG 1.60 anchored to 0.36 g

———— 2,000 years, smoothed, PHA=0.30g*

*The response spectra is preliminary and may possibly change based on incorporation of recently acquired data from boreholes drilled at the ISFSI site.

TABLE 2.6-3. TIME PERIODS OF EARTHQUAKE DATA COMPLETENESS
(Showing Additions and Deletions)

Magnitude Interval	Completeness Period
2.0-4.0	1975-1995
4.0-5.0	1963-1995
5.0-5.5	1950-1995
5.5-6.0	1925-1995
6.0-6.5	1900-1995
6.5-7.0	1875-1995
7.0 +	1850-1995

Modified from Woodward-Clyde Consultants ~~(1992a).~~ [2.52].

TABLE 2.6-4. EARTHQUAKES WITH MAGNITUDES GREATER THAN 5.5 WITHIN 200 MILES OF INEEL (Showing Additions and Deletions)

Earthquake Date & Time (Hr:Mn - UTC)[a]	Magnitude[b]	Modified Mercalli Intensity at the ISFSI site[c]	Geographical Location[d]	Radial Distance (km)[e]	References
1884 November 10 08:50	6.3 M_I	~~VIII~~	Bear Lake, Utah	225	1
1905 November 11 21:26	5.5 M_L	~~VII~~ IV	Shoshone, Idaho	164	2
1909 October 6 02:50	6.3 M_I	~~VIII~~	Hansel Valley, Utah	216	1
1914 May 13 17:15	5.7 M_I	~~VII~~	Ogden, Utah	283	1
1925 ~~July 10~~June 28 ~~14:45~~01:21	6.8 M 6.6 M_w	~~VI~~	Clarkston, Montana	~~201~~275	3,4,5
1925 June 29 01:12	6.3 M		Clarkston, Montana	~~201~~292	21
1930 June 12 09:15	5.8 M_L	~~VI~~	E of Soda Springs, Idaho	190	5
1934 March 12 15:05	6.6 M_L 6.6 M_w	~~IX~~	Hansel Valley, Utah	222	1,3,6
1934 March 12 18:20	6.2 M_L 5.9 M_w	~~VII~~	Hansel Valley, Utah[f]	222	1,3,6
1934 April 14 21:26	5.6 M_L	~~VII~~	Hansel Valley, Utah[f]	245	1
1934 May 06 08:09	5.6 M_L	~~VI~~	Hansel Valley, Utah[f]	222	1
1944 July 12 19:30	6.1 M_b	~~VII~~	N of Stanley, Idaho	235	7
1945 February 14 03:01	6.0 M_L	~~VI~~	N of Stanley, Idaho	235	7
1947 ~~December 17~~November 23 ~~12:38~~09:46	6.3 M 6.1 M_w	~~ND~~	Virginia City, Montana	~~225~~138	3,4
1959 August 18[g] 06:37	7.5 M_s 6.3, 7.3 M_w	~~X~~ VI	Hebgen Lake, Montana	187	3,8,9,10
1959 August 18 07:56	6.5 M	~~ND~~	Hebgen Lake, Montana[h]	208	3
1959 August 18 08:41	6.0 M	~~ND~~	Hebgen Lake, Montana[h]	208	3

TABLE 2.6-4 Continued. EARTHQUAKES WITH MAGNITUDES GREATER THAN 5.5 WITHIN 200 MILES OF INEEL

Earthquake Date & Time (Hr:Mn - UTC)[a]	Magnitude[b]	Modified Mercalli Intensity at the ISFSI site[c]	Geographical Location[d]	Radial Distance (km)[e]	References
1959 August 18 11:03	5.6 M	~~ND~~	Hebgen Lake, Montana[h]	182	3
1959 August 18 15:26	6.5 M_b 6.3 M_w	~~ND~~	Hebgen Lake, Montana[h]	209	10
1959 August 19 04:04	5.9 M_s 6.0 M_w	~~ND~~	Hebgen Lake, Montana[h]	209	4,10
1962 August 30 13:35	5.7 M_s 5.9 M_w	~~VII~~	Cache Valley, Utah	208	1,3,11
1964 October 21 07:38	5.8 M_b 5.6 M_w	~~ND~~	Hebgen Lake, Montana[h]	154	3,4
1975 March 28 02:31	6.1 M_b 6.2 M_w	~~VIII~~III	Pocatello Valley, Utah	183	3,12
1975 June 30 18:54	6.1 M_L	~~VII~~NF	Yellowstone Park, Wyoming	209	3,13
1976 December 8 14:40	5.5 M_b	~~ND~~	Yellowstone Park, Wyoming	198	5
1983 October 28 14:06	7.3 M_s 6.8 M_w	~~IX~~VI	N W of Mackay, Idaho	93	3,8,9,14
1983 October 28 19:51	5.8 M_L 5.4 M_w	~~ND~~	N W of Mackay, Idaho[i]	98	3,15
1983 October 29 23:29	5.8 M_L 5.5 M_w	~~ND~~	N W of Mackay, Idaho[i]	121	3,15
1984 August 22 09:46	5.8 M_L 5.6 M_w	~~ND~~	Challis, Idaho[i]	127	3,15
1994 February 3 09:05	5.9 M_W 5.7 M_W	NF	W of Afton Wyoming	172	16, 17, 18

a - UTC - Universal Time Coordinated (Greenwich Mean Time).

b - — Highest magnitude value is reported in this Table. Moment magnitudes are included, if calculated. Magnitude Scales: M_I - Conversion from Intensity; M_L - Local or Richter; M - magnitude type not specified; M_w - Moment; M_b - Body-wave; M_s - Surface-wave.

c - Modified Mercalli intensity ~~based on Wood and Neumann, 1931~~documented at the INEEL. NF indicated "Not Felt" where documented. Blanks indicate no information available.

d - Latitude and Longitude coordinates are listed in Table 3.7-4.

e - Radial distances based on coordinates 43° 42.0', 112° 48.0'.

f - Aftershock following the M_L = 6.6, 1934 Hansel Valley, Utah earthquake.

g - Hebgen Lake usually referred to as M_s 7.5, but is actually ~~a~~ two events having magnitudes of M_w 6.3 and 7.3 per Doser, 1985.

h - Aftershock following the M_s = 7.5, 1959 Hebgen Lake, Montana earthquake.

i - Aftershock following the M_s = 7.3, 1983 Borah Peak, Idaho earthquake.

References: (1) Richins, 1979; (2) Oaks, 1992; (3) Doser and Smith, 1989; (4) Doser, 1989a; (5) National Earthquake Information Center, unpublished data; (6) Doser, 1989b; (7) Stover et al., 1986; (8) Doser, 1985a; (9) Stover, 1985; (10) Doser, 1985b; (11) Westaway and Smith, 1989; (12) Arabasz et al., 1979; (13) Pitt et al., 1979; (14) Doser and Smith, 1985; (15) Richins et al., 1987, (16) Dewey, 1994; (17) Nava et al., 1994; (18) Pechmann et al., 1997; (19) Cook and Nye, 1979; (20) Stover et al., 1977.

Table 2.6-5. Ground motions recorded during the Borah Peak earthquake at CPP-601 (~1000 feet north of the TMI-2 ISFSI site). **(Showing Additions and Deletions)**

Location		Acceleration	Velocity	Displacement
CPP-601 1st Floor	L	0.043	1.38	0.25
	T	0.065	2.76	0.13
	V	0.033	1.28	0.16
CPP-601 2nd Basement	L	0.038	1.32	0.12
	T	0.044	2.19	0.16
	V	0.038	1.46	0.11
CPP-601 Free Field	L	0.078	2.03	0.23
	T	0.058	2.80	0.34
	V	0.035	1.39	0.25

TABLE 2.6-7. EARTHQUAKES WITHIN 200 MILES THAT HAVE OCCURRED ON TECTONIC STRUCTURES (Showing Additions and Deletions)

Earthquake Date & Time (Hr:Mn - UTC)[a]	Seismic Moment[b] ($\times 10^{25}$ dyne-cm)	Focal Mechanism Strike/Dip/Rake[c] (Degrees)	Tectonic Structure, Source Parameters and Dimensions, and References[d]
1925 ~~July 10~~June 28 ~~14:45~~01:21	10 ± 2 B	30 80 -175 FM 250 56 - 38 BW	Associated with a fault oriented in an oblique manner north of the Clarkston Valley Fault north of Bozeman, Montana. Z=9±5 km (LP); RL=25±5 km (BW), 59±5 km (SF); SD=2.0±1.0 m (v). (1,2)
1934 March 12 15:05	0.95 G 8.6 ± 2 B	7 80 - 70 FM 40 87 - 11 BW 0 73 -110 SF	Caused a fault scarp along an unnamed fault in Hansel Valley, Utah. Z= 8±2 km (LP); RL=11±3 km (BW), 6±2 km (SF); BWD= -2.1±0.1 m (h), 0.2±0.05 m (v); SD= -0.2 (h), 2.0±1.0 m (v); GD= 0.4±0.1 m (v). (1,3)
1934 March 12 18:20	0.77 ± 0.3 B	25 85 - 20 BW	Aftershock to March 12, 1934 earthquake. Z= 8±7 km (LP); RL=7±3 km (BW); BWD= -0.5±0.1 m (h). (1,4)
1947 ~~December 17~~November 23 ~~12:38~~09:46	1.8 ± 0.5 B	120 60 -120 FM 104 48 -170 BW	Possibly associated with the Madison Fault northwest of Hebgen Lake, Montana. Z= 8±2 km (LP); RL=9±2 km (BW); BWD= -0.7±0.2 m (h). (1,2,5)
1959 August 18 06:37 (M_s 7.5)	41 G 150 L 120 S	102 60 - 90 SW 120 70 - 90 SF 132 45 - 90 GE	Caused a fault scarp along the Hebgen and Red Canyon faults near Hebgen Lake, Montana. No distinction between subevents: Z= 11±2 km (LP); RL=24±4 km (SF), 40±4 km (GE); SD= 4.4 m (v); GD= 7.4±0.4 m (v). (1,6)
1959 August 18 06:37 (M_w 6.3)	2.8 B	102 60 - 90 FM 95 42 - 90 BW	Subevent 1: Z= 10±2 km (LP); RL=7±1 km (BW); BWD= 0.95 m (v). (1,6)
1959 August 18 06:37 (M_w 7.3)	92 B	100 54 - 90 FM 95 42 - 90 BW	Subevent 2: Z= 15±3 km (LP); RL=21±5 km (BW); BWD= 6.8 m (v). (1,6)

TABLE 2.6-11 DETERMINISTIC SEISMIC HAZARD STUDIES APPLICABLE TO THE ISFSI SITE (REWRITE)

Seismic Hazard Study	Methodology	Input Parameters	Peak Horizontal Acceleration (g) Bedrock	Soil
Woodward-Lungren and Associates, 1971 [2.175] & Allied Chemical Corporation, 1975 [2.177]	Based on empirical attenuation relationship — maximum acceleration of rock as functions of magnitude and distance (Seed et al., 1969). Soil based on amplification factor of 1.4 derived from lumped-mass method incorporating representative dynamic soil properties.	M_L 7.75 earthquake at the southern end of the Lost River fault at a distance of 24 km to the ICPP. Representative soil profile 50 ft of gravel and sand. This evaluation was for the NWCF site at the ICPP located 320 m from the ISFSI site.	0.33	0.46
Agbabian Associates, 1977 [2.178]	Reviewed the deterministic study conducted by Allied Chemical Corporation [2.177] with respect to NRC regulations. Suggested an alternative deterministic evaluation that considered use of: 1) fault surface length versus earthquake magnitude; and 2) an empirical attenuation relationship developed from earthquakes worldwide (Woodward-Clyde Consultants, 1975 [2.176]). No soil values calculated.	M_L 6.75 earthquake at the southern end of the Lost River fault at a distance of 24 km to the ICPP. This evaluation was for the NWCF site at the ICPP located 320 m from the ISFSI site.	0.30	
Woodward-Clyde Consultants, 1990 [2.51]	Site-specific evaluation using the a stochastic numerical modeling technique known as the band-limited-white-noise ground motion model combined with random vibration theory. The ground motions are modeled as a point source described by M_w, stress drop $\Delta\sigma$, and source region V_s, and ρ_s; crustal attenuation described by Q_o and η; and the local site response based on V_s, intrinsic damping Q_s, and ρ_s. Ground motions were modeled to the ground surface for both rock and soil. Results are in the form of horizontal peak acclerations and response spectra for the 16^{th}, 50^{th}, and 84^{th} percentiles. An evaluation of the vertical to horizontal ratio resulted in an average value of 0.72.	M_w 6.9 on the Lemhi fault at a distance of 21 km, the closest point of the rupture plane to ICPP. $\Delta\sigma$= 50 bars; V_s= 3.55 km/sec; ρ_s = 2.7 gm/cm3; Q_o = 450; and η = 0.2. Local site response based on V_s and V_p measurements in boreholes and empirical earthquake recordings. Sites selected for evaluation at the ICPP were called FPR for rock and SIS for soil, located approximately 500 m from each other and 200 m and 600 m from the ISFSI site, respectively.	0.20 (84^{th})	0.30 (84^{th})

TABLE 2.6-11 Continued. DETERMINISTIC SEISMIC HAZARD STUDIES APPLICABLE TO THE ISFSI SITE

Seismic Hazard Study	Methodology	Input Parameters	Peak Horizontal Acceleration (g) Bedrock	Soil
Woodward-Clyde Federal Services, 1996b [2.179]	Incorporated results of detailed paleoseismic investigations at the southern end of the Lemhi fault [2.94]. Combined four empirical attenuation relationships [2.53] with an attenuation relationship based on the same stochastic modeling approach as in Woodward-Clyde Consultants [2.51] to calculate a weighted mean peak horizontal acceleration for a maximum credible earthquake. Soil value was estimated by using an amplification factor of 2 [2.53]. Results are in the form of peak horizontal accelerations at the 50^{th} and 84^{th} percentiles.	M_w 7.1 on the Lemhi fault at a distance of 22 km, the closest point of the rupture plane to ISFSI site. $\Delta\sigma = 75$ bars; $V_s = 3.55$ km/sec; $\rho_s = 2.7$ gm/cm3; $Q_o = 150$; and $\eta = 0.6$. Local site response based on V_s and V_p measurements in boreholes drilled at the ISFSI site.	0.28 (84^{th})	0.56 (84^{th})

TABLE 2.6-12 PROBABILISTIC SEISMIC HAZARD STUDIES APPLICABLE TO THE ISFSI SITE (REWRITE)

Seismic Hazard Study	Methodology	Input Parameters	Peak Horizontal Acceleration (g) Bedrock	Soil
Agbabian Associates, 1977 [2.178]	Calculated the probability of experiencing the design earthquake during the service life of the facility. Calculation procedure uses the mathematical model by Der-Kiureghian and Ang (1977). Evaluation performed for the NWCF site at the ICPP located 320 m from the ISFSI site.	Three source areas located around the ESRP having maximum magnitudes (6.75-7.5) corresponding to Modified Mercalli Intensities (MMI) IX-X, recurrence intervals based on the historical earthquake record, and intensity attenuation relationships developed from five regional earthquakes.	0.4 /MMI VIII-IX (0.01% chance of exceedance in 100 years)	None
Tera Corporation, 1984	Calculated probabilities of peak horizontal accelerations with return periods of 100, 1,000, and 10,000 yrs. Procedure uses the Tera (1978) model based on the work of Mortgat et al. (1977) and Mortgat and Shah (1979). Analysis done for Argonne National Laboratory site, but hazard maps include the ICPP.	Nine source regions, three are the major range-bounding faults northwest of the ESRP. Magnitudes range 6.5-7.75 and recurrence based on 17 years of earthquake data. Attenuation based on Campbell (1982) and Tera (1984) with Q_o=450, η=0.2 outside the ESRP; Q_o=150, η=0.55 inside the ESRP.	0.18 (1,000 yrs) 0.30 (10,000 yrs)	None
Woodward-Clyde Federal Services, 1996a [2.53]	Calculated annual exceedance probabilities (500, 1,000, 2,000, and 10,000) for peak horizontal accelerations. Procedure is based on Cornell (1968) and Youngs and Coppersmith (1990). Results are in the form of mean peak horizontal accelerations and uniform hazard spectra for rock. Evaluation performed for the ICPP.	Source zones: basin and range faults, M6.5-7.75; volcanic rift zones, M4.5-5.5; ESRP background seismicity, M5-6; northern basin and range background seismicity, M6.25-6.75. Recurrence based on earthquake catalog 1884-1992. Attenuation includes four empirical relationships and stochastic numerical modeling ($\Delta\sigma$ = 75 bars; V_s= 3.55 km/sec; ρ_s = 2.7 gm/cm3; Q_o = 150; and η = 0.6. Site response V_s and V_p measured in boreholes drilled at ICPP and INEEL).	0.10 (1,000 yrs) 0.13 (2,000 yrs) 0.22 (10,000 yrs)	None

TABLE 2.6-12 Continued. PROBABILISTIC SEISMIC HAZARD STUDIES APPLICABLE TO THE ISFSI SITE

Seismic Hazard Study	Methodology	Input Parameters	Peak Horizontal Acceleration (g) Bedrock	Soil
Woodward-Clyde Federal Services, 1996b [2.179]	Developed seismic design parameters for the ISFSI site. Procedures include: deaggregation of mean uniform hazard spectra and adjustment of the normalized spectral shapes to produce bedrock response spectra; soil response analysis using a frequency-domain equivalent-linear formulation (Silva et al. [2.180]); and development of acceleration time histories by combining a Fourier amplitude spectrum with a phase spectrum from an observed strong ground motion record based on (Silva and Lee, 1987). Results in the form of peak horizontal and vertical accelerations for rock, preliminary peak horizontal and vertical accelerations for soil, smoothed response spectra, and time histories.	Mean uniform hazard spectra for bedrock at the ICPP developed by Woodward-Clyde Federal Services, 1996a [2.53]. Soil analysis includes: depths 7.5 - 18 m; shear wave velocites 234 - 604 m/s obtained from boreholes drilled at the ISFSI site. Acceleration time histories developed from strong ground motion rock records of the 1989 M_w 7.0 Loma Prieta, California and the 1980 M_w 6.9 Irpinia earthquakes.	0.10 (1,000 yrs) 0.13 (2,000 yrs) 0.22 (10,000 yrs)	0.23[a] (1,000 yrs) 0.30[a] (2,000 yrs) 0.47[a] (10,000 yrs)

a - This value is preliminary and may possibly change based on incorporation of recently acquired data from boreholes drilled at the ISFSI site.

Changes to Section 2.8 (References)

Revision

Replace Reference 2.1.7.4 with the following:

2.174 DOE (1992), Seismic, wind, and flood design, Section 0112, *INEL Architectural Engineering Standards*, Revision 13, September 21, 1992

New References:

- Campbell, K.W. (1982), A preliminary methodolgy for the regional zonation of peak ground acceleration, Proceedings of 3rd International Conference on Earthquake Microzonation 1, Seattle, p. 365-376.
- Campbell, K.W. and Y. Bozorgnia (1994), Near-source attenuation of peak horizontal acceleration from worldwide accelerograms recorded from 1957 to 1993, Fifth U.S. International Conference on Earthquake Engineering, Chicago, Illinois.
- Corbett, M.K. (1975), Structural development of the eastern Snake River Plain, Idaho as an intracontinental rift, Geological Society of America Abstracts with Programs 7, p. 599-600.
- Cornell, C.A. (1968), Engineering seismic risk analysis, Bulletin of the Seismological Society of America 58, p. 1583-1606.
- Der Kiuergahian, A. and A. H-S. Ang (1977), A fault-rupture model for seismic risk analysis, Bulletin Seismological Society of America 67, p. 1173-1194.
- Dewey, J. (1994), Letter transmittal of the 1994 Draney Peak, Idaho earthquake isoseismals, U.S. Geological Survey, March 4, Denver Colorado.
- DOE (1978), INEL Architectural Engineering Standards, Idaho Falls, Idaho, Original Issue, December.
- Geomatrix Consultants (1995), Seismic design mapping for the State of Oregon, unpublished Final Report prepared for the Oregon Department of Transportation.
- Hamiton, W. (1987), Plate-tectonic evolution of the western U.S.A., Episodes 10, p. 271-301.
- Harris, B.G. (1989), Seismic design criteria at the Idaho National Engineering Laboratory (INEL), Proceedings of the Second DOE Natural Phenomena Hazards Mitigation Conference, Knoxville, Tennessee, p.
- Idriss, I.M. (1991), earthquake ground motions at soft soil sites, Second International Conference on Recent Advances in Geotechnical Earthquake Engineering and Soil Dynmaics 3, p. 2265-2272.

- Joyner, W.B. and D.M. Boore (1982), Prediction of earthquake response spectra, U.S. Geological Survey Open-File Report 82-977.

- Mabey, D.R. (1978), Regional gravity and magnetic anomalies in the eastern Snake River Plain, Idaho, U.S. Geological Survey, Journal of Research 6, p. 553-562.

- Morgat and Shah (1979)

- Mortgat, C.P., T.C. Zsutty, H.C. Shah, and l. Lubetkin (1977), A study of seismic risk for Costa Rica, John A. Blume Earthquake Engineering Center, Stanford University, California, Report 25.

- Nava, S.J., W.J. Arabasz, and J.C. Pechmann (1994), The M 5.9 Draney Peak, Idaho (Idaho-Wyoming border) earthquake of February 3, 1994: A preliminary report, Seismological Research Letters 65, No. 3-4, p. 239.

- Parsons, T., G.A. Thompson, and R.P. Smith (1998), More than one way to stretch: A tectonic model for extension along the plume track of the Yellowstone Hotspot and adjacent Basin and Range Province, U.S.A., accepted for publication in Tectonics.

- Pechmann, J.C., D.A. Brumbaugh, S.J. Nava, T.G. Skelton, G.P. Fivas, W.J. Arabasz, and S.M. Jackson (1997), The 1994 Draney Peak, ID earthquake and its aftershocks, Eos, Transactions, American Geophysical Union, 78, No. 46, p. F480.

- Sadigh, K., C-Y. Chang, N.A. Abrahamson, S.J. Chiou, and M.S. Power (1993), Specification of long-period ground motions: Updated attenuation relationships for rock site conditions and adjustment factors for near-fault effects, in Proceedings of ATC-17-1 Seminar on Seismic Isolation, Passive Energy Dissipation, and Active Control 1, p. 59-70.

- Seed, I., M. Idriss, and F.W. Kiefer (1969), Characteristics of rock motions during earthquakes, Journal of the Soil Mechanics and Foundations Division, American Society of Civil Engineers 95, No. SM5, September.

- Silva, W.J. and K. Lee (1987), WES RASCAL code for synthesizing earthquake ground motions, State-of-the-Art for Assessing Earthquake Hazards in the United States, Report 24, U.S. Corps of Engineers Waterways Experiment Station, Misc. Paper S-73-1, 120 p.

- Singh, S. and R.B. Herrmann (1983), Regionalization of crustal coda Q in the continental U.S., Journal of Geophysical Research 88, p. 527-538.

- Stanley, W.D. (1982), Magnetotelluric soundings on the Idaho National Engineering Laboratory Facility, Idaho, Journal of Geophysical Research 87, p. 2683-2691.

- Stover, C.W., R.B. Simson, and W. Person (1977), Earthquake in the United States, April-June 1975, U.S. Geological Survey Circular 749-B, 29 pp.
- Tera Corporation (1978), Influence of seismic modeling on seismic exposure evaluation, Tera Corporation, Berkeley, California.
- Tera Corporation (1984), Seismic hazard analysis for Area 410, Nevada Test Site, Tera Corporation, Berkeley, California.
- Tera Corporation (1984), Seismic hazard analysis for the Idaho National Engineering Laboratory, unpublished report prepared for Lawrence Livermore National Laboratory, 55 p.
- Youngs, R.R. and K.J. Coppersmith (1990), Keeping pace with the science: Seismic hazard analysis in the western U.S., Proceedings of the Second Natural Phenomena Hazards Mitigation Conference, p. 262-270.
- Woodward-Clyde Federal Services (1997), Letter transmittal of update earthquake catalog 1884-1995, Ivan Wong Letter, December 30, Oakland, California.

Contents of Attachment 23
Geotechnical data package for the TMI-2 ISFSI site

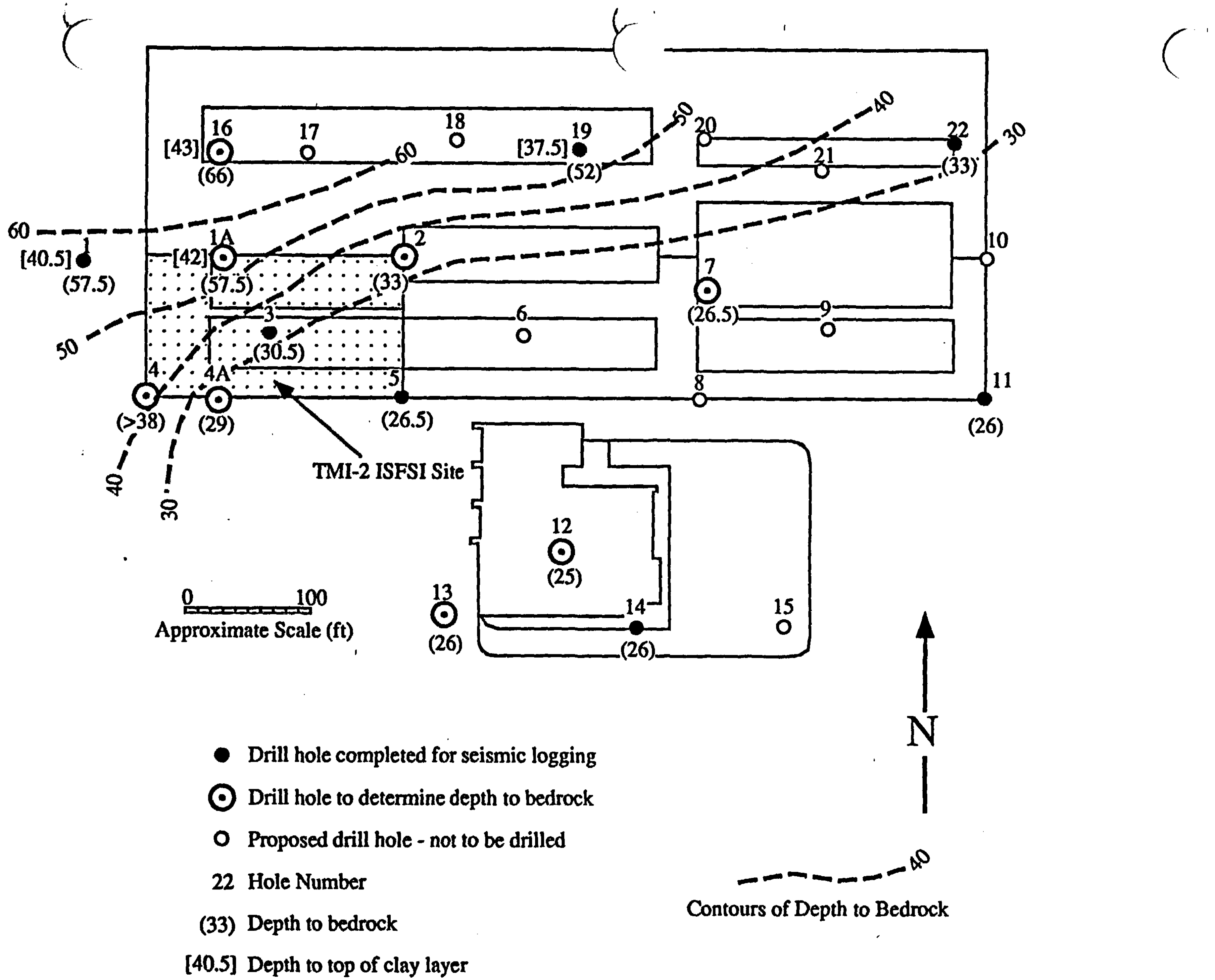

TMI-2 ISFSI Site
0 100
Approximate Scale (ft)
N
Drill hole completed for seismic logging
Drill hole to determine depth to bedrock
Proposed drill hole - not to be drilled
22 Hole Number
(33) Depth to bedrock
[40.5] Depth to top of clay layer
Contours of Depth to Bedrock

Standard Penetration Test Results for TMI-2 ISFSI Site Boreholes at ICPP
November, 1997

Hole Number	Blows/ft at 5.5-6.5 ft	Blows/ft at 20.5-21.5 ft
1	106	69
1A	32	167
2	32	69
3	-	-
4A	178	90
5	31	79
7	28	108
11	30	121
12	62	98
13	59	188
14	62	224
16	18	166
19	62	113
22	53	135

Table 1 DOWNHOLE SEISMIC VELOCITIES

Depth (m)	Depth (feet)	BH-1		BH-11		BH-14		BH-19		BH-22		BH-3		BH-5	
		S-wave velocity Average	P-wave Velocity Average	S-wave velocity Average	P-wave Velocity Average	S-wave velocity Average	P-wave Velocity Average	S-wave velocity Average	P-wave Velocity Average	S-wave velocity Average	P-wave Velocity Average	S-wave velocity Average	P-wave Velocity Average	S-wave velocity Average	P-wave Velocity Average
1	3.28	375	549							367	595	322	545	234	410
2	6.56	375	549			353	514	296	565	367	595	322	545	234	410
3	9.84	375	549			353	514	296	565	367	595	322	545	234	410
4	13.12	469	827	498	1328	497	1009	296	565	367	595	322	545	234	410
5	16.40	469	827	498	1328	497	1009	296	565	367	595	322	545	604	1018
6	19.69	469	827	498	1328	497	1009	430	844	421	1127	586	864	604	1018
7	22.97	469	827	498	1328	497	1009	430	844	421	1127	586	864	604	1018
8	26.25	469	827	498	1328	497	1009	430	844	421	1127	586	864	604	1018
9	29.53	469	827	498	1328	497	1009	430	844	421	1127	586	864	1005	2444
10	32.81	469	827	498	1328	857	2497	430	844	421	1127	586	864	1005	2444
11	36.09	469	827	882	2719	857	2497	430	844	679	2443	586	864	1005	2444
12	39.37	387	669	882	2719	857	2497	430	844	679	2443	1215	2700	1005	2444
13	42.65	387	669	882	2719	857	2497	430	844	679	2443	1215	2700	1005	2444
14	45.93	387	669	882	2719			430	844	679	2443	1215	2700	1005	2444
15	49.21	387	669					430	844	679	2443	1215	2700		
16	52.49	387	669					430	844			1215	2700		
17	55.77	387	669					733	2291						
18	59.06	939	1857					733	2291						
19	62.34	939	1857					733	2291						
20	65.62	939	1857					733	2291						
21	68.90	939	1857					733	2291						
22	72.18	939	1857												
23	75.46	939	1857												

NOTE: Horizontal lines indicate the location of bedrock contact from Figure 1

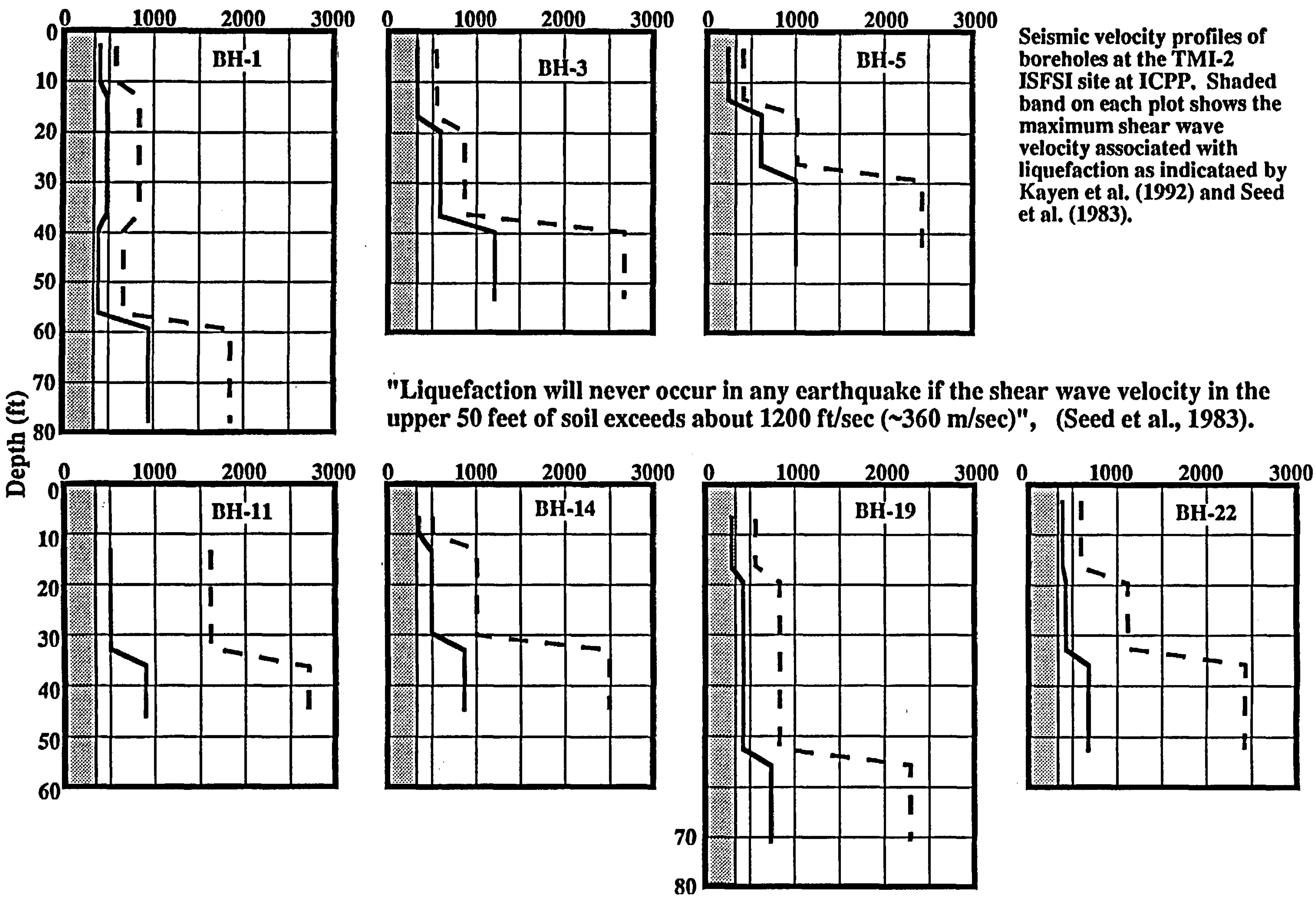

Seismic velocity profiles of boreholes at the TMI-2 ISFSI site at ICPP. Shaded band on each plot shows the maximum shear wave velocity associated with liquefaction as indicataed by Kayen et al. (1992) and Seed et al. (1983).

"Liquefaction will never occur in any earthquake if the shear wave velocity in the upper 50 feet of soil exceeds about 1200 ft/sec (~360 m/sec)", (Seed et al., 1983).

Cyclic Stress Ratio vs Modified SPT N Value (N_1)

Source: Seed R.B., Idriss, I.M., and Arango, I. (1983) Evaluation of liquefaction potential using field performance data; Journal of Engineering Division, ASCE, vol.97, no.3.

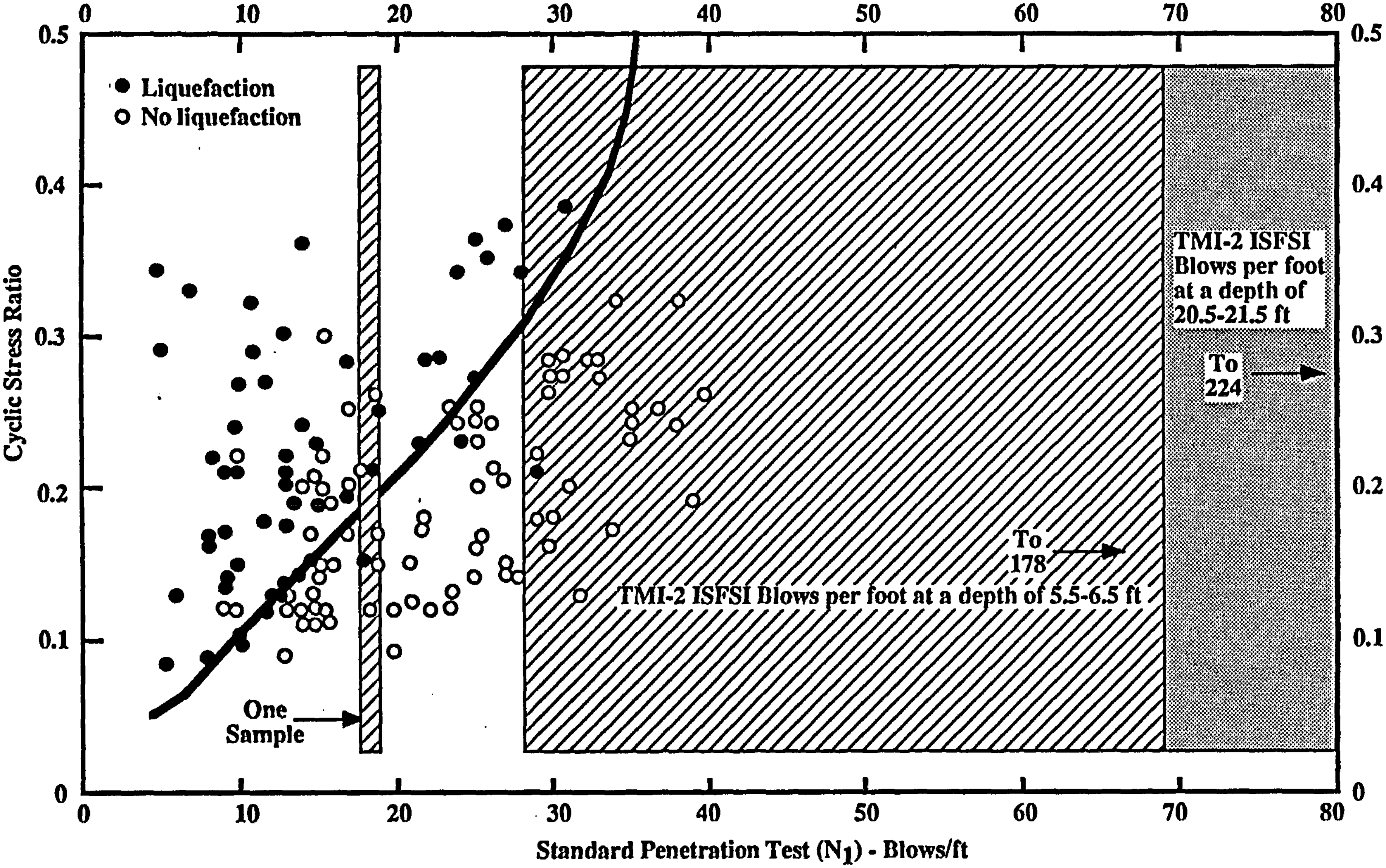

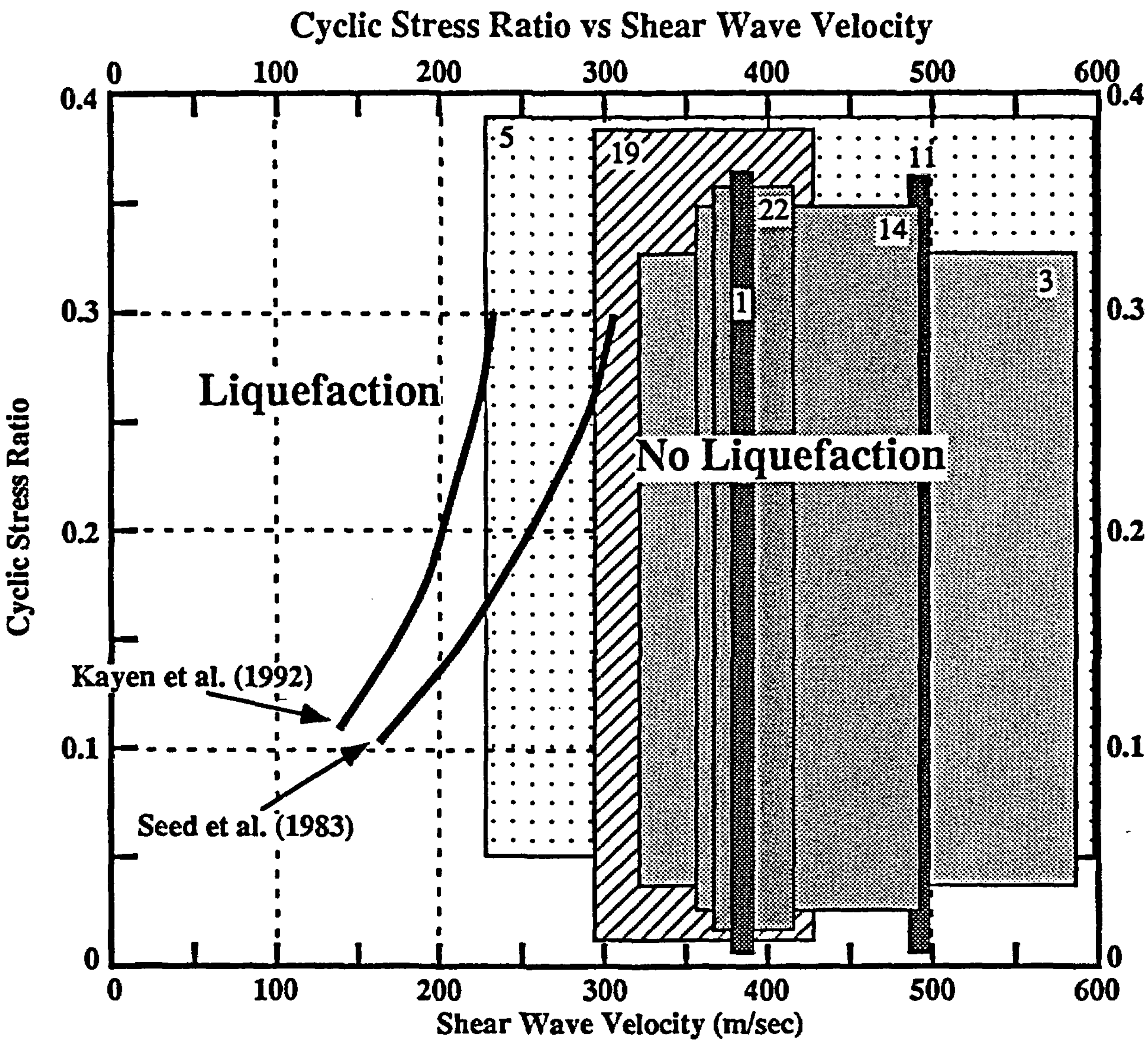

Pattterned boxes show range of shear wave velocities for 7 boreholes at the ISFSI site at ICPP. The 7 boreholes penetrated the entire thickness of the surficial sediment at ICPP (25 to 66 feet). Box numbers correspond to borehole numbers shown on the ISFSI borehole location map.

References:

Kayen, R.E., et al. (1992) Evaluation of SPT-CPT- and shear wave-based methods for liquefaction potential assessment using Loma Prieta Data; Proced. of 4th Japan-US Workshop on Earthquake Resistance Design of Lifetime Facilities and Counter Measures for Liquefaction, v.1.

Seed, R.B., Idress, I.M., and Arango, I. (1983) Evaluation of liquefaction potential using field performance data; Journal of Geotechnical Engineering Division, ASCE, V.97, no.3.

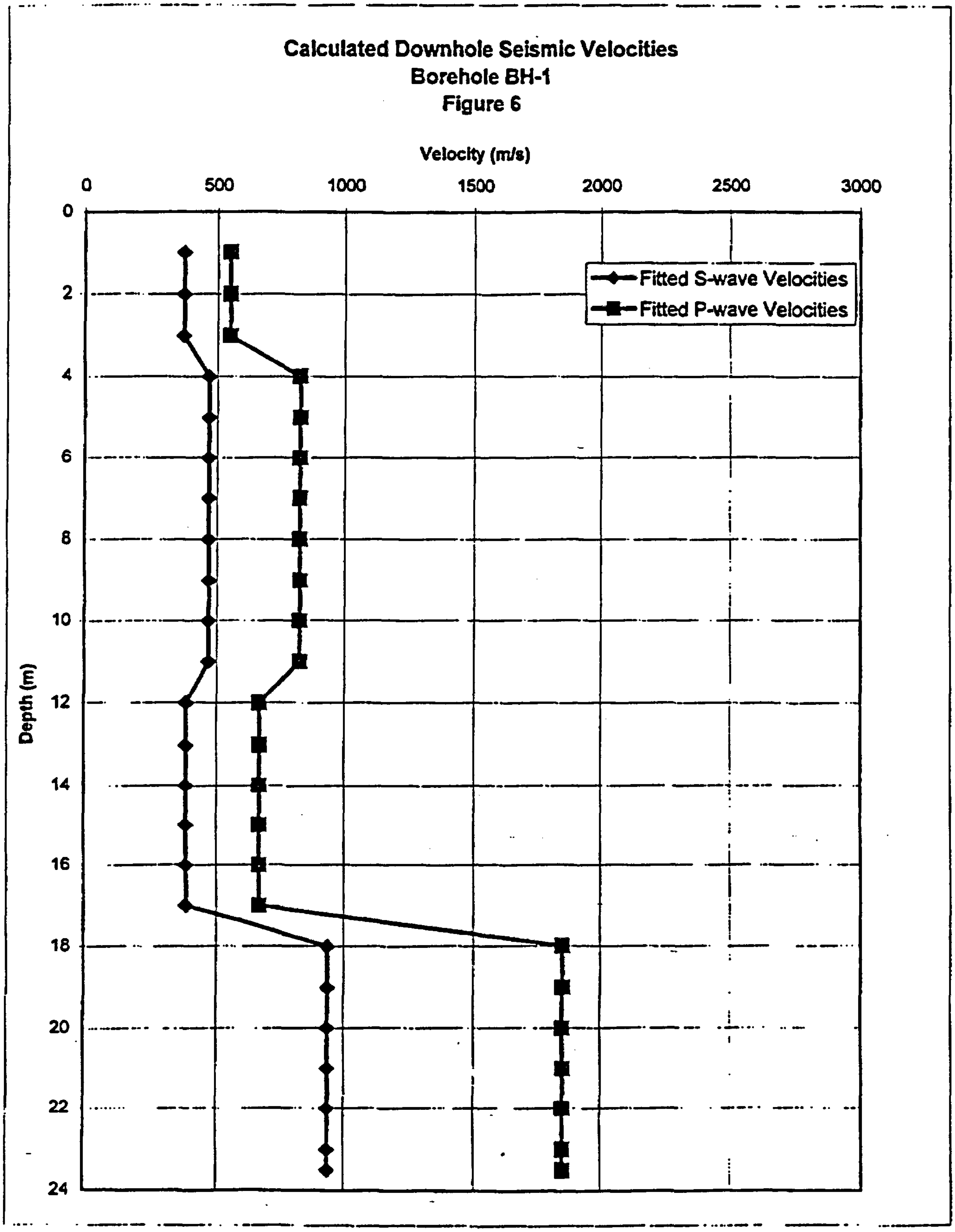
Calculated Downhole Seismic Velocities
Borehole BH-1
Figure 6
Velocity (m/s)
0
500
1000
1500
2000
2500
3000
Depth (m)
0
2
4
6
8
10
12
14
16
18
20
22
24
Fitted S-wave Velocities
Fitted P-wave Velocities

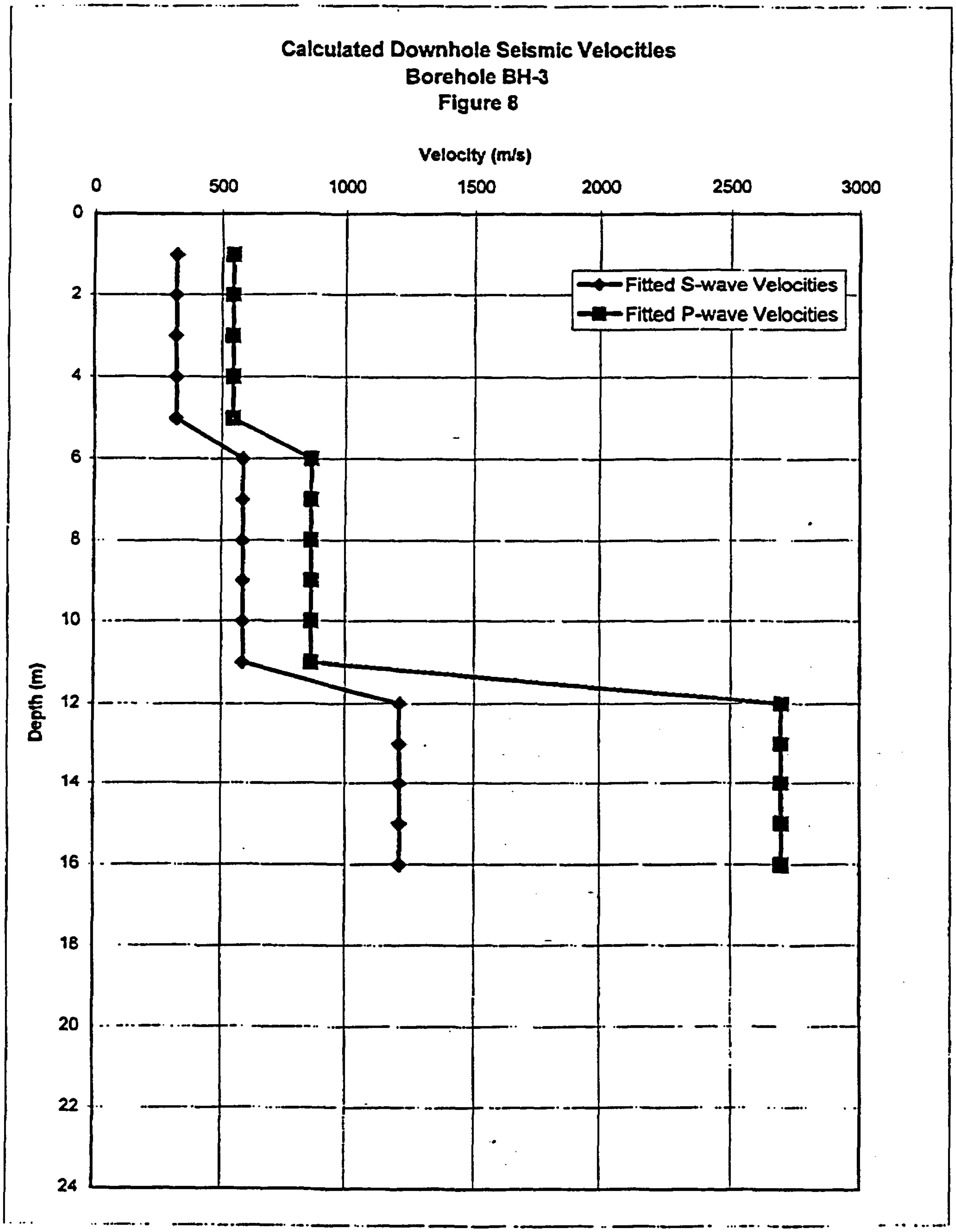
Calculated Downhole Seismic Velocities
Borehole BH-3
Figure 8
Velocity (m/s)
0
500
1000
1500
2000
2500
3000
Depth (m)
0
2
4
6
8
10
12
14
16
18
20
22
24
Fitted S-wave Velocities
Fitted P-wave Velocities

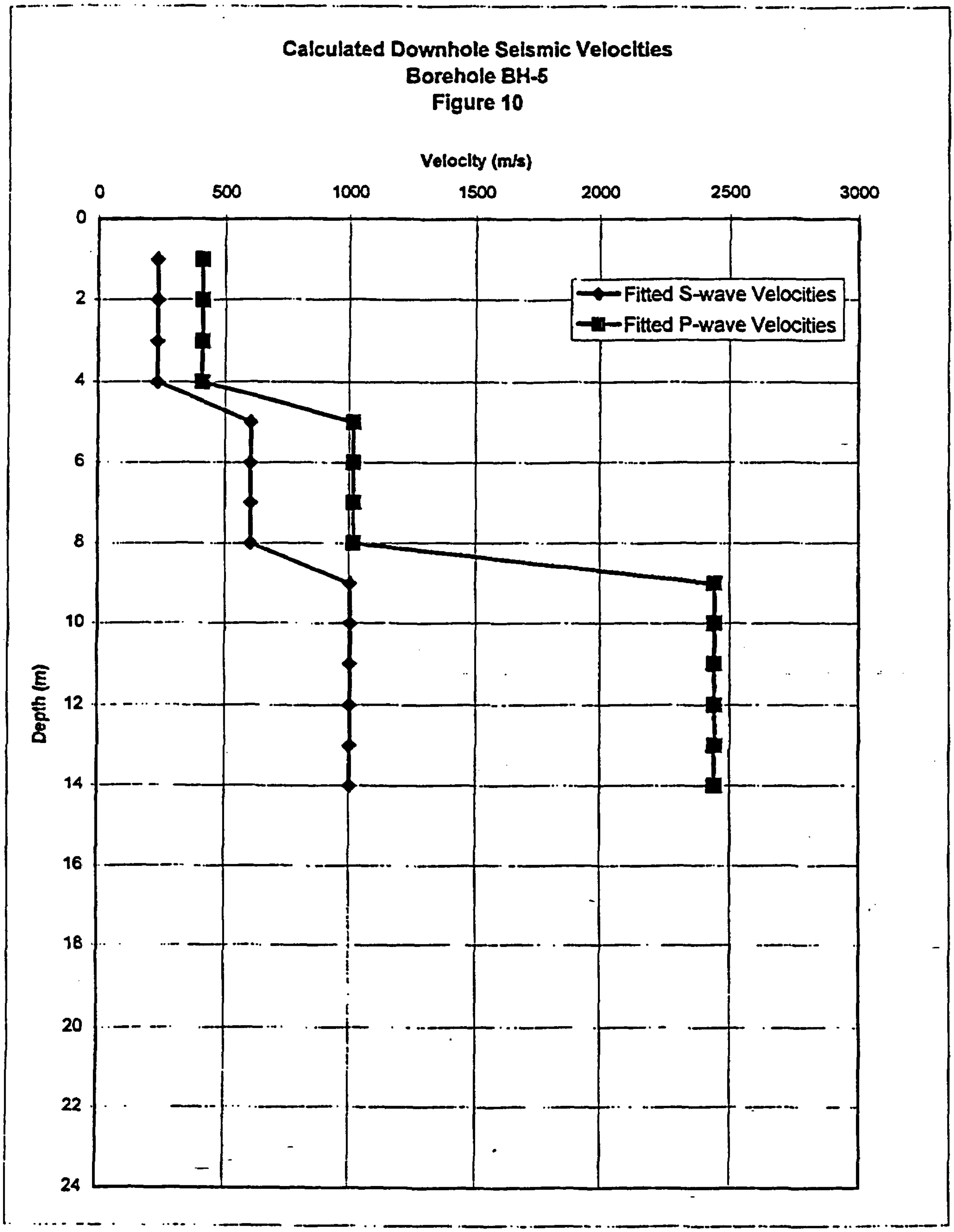
Calculated Downhole Seismic Velocities
Borehole BH-5
Figure 10
Velocity (m/s)
0
500
1000
1500
2000
2500
3000
Depth (m)
0
2
4
6
8
10
12
14
16
18
20
22
24
Fitted S-wave Velocities
Fitted P-wave Velocities

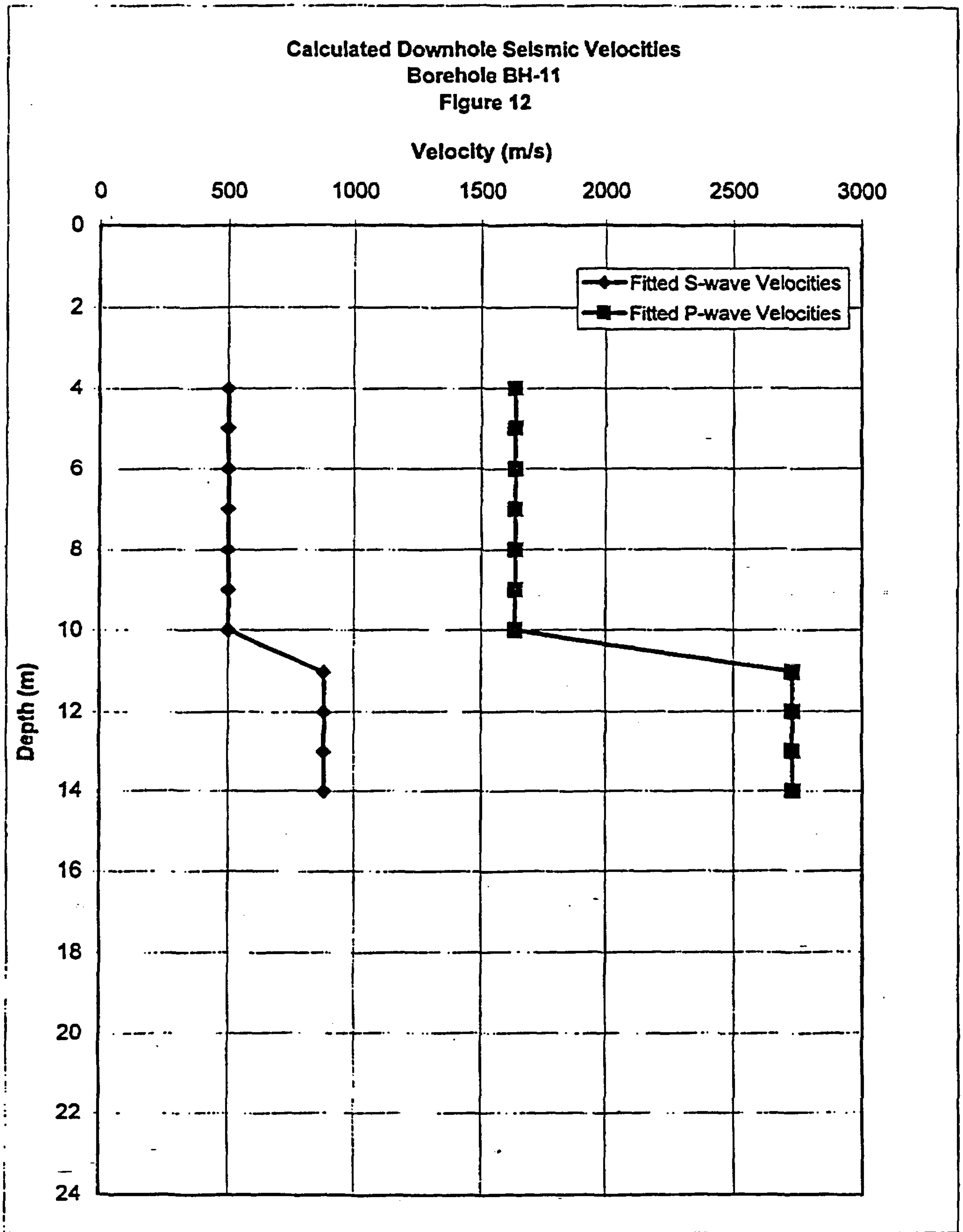
Calculated Downhole Seismic Velocities
Borehole BH-11
Figure 12
Velocity (m/s)
0
500
1000
1500
2000
2500
3000
Depth (m)
0
2
4
6
8
10
12
14
16
18
20
22
24
Fitted S-wave Velocities
Fitted P-wave Velocities

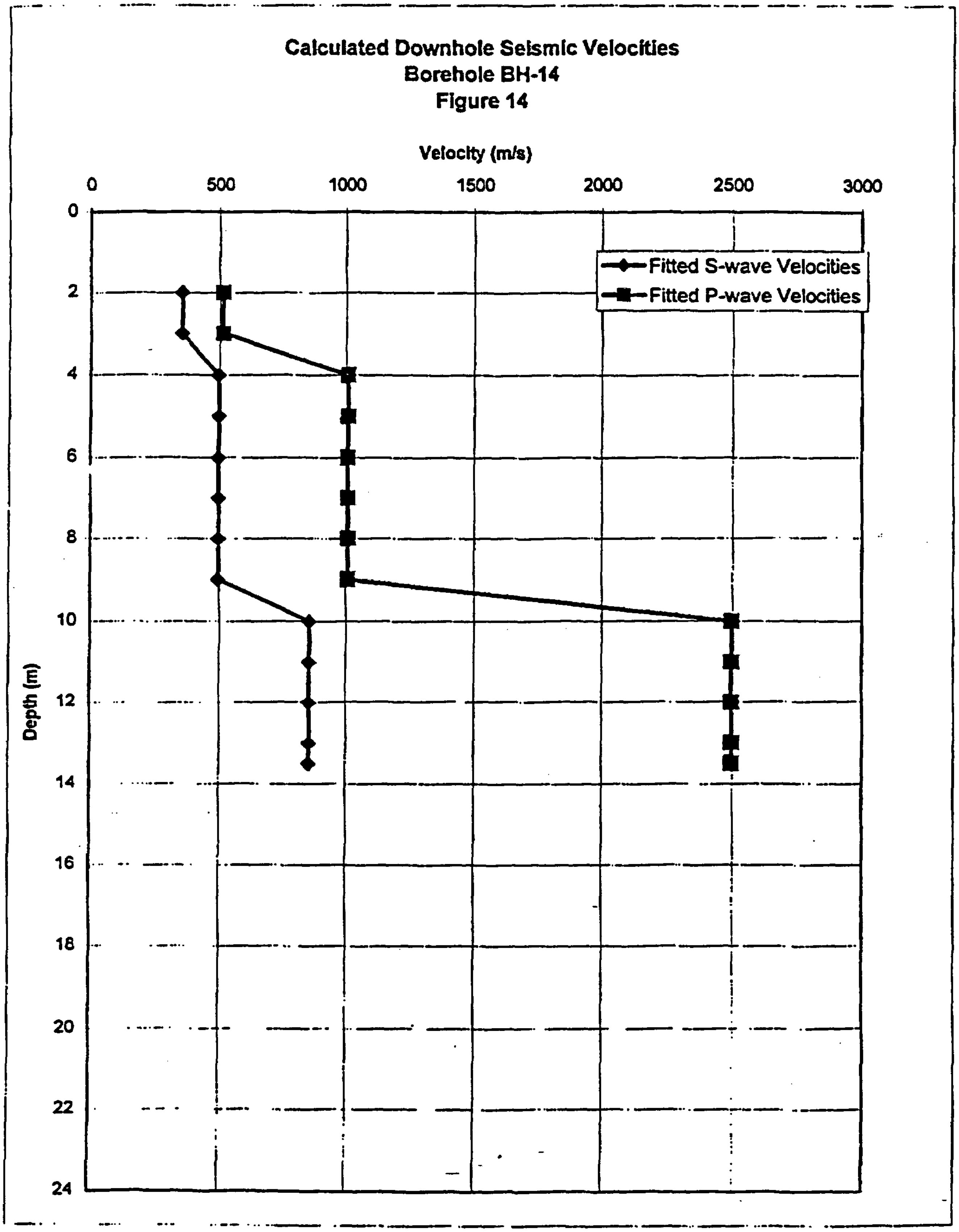
Calculated Downhole Seismic Velocities
Borehole BH-14
Figure 14
Velocity (m/s)
0
500
1000
1500
2000
2500
3000
Depth (m)
0
2
4
6
8
10
12
14
16
18
20
22
24
Fitted S-wave Velocities
Fitted P-wave Velocities

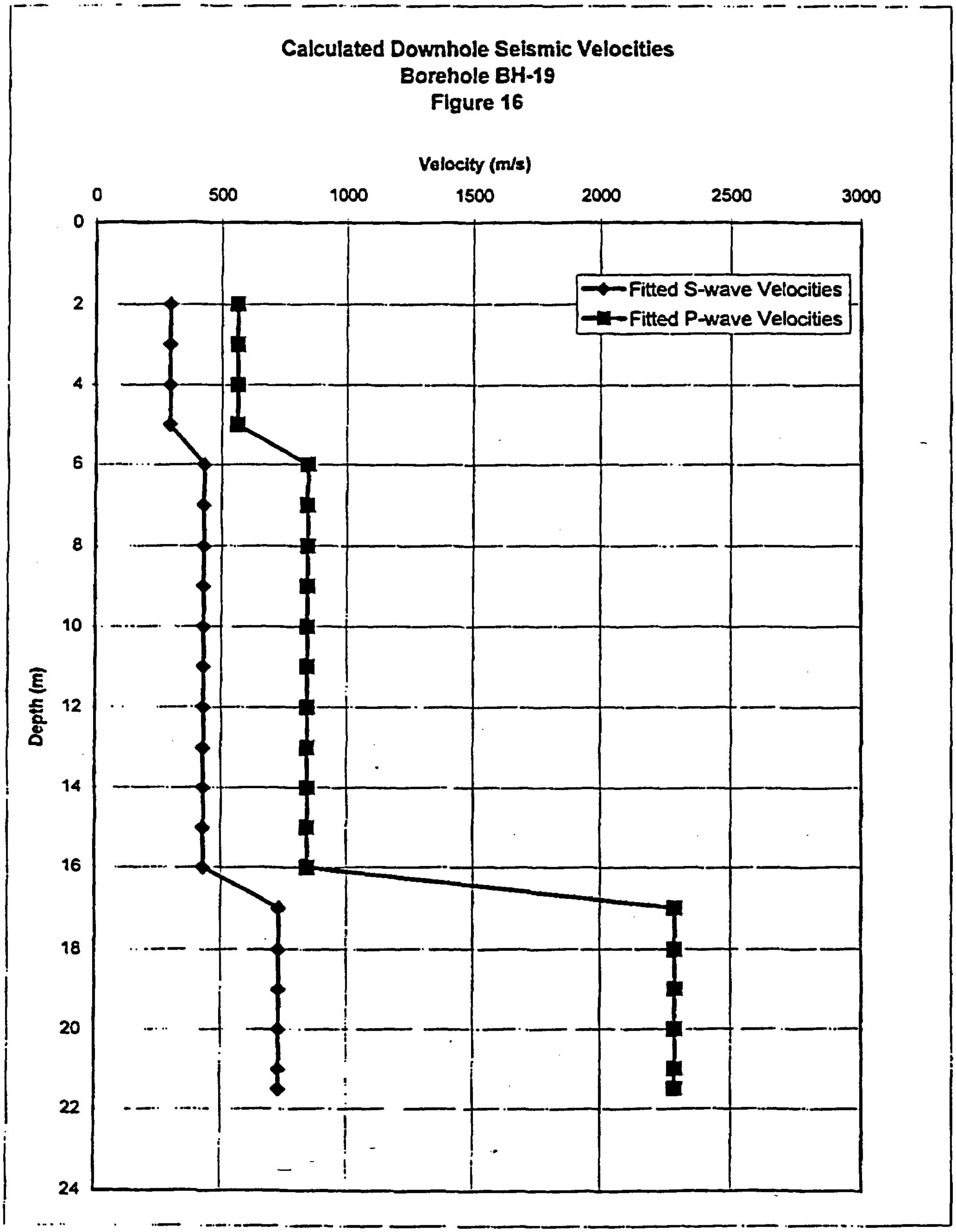
Calculated Downhole Seismic Velocities
Borehole BH-19
Figure 16
Velocity (m/s)
0
500
1000
1500
2000
2500
3000
Depth (m)
0
2
4
6
8
10
12
14
16
18
20
22
24
Fitted S-wave Velocities
Fitted P-wave Velocities

Calculated Downhole Seismic Velocities
Borehole BH-22
Figure 18

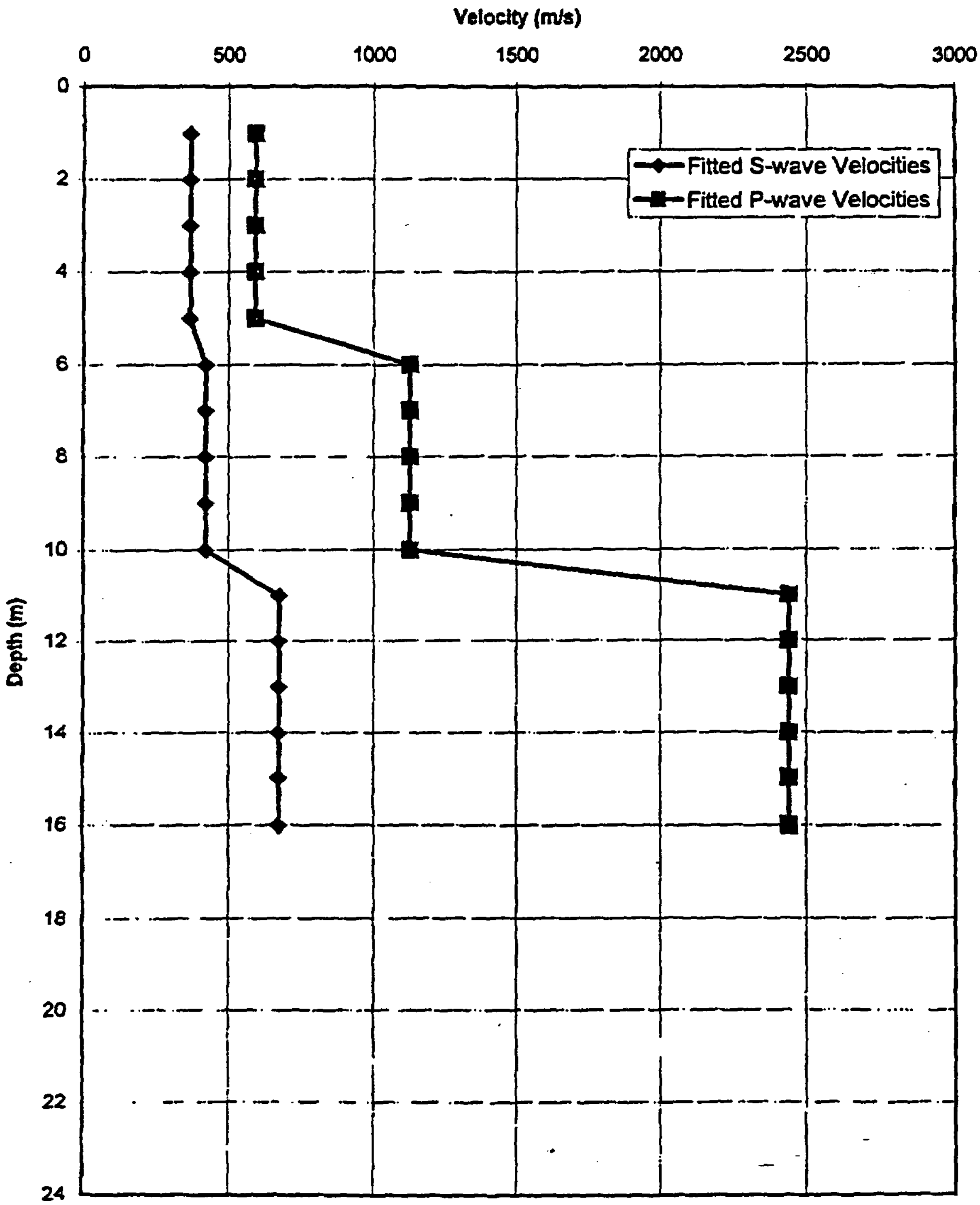

WELL NAME: ICPP-BH-1
Facility: ICPP
Well Type: GEOTECHNICAL
Well Status: Seismic logging
Year Drilled: 1997
Total Depth: 57.5

Easting:
Northing:
Longitude:
Latitude:
Completion Depth:

Driller: DANIELSON/TOWLER
Geologist: HERSLEY
Drill Method: HOLLOW STEM AUGER
Drill Fluid:
Land Surface:

Date: 12/2/97
Water Level: N/A
Water Level Date: N/A
Water Level Access: N/A

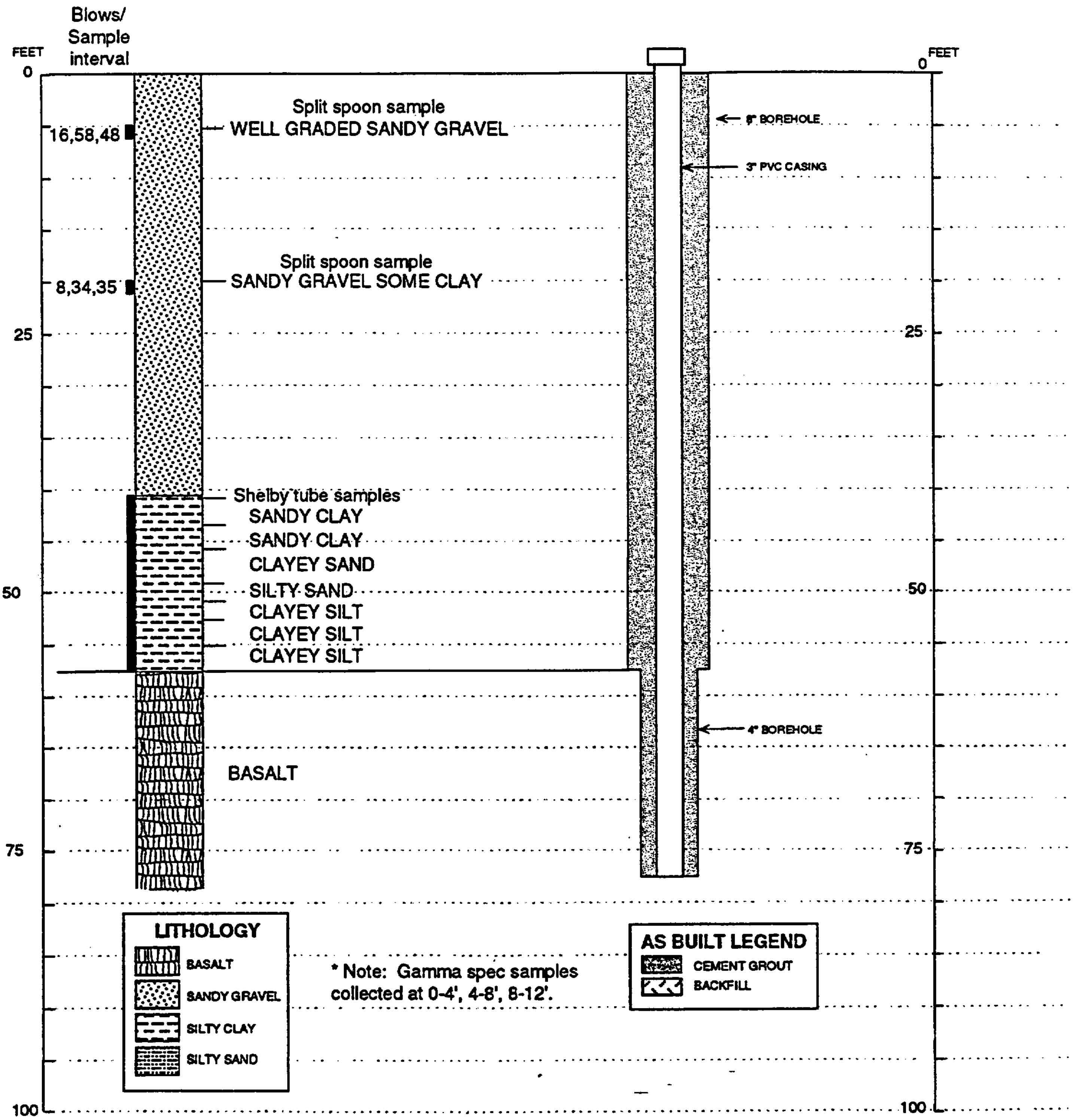

WELL NAME: ICPP-BH-1A	Easting:	Driller: DANIELSON/TOWLER	Date: 12/2/97
Facility: ICPP	Northing:	Geologist: HERSLEY	Water Level: N/A
ell Type: GEOTECHNICAL	Longitude:	Drill Method: HOLLOW STEM AUGER	
ell Status ABANDONED	Latitude:	Drill Fluid:	Water Level Date: N/A
Year Drilled: 1997			
Total Depth 57.5	Completion Depth:	Land Surface:	Water Level Access: N/A

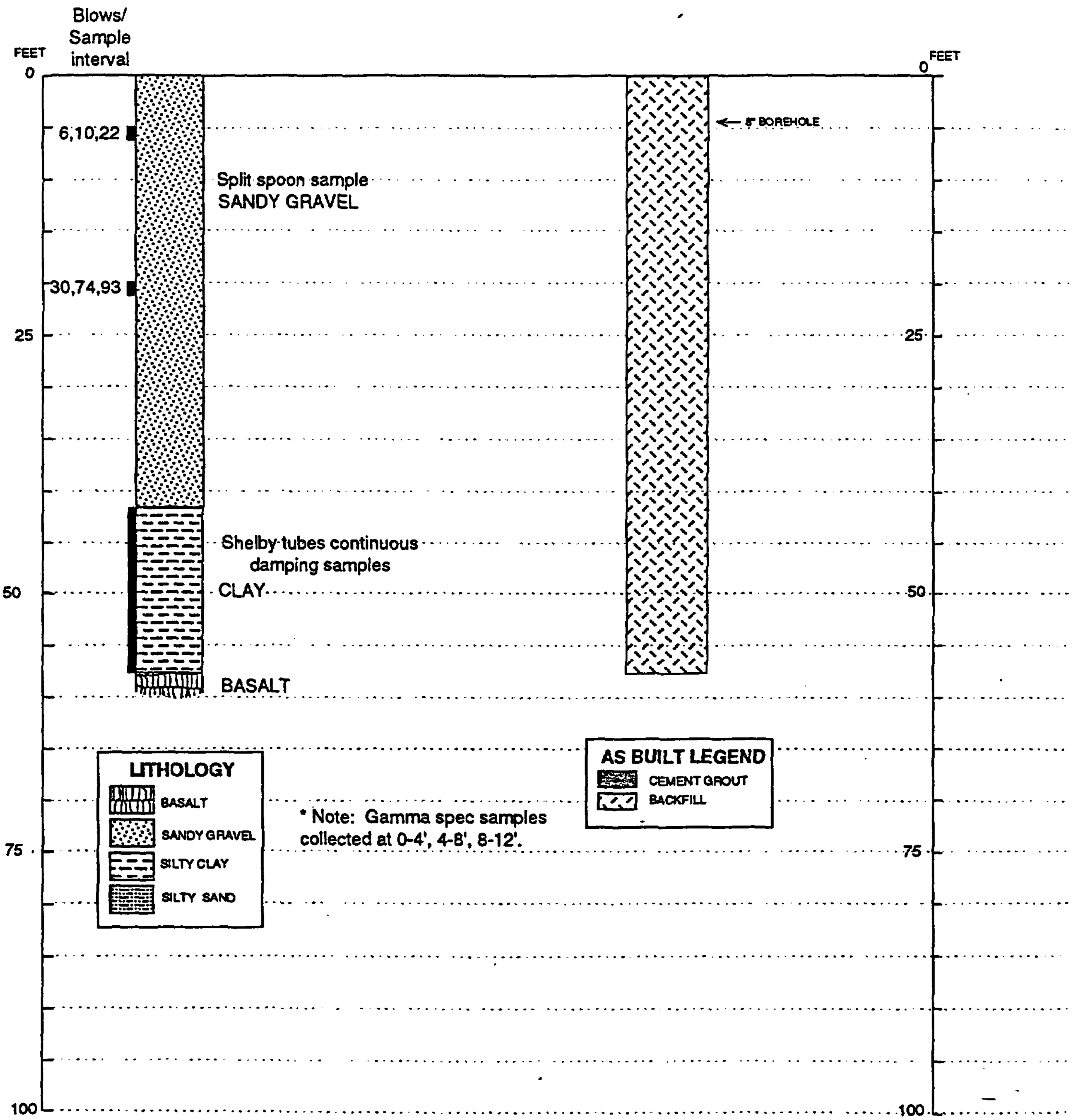

WELL NAME: ICPP-BH-2
Facility: ICPP
'ell Type: GEOTECHNICAL
ell Status ABANDONED
Year Drilled: 1997
Total Depth 33.2

Easting:
Northing:
Longitude:
Latitude:
Completion Depth:

Driller: DANIELSON/TOWLER
Geologist: HERSLEY
Drill Method: HOLLOW STEM AUGER
Drill Fluid:
Land Surface:

Date: 12/2/97
Water Level: N/A
Water Level Date: N/A
Water Level Access: N/A

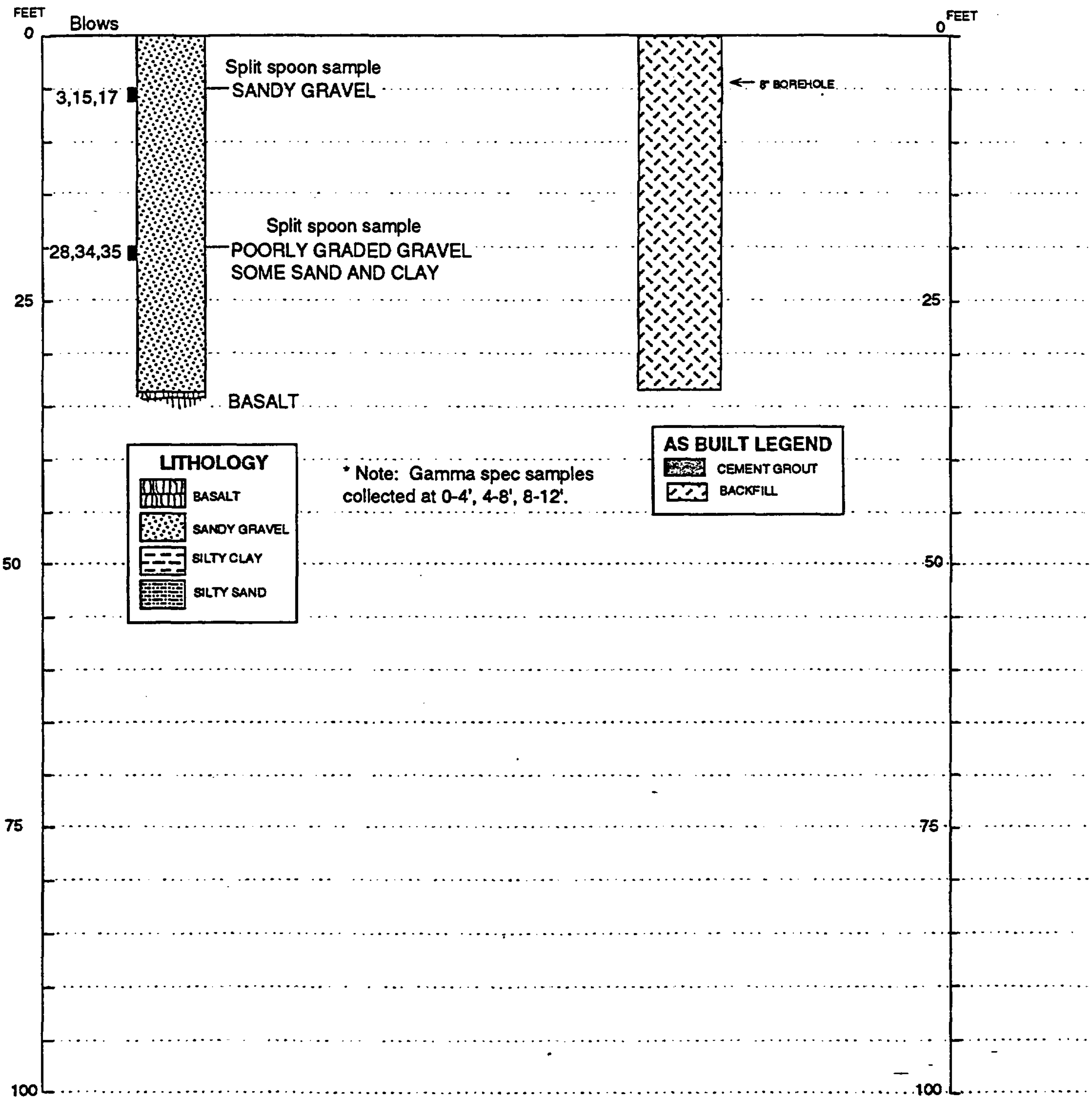

* Note: Gamma spec samples collected at 0-4', 4-8', 8-12'.

WELL NAME: ICPP-BH-3	Easting:	Driller: DANIELSON/TOWLER	Date: 12/2/97
Facility: ICPP	Northing:	Geologist: HERSLEY	Water Level: N/A
Well Type: GEOTECHNICAL	Longitude:	Drill Method: HOLLOW STEM AUGER	Water Level Date: N/A
Well Status: Seismic logging	Latitude:	Drill Fluid:	Water Level Access: N/A
Year Drilled: 1997	Completion Depth:	Land Surface:	
Total Depth: 50.75			

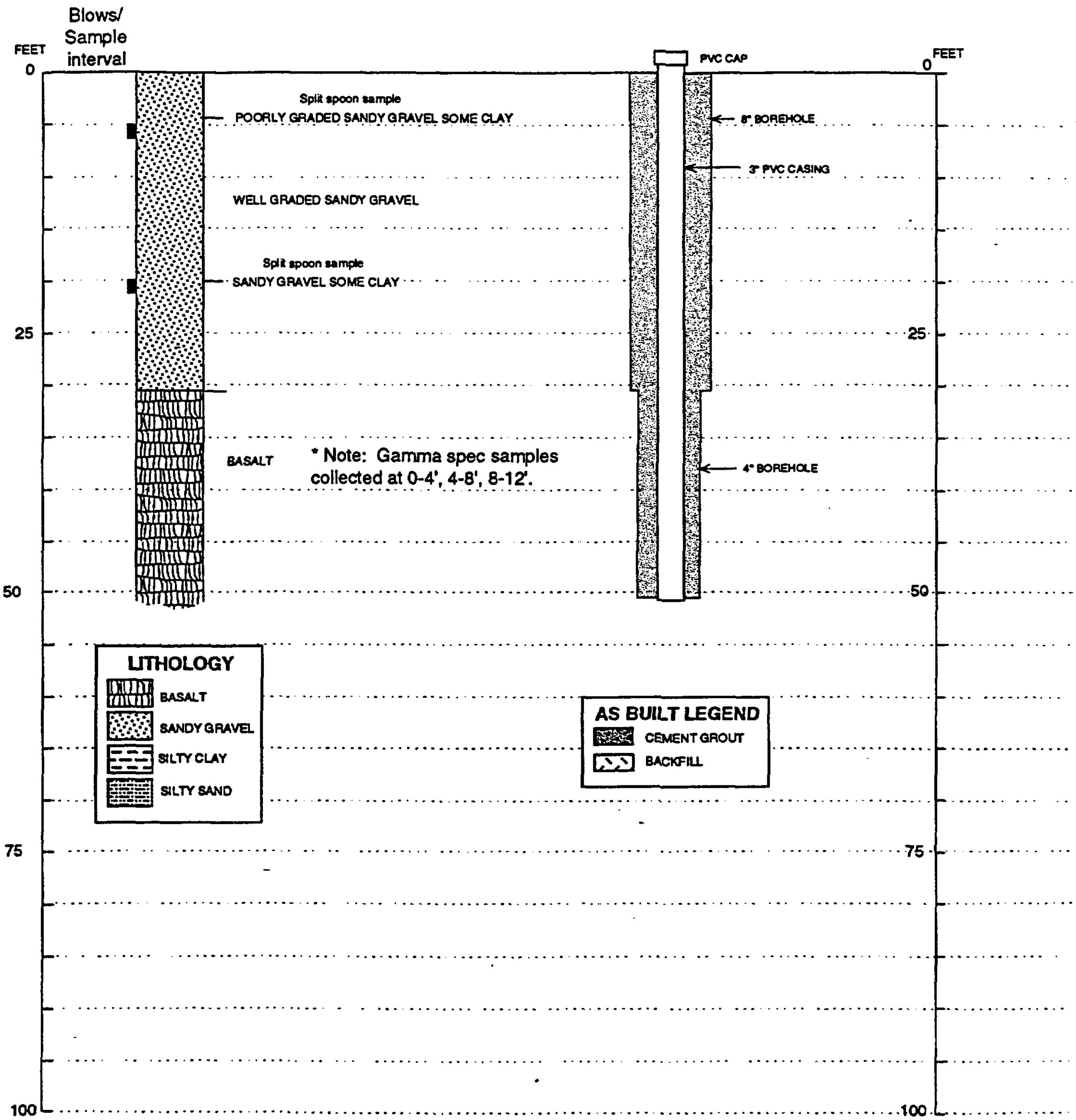

WELL NAME: ICPP-BH-4A	Easting:	Driller: DANIELSON/TOWLER	Date: 12/2/97
Facility: ICPP	Northing:	Geologist: HERSLEY	Water Level: N/A
Well Type: GEOTECHNICAL	Longitude:	Drill Method: HOLLOW STEM AUGER	Water Level Date: N/A
Well Status ABANDONED	Latitude:	Drill Fluid:	
Year Drilled: 1997			
Total Depth 28.75	Completion Depth:	Land Surface:	Water Level Access: N/A

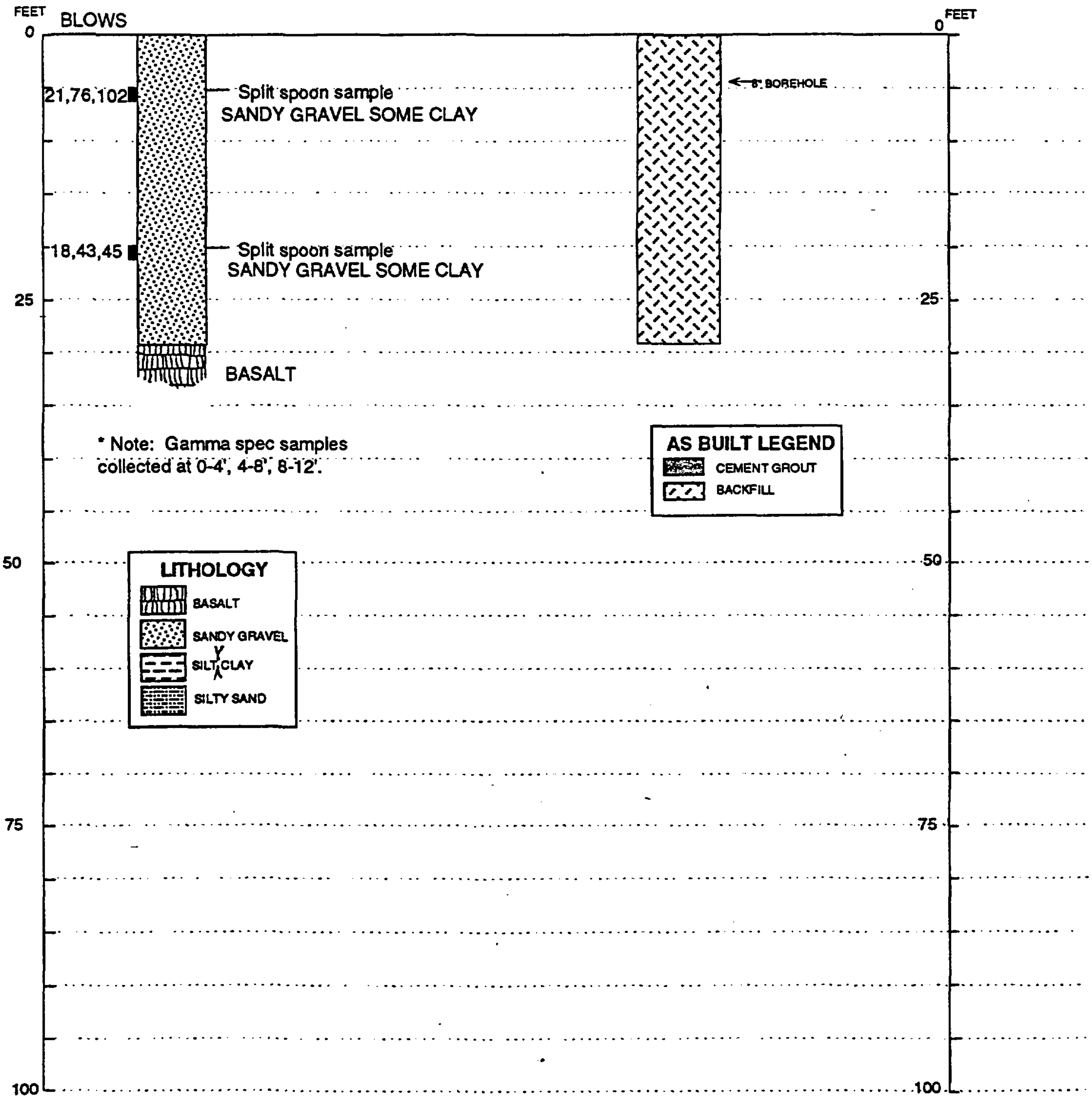

WELL NAME: ICPP-BH-5	Easting:	Driller: DANIELSON/TOWLER	Date: 12/2/97
Facility: ICPP	Northing:	Geologist: HERSLEY	Water Level: N/A
'ell Type: GEOTECHNICAL	Longitude:	Drill Method: HOLLOW STEM AUGER	Water Level Date: N/A
ell Status: Seismic logging	Latitude:	Drill Fluid:	Water Level Access: N/A
Year Drilled: 1997	Completion Depth:	Land Surface:	
Total Depth: 26.5			

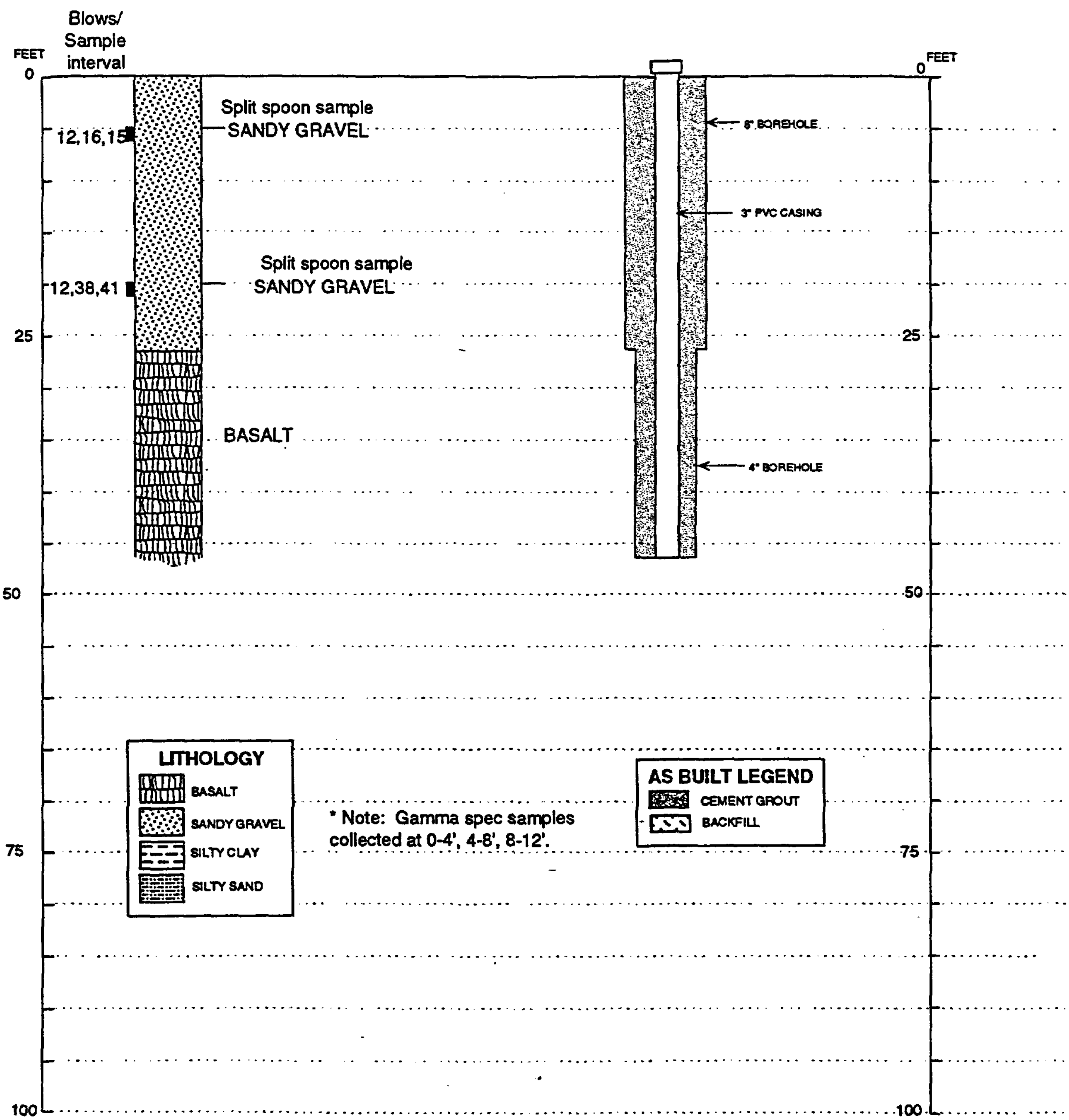

WELL NAME: ICPP-BH-7
Facility: ICPP
Well Type: GEOTECHNICAL
Well Status ABANDONED
Year Drilled: 1997
Total Depth 26.5

Easting:
Northing:
Longitude:
Latitude:
Completion Depth:

Driller: DANIELSON/TOWLER
Geologist: HERSLEY
Drill Method: HOLLOW STEM AUGER
Drill Fluid:
Land Surface:

Date: 12/2/97
Water Level: N/A
Water Level Date: N/A
Water Level Access: N/A

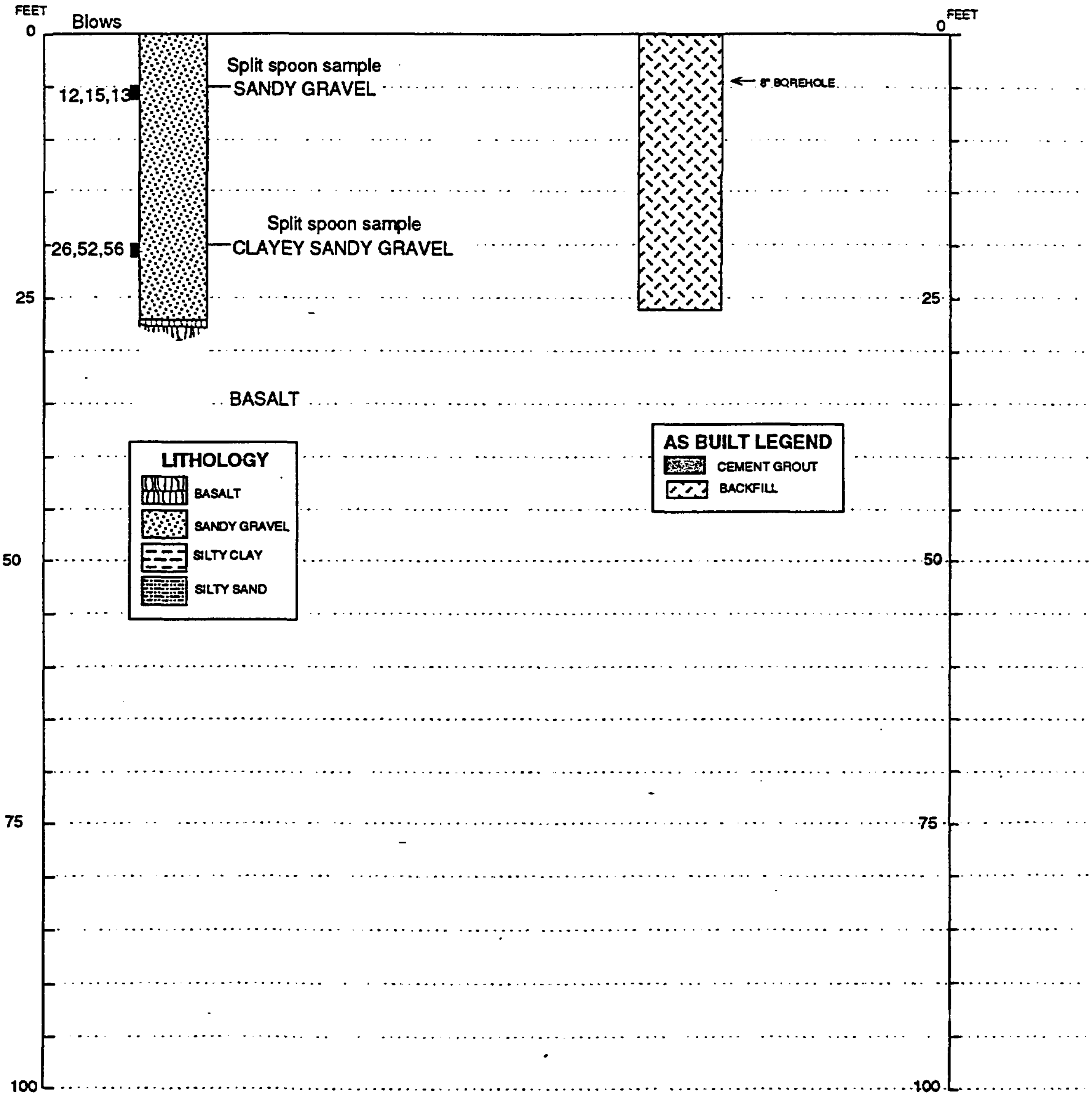

WELL NAME: ICPP-BH-11

Facility: ICPP

Well Type: GEOTECHNICAL

Well Status: Seismic logging

Year Drilled: 1997

Total Depth 48

Easting:

Northing:

Longitude:

Latitude:

Completion Depth:

Driller: DANIELSON/TOWLER

Geologist: HERSLEY

Drill Method: HOLLOW STEM AUGER

Drill Fluid:

Land Surface:

Date: 12/2/97

Water Level: N/A

Water Level Date: N/A

Water Level Access: N/A

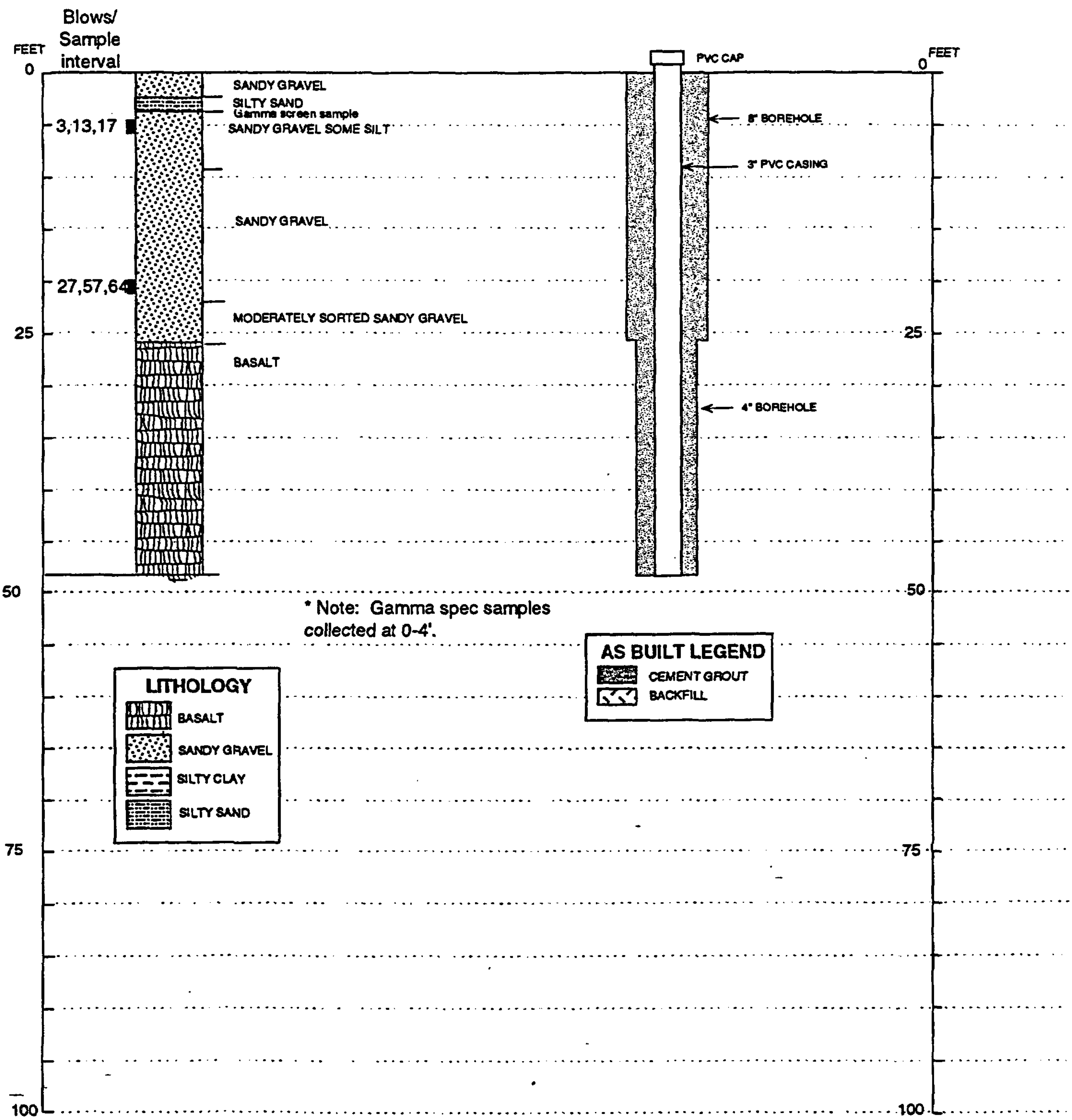

WELL NAME: ICPP-BH-12	Easting:	Driller: DANIELSON/TOWLER	Date: 12/2/97
Facility: ICPP	Northing:	Geologist: HERSLEY	Water Level: N/A
Well Type: GEOTECHNICAL	Longitude:	Drill Method: HOLLOW STEM AUGER	
Well Status ABANDONED	Latitude:	Drill Fluid:	Water Level Date: N/A
Year Drilled: 1997			
Total Depth 25.0	Completion Depth:	Land Surface:	Water Level Access: N/A

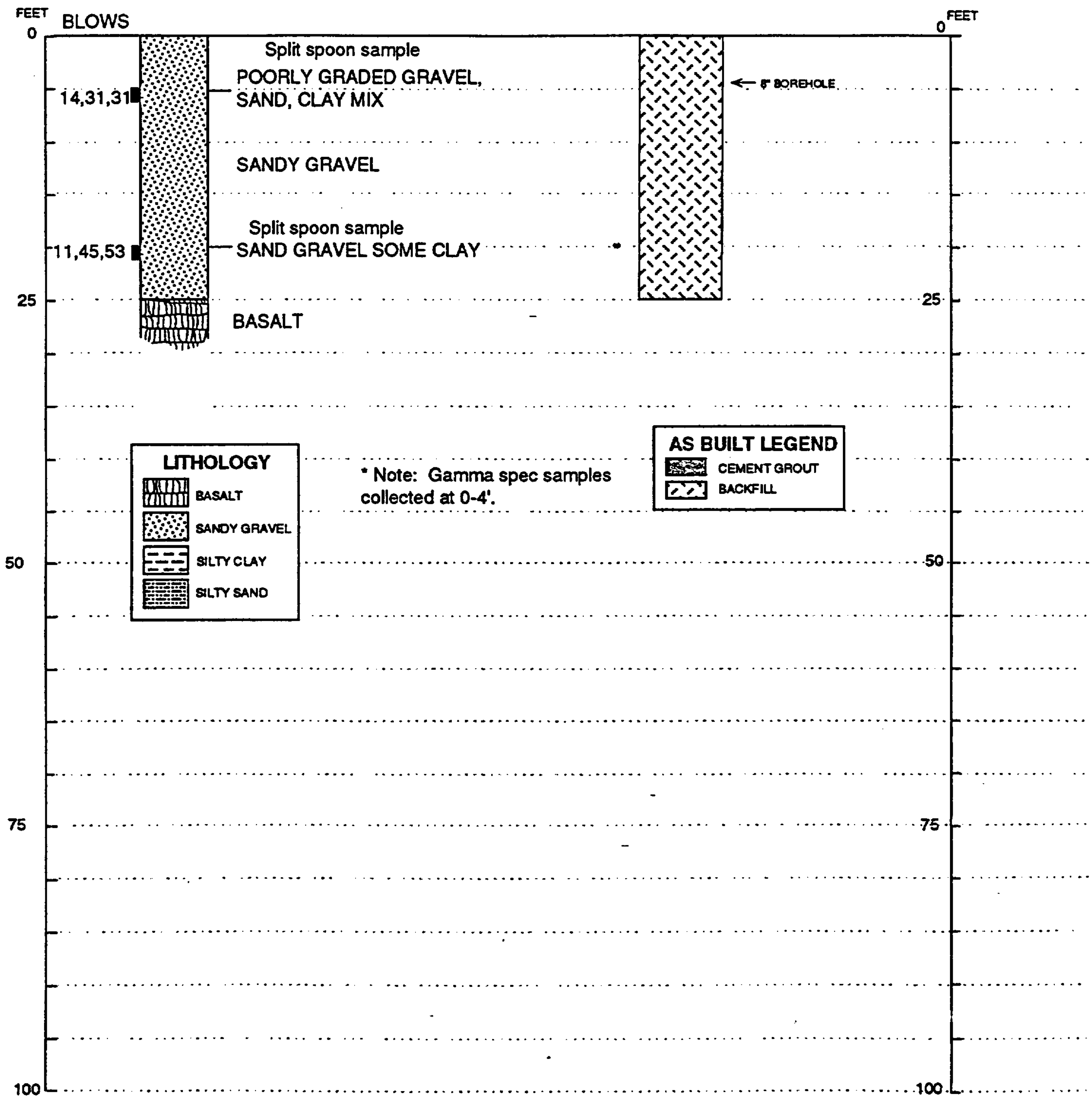

WELL NAME: ICPP-BH-13	Easting:	Driller: DANIELSON/TOWLER	Date: 12/2/97
Facility: ICPP	Northing:	Geologist: HERSLEY	Water Level: N/A
Well Type: GEOTECHNICAL	Longitude:	Drill Method: HOLLOW STEM AUGER	
Well Status: ABANDONED	Latitude:	Drill Fluid:	Water Level Date: N/A
Year Drilled: 1997			
Total Depth: 25.9	Completion Depth:	Land Surface:	Water Level Access: N/A

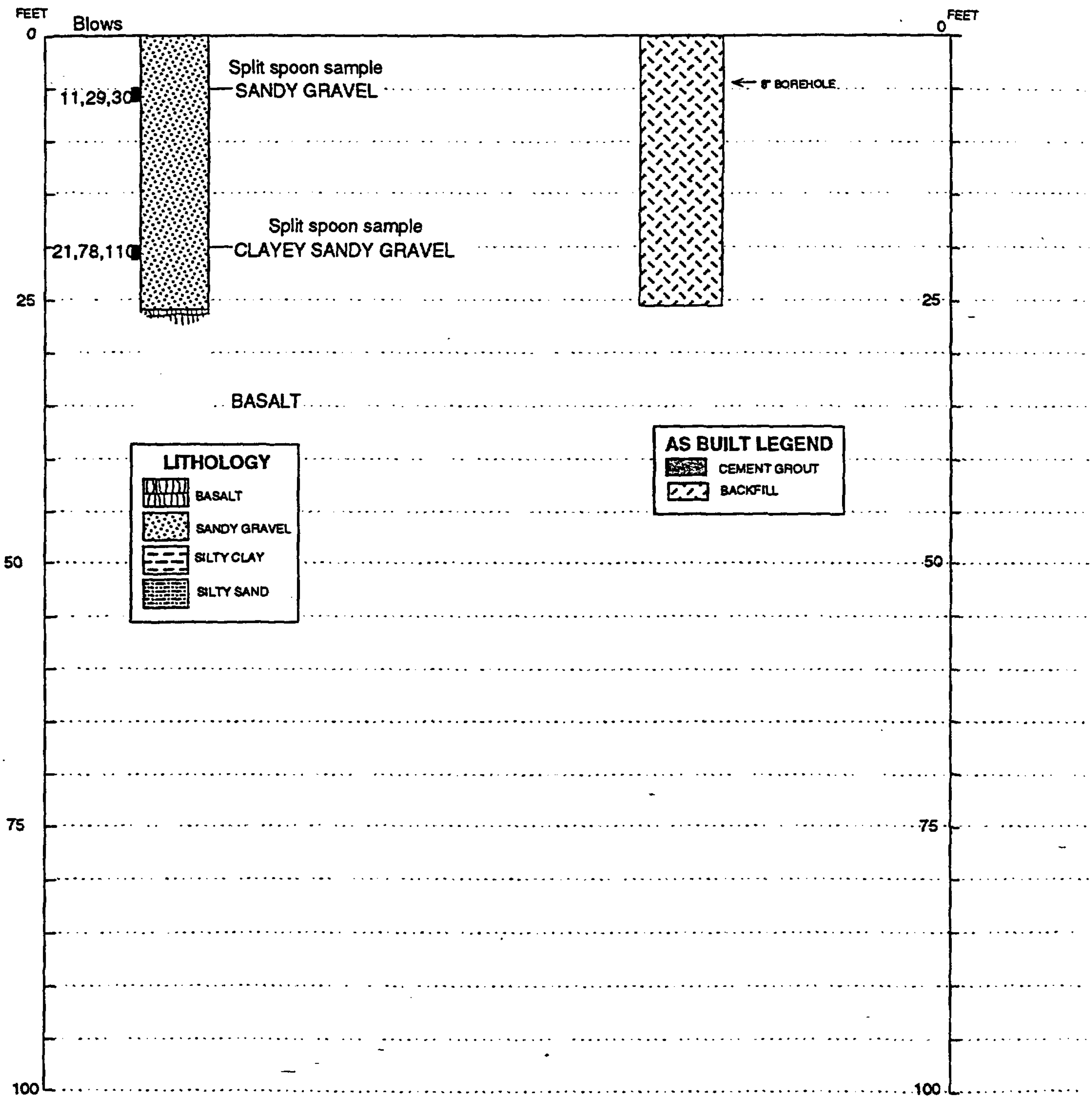

WELL NAME: ICPP-BH-14	Easting:	Driller: DANIELSON/TOWLER	Date: 12/2/97
Facility: ICPP	Northing:	Geologist: HERSLEY	Water Level: N/A
Well Type: GEOTECHNICAL	Longitude:	Drill Method: HOLLOW STEM AUGER	
Well Status: Seismic logging	Latitude:	Drill Fluid:	Water Level Date: N/A
Year Drilled: 1997			
Total Depth: 26.33	Completion Depth:	Land Surface:	Water Level Access: N/A

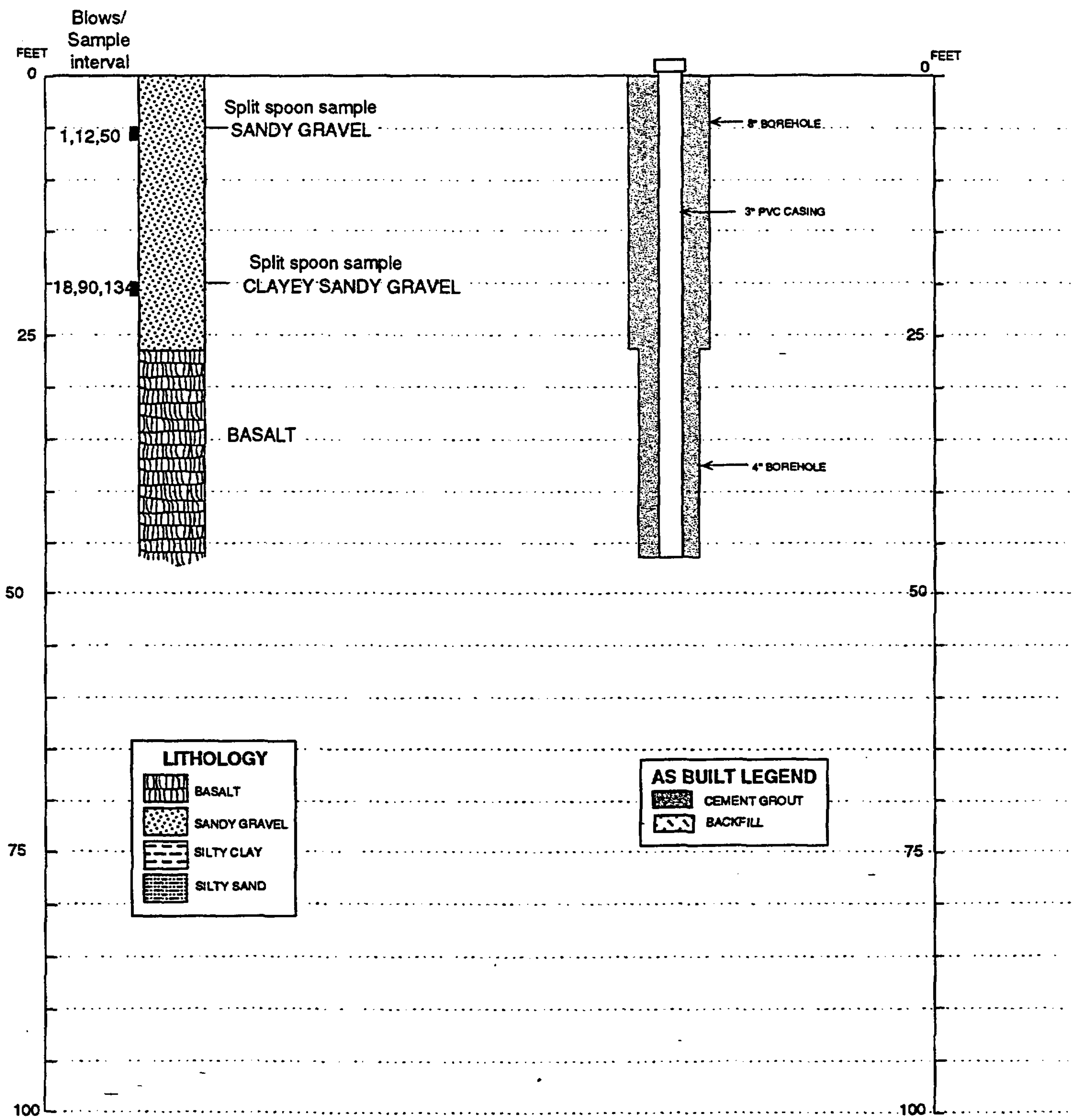

WELL NAME: ICPP-BH-16	Easting:	Driller: DANIELSON/TOWLER	Date: 12/2/97
Facility: ICPP	Northing:	Geologist: HERSLEY	Water Level: N/A
ll Type: GEOTECHNICAL	Longitude:	Drill Method: HOLLOW STEM AUGER	
ll Status ABANDONED	Latitude:	Drill Fluid:	Water Level Date: N/A
Year Drilled: 1997			
Total Depth 66.	Completion Depth:	Land Surface:	Water Level Access: N/A

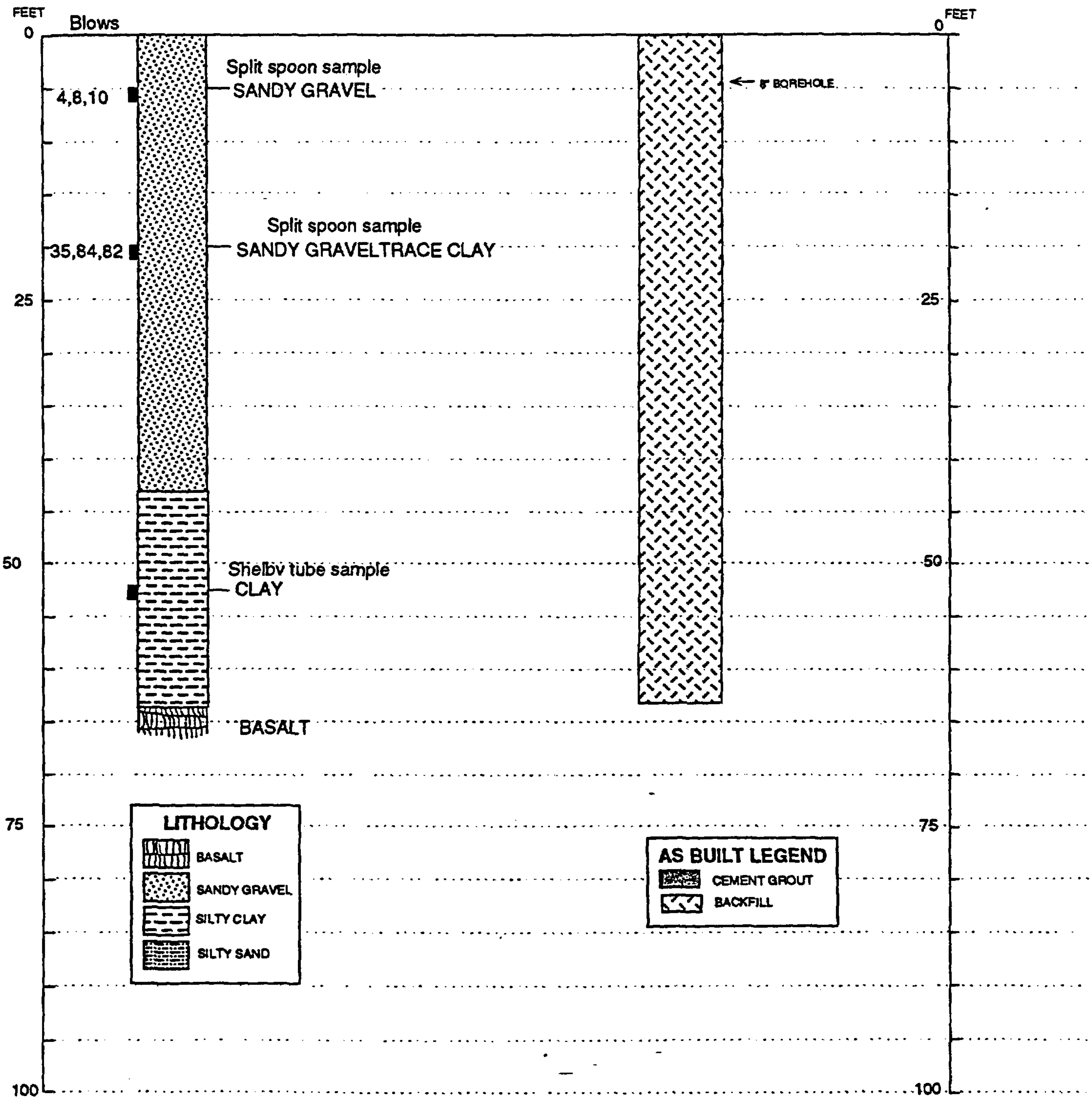

WELL NAME: ICPP-BH-19
Facility: ICPP
Well Type: GEOTECHNICAL
Well Status: Seismic logging
Year Drilled: 1997
Total Depth: 51.75

Easting:
Northing:
Longitude:
Latitude:
Completion Depth:

Driller: DANIELSON/TOWLER
Geologist: HERSLEY
Drill Method: HOLLOW STEM AUGER
Drill Fluid:
Land Surface:

Date: 12/2/97
Water Level: N/A
Water Level Date: N/A
Water Level Access: N/A

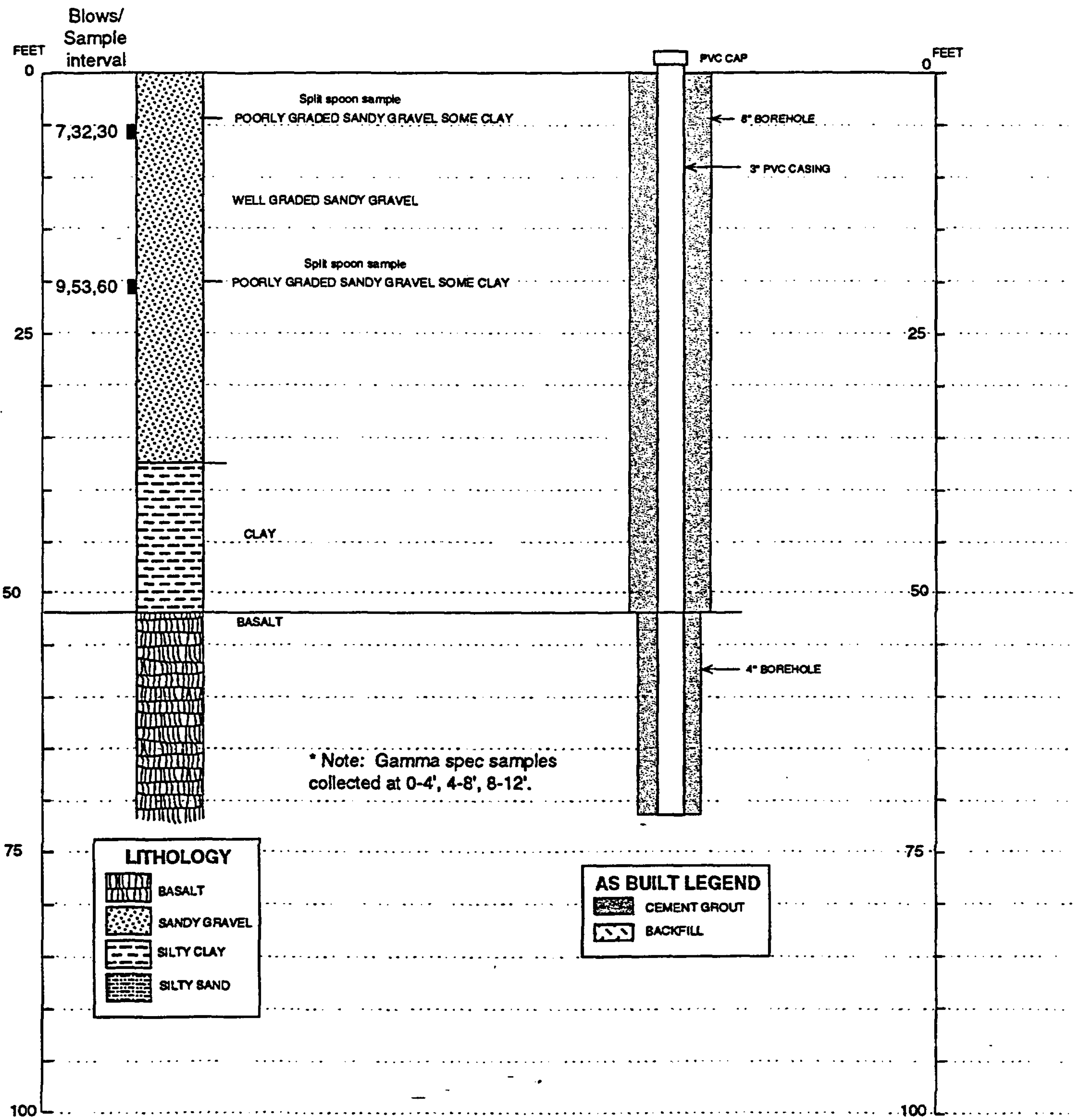

WELL NAME: ICPP-BH-22
Facility: ICPP
Well Type: GEOTECHNICAL
Well Status: Seismic logging
Year Drilled: 1997
Total Depth: 53

Easting:
Northing:
Longitude:
Latitude:
Completion Depth:

Driller: DANIELSON/TOWLER
Geologist: HERSLEY
Drill Method: HOLLOW STEM AUGER
Drill Fluid:
Land Surface:

Date: 12/2/97
Water Level: N/A
Water Level Date: N/A
Water Level Access: N/A

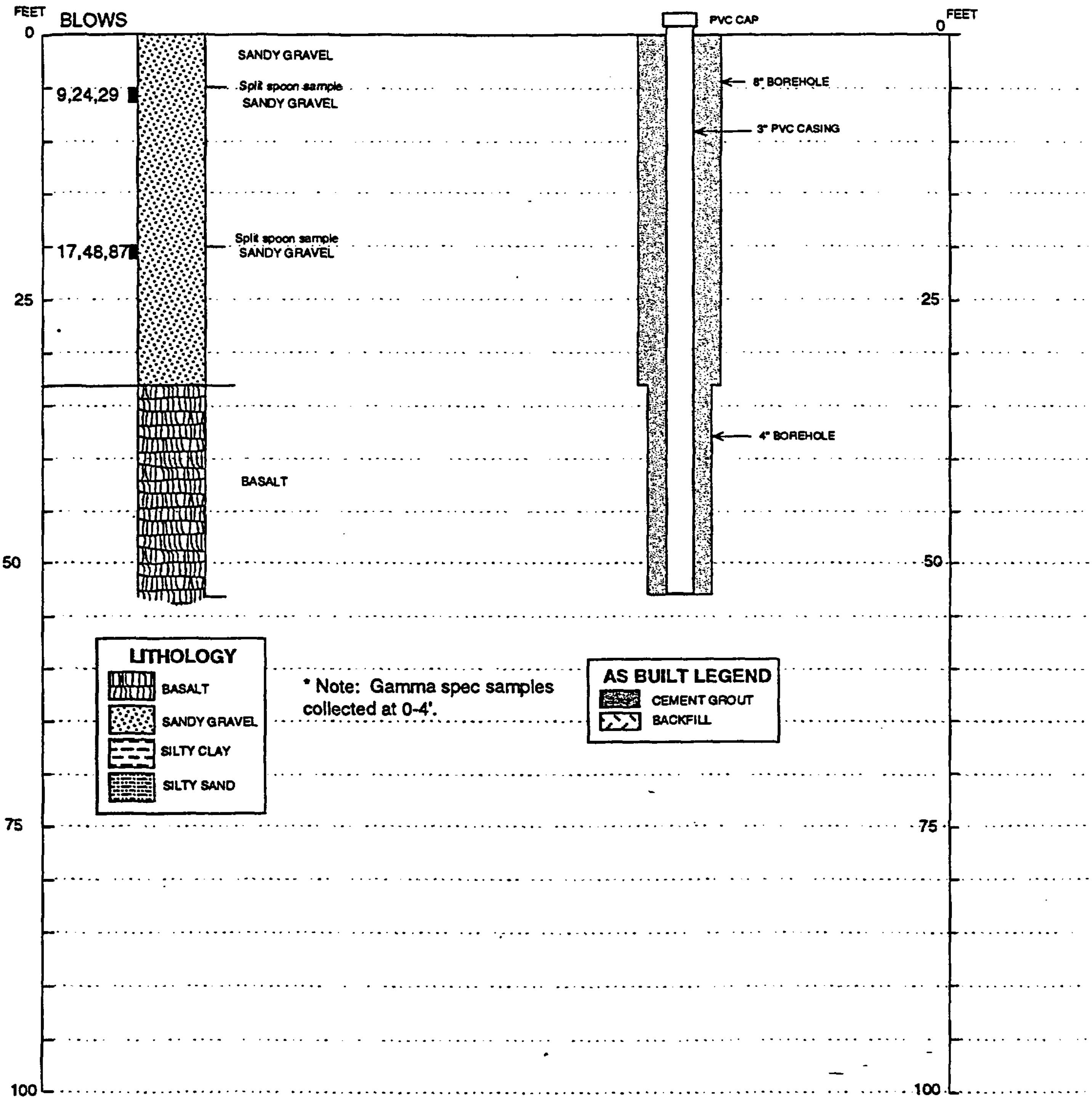

PARTICLE SIZE DISTRIBUTION TEST REPORT

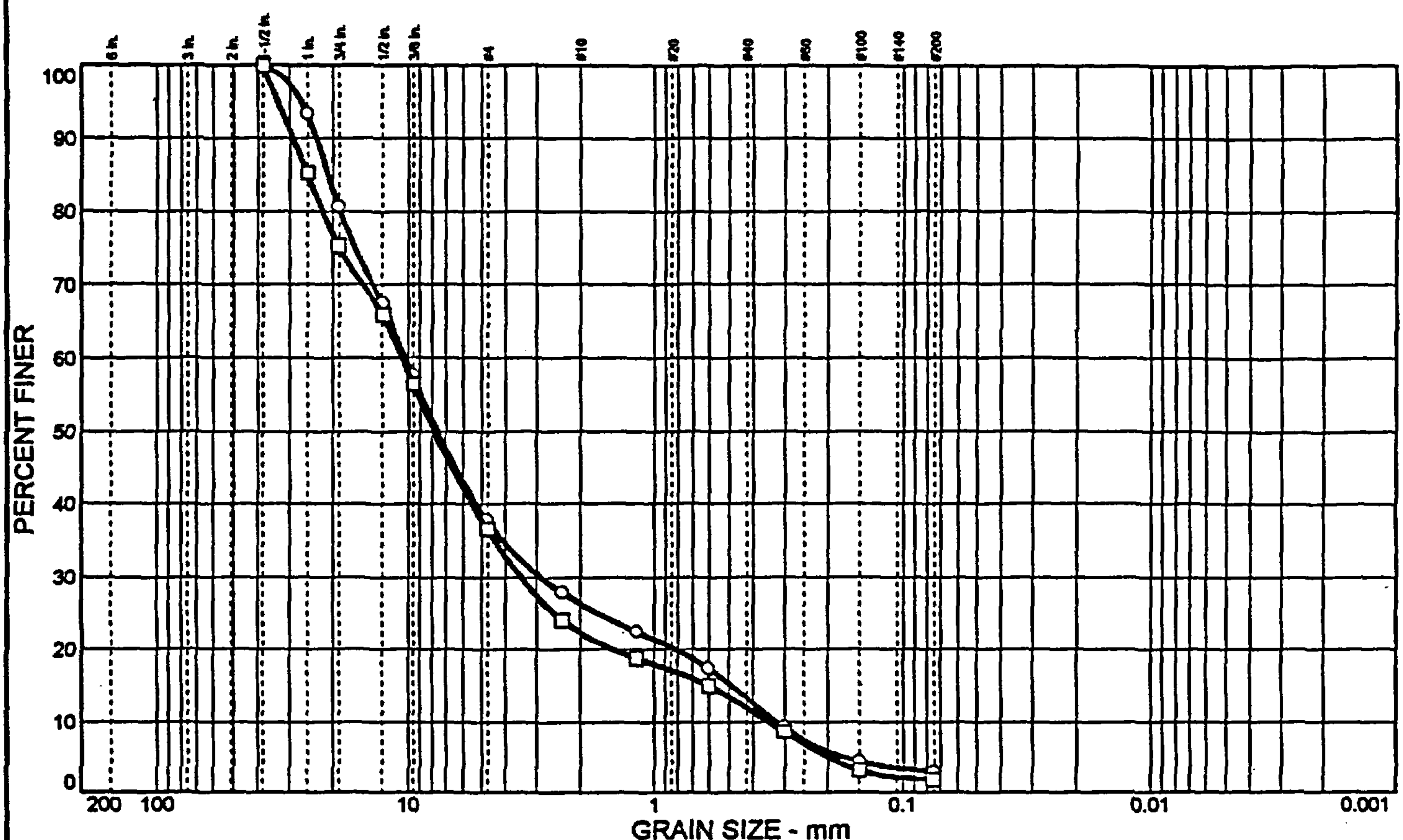

	% + 3"	% GRAVEL	% SAND	% SILT	% CLAY	USCS	AASHTO	PL	LL
○		62.3	34.7			GW	A-1-a	None	None
□		63.4	34.7			GP	A-1-a	None	None

SIEVE inches size	PERCENT FINER ○	PERCENT FINER □	
1.5"	100.0	100.0	
1.0"	93.4	85.3	
0.75"	80.7	75.3	
0.50"	67.4	65.9	
0.375"	57.5	56.4	
	GRAIN SIZE		
D_{60}	10.2	10.6	
D_{30}	2.89	3.46	
D_{10}	0.323	0.346	
	COEFFICIENTS		
C_c	2.53	3.28	
C_u	31.70	30.54	

SIEVE number size	PERCENT FINER ○	PERCENT FINER □	
#4	37.7	36.6	
#8	27.9	24.1	
#16	22.4	18.8	
#30	17.4	15.0	
#50	9.2	8.6	
#100	4.4	3.2	
#200	3.0	1.9	

SOIL DESCRIPTION

○ Well-graded gravel with sand

□ Poorly graded gravel with sand

REMARKS:

○ Sampled at 5'-6'6"

□ Sampled at 5'-6'6"

○ Location: Bore Hole #BH1 5'-6'6"

□ Location: Bore Hole #BH1A 5'-6'6"

INEL MATERIALS LAB

Client: LMITCO Spent Fuel Program

Project: Spent Fuel Installation CPP area

Project No.: 974595150

Page

PARTICLE SIZE DISTRIBUTION TEST REPORT

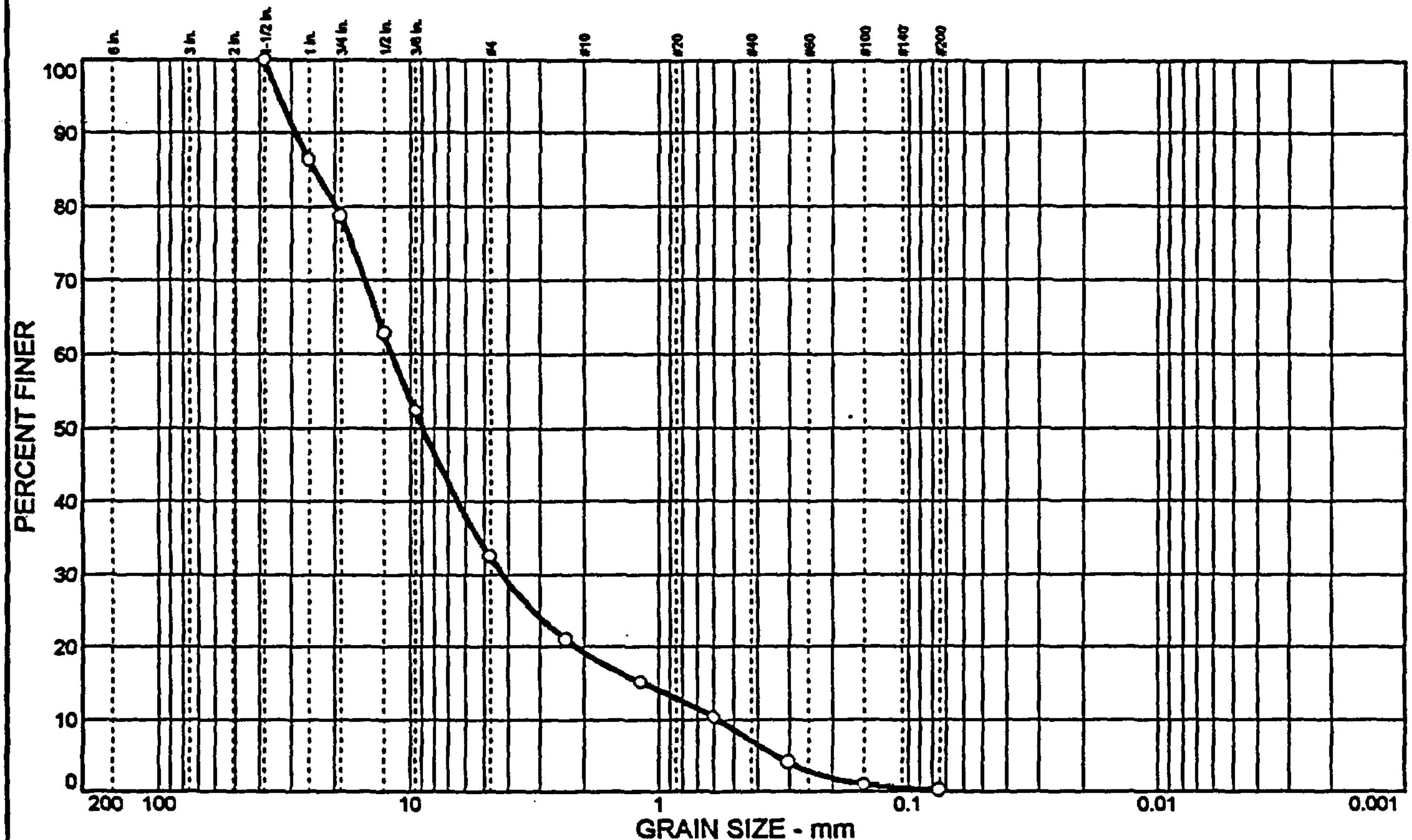

	% + 3"	% GRAVEL	% SAND	% SILT	% CLAY	USCS	AASHTO	PL	LL
O		67.5	32.2			GW	A-1-a	None	None

SIEVE inches size	PERCENT FINER O		
1.5"	100.0		
1.0	86.4		
0.75	78.7		
0.50	62.8		
0.375	52.3		
	GRAIN SIZE		
D_{60}	11.8		
D_{30}	4.22		
D_{10}	0.580		
	COEFFICIENTS		
C_c	2.60		
C_u	20.40		

SIEVE number size	PERCENT FINER O		
#4	32.5		
#8	21.0		
#16	15.1		
#30	10.3		
#50	4.1		
#100	1.1		
#200	0.3		

SOIL DESCRIPTION

O Well-graded gravel with sand

REMARKS:

O Sampled at 5'-6'6"

O Location: Bore Hole #BH2 5'-6'6"

INEL MATERIALS LAB

Client: LMITCO Spent Fuel Program

Project: Spent Fuel Installation CPP area

Project No.: 974595150

Page

PARTICLE SIZE DISTRIBUTION TEST REPORT

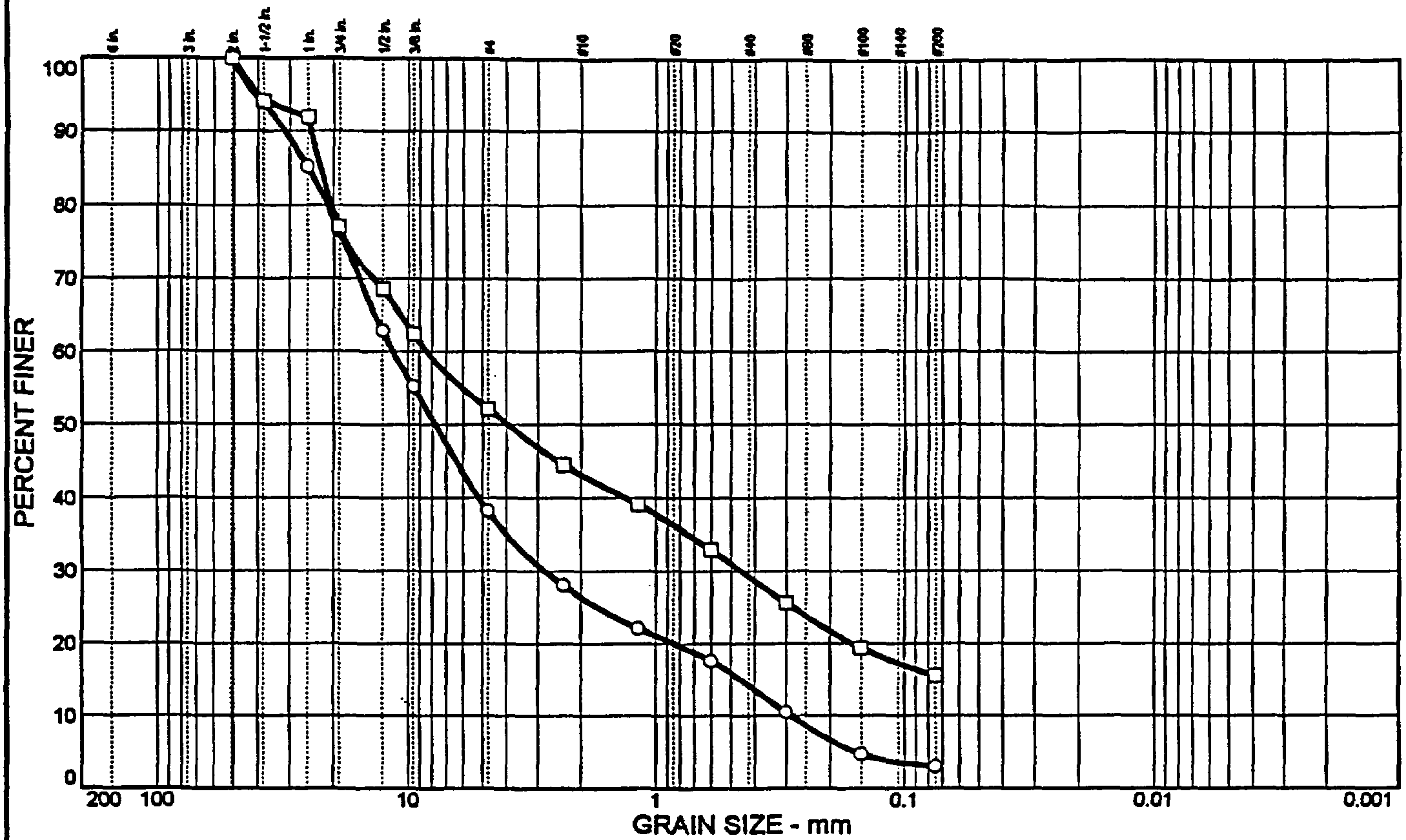

	% + 3"	% GRAVEL	% SAND	% SILT	% CLAY	USCS	AASHTO	PL	LL
O		61.8	35.1			GW	A-1-a	None	None
□		47.9	36.6			GM	A-1-b	None	None

SIEVE inches size	PERCENT FINER O	PERCENT FINER □	
2.0	100.0	100.0	
1.5	94.0	94.1	
1.0"	85.2	91.9	
0.75"	76.6	77.2	
0.50"	62.9	68.6	
0.375"	55.2	62.5	
	GRAIN SIZE		
D_{60}	11.5	8.37	
D_{30}	2.80	0.455	
D_{10}	0.286		
	COEFFICIENTS		
C_c	2.39		
C_u	40.11		

SIEVE number size	PERCENT FINER O	PERCENT FINER □	
#4	38.2	52.1	
#8	28.1	44.5	
#16	22.1	39.1	
#30	17.6	32.9	
#50	10.5	25.6	
#100	4.8	19.4	
#200	3.1	15.5	

SOIL DESCRIPTION

O Well-graded gravel with sand

□ Silty gravel with sand

REMARKS:

O Sampled from 10' - 12'6"

□ Sampled from 28'6" - 30'6"

O Location: Bore Hole #BH3 10'-12'6"

□ Location: Bore Hole #BH3 28'6"-30'6"

INEL MATERIALS LAB

Client: LMITCO Spent Fuel Program

Project: Spent Fuel Installation CPP area

Project No.: 974595150

Page

PARTICLE SIZE DISTRIBUTION TEST REPORT

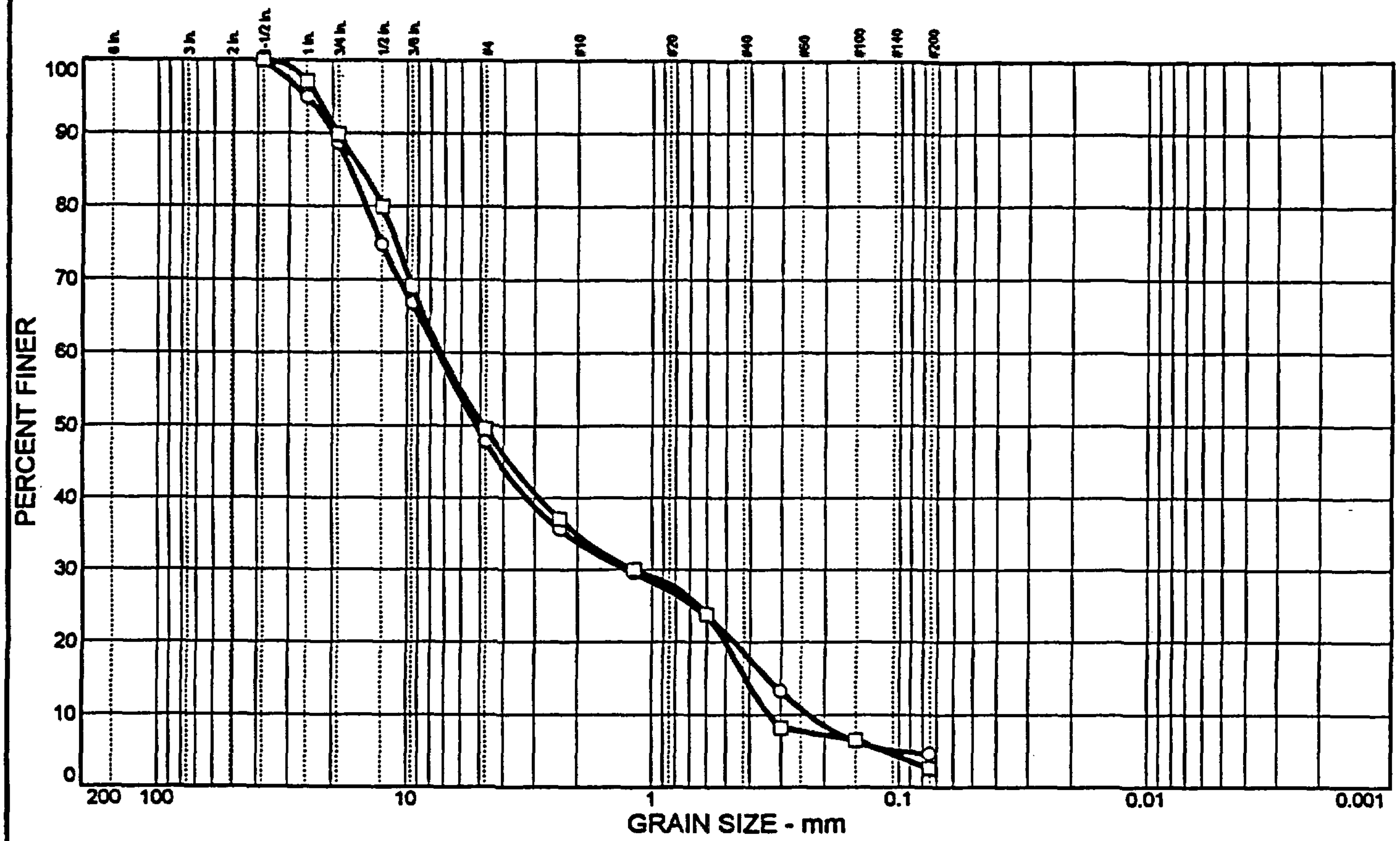

	% + 3"	% GRAVEL	% SAND	% SILT	% CLAY	USCS	AASHTO	PL	LL
○		52.2	43.1			GP	A-1-a	None	None
□		50.5	46.8			GP	A-1-a	None	None

SIEVE inches size	PERCENT FINER ○	PERCENT FINER □	
1.5"	100.0	100.0	
1.0"	94.9	97.1	
0.75"	88.7	89.9	
0.50"	74.8	80.0	
0.375"	66.8	69.1	
	GRAIN SIZE		
D_{60}	7.46	7.25	
D_{30}	1.27	1.18	
D_{10}	0.231	0.332	
	COEFFICIENTS		
C_c	0.93	0.58	
C_u	32.30	21.83	

SIEVE number size	PERCENT FINER ○	PERCENT FINER □	
#4	47.8	49.5	
#8	35.6	37.0	
#16	29.5	30.0	
#30	23.6	23.8	
#50	13.3	8.3	
#100	6.4	6.6	
#200	4.7	2.7	

SOIL DESCRIPTION

○ Poorly graded gravel with sand

□ Poorly graded gravel with sand

REMARKS:

○ Sampled at 5'-6'6"

□ Sampled at 5'-6'6"

○ Location: Bore Hole #BH4 5'-6'6"

□ Location: Bore Hole #BH4A 5'-6'6"

INEL MATERIALS LAB

Client: LMITCO Spent Fuel Program

Project: Spent Fuel Installation CPP area

Project No.: 974595150

Page

PARTICLE SIZE DISTRIBUTION TEST REPORT

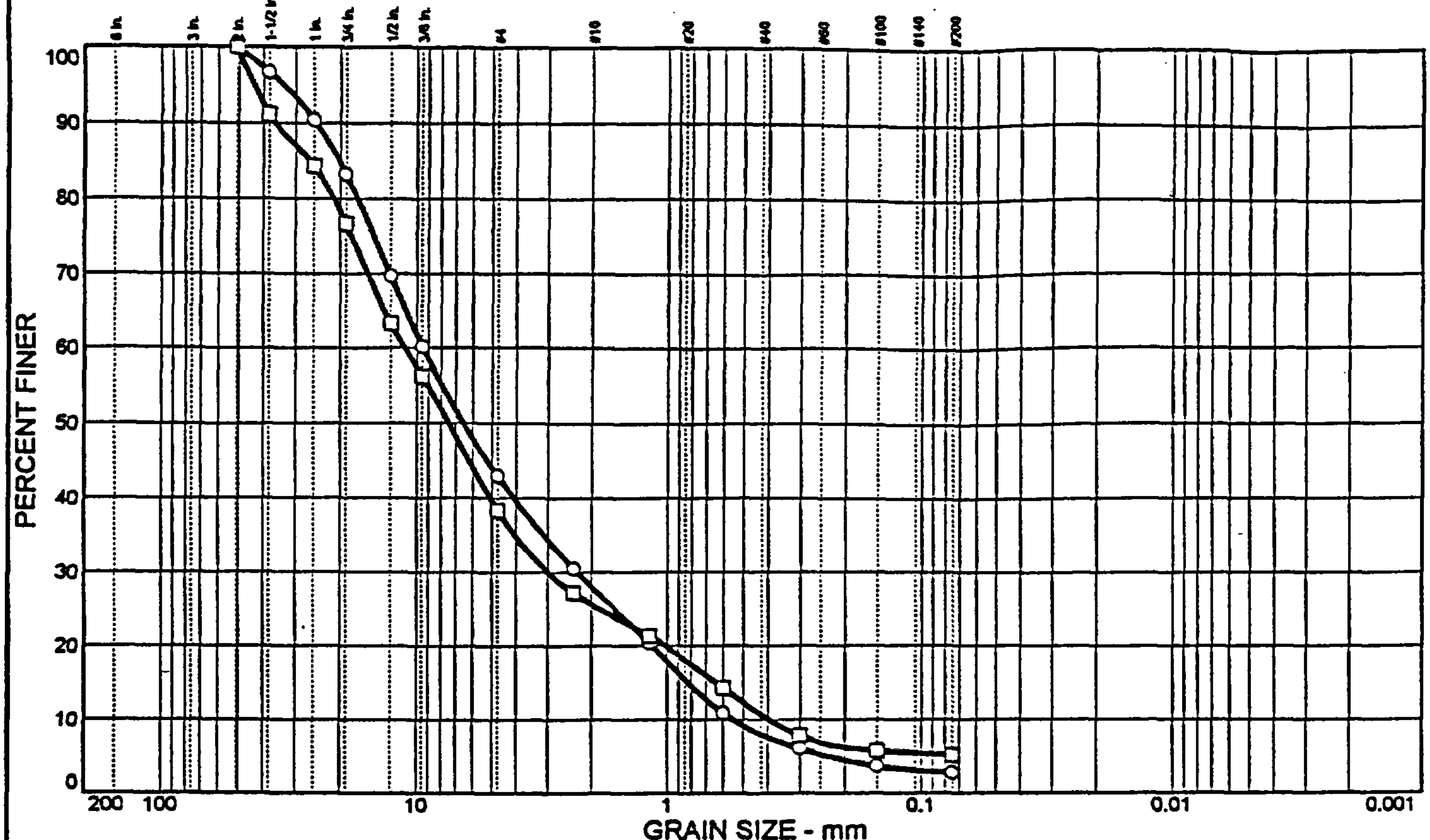

	% + 3"	% GRAVEL	% SAND	% SILT	% CLAY	USCS	AASHTO	PL	LL
○		57.1	40.1			GW	A-1-a	None	None
□		61.7	33.1			GW-GM	A-1-a	None	None

SIEVE inches size	PERCENT FINER ○	□	
2.0	100.0	100.0	
1.5	96.7	91.2	
1.0"	90.4	84.3	
0.75"	83.2	76.7	
0.50"	69.7	63.3	
0.375"	60.2	56.2	
	GRAIN SIZE		
D_{60}	9.46	11.2	
D_{30}	2.28	2.98	
D_{10}	0.549	0.397	
	COEFFICIENTS		
C_c	1.00	2.00	
C_u	17.22	28.16	

SIEVE number size	PERCENT FINER ○	□	
#4	42.9	38.3	
#8	30.5	27.2	
#16	20.4	21.3	
#30	10.9	14.3	
#50	6.1	7.8	
#100	3.7	5.8	
#200	2.8	5.2	

SOIL DESCRIPTION

○ Well-graded gravel with sand

□ Well-graded gravel with silt and sand

REMARKS:

○ Sampled from 5' - 6'6"

□ Sampled from 20' - 21'6"

○ Location: Test Hole #BH5 5'-6'6"

□ Location: Bore Hole #BH5 20'-21'6"

INEL MATERIALS LAB

Client: LMITCO Spent Fuel Program

Project: Spent Fuel Installation CPP area

Project No.: 974595150

Page

PARTICLE SIZE DISTRIBUTION TEST REPORT

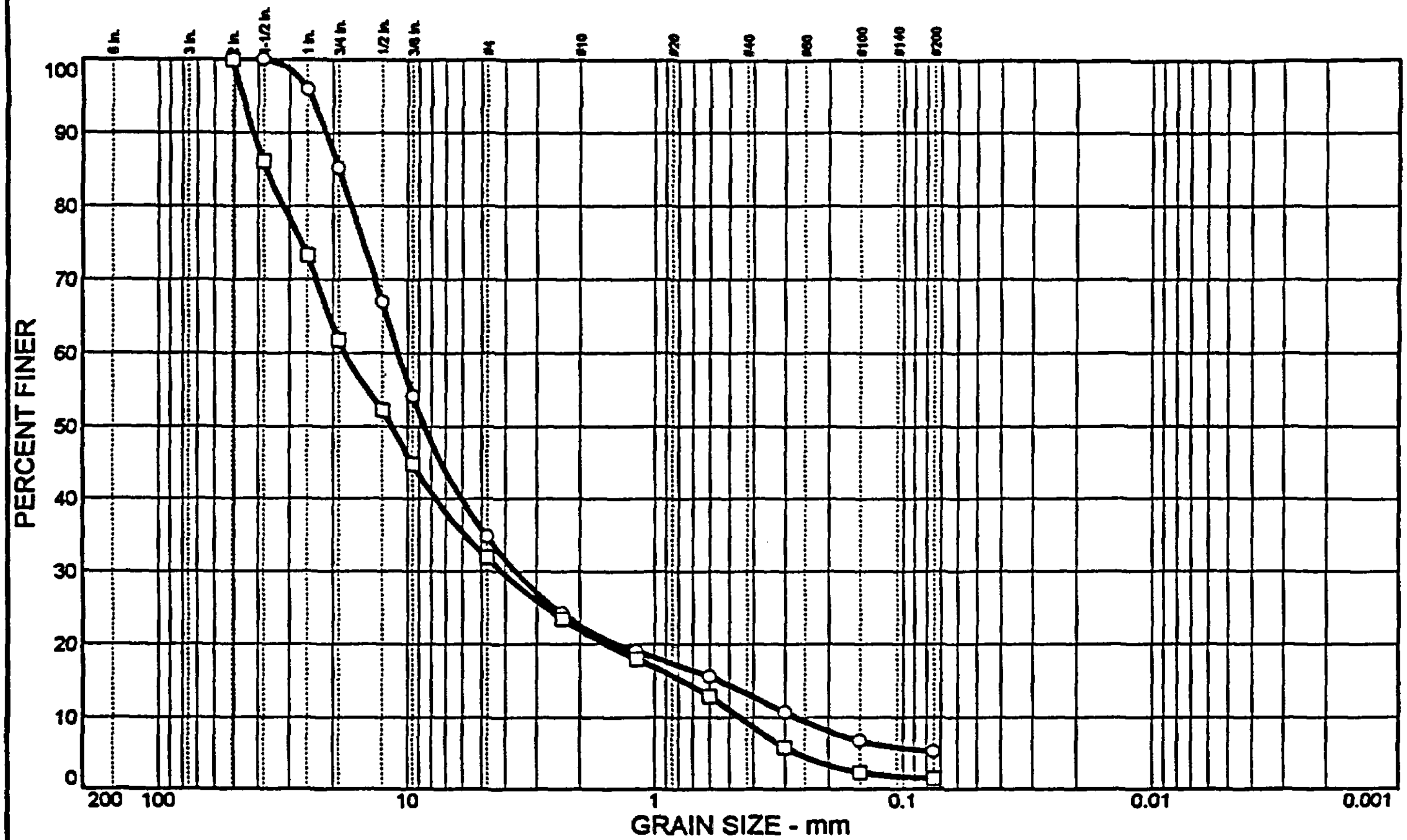

	% + 3"	% GRAVEL	% SAND	% SILT	% CLAY	USCS	AASHTO	PL	LL
○		65.2	29.5			GP-GM	A-1-a	Non	None
□		68.1	30.4			GW	A-1-a	None	None

SIEVE inches size	PERCENT FINER ○	PERCENT FINER □	
2.0		100.0	
1.5	100.0	86.1	
1.0	95.9	73.3	
0.75	85.3	61.9	
0.50	67.0	52.2	
0.375	54.2	44.8	
	GRAIN SIZE		
D_{60}	10.9	17.9	
D_{30}	3.63	4.14	
D_{10}	0.271	0.452	
	COEFFICIENTS		
C_c	4.45	2.11	
C_u	40.22	39.65	

SIEVE number size	PERCENT FINER ○	PERCENT FINER □	
#4	34.8	31.9	
#8	24.2	23.5	
#16	19.0	18.0	
#30	15.6	12.9	
#50	10.7	5.9	
#100	6.8	2.4	
#200	5.3	1.5	

SOIL DESCRIPTION

○ Poorly graded gravel with silt and sand

□ Well-graded gravel with sand

REMARKS:

○ Sampled at 20' - 21'6"

□ Sampled at 5' - 6'6"

○ Location: Bore Hole #BH19 20'-21'6"

□ Location: Bore Hole #BH19 5'-6'6"

INEL MATERIALS LAB

Client: LMITCO Spent Fuel Program

Project: Spent Fuel Installation CPP area

Project No.: 974595150

Page

ATTACHMENT 24
Reference RAI 2-15

MAP I-2330

U.S. DEPARTMENT OF THE INTERIOR
U.S. GEOLOGICAL SURVEY

TITLE: GEOLOGICAL MAP OF THE IDAHO NATIONAL ENGINEERING LABORATORY AND ADJOINING AREAS, EASTERN IDAHO

Please refer to the NRC's Document Control Center Package for the referenced map.

Copies are available through:
U.S. Geological Survey Map Distribution
Box 25286, Federal Center, Denver, DO 80225

Idaho National Engineering and Environmental Laboratory
Volcanic Vents and Topography

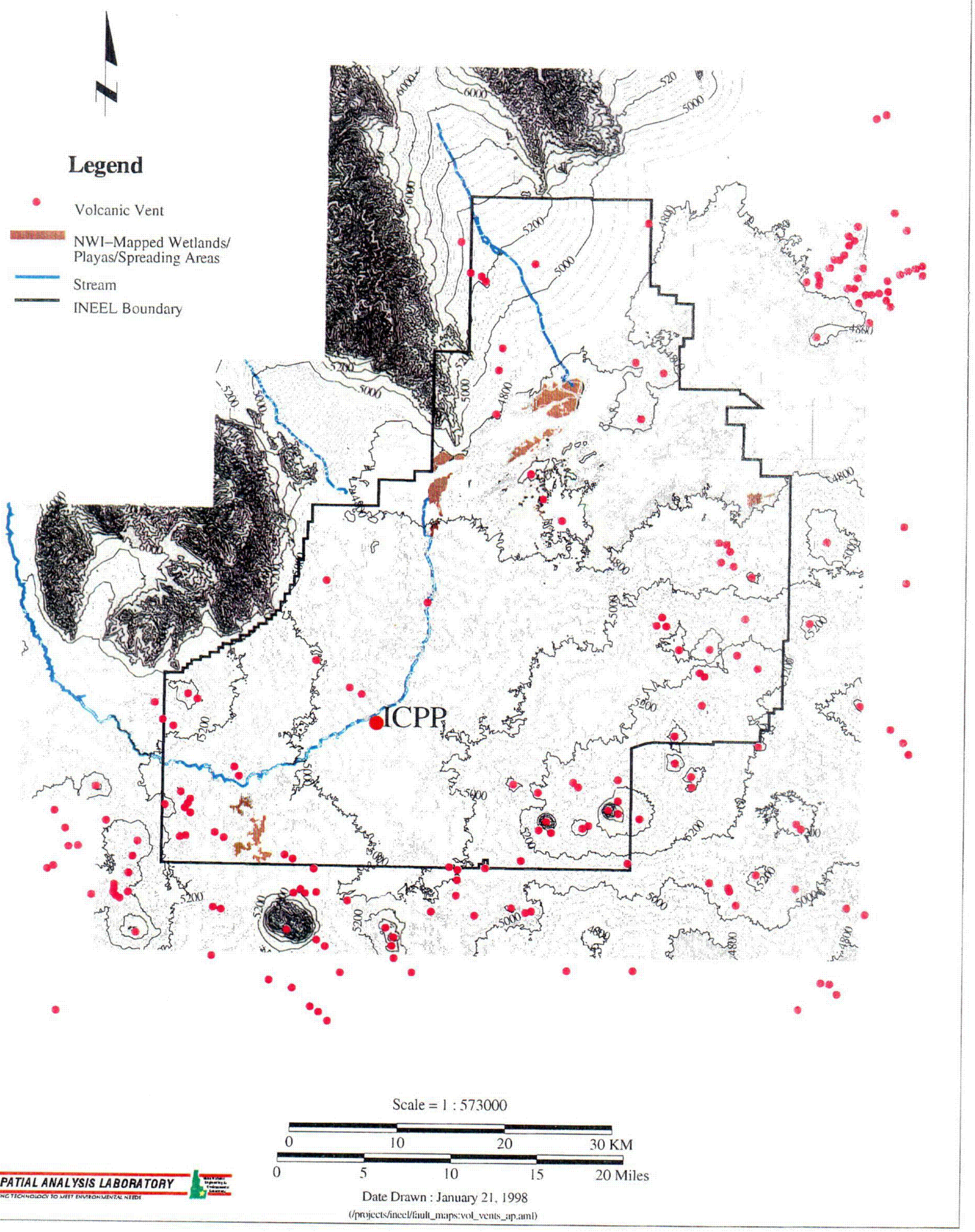

C-04

Generalized Geologic Map of the INEEL Area

(adapted from Kuntz et al., 1994 and Scott, 1982).

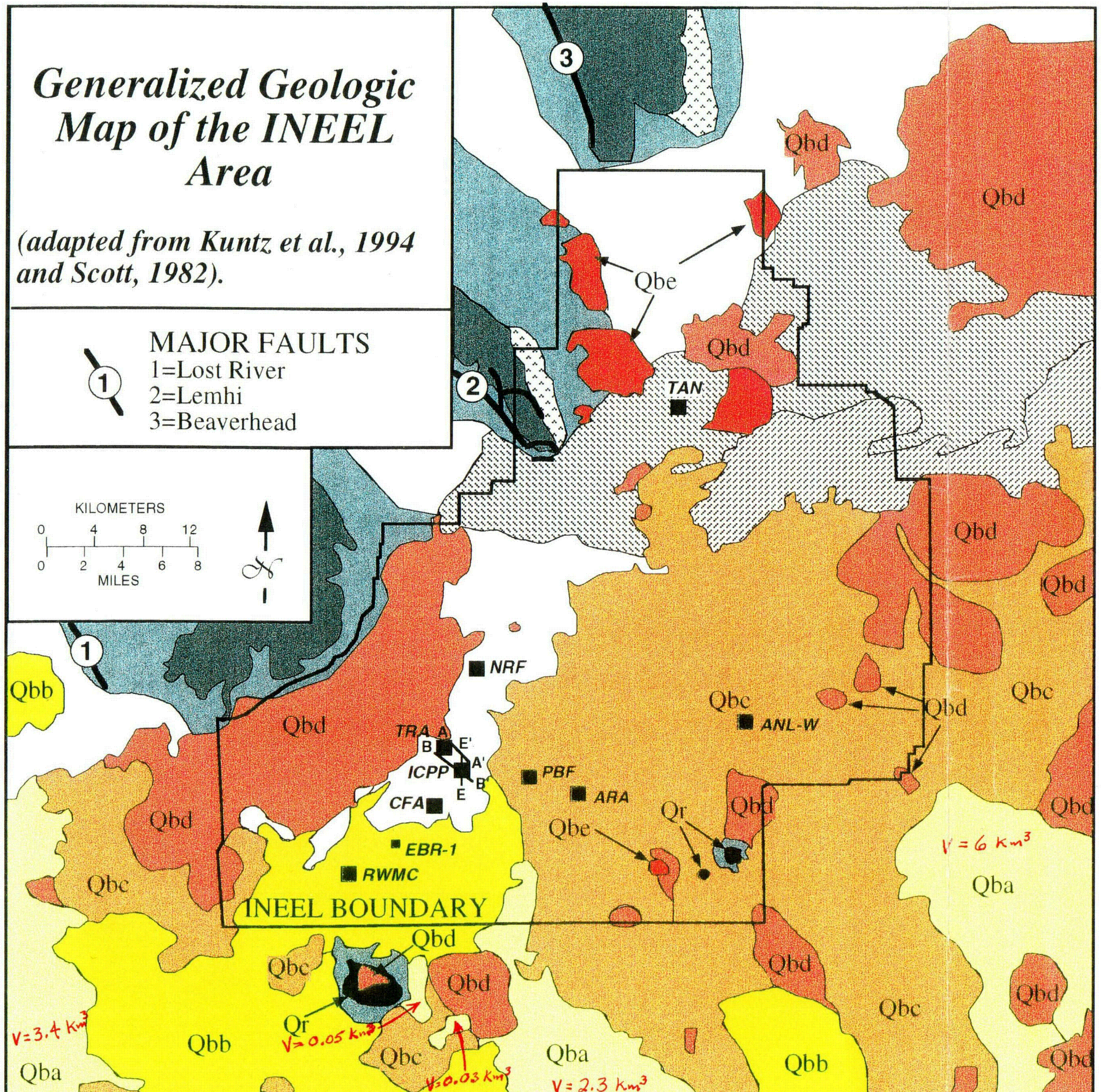

Mainstream Alluvium. Includes deposits of modern flood plains (Holocene) and older deposits in terraces above modern floodplains (upper to middle Pleistocene). Composed mostly of gravel and sand with minor silt and clay. Older deposits host well developed soils and partial to complete loess cover. Up to 20 m thick in southern INEEL, and much thicker in mainstreams to the north.

Alluvial Fans Deposits. Debris flow and stream deposits of clast supported pebble and boulder gravels with matrix of silty sand to clayey silt. Holocene to upper Pliocene. Middle to lower Pleistocene units commonly locally faulted along the west flanks of the Lost River, Lemhi, and Beaverhead Ranges. Includes colluvial debris fans on steep slopes of East, Middle, and Big Southern Buttes.

Eolian Deposits. Very fine to coarse sand in mostly stabilized dunes, 1 to 5 m thick. Some areas of active deflation and migrating sand. Holocene to upper Pleistocene.

Lacustrine Deposits. Mostly lake floor deposits of Pleistocene Lake Terreton. Silty clay to sandy silt. 1 to >100 m thick. Locally includes sandy lake margin deposits and Holocene playa deposits.

BEDROCK UNITS

Basaltic Lava Flows. Black to gray pahoehoe and a'a lava flows, with bedded, oxidized, scoria, cinders, and ash near vents. Locally weathered and oxidized. Olivine basalts composed of crystals of olivine, pyroxene, plagioclase, titanomagnetite, and ilmenite in a matrix of brown glass.

Qba	Holocene to uppermost Pleistocene (<15 kyr). No cover of eolian or alluvial deposits.
Qbb	Upper to Middle Pleistocene (15-200 kyr). Locally covered by up to 1 m of eolian sand and loess.
Qbc	Middle Pleistocene (200-400 kyr). Covered by as much as several m of eolian sand and loess.
Qbd	Middle to Lower Pleistocene (400-730 kyr). Mostly covered by several m of eolian sand and loess.
Qbe	Lower Pleistocene (>730 kyr) Mostly covered by several m of eolian sand and loess. Reversed magnetic polarity.

Quaternary Rhyolite (Qr)

Qr

Rhyolite Domes. Pleistocene (0.3-1.2 Myr) tan to pink, flow laminated rhyolite, with minor vent breccia and banded obsidian composed of microcrystaline intergrowths of quartz, and alkali fledspar with rare phenocrysts of quartz clinopyroxene, and magnetite.

Tertiary Volcanics

Volcanic Rocks. Basaltic lava flows, rhyolitic ash flow tuffs, and rhyolitic lava flows. Mostly Miocene and Pliocene (~4-12 Myr).

Pre-Tertiary Rocks

Pre-Tertiary Rocks. Late Precambrian to Triassic. Mostly Mississippian shelf carbonates of the Overthrust Belt. Also includes Permian to Triassic fine clastic deposits and phosphatic silts; Cambrian to Ordovician quartzites, sandstone, conglomerates, and siltstones; Devonian dolostones and argillites; and Precambrian sandstones and quartzites.

A E' B A' B' E

Positions at cross sections shown in figures 2.6-14, 2.6-15, and 2.6-16.

V= 6 Km³ Volume of lava fed in cubic kilometers. Estimates of volume have been made only for Qba fields.

9802200317-09 C-05

From Kuntz et al. (1992)
Reference 2.45

TABLE 1. CHARACTERISTICS OF FISSURE VENTS AND FLOWS FOR SELECTED ERUPTIONS IN LATEST PLEISTOCENE AND HOLOCENE LAVA FIELDS OF THE EASTERN SNAKE RIVER PLAIN, IDAHO*

LAVA FIELD Flow Name	Length of Eruptive Fissures Single Fissures (km^2)	Length of Eruptive Fissures Whole Zone (km^2)	Estimated Width of Fissures (m)	Area of Lava (km^2)	Estimated Flow/Field Volume (km^3)	Flow Type	Comments
CRATERS OF THE MOON							
Broken Top	Unknown	<0.3	Unknown	11	0.1	Surface- and tube(?)-fed pahoehoe flows.	Intermediate-volume stage-2 eruption. Flow issued from two obscure vents on east and south sides of Broken Top cinder cone. Vents now largely obscured by colluvium
Blue Dragon	0.6	1	1 to 2	280	3.4	Tube-fed pahoehoe flows.	Large-volume sustained lava-cone eruption of stage 3. Eruptions from southernmost cinder cone in Big Crater complex and from 0.5-km-long fissure south of Big Craters. Spatter cones along fissure have internal diameters of 1 to 3 m. Fissure width estimated from smallest diameters.
Trench Mortar Flat	0.3 to 1.3	6	≤2	6	0.03	Shelly, thin pahoehoe flows.	Small-volume stage-1 fissure eruption. Flows erupted from 0.3- to 1.3-km en echelon segments in 6-km zone of eruptive fissures. Fissure widths estimated where enlargement by erosion seemed minimal.
North Crater	Unknown	Unknown	Unknown	1.5	0.01	Surface-fed pahoehoe.	Small-volume eruption from pipelike vent, which is now covered by colluvial cinders from inner wall of North Crater.
Big Craters	≤0.2	0.9	1 to 2	9	0.05	Surface-fed pahoehoe and slab pahoehoe flows.	Small-volume stage-2 eruption. Two source fissures north of Big Craters cinder cone complex are short (≤0.2 km), but Big Craters cinder cone complex is aligned along fissure system 0.9 km long. Fissure width estimated from deepest part of eastern eruptive fissure.
Serrate, Devils Orchard, and Highway	Unknown	...	Unknown	27†	0.5†	Bulbous, block flows.	Vent area near North Crater largely destroyed by eruptions, also covered by younger North Crater flow. Eruption was explosive because remnants of crater walls are contained in flow. Eruptions may have been from central pipelike vent in North Crater.
Vermillion Chasm	0.6 to 1	2.9	1 to 2	20	0.1	Shelly, thin pahoehoe flows.	Small-volume stage-1 fissure eruption. Eruptive fissures enlarged at most localities by explosive venting. Fissure width estimated at deepest, narrowest part of fissure system. Fissure system is 2.9 km long; consists of 3 fissures that range from 0.6 to 1 km in length.
Deadhorse	0.1 to 0.6	10	≤1.5	8	0.04	Shelly pahoehoe and thin pahoehoe flows.	Small-volume stage-1 fissure eruption. Many thin flows were erupted from numerous (>13) en echelon, right-stepping eruptive fissures that range from 0.1 to 0.6 km in length. The Deadhorse fissure system is the longest known fissure system that was active along the Great Rift volcanic rift zone during a single eruptive pulse.
Devils Cauldron	(>0.3)	...	Unknown	90	0.9	Tube- and surface-fed pahoehoe flows.	Intermediate-volume stage-2 eruption from central vent on lava cone. Lava lakes perched above vents. Fissure and vent are obscured by flows and lava lakes.
Minidoka	Unknown	...	Unknown	250	3.0	Chiefly tube-fed pahoehoe flows.	Large-volume, sustained stage-3 eruption from central vent complex that is now covered by flows.

TABLE 1. CHARACTERISTICS OF FISSURE VENTS AND FLOWS FOR SELECTED ERUPTIONS IN LATEST PLEISTOCENE AND HOLOCENE LAVA FIELDS OF THE EASTERN SNAKE RIVER PLAIN, IDAHO (continued)

LAVA FIELD Flow Name	Length of Eruptive Fissures Single Fissures (km²)	Whole Zone (km²)	Estimated Width of Fissures (m)	Area of Lava (km²)	Estimated Flow/Field Volume (km³)	Flow Type	Comments
HELLS HALF ACRE	Unknown	2	Unknown	400	6	Chiefly tube-fed pahoehoe flows with minor surface-fed shelly, and slab pahoehoe flows near vent area.	Large-volume, sustained stage-3 eruption from central vent complex that contained a large lava lake. Collapse pits, spatter cones, and the main depression define the length of main eruptive fissure.
NORTH ROBBERS	<0.5	2.9	Unknown	5	0.05	Chiefly surface-fed pahoehoe and minor shelly pahoehoe flows near vents.	Small-volume stage-1 fissure eruption. Eruptive features defined by spatter ramparts and small cinder cones. Noneruptive fissure 0.7 km long extends north of eruptive fissures.
SOUTH ROBBERS	1.1	1.7	Unknown	3	0.03	Chiefly surface-fed pahoehoe and minor shelly pahoehoe flows near vents.	Small-volume stage-1 fissure eruption. Eruptive fissures defined by spatter ramparts and small cinder cones. A 0.6-km-long noneruptive fissure extends north of eruptive fissures.
CERRO GRANDE	Unknown	Unknown	Unknown	175	2.3	Chiefly tube- and surface-fed pahoehoe flows.	Relatively large-volume stage-3 eruption. Poorly defined vent area filled by a lava lake.
KINGS BOWL	0.1 to 0.5	6.2	0.5 to 1[§]	3.3	0.005	Shelly pahoehoe and thin pahoehoe flows.	Small-volume stage-1 fissure eruption. Eruptions from about a dozen fissures in a zone about 6.5 km long. Dikes ≤1.5 m thick exposed in fissure at Kings Bowl (see Greeley and others, 1977, Figs. 11-14, 11-16; Greeley, 1977, Fig. 3-19).
WAPI	...	>0.6	Unknown	325	6	Surface- and tube-fed pahoehoe flows.	Large-volume stage-3 eruption. Vent complex consists of 11 eruptive centers aligned over a buried eruptive fissure (Champion and Greeley, 1977).
SHOSHONE	Unknown	Unknown	Unknown	190	1.5	Chiefly tube- and surface-fed pahoehoe flows. Shelly pahoehoe and slab pahoehoe flows near vent.	Relatively large-volume stage-3 eruption. Vent area modified by late-stage lava lake. Lava tubes recognized only in proximal parts of lava field. Lava lake activity with pistonlike draining and filling of vent depression.

*Data from Kuntz, Champion, and others (1986, 1992); Kuntz, Lefebvre, and Champion (1989a, b); Kuntz, Champion, and Lefebvre (1989); and this chapter.

[†]Total for all three flows.

[§]Measured width.

Attachment 24

MAP I-2330

U.S. DEPARTMENT OF THE INTERIOR
U.S. GEOLOGICAL SURVEY

GEOLOGIC MAP OF THE IDAHO NATIONAL ENGINEERING LABORATORY AND ADJOINING AREAS, EASTERN IDAHO

By Mel A. Kuntz, Betty Skipp, Marvin A. Lanphere, William E. Scott, Kenneth L. Pierce, G. Brent Dalrymple, Duane E. Champion,[1] Glenn F. Embree,[2] William R. Page,[1] Lisa A. Morgan,[1] Richard P. Smith,[3] William R. Hackett,[4] and David W. Rodgers[4]

[1]U.S. Geological Survey
[2]Department of Geology, Ricks College, Rexburg, Idaho
[3]EG&G Idaho Inc., Idaho Falls, Idaho
[4]Department of Geology, Idaho State University, Pocatello, Idaho

Prepared in cooperation with the
U.S. DEPARTMENT OF ENERGY

MISCELLANEOUS INVESTIGATIONS SERIES
Published by the U.S. Geological Survey, 1994

KUNTZ AND OTHERS—GEOLOGY, IDAHO NATIONAL ENGINEERING LABORATORY AND ADJOINING AREAS, EASTERN IDAHO 1:100,000 MAP I-2330

THIS PAGE IS AN OVERSIZED DRAWING OR FIGURE,

THAT CAN BE VIEWED AT THE RECORD TITLED:
"GEOLOGIC MAP OF THE IDAHO NATIONAL ENGINEERING LABORATORY AND ADJOINING AREAS, EASTERN, IDAHO"

WITHIN THIS PACKAGE

D-07A
D-07B